

Doctoral Thesis
Madrid, Spain 2016

Aggregation of Plug-in Electric Vehicles in Power Systems for Primary Frequency Control

SEYEDMAHDI IZADKHAST



Aggregation of Plug-in Electric Vehicles in Power Systems for Primary Frequency Control

SEYEDMAHDI IZADKHAST

Doctoral Thesis supervisors:

Dr. Pablo García González, Universidad Pontificia Comillas, main director
Dr. Pablo Frías Marín, Universidad Pontificia Comillas, co-director

Members of the Examination Committee:

Prof.dr.ir.
Prof.dr.ir.
Prof.dr.ir.
Prof.dr.ir.
Prof.dr.ir.

This research was funded by the European Commission through the SETS Program, an Erasmus Mundus Joint Doctorate, and also partially supported by the Institute for Research in Technology at Universidad Pontificia Comillas.

TRITA-EE:

ISSN:

ISBN:

Copyright © 2016 by S. Izadkhast. All rights reserved. No part of the material protected by this copyright notice may be reproduced or utilized in any form or by any means, electronic or mechanical, including photocopying, recording or by any information storage and retrieval system, without written permission from the author.

Printed by US-AB in Stockholm, Sweden

Aggregation of Plug-in Electric Vehicles in Power Systems for Primary Frequency Control

PROEFSCHRIFT

ter verkrijging van de graad van doctor
aan de Technische Universiteit Delft,
op gezag van de Rector Magnificus prof. ir. K.C.A.M. Luyben,
voorzitter van het College voor Promoties,
in het openbaar te verdedigen
op woensdag X om X uur

door

Seyedmahdi IZADKHAST
Van de Graad van Master of Science,
Technische Universiteit Sharif, Iran
geboren te Teheran, Iran

This dissertation has been approved by:

Prof.dr.ir. , Technische Universiteit Delft, promotor

Composition of the doctoral committee:

Prof.dr.ir.

Prof.dr.ir.

Prof.dr.ir.

Prof.dr.ir.

Prof.dr.ir.

The doctoral research has been carried out in the context of an agreement on joint doctoral supervision between KTH Royal Institute of Technology, Stockholm, Sweden, Universidad Pontifical de Comillas, Madrid, Spain and Delft University of Technology, The Netherlands.

This research was funded by the European Commission through the SETS Program, an Erasmus Mundus Joint Doctorate, and also partially supported by the Institute for Research in Technology at Universidad Pontificia Comillas.

Keywords: Aggregation, Plug-in Electric Vehicles, Primary Frequency Control

ISBN

Copyright © 2016 by S. Izadkhast. Madrid, Spain. All rights reserved. No part of the material protected by this copyright notice may be reproduced or utilized in any form or by any means, electronic or mechanical, including photocopying, recording or by any information storage and retrieval system, without written permission from the author.

Printed by

SETS Joint Doctorate

The Erasmus Mundus Joint Doctorate in **Sustainable Energy Technologies and Strategies**, SETS Joint Doctorate, is an international programme run by six institutions in cooperation:

- Comillas Pontifical University, Madrid, Spain
- Delft University of Technology, Delft, the Netherlands
- Florence School of Regulation, Florence, Italy
- Johns Hopkins University, Baltimore, USA
- KTH Royal Institute of Technology, Stockholm, Sweden
- University Paris-Sud 11, Paris, France

The Doctoral Degrees issued upon completion of the programme are issued by Comillas Pontifical University, Delft University of Technology, and KTH Royal Institute of Technology.

The Degree Certificates are giving reference to the joint programme. The doctoral candidates are jointly supervised, and must pass a joint examination procedure set up by the three institutions issuing the degrees.

This Thesis is a part of the examination for the doctoral degree.

The invested degrees are official in Spain, the Netherlands and Sweden respectively.

SETS Joint Doctorate was awarded the Erasmus Mundus **excellence label** by the European Commission in year 2010, and the European Commission's **Education, Audiovisual and Culture Executive Agency**, EACEA, has supported the funding of this programme.

The EACEA is not to be held responsible for contents of the Thesis.



*To my parents and my sister,
for their love, support, and encouragement*

Abstract in English Language

Author: Seyedmahdi Izadkhast

Thesis Title: Aggregation of Plug-in Electric Vehicles in Power Systems for Primary Frequency Control

Language: Written in English

Keywords: Aggregation, Plug-in Electric Vehicles, Primary Frequency Control

The number of plug-in electric vehicles (PEVs) is likely to increase in the near future and these vehicles will probably be connected to the electric grid most of the day time. PEVs are interesting options to provide a wide variety of services such as primary frequency control (PFC), because they are able to quickly control their active power using electronic power converters. However, to evaluate the impact of PEVs on PFC, one should either carry out complex and time consuming simulation involving a large number of PEVs or formulate and develop aggregate models which could efficiently reduce simulation complexity and time while maintaining accuracy.

This thesis proposes aggregate models of PEVs for PFC. The final aggregate model has been developed gradually through the following steps. First of all, an aggregate model of PEVs for the PFC has been developed where various technical characteristics of PEVs such as operating modes (i.e., idle, disconnected, and charging) and PEV's state of charge have been formulated and incorporated. Secondly, some technical characteristics of distribution networks have been added to the previous aggregate model of PEVs for the PFC. For this purpose, the power consumed in the network during PFC as well as the maximum allowed current of the lines and transformers have been taken into account. Thirdly, the frequency stability margins of power systems including PEVs have been evaluated and a strategy to design the frequency-droop controller of PEVs for PFC has been described. The controller designed guarantees similar stability margins, in the worst case scenario, to those of the system without PEVs. Finally, a method to evaluate the positive economic impact of PEVs participation in PFC has been proposed.

Affiliations:

Inst. de Investigación Tecnológica
Universidad Pontificia Comillas
C. Sta Cruz de Marcenado 26
28015 Madrid, Spain

KTH Electric Power Systems
School of Electrical Engineering
Royal Institute of Technology
Teknikringen 33, 100-44
Stockholm
Sweden

Technology Policy & Management
Technische Universiteit Delft
Jaffalaan 5, 2628 BX Delft
The Netherlands

Acknowledgments

I would like to deeply thank my supervisors Professor Pablo García and Professor Pablo Frías for their expert guidance, wise advise and help during the last five years. I would also like to sincerely thank Professor Pavol Bauer and Dr. Laura Ramírez Elizondo for their ongoing support and invaluable guidance over the last three years.

I would like to express my gratitude towards all partner institutions within the SETS programme as well as the European Commission for its financial support. My gratitude goes to my colleagues in the DCE&S group at the Delft University of Technology & IIT who provided suggestions and support. Finally, many thanks, from the bottom of my heart, to my parents for their endless love and all their support without whom this research would not have been possible.

Dissertation

This doctoral thesis develops and evaluates aggregate models of PEVs satisfactorily representing the substantial dynamic behaviour of PEVs during the provision of PFC. Note that this document is a full-classic doctoral thesis.

Papers in Science Citation Index (JCR) Journals:

- Paper J1** S. Izadkhast, P. Garcia-Gonzalez, and P. Frías, “An aggregate model of plug-in electric vehicles for primary frequency control,” *IEEE Transactions on Power Systems*, vol. 30, no. 3, pp. 1475–1482. May 2015.
- Paper J2** S. Izadkhast, P. Garcia-Gonzalez, and P. Frías, L. Ramirez-Elizondo, and P. Bauer, “An aggregate model of plug-in electric vehicles including distribution network characteristics for primary frequency control,” *IEEE Transactions on Power Systems*, vol. 31, no. 4, pp. 2987–2998. Jul 2016.
- Paper J3** S. Izadkhast, P. Garcia-Gonzalez, P. Frías, and P. Bauer, “Design of plug-in electric vehicle’s frequency-droop controller for primary frequency control and performance assessment,” *IEEE Transactions on Power Systems*, accepted and to be published.

Conference Papers:

With Proceedings

- Paper C1** S. Izadkhast, P. Garcia-Gonzalez, and P. Frías, L. Ramirez-Elizondo, and P. Bauer, “Aggregation of plug-in electric vehicles in distribution networks for primary frequency control,” in *IEEE International Electric Vehicle Conference*, Dec. 2014 Florence, Italy.
- Paper C2** S. Izadkhast, P. Garcia-Gonzalez, and P. Frías, “An aggregate model of plug-in electric vehicles for primary frequency control,” *Power & Energy Technology Systems (PES) General Meeting*, Jul. 2016 IEEE Boston, Massachusetts, USA.
- Paper C3** S. Izadkhast, P. Garcia-Gonzalez, and P. Frías, L. Ramirez-Elizondo, and P. Bauer, “An aggregate model of plug-in electric vehicles including distribution network characteristics for primary frequency control,” *Power & En-*

ergy Technology Systems (PES) General Meeting, Jul. 2016 IEEE Boston, Massachusetts, USA.

Without Proceedings

Paper C4 S. Izadkhast, “Plug-in electric vehicle participation in primary frequency control considering characteristics of distribution networks,” in *Young Energy Engineers & Economists Seminar*, Nov. 2014 KU Leuven, Belgium.

Co-authored Papers:

With Relevance for This Thesis Research

Paper C5 A. Rodriguez-Calvo, S. Izadkhast, R. Cossent, and P. Frías, “Evaluating the determinants of the scalability and replicability of islanded operation in medium voltage networks with cogeneration,” in *Smart Electric Distribution Systems & Technologies (EDST)*, Sep. 2015 IEEE Vienna, Austria.

Paper C6 R. Moreno, H. R. Chamorro, and S. Izadkhast, “A framework for the energy aggregator model,” in *Workshop on Power Electronics & Power Quality Applications (PEPQA)*, Jul. 2013 IEEE Bogota, Colombia.

Technical reports:

With Relevance for This Thesis Research

Report R1 S. Izadkhast, “Evaluating the impact of plug-in electric vehicles on the cellular smart grid platform (CSGriP) cells”, Cellular Smart Grid Platform (CSGriP) Project, the Netherlands, 2016.

Report R2 S. Izadkhast, A. Rodriguez, R. Cossent, and P. Frías, “Islanded operation of the NICE distribution zone equipped with the battery energy storage unit – French demo project” Grid4EU Technical Project & NICE GRID (EDF, France) Technical Report, 2015.

Report R3 S. Izadkhast, A. Rodriguez, R. Cossent, and P. Frías, “Islanded operation of a distribution zone equipped with the CHP unit – Czech demo project” Grid4EU Technical Project Report, 2015.

Report R4 S. Izadkhast, A. Rodriguez, R. Cossent, and P. Frías, “Evaluation of anti-islanding schemes for grid-connected photovoltaic systems – Italian demo project” Grid4EU Technical Project Report, 2015.

Served as a Peer-Reviewer for Prestigious Journals and Conferences:

- IEEE Transactions on Power Systems
- IEEE Transactions on Industrial Informatics
- IEEE Transactions on Smart grid
- IET Generation, Transmission, Distribution (GTD)
- Elsevier, Sustainable Energy, Grids, and Networks (SEGAN)
- IEEE PES General Meeting

Contents

Acknowledgments	ii
Dissertation	iii
List of Acronyms	ix
Nomenclature	xi
1. Introduction	1
1.1. Background	1
1.2. Challenges And Motivation	5
1.3. Doctoral Thesis Objectives	7
1.3.1. Main Objective	7
1.3.2. Specific Objectives	7
1.4. Thesis Outline and Document Structure	8
2. Background Review of Primary Frequency Control by Plug-in Electric Vehicles in Electric Power Systems	10
2.1. Introduction	11
2.2. PEVs Key Components and Modelling from the Grid Point of View	11
2.2.1. PEVs Components	11
2.2.2. PEV Modelling from the Grid Point of View	15
2.3. Provision of Ancillary Services by PEVs	18
2.3.1. Overview of Ancillary Services Provision by PEVs	18
2.3.2. Provision of PFC by PEVs	23
2.4. Aggregation of PEVs in Electric Power Systems	24
2.4.1. Review of DER Aggregation in Electric Power Systems	25
2.4.2. PEV Aggregation in Electric Power Systems	28
2.5. Conclusions On the State-of-the-art	29
3. An Aggregate Model of PEVs for PFC	31
3.1. Introduction	32
3.2. PFC by PEVs Over Time	34
3.3. Decentralized Model of PEVs for the PFC	37
3.4. Proposed Model of a Single PEV for PFC	39
3.4.1. Previously Developed Model of a PEV for PFC	40
3.4.2. Proposed Model of a PEV for PFC	42

3.5.	Proposed Aggregate Model of PEVs	47
3.5.1.	Average PFC Loop of PEVs for PFC	47
3.5.2.	Average Battery Charger Model	51
3.6.	Case Study and Simulation Scenarios	56
3.6.1.	Modeling Conventional Power Plants	57
3.6.2.	Calculation of the Inertia H for the Worst Case	58
3.6.3.	Aggregate Model of PEV Fleet	60
3.6.4.	Simulation Scenarios	67
3.7.	Simulation Results	68
3.7.1.	Simulation Results of PEV's Participation in the PFC	68
3.7.2.	Simulation Results of the Impact of PEV's Upward Power Reserve on the PFC	70
3.8.	Conclusions and Out-Look	72
4.	An Aggregate Model of PEVs Including Distribution Networks	73
4.1.	Introduction	74
4.2.	Context of PFC by PEVs Within Distribution Networks Over Time	77
4.3.	Equivalent Model of A Single PEV for PFC in a Radial Distribution Network	79
4.3.1.	Power Consumed in Distribution Network	80
4.3.2.	Maximum Allowed Current of A Single PEV for PFC	89
4.3.3.	PEV Equivalent Model for PFC Including Proposed Distribution Network and Transformer Limit	91
4.4.	Aggregate Model of a Large-scale PEV Fleet in a Radial Distribution Network for PFC	95
4.4.1.	Aggregate Fleet's Instantaneous Power Including Power Consumption in the Network During PFC	95
4.4.2.	Maximum Allowed Current of Average PEV for PFC	99
4.4.3.	Aggregate Model of PEVs for PFC Including Distribution Network and Transformer Limit	100
4.5.	Case Study and Simulation Scenarios	102
4.5.1.	Case Study	102
4.5.2.	Simulation Scenarios and Sensitivity Analysis	109
4.6.	Simulation Results	111
4.6.1.	Simulation Results of the Case Study for Scenario 1	111
4.6.2.	Simulation Results of the Case Study for Scenario 2	113
4.6.3.	Validation of Aggregate Models With And Without Network & Sensitivity Analysis Results &	116
4.6.4.	Discussion	117
4.7.	Conclusions and Out-Look	118
5.	Design of PEVs Frequency-Droop Controller for PFC and Economic Performance Assessment	121
5.1.	Introduction	122

5.2.	Technical Implementation: Strategy to Design Frequency-Droop Controllers of PEVs	125
5.2.1.	System Stability Margin Analysis	128
5.2.2.	Design of the Overall Controller Gain of PEVs	133
5.2.3.	Design of the Frequency-Droop Controller of Individual PEVs	137
5.2.4.	Replacement of PEV's reserve by CGU's reserve during PFC	140
5.3.	Case Studies and Simulation Scenarios	142
5.3.1.	Base Case Study of Small-Scale Distribution Network	142
5.3.2.	Simulation Scenarios	143
5.4.	Simulation Results	147
5.4.1.	Results of Scenario A for Different PEV Penetration Rates	147
5.4.2.	Results of Scenario B For Different PEV Penetration Rates	150
5.4.3.	Results of Scenarios A and B With and Without Maximum Power Limits of PEVs for PFC	152
5.4.4.	PEV's Power Reserve Release Moments After the Disturbance	153
5.5.	Brief Description And Discussion On Economic Evaluation of PEVs for PFC (Outside the Scope of This Technical Research)	155
5.5.1.	Introduction To Economic Value Of PFC In Power Systems	155
5.5.2.	Economic Evaluation of PFC Including PEVs	162
5.5.3.	UFLS Scheme For Previous Case Study And Simulation Scenarios	166
5.5.4.	Results	167
5.6.	Discussion	170
5.7.	Conclusions and Out-Look	170
6.	Conclusions and Future Work	172
6.1.	Conclusions	172
6.2.	Future Work	175
6.3.	List of Thesis-Related Publications in Prestigious (JCR) Journals & International Conferences	176
A.	Review on Regulation- and Market-Oriented Aggregation Approaches	178
A.1.	Regulation-Oriented Approach	180
A.1.1.	Aggregation Provision Under the Regulatory Framework	180
A.2.	Market-Oriented Approach	181
A.2.1.	Aggregation Provision Under the Competitive Electricity Market Environment	181
B.	Models of Governor-Turbine	185
	Bibliography	186
	Curriculum Vitae	xxiii

List of Acronyms

AC	Alternating Current
AGC	Automatic Generation Control
BBC	Bidirectional Battery Charger
BEV	Battery Electric Vehicle
CAGR	Compound Annual Growth Rate
CC	Constant Current
CCGT	Combined Cycle Gas Turbine
CDF	Cumulative Distribution Function
CGU	Conventional Generating Unit
CHP	Combined Heat and Power
CI	Constant Impedance
CP	Constant Power
CV	Constant Voltage
DC	Direct Current
DER	Distributed Energy Resources
DFIG	Doubly-Fed Induction Generator
DNPC	Distribution Network Power Consumption
DSO	Distribution System Operator
DSO	Distribution System Operators
E-Mobility	Electric Mobility
ESP	Energy Service Provider
EU	European Union
FERC	Federal Energy Regulatory Commission
GHG	GreenHouse Gas
HV	High Voltage
ICE	Internal Combustion Engine
ICT	Information and Communication Technology
ISO	Independent System Operator
LF	Line Factor
LFC	Load Frequency Control
LFC	Load Frequency Control
LV	Low Voltage
MAC	Maximum Allowed Current
MV	Medium Voltage

NHTS	National Household Travel Survey
PCC	Point of Common Coupling
PEV	Plug-in Electric Vehicle
PFC	Primary Frequency Control
PHEV	Plug-in Hybrid Electric Vehicle
PLL	Phase-Locked-Loop
PSO	Power System Operator
PU	Per Unit
PV	Photo-Voltaic
PWM	Pulse Width Modulation
RES	Renewable Energy Sources
SA	Sensitivity Analysis
SCUC	Security Constrained Unit Commitment
SFC	Secondary Frequency Control
SOC	State Of Charge
TSO	Transmission System Operator
TSO	Transmission System Operator
UBC	Unidirectional Battery Charger
UCTE	Union for the Coordination of the Transmission of Electricity
UFLS	Under Frequency Load Shedding
V2G	Vehicle-to-Grid
V2G	Vehicle-to-Grid
VOLL	Value of Lost Load

Nomenclature

Indexes and Sets

- $h \in \mathcal{H}$ Hourly periods, running from 1 to H hours.
 $i \in \mathcal{I}$ Plug-in Electric Vehicles, running from 1 to I .
 $m \in \mathcal{M}$ Generating units, running from 1 to M .
 $n, j \in \mathcal{N}$ Buses and corresponding lines, running from 1 to N .

Parameters

- a_1 Corresponding coefficient of constant impedance loads.
 a_2 Corresponding coefficient of constant current loads.
 a_3 Corresponding coefficient of constant power loads.
 AV^{CGU} Average clearing price offered by CGUs for the PFC [€/MW/Week].
 $AV^{CGU+PEV}$ Average clearing price offered by CGUs together with PEVs for the PFC [€/MW/Week].
 C Number of grid-connected PEVs.
 C_{pev} Effective number of grid-connected PEVs considering distribution network characteristics.
 C_{PFC}^{COST} Total PFC costs [€].
 $C_{PFC,A}^{COST}$ Total availability costs of units for PFC [€].
 $C_{PFC,O}^{COST}$ Total opportunity costs of units for PFC [€].
 D_n Distance of bus n from the MV bus [km].
 D_{PFC} Total primary reserve demand in the PFC market [MW].
 D Equivalent damping [MW/Hz].
 E_m Kinetic energy stored in the rotating mass of conventional generating unit m [$\frac{Kg.m^2}{s^2}$].
 ENS Energy not served [MWh].
 F^{nom} Nominal frequency [Hz].

f^{min}	Minimum frequency threshold to activate the UFLS [Hz].
G	Gravity index for average distance of PEVs from MV bus [km].
H	Equivalent inertia constant [s].
I_d	d - axis steady-state current before PFC [A].
I_q	q - axis steady-state current before PFC [A].
I^{max}	Maximum current limit of the unit [A].
I^{min}	Minimum current limit of the unit [A].
I_z^{max}	Maximum allowed current of transformer [A].
ΔI_z^{max}	Maximum allowed current variation of PEV for PFC [A].
K^I	Participation factor of PEV in idle mode.
K^C	Participation factor of PEV in charging mode.
K_{av}	Average participation factor of all PEVs .
K_{av}^C	Average participation factor of PEVs in charging mode.
K_{av}^I	Average participation factor of PEVs in idle mode.
K_{pev}	Overall gain of aggregate model of PEVs for the PFC [p.u./Hz].
$K_{pev}^{Desired}$	Desired gain of PEVs for the PFC according to stability margins [p.u./Hz].
LF	Introduced line factors.
L_n^L	Inductance [H].
P^{max}	Maximum power limit of the unit [kW].
P^{min}	Minimum power limit of the unit [kW].
ΔP^{max}	Upward power limit of the unit [kW].
ΔP^{min}	Downward power limit of the unit [kW].
P_{av}^{max}	Average maximum power limit of the units [kW].
P_{av}^{min}	Average minimum power limit of the units [kW].
ΔP_{av}^{max}	Average upward power limit of the units [kW].
ΔP_{av}^{min}	Average downward power limit of the units [kW].
P_0	Rated power consumption of the load [kW].
P^B	Total active power consumption at each bus before PFC [kW].
PR^{DST}	Estimated number of disturbances for a given year.
PF_{PFC}	Penalty factor for the PFC [$\text{€}/Hz^2$].
Q^B	Total reactive power consumption at each bus before PFC [kVar].

R_n^L	Resistance [ohms].
R_{int}	Internal resistance of the battery [ohms].
R_{cgu}	Frequency droop coefficient of conventional units [Hz/p.u.].
R_{pev}	Frequency droop coefficient of PEVs [Hz/p.u.].
R_{fin}^{rlc}	Final expected replacement of PEV's reserve by CGU's reserve.
S_m	Installed capacity of conventional generating unit m [MVA].
S_L^B	Loads apparent power [kVA].
S_{base}	Total base power conversion for per unit [MVA].
SOC_0	Minimum SOC of a single PEV.
SOC_{av}	Average SOC of PEVs.
T_{conv}	Time constant of the converter [ms].
TG	Time constant of the governor [ms].
T_{int}	Intentional delay for the UFLS [s].
T_{PFC}^{full}	Time at which the PFC response must be fully deployed [s].
T_{PFC}^{rlc}	Time after which PEVs start to release some portion of their power reserve replacing it by conventional unit's reserve [s].
V_d	d - axis steady-state voltage before PFC [V].
$V_{d,av}$	Average d - axis steady-state voltage of all buses before PFC [V].
V_q	q - axis steady-state voltage before PFC [V].
V_0	Rated voltage of the load [V].
V_{dc}	DC link voltage [V].
$VOLL$	Value of lost load.
V_n	AC voltage [V].
Z_n	Impedance [ohms].
α^I	Share of PEVs in idle mode in the fleet.
α^C	Share of PEVs in charging mode in the fleet.
ϕ	Beta density distribution function.
σ	Standard deviation.
ρ_{pev}	Penetration rate of PEVs [%].

Variables

Δe_L	Variation of stored energy in line inductance during PFC [$\text{H}\cdot\text{A}^2$].
f	Frequency [Hz].
Δf	Frequency deviation [Hz].
i_d	d - axis current during PFC [A].
i_q	q - axis current during PFC [A].
Δi_d	d - axis current variation during PFC [A].
Δi_q	q - axis current variation during PFC [A].
Δp_{PFC}	Power variation of unit for the PFC service [kW].
Δp_{pev}	Power variation of PEV for the PFC [kW].
$p_{c,i}$	Charging power of PEV i [kW].
p_{av}	Average charging power of PEVs [kW].
Δp_R	Variation of power consumed in line resistance during PFC [kW].
p_R	Power consumed in line resistance during PFC [kW].
Δp_L	Variation of power consumed in line inductance during PFC [kW].
p_L	Power consumed in line inductance due to stored energy variation during PFC [kW].
Δp_z	Power variation in impedance Z [kW].
$\Delta p_{n,j}$	Power variation in bus n due to the PEV power variation in bus j [kW].
Δp_{DNPC}	Total power consumed in lines during PFC [kW].
Δp_{ag}	Aggregate power variation at MV [kW].
r^{rlc}	Percentage of PEV's reserve replaced by CGU's reserve over time during PFC.
v_d	d - axis voltage during PFC [V].
v_q	q - axis voltage during PFC [V].
Δv_d	d - axis voltage variation during PFC [V].
Δv_q	q - axis voltage variation during PFC [V].
v_{oc}	Open circuit voltage of the battery [V].

1. Introduction

Contents

1.1. Background	1
1.2. Challenges And Motivation	5
1.3. Doctoral Thesis Objectives	7
1.3.1. Main Objective	7
1.3.2. Specific Objectives	7
1.4. Thesis Outline and Document Structure	8

This chapter firstly addresses the background of this doctoral thesis where the provision of primary frequency control by plug-in electric vehicles is described. Then, the key technical challenges and original contributions of this thesis research are explored and accordingly the main and specific scientific objectives are defined and highlighted. Finally, the structure of this dissertation is described.

1.1. Background

Over the past decade, the growing energy demand worldwide, greenhouse gas (GHG) and other pollutant emissions, depletion of fossil fuels, and emerging other international environmental concerns have motivated many countries around the globe to propose renewable energy targets (Beck & Martinot, 2004). Among the world’s first initiatives for renewable energy development, in particular, the European Union (EU) has widely adopted a number of mandatory national targets and renewable energy directives (e.g., directives 2001/77/EC, 2003/30/EC, and 2009/28/EC) over the last couple of decades. As one of the most prominent examples, directive 2009/28/EC obliged all member states to achieve 20% and 10% shares of energy from renewable energy sources (RESs) in the community’s gross final consumption and the transport energy consumption by 2020, respectively (parliament & the council, 2009). More importantly, to successfully achieve not only the EU’s short term (2020 horizon) targets, but also the EU’s medium term (2030 horizon) and long term (2050 horizon) objectives, undoubtedly electric mobility (E-mobility) based on plug-in electric vehicles (PEVs)¹ plays a fundamental role in both the electricity and transport sectors.

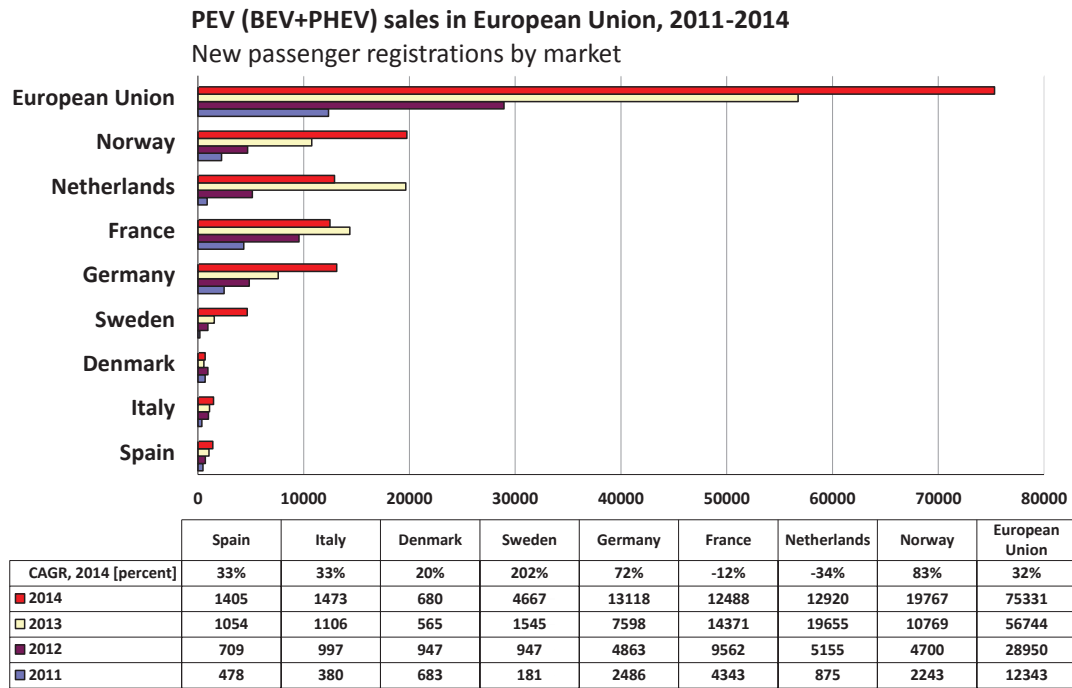


Figure 1.1.: New registrations of PEVs including both BEVs and PHEVs by market in the European Union from 2011 to 2014 (ACEA, 2014; Company, 2014).

Generally speaking, on the one hand, the transport sector in the EU that mainly relies on oil-based internal combustion engines (ICE) is notably responsible for roughly one-third of the EU's total carbon dioxide (CO₂) emissions. In this context, PEVs could remarkably help establish a safe, clean, and sustainable transport system, since they are very quiet, environmentally friendly, pollution free, and three-times more energy efficient compared to ICE vehicles. To increase the share of PEVs in the transport sector, the EU has just promoted the initial adoption phase of e-mobility at a relatively fast pace over the past few years. To defend this statement, for instance, PEV sales in Europe have notably increased at a compound annual growth rates (CAGRs) of 57.18% and 32% over the periods of 2011-2014 and 2013-2014, respectively, as shown in Figure 1.1. Most prominently, Norway topped the list of European countries by 19,767 new passenger registrations in 2014.

On the other hand, the electricity sector in the EU is currently undergoing a series of profound transformations following the widespread introduction of renewable energy support schemes (e.g., feed-in tariffs, market premiums, or green certificates). In fact, this support has greatly facilitated the integration of distributed energy resources (DERs) such as wind turbine generators, solar photovoltaic (PV), and

¹In this doctoral thesis, PEVs refer to both plug-in hybrid electric vehicles (PHEVs) and battery electric vehicles (BEVs), which have the capability of connecting to the electric power grid. In brief, while PHEVs possess both electric and conventional drives, BEVs are only propelled by the electric drive train.

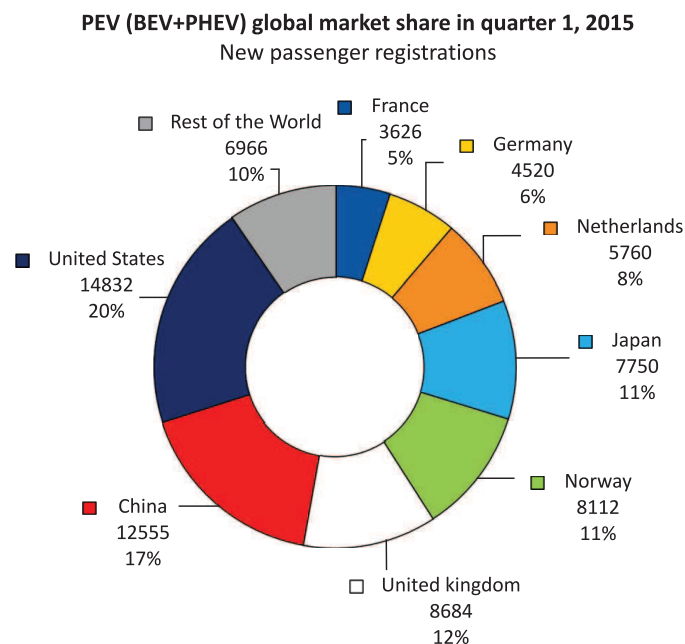


Figure 1.2.: Global market share of PEVs including BEVs and PHEVs based on the number of new registrations in the first quarter of 2015 (ACEA, 2015; Automotive, 2015; Office of Energy Efficiency & Renewable Energy, 2015).

specially PEVs into electric power systems. In particular, as mentioned above, currently PEVs are increasingly gaining importance in Europe where the electrification of the transport sector potentially and additionally plays a key role in enabling large-scale deployment of PEVs. For instance, in the first quarter of 2015, 8,112 PEVs were registered in Norway accounting for not only the largest market share of new PEV registrations in Europe, as shown in Figure 1.2, but also importantly for the first time a third of the country's total vehicle registrations (Automotive, 2015). On top of this, taking a look at the global market share of PEVs in the first quarter of 2015 in Figure 1.2, while the United States held the largest market share of 20% new PEV registrations (a moderate growth rate of 17.7% from 2014 to 2015), China accounted for the second-largest market share of 17% new PEV registrations (a moderate growth rate of 22.2% from 2014 to 2015). As a result on the power system side, in general the connection of a large number of PEVs in the future certainly creates new challenges and opportunities for power system operators in terms of the electricity grid planning, asset management, design, operation, and ancillary service procurement (Rebours et al., 2007a,b), where the latter term is the actual focus of this document.

Generally speaking, power system ancillary services from a technical point of view are *“those functions carried out by - generation, transmission, system-control, and distribution - system equipment and persons that support the fundamental services of generating capacity, electricity supply, and active power delivery”* (Hirst & Kirby,

1996). In addition, the federal energy regulatory commission (FERC) of the United States has defined ancillary services from an economic point of view as “*those electricity services required to support the transmission of electrical power from seller to purchaser provided the obligations of control areas and transmitting utilities within those control areas to achieve reliable operations of the interconnected transmission and distribution system*” (Hirst & Kirby, 1996). In principle, the most important electricity services, which have a vital role in ensuring power systems reliability, security, and stability, are listed as follows:

1. *Primary frequency control* (PFC): This essential service is automatically and locally activated to arrest the initial frequency drop right after a contingency event within a few seconds in a decentralized manner.
2. *Secondary frequency control* (SFC): SFC, which might be also called the load frequency control or automatic generation control of the interconnected power systems, is typically employed to automatically recover the system frequency to the rated value within a few minutes in a centralized manner².
3. *Black start capability*: It is the practice of restoring the bulk power system from a shut down to a steady-state condition.
4. *Reactive power and voltage control*: This control is the process by which the voltage quality in terms of sag, swell, flickers, and total harmonic distortion are always properly monitored and controlled employing resources such as distributed energy units.
5. *Islanding operation and emergency backup*: Technical speaking, the islanded condition can be defined as a portion of the electricity system that contains both load and distributed energy resources that could remain energized while it is isolated from the remainder of the utility system following the grid disconnection due to the scheduled maintenance or faults (Estebanez et al., 2011).
6. *Power loss minimization*: Both active and reactive power capabilities of distributed energy resources like PEVs can be employed to minimize power losses across the electrical distribution networks.
7. *Congestion management*: Congestion management is one of the most strategic functions of system operators to assure that the operating and functional limits of electrical distribution and transmission grids are not exceeded or violated during normal operating conditions.

This thesis research will mainly focus on the provision of the former, i.e., primary frequency control, by PEVs. Next, we address why PEVs are interesting options for the PFC and then the most important challenges of this work are described.

²SFC is also known as the load frequency control (LFC) or automatic generation control (AGC) of interconnected areas. In brief, following a severe contingency event, on the one hand, the SFC is employed to recover the system frequency to the rated value within a few minutes in a centralized way. On the other hand, the PFC is directly and locally implemented to arrest the initial frequency drop right after a contingency event within a few seconds in a decentralized manner.

1.2. Challenges And Motivation

The provision of PFC in electric power systems is a complex and challenging task. To briefly introduce the PFC, it is an essential ancillary service which maintains an instantaneous balance between the active power production and consumption under either normal operation (e.g., load power fluctuations or intermittent power production causing a continuous active power mismatch over the day) or emergency conditions (e.g., sudden outages of generating units). In the past, in principle the PFC has been satisfactorily provided only by conventional generating units such as thermal and hydro power plants (Kundur et al., 1994), however recent studies have reported that the overall desired PFC response has been gradually declining in the real-world power systems like the Eastern Interconnection of the United States (Ingleson & Allen, 2010). In fact, this has been taking place in present-day power systems due to a number of reasons such as large speed governor dead bands, blocked governor valves, and particularly the recent considerable increase in the penetration of electronically-interfaced DERs, which are not typically equipped with the PFC (Ela et al., 2014a,b). To cope up with such severe declines in the system PFC response, PEVs, which are able to be specially equipped with the PFC loop, together with the conventional generating units are potentially able to further participate in the PFC.

Over the past years, a great deal of literature has been dealing with the provision of ancillary services like PFC by PEVs (Almeida et al., 2015; Liu et al., 2013; Mu et al., 2013a; Pillai & Bak-Jensen, 2010b). In fact, technically speaking, PEVs are potentially able to provide all the above-mentioned ancillary services in general and the PFC in particular due to the following reasons:

1. As detailed above, PEVs could have a considerable impact on the performance of power systems, as they are expected to be connected to electric power systems in a large number in the near future,
2. PEVs are mostly connected to the electrical grid during the day or night, and consequently available to procure electricity services,
3. The battery of PEVs connected to the electrical networks has the capacity to absorb, store, and produce electrical energy when needed,
4. PEVs are connected to the low voltage (LV) electrical distribution networks, therefore they are located spatially close to a large portion of demand,
5. When connected, PEVs are able to charge /or discharge at any time of the day or night with almost negligible start-up and shut-down costs,
6. Last but not least, the PEVs battery charger is able to quickly monitor, control, and track the active and reactive power reference values, for instance within a few tens of milliseconds. In particular, this makes PEVs highly attractive future options for the provision of the PFC, for which the relatively quick active power response is essentially required.

In the scientific literature, the provision of PFC by PEVs together with conventional units has been extensively addressed over the past years. Despite the fact that the PFC analysis could be conveniently performed on the conventional generating units with a certain number of generators, it might be quite computationally complex and time consuming for a large number of PEVs ranging from thousands to millions. In previous research, the PFC analysis has been typically performed on either small-scale power systems including a limited number of PEVs (Pecas Lopes et al., 2009; Pillai & Bak-Jensen, 2010b) or large scale power systems including a large number of PEVs (Liu et al., 2013; Mu et al., 2013a) but using extremely over-simplified models with a relatively poor accuracy. In fact, these over-simplified models fall short in properly representing a large number of distributed PEVs with various operating characteristics at the LV distribution side, and consequently could not capture the fairly accurate dynamic behavior of the PEV fleet for PFC. On top of this, unlike conventional generating units interfaced with real-time data acquisition systems, the real-time operational data of PEVs for the PFC analysis are not currently available for system operators.

To effectively overcome the above-mentioned severe problems, PEVs connected to either small- or large-scale power systems are to be aggregated in an efficient and effective manner for the PFC analysis. Undoubtedly, aggregation of PEVs in electric power systems can be a feasible and useful approach, by using which power system's electrical engineers or power system operators (PSOs) are able to efficiently study the PFC in power systems. Therefore, the original contribution of this thesis research is to properly develop and carefully examine dynamic aggregate models of PEVs for the PFC study. To this end, the following relevant technical considerations on the large-scale aggregation of PEVs for PFC are highlighted and addressed as follows:

1. ***PEV fleet characteristics:*** Since PEVs with various technical features are connected /or disconnected to power system at any time of day or night, and furthermore in future PEV owners might be able to fully control the PEV charging power and charging time according to their preferences, the aggregate dynamic behaviour of the PEV fleet could be notably varied over the day. Thus, to properly aggregate the PEV fleets for PFC, several PEV fleet characteristics which could potentially and largely affect the PEV fleet performance during the PFC must be carefully identified and considered. For instance, the minimum desired state of charge (SOC) of the PEV owners, the maximum and minimum power limits of battery chargers, constant current (CC) and constant voltage (CV) charging modes of PEV are some important characteristics that must be further taken into account.
2. ***Distribution network considerations:*** Since PEVs are typically connected to the LV electrical distribution networks, several distribution network characteristics are to be carefully identified and considered particularly when the PFC analysis is performed. In the past, the PFC response of conventional generating units, e.g., hydro and fuel gas units, has been mainly analysed while they are connected to the high voltage (HV) transmission system us-

ing traditional frequency control schemes. While these schemes are able to properly represent the dynamic behaviour of conventional units at the HV transmission side, their implementation in PEVs at the LV distribution side could potentially result in a considerable error. In reality, when the charging power of PEVs deviates for the PFC provision, the distribution lines power flow can significantly change from downstream LV distribution system to upstream HV transmission system. Hence, the total distribution network power consumption (DNPC) can vary with respect to the PEVs power variation for PFC. In other words, the total PEVs power variation in the downstream LV distribution system is not equal to the total power variation, which is reflected in the upstream HV transmission system. Moreover, if PEVs participate in PFC by massively increasing their charging power, then this could cause the overload of the distribution lines and transformers, and consequently the fuse /or overcurrent relay protection is undesirably activated. Hence for example, the DNPC and the maximum allowed current (MAC) of the lines and transformers are two essential characteristics of distribution networks for PFC analysis that must be further taken into account.

3. ***Technical implementation and economic evaluation of aggregate models of PEVs for the PFC:*** To effectively evaluate the performance of PEVs for the primary frequency control from both technical and economic aspects, firstly a novel design strategy of PEV's frequency-droop controller for PFC is proposed, and secondly considering the designed PEV droop, the economic impact of relatively fast-controlled PEVs on the PFC costs is assessed in both islanded networks and large-scale power systems.

1.3. Doctoral Thesis Objectives

1.3.1. Main Objective

The main objective of this research work is to develop and validate aggregate models of PEVs for the PFC service that are able to satisfactorily represent the substantial dynamic behaviour of electric power systems including PEVs. Also, we describe a strategy to well design the frequency droop controller of PEVs considering the trade-off between the frequency stability and performance.

1.3.2. Specific Objectives

With respect to the above-stated main objective, several specific objectives are addressed and detailed as follows:

1. To carry out a comprehensive literature study using which the main drawbacks of previous models of PEVs for the PFC are carefully discovered and the critical

research gaps are identified. Furthermore, some aggregation techniques are introduced to later obtain a fairly accurate aggregate model of PEVs for the provision of PFC.

2. To incorporate the essential characteristics of each individual PEV such as minimum desired SOC of the PEV owner, maximum and minimum power limits of battery chargers, constant current and constant voltage charging modes of PEVs, into the aggregate model of PEVs using arithmetic average technique.
3. To incorporate the distribution network characteristics, e.g., power consumed in the network and maximum allowed current of lines and transformers, into the model of PEVs for the PFC.
4. To analyse and evaluate the technical implementation and economic evaluation of the previously-developed aggregate models of PEVs for PFC.

1.4. Thesis Outline and Document Structure

In summary, this section presents the thesis outline and the structure of this document, as shown in Figure 1.3. The major outcomes of this thesis have been three JCR peer reviewed articles and four international conference papers. This thesis, which is fundamentally a full-classic thesis, comprises six chapters (including this chapter) as follows:

Chapter 2: This chapter addresses and highlights in detail a background review of the PEV aggregation in power systems for the PFC. To this end, in regard to the background review on the PFC, first the generic models of PEVs for PFC are reviewed mainly from the literature, where also an introduction is given on various battery models and battery charger topologies. Later on, several aggregation methods are discussed and compared and the main research gaps will be identified.

Chapter 3: This chapter presents an aggregate model of PEVs for the PFC. To obtain this, first, the model of a single PEV for the PFC is developed and obtained according to the battery and battery charger models reviewed in chapter 2. Afterwards, the model of a single PEV is generalized into the model of whole PEV fleet. To this end, according to the aggregation methodologies addressed in chapter 2, the arithmetic averaging technique is selected and employed to represent the whole PEV fleets. In spite of this, distribution networks to which PEVs are mostly to be connected are not yet addressed and considered in this chapter. Next, we will include and discuss in detail in the following chapter.

Chapter 4: This chapter provides an enhanced aggregate model of PEVs for the PFC where the distribution network characteristics are further included. To

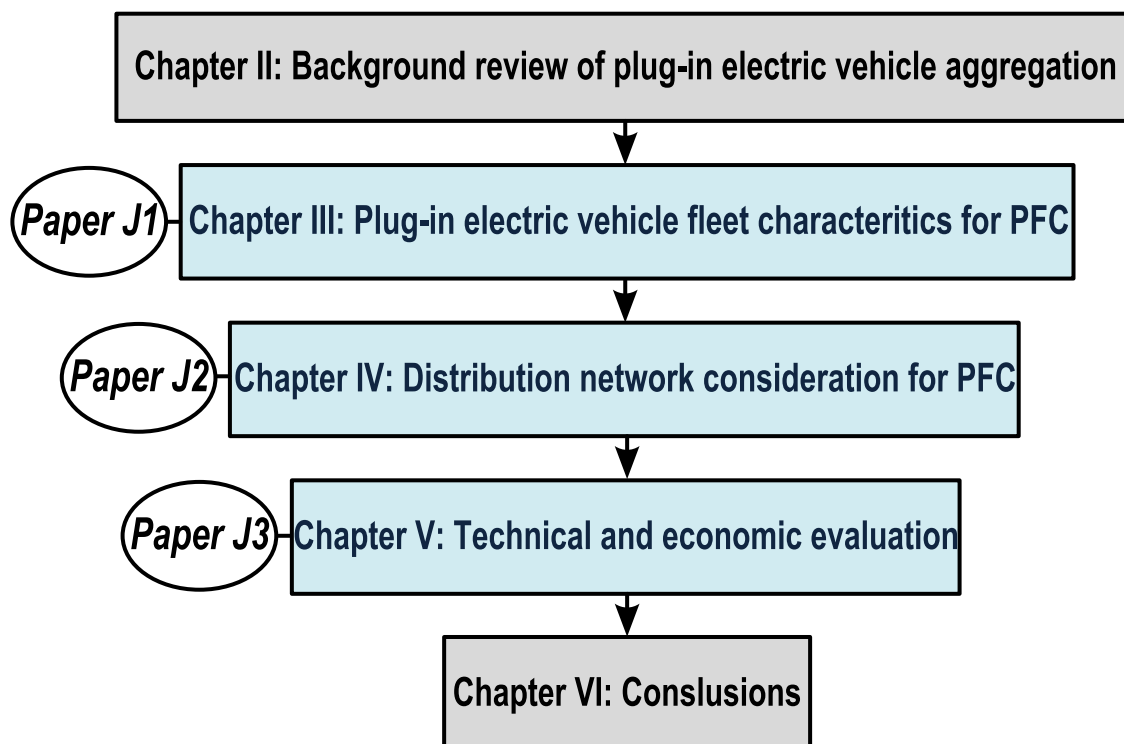


Figure 1.3.: Dissertation structure and outline of the full-classic thesis.

incorporate characteristics of the distribution networks into the previously-presented aggregate model of PEVs, first, the system dynamic behaviour is formulated. In short, two essential characteristics of distribution networks for the PFC provision through PEVs are selected and identified: 1) power consumed in the distribution network, and 2) maximum current limit of the distribution transformers and lines. Finally, the simulation results are briefly presented, and a short discussion is given.

Chapter 5: This chapter provides the technical implementation and economic evaluation for aggregate models of PEVs for PFC. To this end, first a strategy is described to well design the frequency droop controller of PEVs for the PFC. Also, the economic aspects of the provision of PEVs by the PFC will be briefly addressed and evaluated.

Chapter 6: Finally, the conclusions are drawn and guidelines for future studies are given.

2. Background Review of Primary Frequency Control by Plug-in Electric Vehicles in Electric Power Systems

Contents

2.1. Introduction	11
2.2. PEVs Key Components and Modelling from the Grid Point of View	11
2.2.1. PEVs Components	11
2.2.2. PEV Modelling from the Grid Point of View	15
2.3. Provision of Ancillary Services by PEVs	18
2.3.1. Overview of Ancillary Services Provision by PEVs	18
2.3.2. Provision of PFC by PEVs	23
2.4. Aggregation of PEVs in Electric Power Systems	24
2.4.1. Review of DER Aggregation in Electric Power Systems	25
2.4.2. PEV Aggregation in Electric Power Systems	28
2.5. Conclusions On the State-of-the-art	29

In the previous chapter, the main and specific objectives of this thesis research were presented in detail. According to these objectives, the global structure and chapter content of this doctoral thesis was outlined and described. It was emphasized that in the first step, a comprehensive survey of the state-of-the-art is to be provided, and then the key research gaps and research questions are to be identified. To this end, this section first introduces the key components of PEVs and then describes the PEV modelling from the grid point of view. Then, various ancillary services, which could be potentially provided by PEVs are addressed. Finally, the aggregation of distributed energy resources like PEVs for PFC in electric power systems will be reviewed and the main research gaps will be identified and classified.

2.1. Introduction

This chapter presents the relevant research background of this thesis on the provision of primary frequency control by PEVs. To this end, first PEV's key components are introduced and later on the PEV modelling from the grid point of view is described. Then, an overview of a wide variety of power system ancillary services, which could be potentially provided by PEVs, is presented. Later on, we provide an overview of aggregation of various DER units including PEVs in power systems mainly with respect to a technical perspective. Finally, the most important conclusions on the state-of-the-art are drawn.

2.2. PEVs Key Components and Modelling from the Grid Point of View

In order to properly study the impact of PEVs on electric power systems, first it is of great importance to properly describe the PEV key components. Then, the PEV modelling from the grid point of view is presented.

2.2.1. PEVs Components

Technically speaking, a grid-connected electric vehicle consists of the following main components: 1) battery pack, and 2) battery charger system.

2.2.1.1. Battery Pack

The battery pack, which is the most costly component of PEVs, stores and supplies the required energy to propel the PEV. In the past, various battery technologies such as lead-acid, li-ion, and NaS have been thoroughly tested and developed for PEVs, and presently the li-ion technology seems to be the most viable and popular technology due to relatively high power and energy density, excellent cycle life, safety, and capacity. In order to properly examine the operating characteristics of the li-ion battery through simulations, certainly appropriate battery models are required. As a consequence, in the literature, there has been a great deal of research recently on the li-ion battery models (Chen & Rincon-Mora, 2006; Dees et al., 2002; Hentunen et al., 2011; Kroeze & Krein, 2008; Rakhmatov et al., 2003).

To shortly address li-ion battery models with respect to the literature, they can be generally categorized into electrochemical, mathematical, or electrical models depending on the degree of complexity (Chen & Rincon-Mora, 2006) as follows:

Electrochemical models: These models have been mainly introduced to optimize the physical design aspects of the battery, and are based on the chemical reactions inside the battery cells. Despite the fact that these models are the most accurate battery models, they are computationally intensive and time consuming due to the non-linear time-varying partial differential equations (Dees et al., 2002).

Mathematical models: These models have been developed based on the empirical data to predict battery system characteristics such as the battery runtime, efficiency, and capacity. However, these models cannot provide any I-V (i.e., current-voltage) battery information for the circuit simulations, and their accuracy to dynamically estimate the state of charge lies poorly between 5% up to 20% (Rakhmatov et al., 2003).

Electrical models: Electrical models which are the most suitable models for device simulation purposes, have been developed based on the electrical equivalent models using a combination of voltage sources, resistors, and capacitors (Chen & Rincon-Mora, 2006). The latter are more intuitive, useful, and easy to handle for electrical engineers, who typically use the commercial circuit simulators. Also, electrical models have been divided into three categories of the thevenin-based, impedance-based, and runtime-based models. Since for the impedance-based models, the fitting process of battery impedance is a very difficult or complex task, in the past a combination of thevenin-based and runtime-based models have been widely developed and used (Kroeze & Krein, 2008). Over the course of this section, a combination of thevenin-based and runtime-based models will be presented in detail (see Figure 2.1).

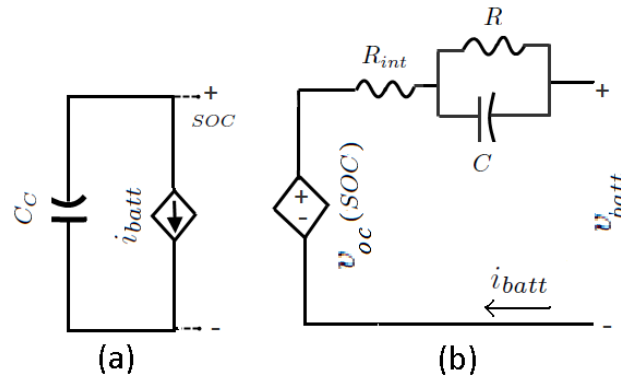


Figure 2.1.: Battery electrical-based model. (a) Run-time based model. (b) Thevenin-based model. C_c : battery capacity, i_{batt} : battery current, v_{oc} : open-circuit voltage of the battery, R_{int} : internal battery resistance, C & R : parasitic capacitance and resistance, v_{batt} : battery terminal voltage.

2.2.1.2. Battery Charger

PEV's battery charger, which is a high-power non-linear device, provides a well-controlled interface between the PEV battery pack and the electrical grid. In summary, the most important properties of battery chargers are addressed and classified with respect to the following aspects:

Independent or Integrated PEV Charging System: PEV's battery chargers can be classified into either independent or integrated PEV charging systems (Haghbin et al., 2011; Shi et al., 2008). While the independent charging system comprises a separate battery charger, integrated charging systems mainly use the PEV traction inverter and motor in order to charge the battery from the grid (Haghbin et al., 2011).

On-board or Off-board Charging System: On-board charging systems refer to the chargers internally implemented inside PEVs (Haghbin et al., 2010), whereas off-board charging systems mainly refer to those chargers, which are typically located in charging stations or parking areas. On the one hand, the former typically has a limited power rating due to space and weight restrictions, however is the preferred choice of PEV owners due to simplicity. On the other hand, the latter typically has a higher power rating that is mainly designed for commercial purposes.

Conductive or Inductive Charging System: Conductive charging is a method to transfer power by direct electrical contact using standard sockets and power cords, while inductive charging is a wireless charging technique for magnetic transfer of power. Conductive charging has inherent advantages in charging accessibility, ease of use, efficiency, and low costs, whereas induction charging provides better safety performance due to electrical insulation.

PEV Charging Levels: According to SAE J1772 standard, depending on the maximum power capacity of the charger, three charging levels for PEVs are recommended as follows (Kisacikoglu et al., 2010; Rosekeit & De Doncker, 2011): 1) charging level 1 represents the low level charging, e.g., single-phase alternating current (AC) charging, 2) charging level 2 is for the medium level charging, e.g. three-phase ac charging, and 3) charging level 3 is for the commercial fast charging, e.g., direct current (DC) charging. In the last few years, some commercially available PEVs have been equipped to receive DC charging (e.g., Nissan Leaf) using CHAdeMO stations (Yilmaz & Krein, 2013).

Battery Charger Topologies: Generally, battery charger topologies can be divided into two major groups as follows (Kisacikoglu et al., 2010; Singh et al., 2003, 2004): 1) Unidirectional battery charger topology: The unidirectional battery charger topologies, e.g., a thyristor-based rectifier or a diode-based rectifier with DC/DC converter, have the ability to only charge the battery pack, or in other words, they are not able to inject the power back into the AC grid. In Figure 2.2.(a) (Yilmaz & Krein, 2013), a unidirectional battery charger based on diode-based rectifier with DC/DC converter is shown. In brief, the AC voltage source provides a regulated voltage at its nominal value, and accordingly the diode bridge rectifier produces a DC voltage, which is smoothed by a filter capacitor. The DC/DC converter is then

responsible for performing the charging control at the battery side. 2) Bidirectional charger topology: The bidirectional battery charger topologies, e.g., thyristor-based rectifier with bidirectional DC/DC converter or AC/DC inverter, works in four quadrants providing Vehicle-to-Grid service. In Figure 2.2.(b) (Yilmaz & Krein, 2013), a bidirectional battery charger based on AC/DC inverter is shown where the DC link voltage and current are controlled using fast semiconductor switches such as GTO thyristors or IGBT. Despite that fact that most of the existing on-board battery chargers are unidirectional (Sun et al., 2014) for PEV technologies (e.g., Nissan Leaf, Mitsubishi i-MiEV, and Tesla Roadster), many charging configurations are able to support bidirectional power flow between the electric vehicle and grid (Yilmaz & Krein, 2013) (for instance, the capability of being connected to the bi-directional off-board battery chargers). To this end, currently, the major electric vehicle's manufacturers such as Tesla and Nissan are working toward bi-directional charger stations (e.g., Leaf-to-Home project of Nissan).

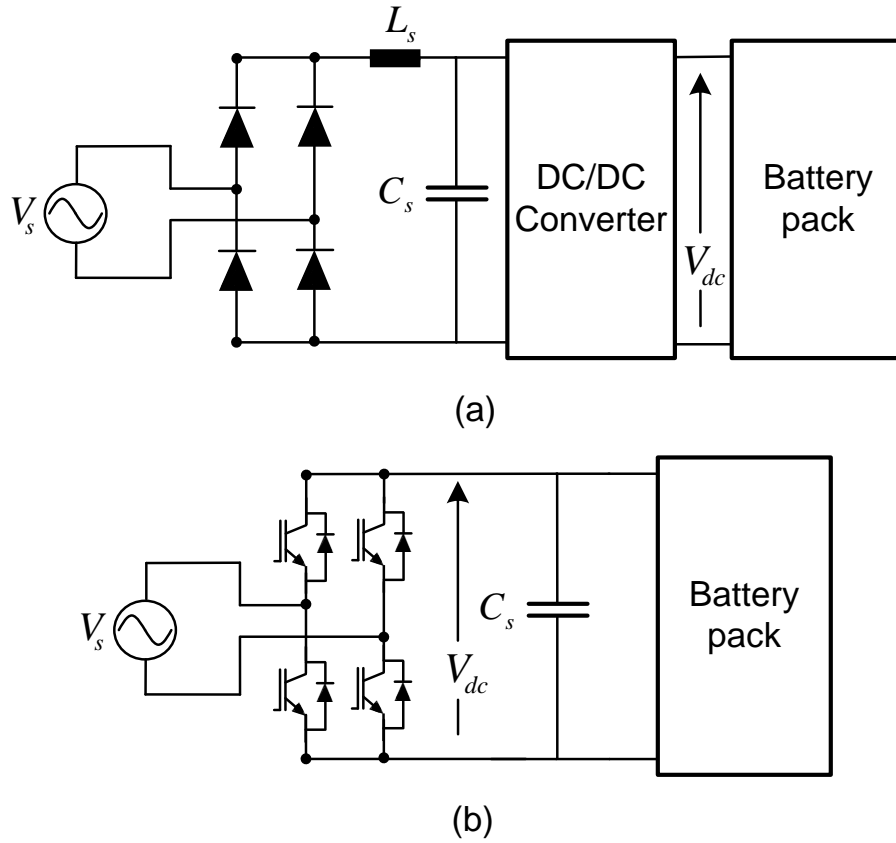


Figure 2.2.: Battery charger topologies. (a) unidirectional charger topology based on diode-based rectifier with DC/DC converter. (b) bidirectional charger topology based on AC/DC inverter.

A summary of battery charger topologies for the commercially available PEVs is

shown in Table 2.1.

Vehicle	Vehicle technology	On-board chargers	Off-board chargers
Nissan Leaf	PEV	Unidirectional	Unidirectional or Bidirectional
Mitsubishi i-MiEV	PEV	Unidirectional	Unidirectional or Bidirectional
Tesla Roadster	PEV	Unidirectional	Unidirectional or Bidirectional

Table 2.1.: Battery charger topology of commercially available PEVs.

2.2.2. PEV Modelling from the Grid Point of View

Here, we first briefly present the detailed model of a single PEV, and later on the appropriate PEV model for PFC is introduced and described.

2.2.2.1. Detailed PEV Modelling

The detailed model of a grid-connected electric vehicle can be represented by a battery and a battery charger. The electrical battery models is shown in Figure 2.1. Also, Figure 2.3 presents the detailed model of battery charger including AC/DC converter, measurement, calculations, and control system blocks.

Detailed battery model: Figure 2.1 shows a combination of thevenin-based and runtime-based models, which have been widely developed and used (Kroeze & Krein, 2008). On the one hand, runtime-based models intend to predict the battery state of charge over a longer period of time considering the electrical storage capacity Cc and the battery charging current i_{batt} , as shown in Figure 2.1.(a). On the other hand, the thevenin-based models are able to predict the battery transient response considering the battery internal resistor R_{int} and the parallel resistor R and capacitor C , as shown in Figure 2.1.(b). As seen, the battery open circuit voltage v_{oc} depends on the battery state of charge, which is obtained from the run-time based models. Accordingly, the battery terminal voltage v_{batt} can be calculated summing v_{oc} and voltage drop across R_{int} and the parallel R and C .

Detailed battery charger model: In Figure 2.3, the battery charger consists of the following components: 1) Measurements: The block is responsible for measuring the instantaneous current and voltage of PEV at the grid connection point. 2) Calculations: In order to instantaneously calculate the PEV's active and reactive power, the dq axis voltages and currents are to be obtained. To this end, the phase-locked-loop (PLL) is used to calculate the frequency and phase angles for the synchronization and transformations. 3) Battery charger control: In Figure 2.3,

the active and reactive power references of PEV are tracked and controlled using the PI outer-loop and current PI inner-loop controllers. Accordingly, the switching command signals are generated employing pulsed width modulation (PWM). 4) AC / DC converter equipped with semiconductor switches: Finally, the switching command signals are fed into semiconductor switches in order to charge/discharge the battery.

2.2.2.2. Simplified PEV Modelling for Primary Frequency Control

Since the main focus of this thesis research is on the short time scale electricity service (i.e., primary frequency control in order of seconds), the detailed PEV model described above can be significantly simplified, as shown in Figure 2.4:

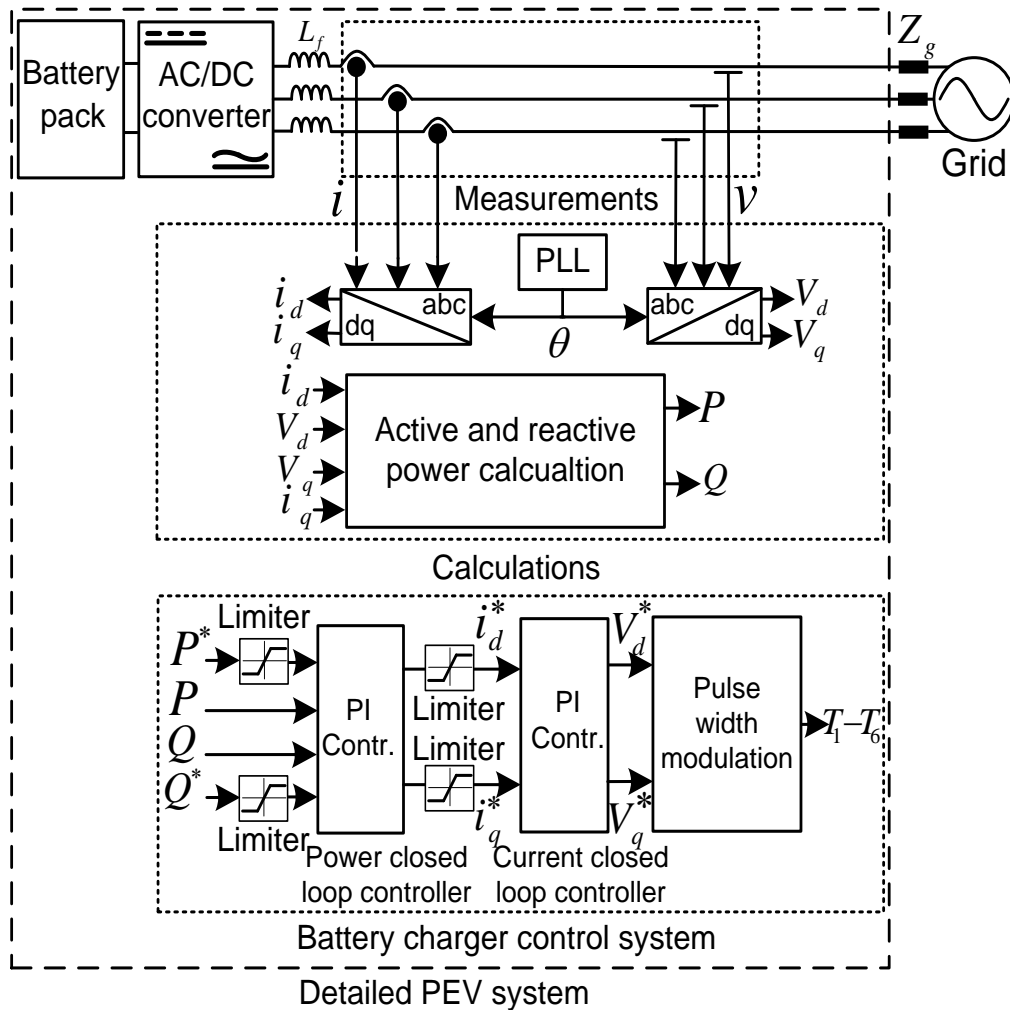


Figure 2.3.: Detailed model of PEV including battery pack, AC/DC converter, measurement, calculations, and control system blocks.

Battery model for the PFC: For the primary frequency control analysis, the battery can be generally neglected (Pecas Lopes et al., 2011, 2009; Pillai & Bak-Jensen, 2010b) or simply considered as a constant DC voltage source (Aghamohammadi & Abdolahinia, 2014). In other words, the battery is not modelled as a combination of thevenin-based and runtime-based models. On the one hand, regarding the runtime based models, since PEVs typically need to be charged for several hours, the impact of these services on the battery state of charge over a short period of time is certainly very negligible (Almeida et al., 2011). Accordingly, it is assumed that the battery state of charge remains constant during the provision of the PFC, and therefore, if needed, the SOC will be only considered as an input. On the other hand, in regard to the thevenin-based models, they are typically capable of representing the battery's fast transient response (e.g., a few hundreds of milliseconds), which is very low compared to the time horizon of this research. It is worth underlying that the fast switching IGBT using PWM algorithm is able to quickly compensate the transient DC voltage variations, and consequently the desired AC voltage can be almost simultaneously applied by the charger.

Battery charger model for the PFC: As the response time of the power control loop of the battery charger has a very low value (e.g., a few tens of milliseconds), the detailed descriptions of the battery charger such as the pulse width modulation scheme, semi-conductor switches, filter, inductors, and capacitors can be neglected. As a result, the battery charger can be simply represented by the following parts, as shown in Figure 2.4: 1) first-order transfer function with a very small time constant T_{conv} (e.g., 40-100 ms), 2) maximum power capacity limit of the charger depending on PEV charging level ΔP^{max} , and 3) minimum power capacity limit ΔP^{min} equal to either minus maximum power capacity (i.e., for bidirectional battery charger topology) or zero (i.e., for unidirectional battery charger topology) depending on the charger topology.

Note that in this thesis, the very fast rate of change of power of PEVs is not relevant to the PFC. Technically speaking, PEVs are able to quickly change their output current, thanks to their fast switching inverters. However, indeed such fast switching devices still have a limitation in term of rate of change of current that is typically within a few microseconds (see (IRF, 2009)). Despite this fact, as also acknowledged in (Morel et al., 2015), such very fast rate of change of current of switches are not considered for the frequency stability analysis, which has a relatively much slower dynamics (e.g., tens of milliseconds). In other words, during the frequency disturbance, the rate of change of power required for the PFC is typically very low compared to the limit in the rate of change of current of fast switching devices. Thus, the limit in the rate of change of power of PEVs is not typically considered for the PFC studies (see (Adrees & Milanovic, 2016; Meng et al., 2015; Mu et al., 2013a; Pecas Lopes et al., 2009; Pillai & Bak-Jensen, 2010b)).

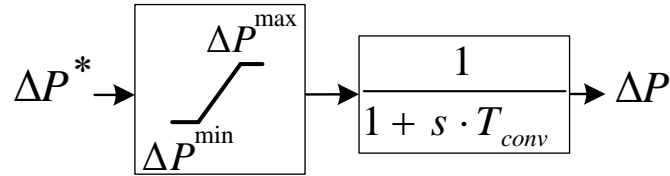


Figure 2.4.: PEV model for the PFC.

2.3. Provision of Ancillary Services by PEVs

The large-scale introduction of PEVs can bring new challenges and opportunities in the grid planning, operation, and ancillary services. As a promising new opportunity, PEVs could be potentially viable options for providing various power system ancillary services from very short to long time scales due to the following reasons: 1) for very short time scale services, PEVs have a high capability to quickly control their active and reactive power thanks to the fast-controlled electronically-switched battery chargers, and 2) for long time scale services, the battery pack of PEVs is typically able to store a large quantity of energy, which could be injected back into the grid when needed.

2.3.1. Overview of Ancillary Services Provision by PEVs

Figure 2.5 provides an overview of various electricity ancillary services (Hirst & Kirby, 1996) by PEVs with respect to the following time scales:

Very short time scale services (order of milliseconds): Within this time scale, PEVs are able to procure services such as transient stability, current /or voltage harmonic mitigation, transient pulsed load regulation, and load profile spikes smoothing. The transient stability stands for the capability of a power system to maintain synchronous operation following a severe disturbance, e.g., the outage of large generating units or load. Thanks to the fast-controlled battery charger, PEVs have a great potential to improve the the dynamic and transient stability of power systems following sever network faults. Note that here harmonics are generally defined as the continuous integral multiples of the fundamental waveform that could produce negative effects on the neighbour system components. When needed, PEVs could reduce voltage or current harmonic distortions, which are typically caused by non-linear devices in the network. Also, PEVs are able to supply transient pulsed loads and mitigate the spurious spikes of the load profile.

Short time scale services (order of seconds): Within a few seconds, as shown in Figure 2.5, PEVs are able to provide various services such as primary frequency control, emulated inertia (Almeida et al., 2015), and seamless islanding transition. In particular, primary frequency control is defined as the service, which is automatically and locally activated to arrest the initial frequency drop right after a contingency event within a few seconds in a decentralized way. As shown in the green block of Figure 2.5, this thesis research mainly sheds light on the provision of PFC by PEVs in power systems that will be presented and reviewed in detail in the next subsection. Besides, here the system inertia refers to the rate of change of the generator's kinetic energy according to the time. In other words, it can be interpreted as the ability of power system to suppress frequency deviations following either small or large mismatch between the total generating power and load consumption. In practice, when the main grid is disconnected due to either upstream scheduled maintenance or faults, the islanded distribution area could remain operational and stable by ensuring a seamless transition from grid-connected to islanded mode (Kwon et al., 2012).

Medium time scale services (order of minutes): In Figure 2.5, within several minutes, various services such as secondary frequency control, local voltage management, wind farms and solar units power swing mitigation, and black start could be provided by PEVs. Secondary frequency control is employed to automatically recover the system frequency to the rated value within a few minutes in a centralized way following a contingency event (Galus et al., 2011). The local voltage management is defined as the process by which the voltage quality in terms of sag and swells across the distribution network are always properly monitored and controlled employing local resources such as PEVs or other types of DER units. The black start refers to the process of restoring the bulk power system from a shut down to a steady state condition.

Long time scale service (order of hours): In Figure 2.5, over long time periods PEVs could provide a wide variety of services such as tertiary frequency control, peak load shaving, peak load shifting and energy arbitrage, islanded operation and emergency back up, power losses minimization, and congestion management. The tertiary frequency control is manually activated to replace the secondary control reserves over periods ranging from minutes to hours (Serban & Marinescu, 2012, 2014). The energy arbitrage is defined here as purchasing and storing energy ("charging") when energy prices are low, then selling energy ("discharging") when energy prices are high. Generally speaking, the islanded condition is defined *as a portion of the utility system that contains both load and distribution resources that remains energized while it is isolated from the remainder of the utility system* following the grid disconnection due to the scheduled maintenance or faults (Estebanez et al., 2011). Finally, the congestion management is one of the strategic functions of system op-

erators to always ensure that the operating limits of distribution and transmission systems are not exceeded and violated.

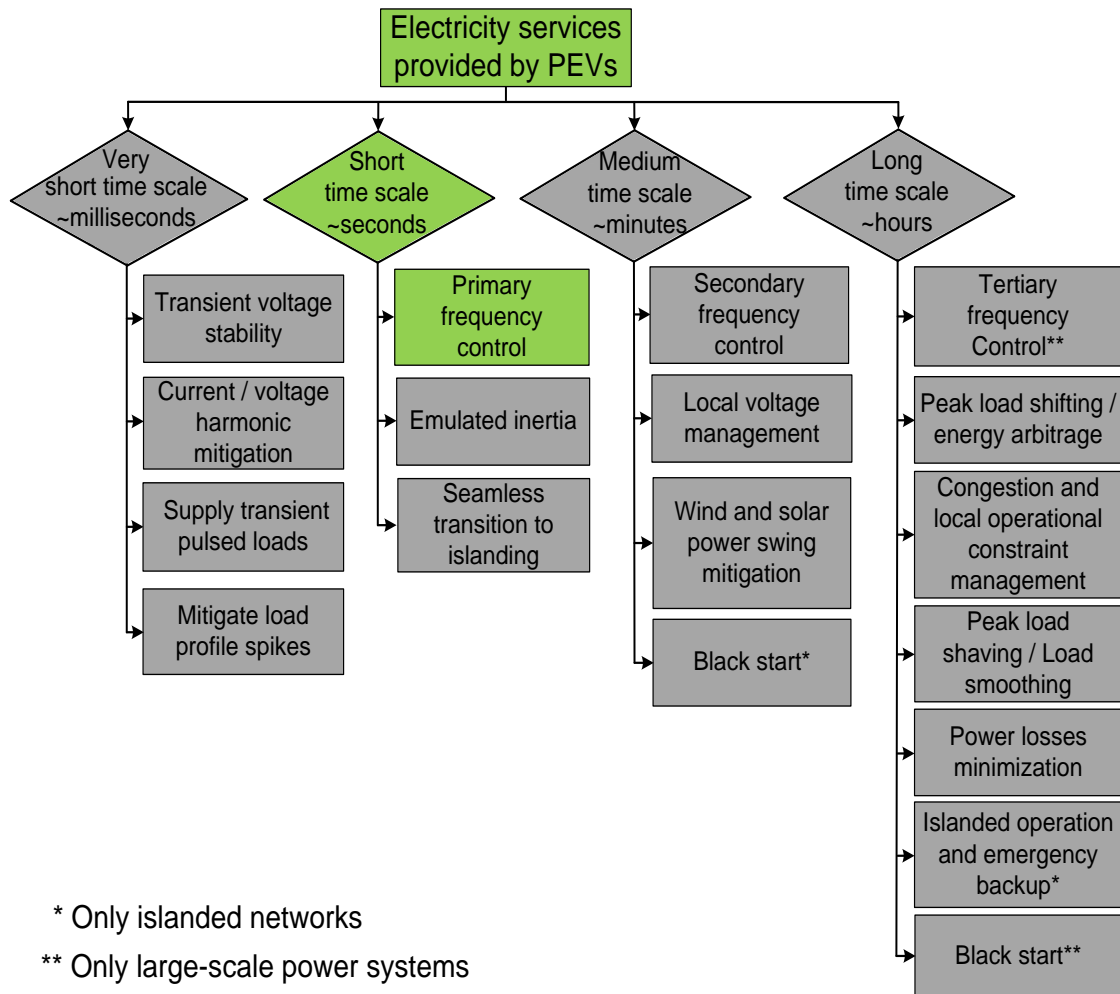


Figure 2.5.: Overview of electricity ancillary services by PEVs (the green blocks are mainly addressed and evaluated in this thesis research).

Most of the above mentioned electricity services are common between large-scale power systems and islanded networks. However, while tertiary frequency control is mainly concerned with the large-scale power systems, the islanded operation and emergency back-up are provided when the main grid is not available in the islanded networks. Besides, whereas the black start might take several minutes in the islanded networks (i.e., considered as a medium time scale service), it could take up to several hours in large-scale power systems in order to start up thermal units (i.e., considered as a long time scale service). In particular, with respect to the PFC and SFC services, islanded networks are typically required to provide a greater amount

of operating reserve compared to the large-scale power systems to cope up with unexpected contingency events. This is because a low number of generating units in islanded networks typically provide a large portion of load. As a result, the outage of one single generating unit in the islanded network could create a relatively large disturbance, for which faster and larger amount of reserves are typically needed.

Before we review the literature on the PFC by PEVs, we present the current grid code requirements on frequency control in Europe.

2.3.1.1. Continental Europe Frequency Regulation & Spanish Mainland System Rules

In electric power systems, ideally speaking, the instantaneous active power balance between the power produced by generating units and the electrical demand must be always maintained and satisfied under either normal operation or emergency conditions. Under normal operation, the power imbalance exists due to either intermittent renewable electricity generation or continuing load fluctuations, while under emergency conditions, it occurs due to sudden outages of generating units, transmission lines, or loads. When the instantaneous active power becomes unbalanced, the system frequency starts to deviate from the nominal value. To continuously mitigate the frequency variations, various frequency control schemes are developed and established in power systems based on three control levels corresponding to three time resolutions as follows (Rebours et al., 2007a,b): 1) primary frequency control, 2) secondary frequency control, and 3) tertiary frequency control.

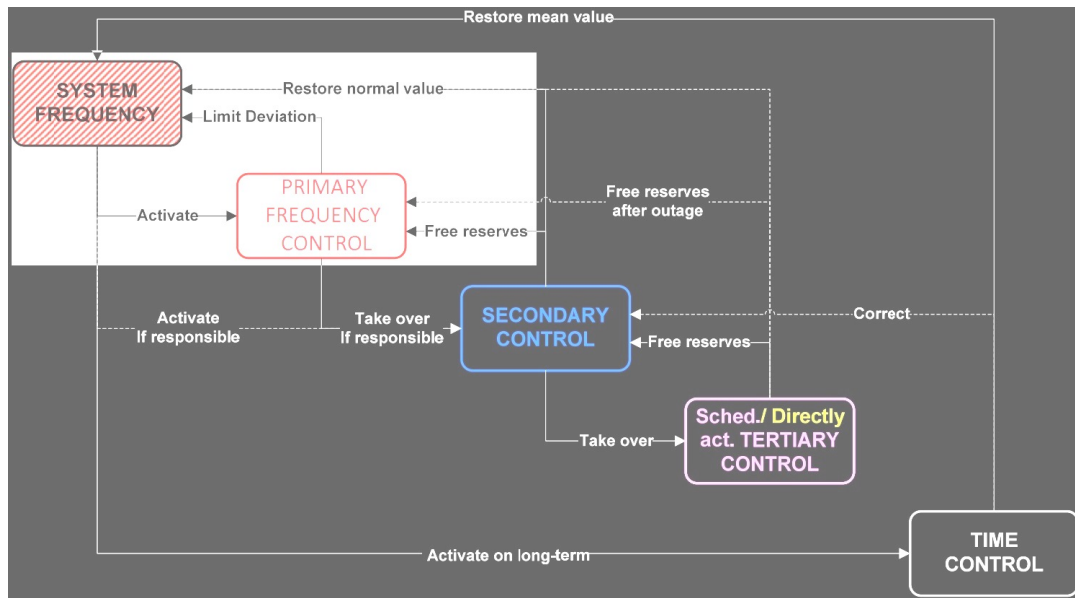


Figure 2.6.: Control scheme and required actions for the system frequency by UCTE (UCTE, 2009).

Figure 2.6 presents the control actions in different successive steps within Union for the Coordination of the Transmission of Electricity (UCTE)¹ (UCTE, 2009). In particular, as a joint action of all interconnected parties involved, PFC starts within a few seconds following a contingency event. In the European countries like Spain (REE, 2006)², the requirements of the PFC reserve have been established according to the UCTE as follows:

- **Standards for PFC reliability and targets:** The main goal of PFC is to maintain reliable system operation during the loss of generation or interruption of power exchanges in an interconnected area without the need for under frequency automatic load shedding or disconnection of generating units.
- **Deployment and duration of PFC:** The PFC shall be fully provided within 15 s following a disturbance of less than or equal to 1500 MW. If the disturbance is larger than 1500 MW, then 50% of the primary reserve shall be activated before 15 s and later, 100% of the primary reserve shall be achieved before 30 s in a linear way. The primary reserve shall be maintained for about 15 minutes (REE, 2006).
- **Activation and insensitivity of PFC:** Typically, the PFC is to be triggered when the frequency deviation exceeds 20 mHz. However, in Spain, the voluntary dead-band is not implemented (REE, 2006).
- **Resolution of frequency measurements:** For the PFC, the resolution of measurement shall be less than or equal to 10 mHz.
- **Droop range of generating units:** The droop coefficient of generators must be between 2 and 5%, where all generators shall be able to vary 1.5% of their nominal power for PFC.
- **Full PFC activation at permissible Quasi-Steady-State frequency deviation:** The maximum permissible quasi-steady state frequency deviation is 200 mHz, at which the PFC is to be fully activated following an incident.
- **Minimum/maximum allowed frequency:** The minimum instantaneous frequency is 49.20 Hz, which agrees with -800 mHz maximum allowed dynamic frequency deviation. Similarly, the maximum instantaneous frequency is 50.80 Hz, which agrees with +800 mHz maximum allowed dynamic frequency deviation.

¹In 2009, the UCTE was merged and integrated into ENTSO-E (European Network of Transmission System Operators for Electricity). The here-provided requirements from the UCTE handbook can be found in the ENTSO-E webpage as follows [last consultation date: Oct 2016]: https://www.entsoe.eu/fileadmin/user_upload/_library/publications/entsoe/Operation_Handbook/Policy_1_final.pdf

²More information on the operation procedure can be found in the REE webpage as follows [last consultation date: Oct 2016]:

http://www.ree.es/sites/default/files/01_ACTIVIDADES/Documentos/ProcedimientosOperacion/procedimientos_operacion_SEIE.pdf

2.3.2. Provision of PFC by PEVs

This thesis research is concerned with the provision of the PFC by PEVs in electric power systems, that has recently attracted a growing research attention. In (Baboli et al., 2010), the participation of PEVs in the PFC was evaluated in a microgrid, where it was shown that PEVs have significant impact on the PFC. In another research work, in the simplest control approach, PEVs were disconnected from the Great Britain power system following a large disturbance (Mu et al., 2013a). Also, the PEV charging power based on the statistical behavior of PEVs was initially estimated, and then according to the battery state of charge of PEVs, the aggregate primary reserve of PEVs for PFC was obtained. As in (Mu et al., 2013a) the PFC is not performed under fully controlled conditions, if a relatively large amount of PEV consumption is immediately disconnected compared to the size of the disturbance, this control approach might introduce undesired over frequency deviations (Mu et al., 2013a). In (Almeida et al., 2011; Liu et al., 2013; Pecas Lopes et al., 2011, 2009; Pillai & Bak-Jensen, 2010b), a more sophisticated approach, i.e., frequency-droop control, for PEVs was used to evaluate the PFC over either short or long time periods. Over short time periods (e.g., several seconds) following a large disturbance, in (Almeida et al., 2011), the provision of PFC by PEVs was assessed in an isolated network with large penetration of intermittent renewable power sources. It was concluded that the usage of PEVs to perform fast control actions using droop control was efficient. In (Pecas Lopes et al., 2009), the amount of wind power, which can be integrated in a large isolated electricity grid, was quantified when PEVs participate in the PFC. It was found that PEVs utilized with power electronic interfaces are capable of responding very fast to frequency deviations that have a great potential to notably improve the overall system dynamic performance in terms of the PFC. In (Pecas Lopes et al., 2011), it was verified that the frequency responses of either a microgrid or a large isolated system were dramatically improved when PEVs additionally participated in the PFC within several seconds. In (Pillai & Bak-Jensen, 2010b), the dynamic frequency response of an islanded Danish distribution network including a large amount of wind power was analyzed and evaluated, in which PEV could provide a faster and stable frequency control than the conventional generating units. In addition to the droop controller, a derivative controller emulating the virtual inertial response (Almeida et al., 2015) can be added to the PFC loop of PEVs. This resulted in an improvement of the frequency response of an islanded network including PEVs reacting very fast to the rate of change of frequency (Almeida et al., 2015).

Over a longer time periods (e.g., several hours), PEVs can continuously participate in PFC. However this might considerably affect the charging schedule of PEVs, and as a consequence, the energy content of PEV's battery varies. Therefore in (Liu et al., 2013), a decentralized method considering the charging demand power of PEV owners was proposed for PEVs to participate in the PFC, and furthermore, a smart charging method was developed to maintain the scheduled charging, while at the

same time providing the frequency regulation. In this control, the droop coefficient was adjusted according to the energy of the PEV's battery. It was demonstrated that PEVs could successfully suppress frequency fluctuations of two-area interconnected power grid while maintaining the charging demand imposed by PEV owners.

As illustrated, a large body of previous research has been dedicated to the distributed models of PEVs for the PFC that typically are computationally complex and time consuming. To tackle such severe problems, PEVs could be fairly represented in an aggregated manner. Thus, next we aim to review in detail the literature related to the aggregation of PEVs in power systems.

2.4. Aggregation of PEVs in Electric Power Systems

Over the past decade, electric power systems have undergone dramatic changes due to the introduction of information and communication technologies (ICTs), the implementation of electricity market reforms, and the integration of a large number of small-scale DER units. Particularly regarding the latter, small-scale DERs have been increasingly connecting to the electric power grids in the past few years, and if the growing trend is sustained in the future, a dramatic increase in the penetration level of DERs will be expected. On the one hand, if not properly controlled and integrated, the large scale introduction of DERs can potentially put at risk the overall stability, security, and performance of the present-day power systems. On the other hand, if properly controlled and integrated, small-scale DERs are able to provide not only a low-cost cleaner electrical energy, but also various technically and economically valuable services to the power grid. Hence undoubtedly, the aggregation of small-scale DERs can potentially bring various opportunities and challenges for system operators in various relevant dimensions such as regulatory, electricity market, and technical perspectives. To define the meaning of aggregation here, it is the process by which a large number of small-scale DERs are combined into a single aggregated DER, which is much easier to be handled and analysed. The resulting aggregate model of DERs could be used by various power system's participants such as transmission system operator (TSOs), distribution system operator (DSOs), or new profit-seeking agents, the so-called aggregators.

The aggregation of distributed energy resources units in general and PEVs in particular has been extensively addressed in the existing literature over the last years (Braun & Strauss, 2008; Galus et al., 2011; Momber et al., 2016; Moreno et al., 2013; Ulbig et al., 2010). To concisely address the literature, this section firstly provides a review of the DER aggregation in electric power systems and afterwards within the technical context, the aggregation of PEVs in electric power systems is reviewed.

2.4.1. Review of DER Aggregation in Electric Power Systems

In accordance with the state-of-the-art, the DER aggregation in electric power system can be classified into three major groups as follows:

1. *Regulation-oriented approach:* Within the regulatory framework, the aggregation of DERs could bring substantial benefits to various power system players such as TSOs, DSOs, retailers, final customers, or aggregators. In previous research, the value of aggregation has been addressed and analysed mainly from the system and private value perspectives. On the one hand, economically speaking, the aggregation of small-scale DERs provides a value to the system only if it improves the static and dynamic efficiency of the economic system (Nordhaus, 1969). On the other hand, the private value results from some regulatory pressures, institutional flaws and market imperfections. While the overall system value might mainly contribute to the fundamental (Armbrust et al., 2010; Littlechild & others, 2000; Markovic et al., 2013) and transitory values of aggregation (Codognet, 2004), the private sector value is represented by the opportunistic value of aggregation. On a universal level, the regulatory framework certainly affects not only the electricity market structure and performance, but also the technical characteristics and performance of power systems.
2. *Market-oriented approach:* In general, the aggregation of small-scale DERs via the aggregator helps these units effectively participate in several electricity markets such as the forward and futures markets, day-ahead market, intra-day market, and real-time balancing markets³ (Bessa et al., 2012; Momber et al., 2016; Pinson et al., 2014). Particularly in the latter, i.e., balancing markets, either dispatchable or non-dispatchable DERs via the aggregator are able to effectively provide various valuable ancillary services such as primary frequency control, secondary frequency control, peak shaving, and power management.
3. *Technically-oriented approach:* Technically speaking, as mentioned, small-scale DERs are able to provide electricity services over a wide range of time scales. In particular, electronically-interfaced small-scale DERs such as wind farms, PV units, and PEVs are able to quickly provide not only short time scale services (e.g., primary frequency control services) over several seconds, but also very short time scale services (e.g., the small-disturbance angle stability and transient stability services) during a few hundred milliseconds. Over medium or long time scales (e.g., from several minutes to hours), a variety of small-scale DERs are able to provide the secondary frequency control, peak shaving, and power management.

Note that the regulation-oriented and market-oriented approaches lie outside the scope of this thesis research (for further information, see Appendix A), and our

³In the power system literature, the real-time balancing market is also called regulation or adjustment market.

main focus here-in is only on the technically-oriented approach.

2.4.1.1. DER Aggregation According to Technically-Oriented Approach

Why aggregation of DERs is needed with respect to technically-oriented approach?

From a technical point of view, the large-scale introduction of DERs, which are typically distributed and connected to the LV distribution networks, can significantly impact on either steady-state or dynamic performance of power systems. To properly analyse this context, aggregate models of a large number of DERs are required due to the following reasons:

1) *Modelling complexity, large execution time and memory requirement:*

In order to analyse the impact of DERs on the system performance, naturally and plainly each individual DER can be separately modelled. Despite this fact, the resulting distributed models could be quite computationally complex and time consuming especially when the number of DERs is large. Moreover, the simulation's execution time and memory usage can be very large, when a large number of DERs are simulated. They can be considerably reduced using appropriate aggregate models of DERs (e.g., from 47 min 45 s to 7 min 40 s in our simulations in Matlab / Simulink (Izadkhast et al., 2016)).

2) *Lack of real-time operational data of DER units:* In present day distribution networks, in fact, the real-time operational data of DERs is not likely to be available either for DSOs and TSOs. As a consequence, the simulations can not be properly performed at each moment of the day, since the required input parameter values of the resulting distributed model for each individual DER are not procurable and not known accurately. As a remedy and alternative to this problem, the aggregate estimated values of the DER units according to their historical statistical data and temporal behaviour can be approximately calculated and used.

Aggregation of DERs for various ancillary services

Within such a technical context, various electricity ancillary services, which can be potentially simulated through TSOs, DSOs, or aggregators using aggregate models of DER units, are presented with respect to the following time scales (see Figure 2.5):

Very short time scale services: In particular, electronically-interfaced fast-controlled DER units like large-scale wind farms and induction machines are able to notably improve the overall system transient response at the point-of-interconnection.

In order to capture the aggregate dynamic response of a number of DERs, aggregate models of DER units have been extensively proposed and developed at both transmission and distribution system sides in the literature. At the high voltage transmission side, aggregate models of wind farms with either fixed (Akhmatov & Knudsen, 2002; Slootweg & Kling, 2003) or variable wind turbines (e.g., doubly-fed induction generator (DFIG) (Fernandez et al., 2008; Garcia et al., 2015) and full-scale converter with permanent magnet synchronous generator (Conroy & Watson, 2009; Mercado-Vargas et al., 2015)) have been proposed. Besides, the transient characteristics of the induction machines, which have been sporadically connected to the distribution system, have been used to calculate the parameters of the aggregate model induction machines (Louie et al., 2007; Nozari et al., 1987; Taleb et al., 1994).

Medium and long time scales services: In previous research, a variety of DER units have been widely introduced and developed in an aggregated manner to provide the SFC (Galus et al., 2011; Liu et al., 2015; Ota et al., 2010), peak shaving (Costanzo et al., 2011; Huang & Lu, 2009; Yang et al., 2014), and energy management services (Battistelli et al., 2012; Su & Wang, 2012; Zhang et al., 2014).

Short time scale services: In previous research, only distributed models of a variety of DER units such as wind farms (Morren et al., 2006; Ullah et al., 2008; Vidyanandan & Senroy, 2013) and PEVs (Almeida et al., 2011; Liu et al., 2013; Mu et al., 2013a) have been widely developed and used for the PFC. Note that in the past, the aggregation of wind farms for the PFC has not been principally considered as a relevant research topic due to the following reasons: 1) wind turbines within the farm are not distributed across the LV distribution networks and they are typically connected to the MV /or HV transmission lines in a centralized way, 2) wind turbines are permanently connected to a specific geographic location, e.g., the point of common coupling (PCC), 3) the number of wind turbines connected to the PCC is typically low and fixed, and 4) the real-time operational data of each individual wind turbine such as wind speed, active and reactive power production are closely monitored and known for the operator. On the other hand, the aggregation of PEVs for the PFC could be quite complex and challenging due to a number of specific reasons, which are addressed below.

Despite the fact that considerable research attention has been recently paid to the provision of short time scale services by DERs in a distributed manner, the existing literature clearly lacks to address aggregate models of DER units in particular PEVs for these services. Therefore, this thesis research aims to mainly tackle the aggregation problem of PEVs for the procurement of the PFC.

2.4.2. PEV Aggregation in Electric Power Systems

Over the past years, PEV aggregation in power systems has achieved increasing importance due to the aforementioned reasons. As a result, in the near future, it is very likely that profit-seeking agents, so-called PEV aggregators, serve as a commercial middleman between the electricity market, DSOs, TSOs, and PEV owners. Also, PEV aggregators are going to be the main provider and controller of vehicle-to-grid (V2G) ancillary services, e.g., primary frequency control and secondary frequency control. Nonetheless, the aggregation of PEVs could be quite complex and challenging task due to the following reasons: 1) the number of PEVs could be relatively very large ranging from tens of thousand to millions, and 2) PEVs are not permanently connected to a specific bus bar of the network, or in other words, they are characterized by a high degree of uncertainty due to their spatial and temporal variability.

There has been a great deal of research recently on the aggregation of PEVs for the medium and long time scales services (e.g., SFC (Galus et al., 2011; Liu et al., 2015; Pillai & Bak-Jensen, 2011)), whereas in general very little research attention has been given to aggregate models of PEVs for short time scale services such as the PFC. In fact as the number of electric vehicles plugged into the grid is expected to significantly increase, decentralized models of PEVs for the PFC could be quite computationally complex and time consuming to be executed and solved. Therefore, on the first attempt in this thesis research, aggregate models of PEVs for the PFC are proposed and developed with respect to the following aspects, as also shown in Table. 2.2: 1) PEV fleet characteristics such as the minimum desired SOC of the PEV owners, PEV fleet operating modes (i.e., disconnected, idle, and charging mods), constant current and constant voltage charging modes of PEV (see Chapter 3), 2) distribution network characteristics such as power consumed in distribution network and maximum current of distribution lines (see Chapter 4), and 3) design of PEV frequency-droop controller and in part economic evaluation of PFC by PEVs (see Chapter 5).

	Freq. droop cont.	Dist./Agg. mdl	SOC	Loctn. of PEVs	Dis. net. char.	PEV ft. opr. modes	CC /or CV	Freq. stab. marg.	Econ. eval. of PFC by PEVs
(Almeida et al., 2011)	✓	Dist.	×	×	×	×	×	×	×
(Pecas Lopes et al., 2011)	✓	Dist.	×	×	×	×	×	×	×
(Baboli et al., 2010)	✓	Dist.	×	×	×	×	×	×	×
(Pecas Lopes et al., 2009)	✓	Dist.	×	×	×	×	×	×	×
(Almeida et al., 2015)	✓	Dist.	×	×	×	×	×	×	×
(Pillai & Bak-Jensen, 2010b)	✓	Dist.	×	×	×	×	×	×	×
(Liu et al., 2013)	✓	Dist.	✓	×	×	×	×	×	×
(Mu et al., 2013a)	×	Agg.	✓	×	×	✓	✓	×	×
Chap. 3	✓	Agg.	✓	×	×	✓	✓	×	×
Chap. 4	✓	Agg.	✓	✓	✓	✓	✓	×	×
Chap. 5	✓	Agg.	✓	✓	✓	✓	✓	✓	Partially- ✓

Table 2.2.: Summary of the literature review on the provision of PFC by PEVs.

2.5. Conclusions On the State-of-the-art

To help identify the existing research gaps of the provision of PFC by PEVs, this chapter reviewed in detail the state-of-the-art. In the past, distributed models of PEVs for the PFC have been extensively used and developed despite the fact that they have major drawbacks (e.g., computationally intensive and time consuming). To solve such problems, a large number of PEVs could be represented in an aggregated manner.

Table. 2.2 presents a summary of the above presented literature review on the PFC by PEVs. In the past, some important aspects such as the location of PEVs, the characteristics of distribution networks, frequency stability margins, and economic evaluation of PFC by PEVs have not been adequately addressed that will be extensively studied in Chapters 3, 4, and 5 of this research thesis.

Therefore, to efficiently analyse the provision of PFC by PEVs in future, there will be an increasing need of PEV aggregate models. In this thesis, aggregate models of PEVs for the PFC are proposed and developed with respect to the following essential aspects:

- PEV fleet characteristics such as the minimum desired SOC of the PEV owners, drive train maximum and minimum power limitations, constant current and constant voltage charging modes of PEVs (see Chapter 3).
- Distribution network considerations such as the total power consumed in distribution network and the maximum allowed current of the lines and transformers (see Chapter 4).
- Design of PEV frequency-droop controller employing the stability margin analysis and in part economic evaluation of PFC by PEVs (see Chapter 5).

3. An Aggregate Model of PEVs for PFC

Contents

3.1. Introduction	32
3.2. PFC by PEVs Over Time	34
3.3. Decentralized Model of PEVs for the PFC	37
3.4. Proposed Model of a Single PEV for PFC	39
3.4.1. Previously Developed Model of a PEV for PFC	40
3.4.2. Proposed Model of a PEV for PFC	42
3.5. Proposed Aggregate Model of PEVs	47
3.5.1. Average PFC Loop of PEVs for PFC	47
3.5.2. Average Battery Charger Model	51
3.6. Case Study and Simulation Scenarios	56
3.6.1. Modeling Conventional Power Plants	57
3.6.2. Calculation of the Inertia H for the Worst Case	58
3.6.3. Aggregate Model of PEV Fleet	60
3.6.4. Simulation Scenarios	67
3.7. Simulation Results	68
3.7.1. Simulation Results of PEV's Participation in the PFC	68
3.7.2. Simulation Results of the Impact of PEV's Upward Power Reserve on the PFC	70
3.8. Conclusions and Out-Look	72

The key research gap identified in the previous chapter was the lack of aggregate models of plug-in electric vehicles to properly simulate and evaluate the behaviour of the fleet for the primary frequency control analysis. Therefore, here we develop an aggregate model of PEVs for the PFC, where first the model of a single PEV is proposed. Since in previous research, some essential characteristics of PEVs such as the vehicle's operating modes were neglected, therefore we further consider and incorporate them into the proposed model. This is carried out by introducing a participation factor for a PEV during the PFC. In the next step, an aggregate model

of PEVs for the PFC is proposed. To obtain this model, the average of the PEV's participation factors is calculated. Then, the aggregate model of PEVs for the PFC is evaluated for the Spanish power system case. Afterwards, dynamic simulations are performed in Matlab / Simulink and the simulation results are discussed. Finally, the main conclusions are drawn.

3.1. Introduction

In the previous chapter, first the PEV key components and the PEV modelling from the grid point of view were presented. In particular, the simplified model of a PEV for the PFC was shown in which the battery dynamics were neglected. Moreover, the battery charger was represented as a first-order transfer function with a small time constant (a few tens of milliseconds). Then, the existing literature on the PFC by PEVs was extensively reviewed and the main research gaps were identified and analysed. It was concluded that to reduce the computational complexity of decentralised models of PEVs, there is a clear need for aggregate models of PEVs for PFC studies.

In this chapter, in particular essential operating modes of the PEV fleet for the PFC are addressed and modelled in detail. To address this research question, here we first provide a comprehensive state of the art review on the provision of PFC by PEVs as follows.

The PFC is a crucial ancillary service, which aims to instantaneously maintain the active power balance between the total power production and consumption in power systems. In the past, the PFC has been mainly provided by conventional generating units (CGUs), however in the near future, it is envisioned that distributed energy resources like PEVs additionally participate in the PFC. PEVs seem effective options for the fast PFC service due to the following reasons:

1. PEVs are able to quickly control their active power within a few tens of milliseconds using IGBT-based battery chargers,
2. Since the number of grid-connected vehicles could be large in future, they could potentially provide a great amount of power reserve for the PFC. Also, though PEVs are primarily used for transportation purposes, according to the National Household Travel Survey (NHTS) (NHTS, 2009), PEVs are typically connected to the grid over 90% of the time. Therefore, they are available for the PFC a large portion of the day.

In previous research, the provision of PFC by PEVs has been extensively reported and analysed utilizing decentralized models of PEVs for the PFC (Almeida et al., 2011; Baboli et al., 2010; Liu et al., 2013; Pecas Lopes et al., 2011; Pillai & Bak-Jensen, 2010a). Within these models, various characteristics of PEV fleets such as the type of frequency controller (Baboli et al., 2010; Liu et al., 2013; Pillai & Bak-

Jensen, 2010a), the penetration rate of PEVs, and the type of the battery charger topology (Mu et al., 2013a) have been considered for the PFC.

In regard to the type of the PEV's frequency controller, using the simplest control approach, PEVs were assumed to be immediately disconnected from the Great Britain's power system following a large disturbance in the target year 2020, and consequently the frequency response was notably improved (Mu et al., 2013a). Alternatively, a simple frequency-droop curve was employed in PEVs to make them able to provide the PFC within several seconds (Almeida et al., 2011; Baboli et al., 2010; Pecas Lopes et al., 2009). The same control loop was implemented in PEVs to improve the minimum transient frequency (Liu et al., 2013). Additionally, a derivative controller was added to the active power control loop of PEVs, through which the virtual inertial response was emulated in an islanded network (Almeida et al., 2015; Pillai & Bak-Jensen, 2010b).

For a wide range of PEV's penetration levels, the provision of PFC by PEVs has been studied in (Mu et al., 2013a). It was shown that if all PEVs are disconnected from the electric grid following the disturbance, then the frequency response might greatly deteriorate¹. Therefore, in future only a portion of PEVs might be allowed to fully participate in the PFC. Alternatively, using an appropriate regulation scheme, all PEVs might be able to participate in the PFC in a controlled or coordinated manner. Moreover, the impact of the battery charger topologies (i.e., unidirectional or bidirectional battery chargers) on the frequency support from PEVs was analyzed in (Mu et al., 2013a). As already expected, PEVs equipped with bidirectional battery chargers (BBCs) had a better performance compared to the ones with unidirectional battery chargers (UBCs).

Although the above-mentioned characteristics of PEV fleets have been addressed in the past, nonetheless, some essential characteristics of PEVs (e.g., operating modes of PEVs) have not been comprehensively analyzed yet. Also, since the decentralized models of PEVs are computationally intensive and time consuming, aggregate models of PEVs for the PFC should be introduced and developed. First of all, the operational data of each PEV will not be likely available to either system operators or PEV owners in the future. Therefore, in principle it will not be very likely to be able to completely create the decentralized model of PEVs due to the lack of data. If the data would be even available, it is a very complex and challenging task to individually model each PEV for the PFC, as the number of PEVs can be very large.

In summary, this chapter mainly provides the following original research contributions:

1. To facilitate the incorporation of some essential PEV fleet characteristics into the PEV's model for the PFC, a participation factor is introduced. In fact,

¹Note that in this thesis, the frequency response refers to the response of typical closed-loop frequency control of the power systems including distributed PEVs after disturbance, as shown in Figure. 3.1.

the participation factor represents the availability level of each PEV for the PFC considering the following essential PEV's characteristics:

- 1.1. PEV's operating modes (i.e., disconnected, idle, or charging)
- 1.2. If in the charging mode, the constant voltage (CV) or constant current (CC) charging modes.
2. The available power reserve of PEVs for the PFC depends on their battery charger topology. The impact of PEVs equipped with unidirectional battery chargers on the frequency response will be compared to the one of PEVs equipped with the bidirectional battery chargers.
3. On the first attempt, to reduce the computational complexity of the decentralized models of PEVs, an aggregate model of a large number of PEVs for the PFC is proposed and formulated using the arithmetic averaging technique. Note that the probability density functions of state of charge of PEVs are taken into account to obtain the average parameter values of the PEV fleet.

This chapter comprises of the following seven Sections:

- Section 3.2 generally describes the provision of primary frequency control by PEVs in electric power systems.
- Section 3.3 provides the frequency control scheme of power systems, in which PEVs are decentrally participating in the PFC.
- Section 3.4 presents an aggregate model of PEVs for PFC. To this end, first the model of a single PEV for the PFC is proposed and developed introducing the participation factor. Then, the aggregate model of PEVs for the PFC is obtained based on the probability distribution functions of PEV's state of charge using the averaging arithmetic technique.
- Section 3.5 characterizes the power system under study for the frequency analysis, and then, provides the numerical calculation of the aggregate model of PEVs. In particular, a case study of the Spanish power system is created and analyzed for the worst scenario. Moreover, simulation scenarios are defined in this section.
- Section 3.6 presents the results of the previously defined scenarios, where the impact of PEVs on the PFC response is evaluated and discussed.
- Finally, Section 3.7 concludes this chapter and the outlook of the next chapter is presented.

3.2. PFC by PEVs Over Time

Technically speaking, PEVs, which are able to be specially equipped with the PFC loop, (Almeida et al., 2011; Liu et al., 2013) together with the CGUs are potentially

able to further participate in the PFC. To this end, the frequency at the connection point of PEVs could be measured and then provided to the PFC loop of PEVs in a decentralize manner. In such power systems, the dynamic response of power systems at each moment of the day is represented not only by the type of conventional generating units, but also by the behavior of PEV fleet. In other words, the overall dynamic response of power systems including PEVs over the day is a function of both conventional generating units and PEV fleets as follows. Note that since the PFC response typically lasts a few seconds, the slow response of the power system including PEVs for the secondary and tertiary frequency control can be neglected. In other words, we only evaluate the quick dynamic behavior of the network for the PFC at a specific moment of the year at which the disturbance occurs, while neglecting the secondary and tertiary frequency control loops.

Regarding the type of conventional generating units, it might highly depend on the load consumption level. If the load level has a low value, then a large portion of the load is typically supplied by either base-load units or renewable energy sources. The base-load units like thermal power plants² have a relatively slow response, and moreover renewable energy sources do not currently provide the PFC. As a result, it is expected that the overall dynamic response of the power system would be very poor, when the load consumption is low. Hence, the worst case can be characterized by the low load, at which the frequency disturbance could lead to high frequency deviations. In order to identify the worst case for a future target year, the minimum expected load during the year could be considered, and then the PFC analysis is performed for that specific moment of the day. In a similar way, the worst case for a specific day can be characterized by the specific moment at which the minimum load occurs.

Regarding the PEV fleet, undoubtedly the dynamic response of the fleet could largely vary over a day depending on the behavior of PEV owners. Therefore in this analysis, inevitably we will have to take into account the probability density functions of various PEV fleet parameters. First, PEV owners have an uncertain and unpredictable behavior with high spatial and temporal variability. Second, the behavior of PEV owners highly varies from one to another. Therefore, the fleet's relevant parameters for the PFC study from the grid point of view highly change over time (from one instant of time to another). The parameters of the fleet, which largely vary from the electrical grid point view over a day, are introduced as follows:

- *Battery state of charge:* When PEVs are connected to the electrical grid, they are either in the idle or charging mode for which the battery state of charge is constant or increasing, respectively. In the idle mode, it is assumed that the PEV charging process is completed or temporarily stopped due to smart charging management strategies. Therefore, the PEV could remain connected

²Since in this analysis the Spanish power system will be evaluated, base-load units can be mainly represented by thermal units, which have a relatively slow response. Nonetheless, this might not always hold true for instance when the power system is largely penetrated with hydro units.

to the grid in the idle mode while the charging power remains always equal to zero. In the charging mode, the PEV's battery state of charge gradually increases, the rate of which depends on the constant current or constant voltage mode. During the constant current charging, the battery is charged at the nominal charger's current and consequently the battery state of charge moderately increases from the initial state of charge. However, during the constant voltage charging, the battery state of charge has a high value (close to full charging), and therefore the battery state of charge slowly increments until the battery is fully charged. Besides, the initial state of charge of PEVs, when they are just connected to the grid, depends on the driving pattern of PEV owners. In conclusion, the state of charge of PEVs largely varies during the day depending on many factors like the charging or idle mode.

- *Number of grid-connected PEVs:* Undoubtedly, the number of grid-connected PEVs could greatly vary during the day depending on the driving habits of PEV owners. A PEV might be connected at various locations (e.g., home or work) during the day, and this way they could be connected to the grid a large portion of the day (e.g., 90% of the day according to NHTS (NHTS, 2009)). For the PFC analysis, obviously the disconnected PEVs are not able to provide the service, and consequently the overall dynamic response of PEV fleets can be significantly affected by the availability of PEVs for the PFC during the day.
- *Upward and downward power reserves of PEVs:* The available upward and downward power reserves of a PEV for the PFC highly changes during the day. At each moment of the day, these power reserves can be calculated according to the topology of the battery chargers and the charging power. To this end, first, the maximum and minimum physical power limit of the battery charger should be considered. The maximum power limit of the battery charger is typically equal to the nominal power of the battery charger. Since a single PEV might be connected to the electrical grid via various chargers in different locations (e.g., a small-scale battery charger at home or a large-scale battery charger at the charging station), the maximum power limit of the PEV could vary during the day. On the one hand, typically, PEVs are charged at home with a relatively low power (e.g., 1-3.3 kW), and consequently, the whole charging process might take up to several hours. On the other hand, at the charging stations, PEVs charging power has a high value (e.g., 11-50 kW), and the whole charging process might take less than one hour. Undoubtedly, the battery size of the PEV is additionally an important factor, which will be described in more detail in the next sections. Besides, the battery charger could be characterized by unidirectional or bidirectional battery charger typologies, which have a different minimum power limits. In brief, both maximum and minimum power limits of PEV battery chargers basically vary over the day. Second, the charging power of PEVs, which depends on the charging or idle mode of the PEV, greatly changes over a day. Typically speaking, the charg-

ing power of PEVs in the constant current mode is very close to the nominal power of the battery charger, however the charging power of PEVs gradually decreases during the constant voltage mode. As mentioned before, the charging power of PEVs in the idle mode is zero. Thus, in summary, the available upward and downward power reserves of PEVs for the PFC highly change during the day. In order to calculate them at each moment of the day, we must consider the charging power of PEVs, the maximum power limit and the topology of the battery chargers.

There are some parameters of the PEV fleet that are assumed constant during a day. For instance, in practice, the PFC loop characteristics of PEVs such as the dead-band function and frequency-droop controllers could be assumed constant. Also, it can be assumed that different battery chargers have a similar power closed loops, and consequently their battery charger time constant is the same. Besides, here we assumed that PEVs are connected to the high-voltage transmission system in the model, and therefore the location of PEVs at the low-voltage distribution network are not considered in this chapter.

It is worth mentioning that the above-mentioned parameters will be taken into account when the single and aggregate model of PEVs for the PFC are proposed and developed in the next sections. Moreover, appropriate case studies of the Spanish power system will be created and described where the worst case of the system will be found and presented.

Next, we describe a decentralized model of PEVs for the PFC, where some major shortcomings of these models are highlighted and discussed.

3.3. Decentralized Model of PEVs for the PFC

As described, the primary frequency control aims to keep the active power balance between total power generation and the electricity demand in the power system, in such a way that the system frequency remains within an acceptable range (Kundur et al., 1994). Figure. 3.1 shows the typical frequency control scheme of the power systems in which distributed PEVs could participate in the PFC together with the conventional generating units. The typical frequency control scheme of power systems shown in Figure. 3.1 mainly consists of the following components:

Load and system model: In Figure. 3.1, the active power mismatch between total load and PEV's consumption, and total power production of wind farms, solar PVs, and the generating units creates the frequency deviation Δf mostly depending on the equivalent system inertia-constant of the generating units H and the equivalent load-damping constant D (Kundur et al., 1994). Note that frequency-sensitive electrical loads such as induction and synchronous machines respond to the

frequency deviations, that is typically represented by an equivalent load-damping constant D .

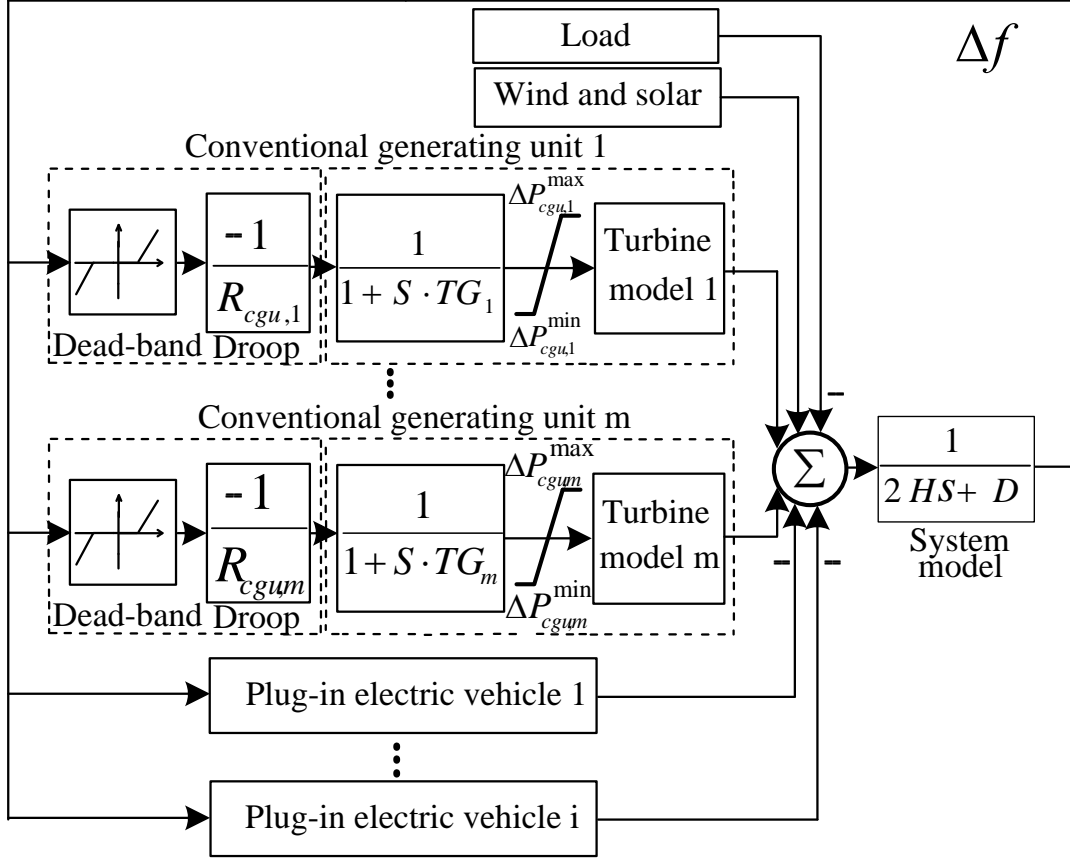


Figure 3.1.: Typical frequency control scheme of the power systems including distributed PEVs.

Wind farm and solar PVs: In present-day power systems, wind farms and solar PV technologies are typically decoupled from the electrical grids by a power electronic converter, and also are not generally equipped with the PFC loop. Therefore, they do not provide the PFC service following the contingency event, and in summary their output power in Figure. 3.1 remains constant during the disturbance³.

Decentralized Conventional generating units from 1 to m : Typically, the shaft rotational speed of conventional generating units is monitored for the PFC by the speed droop governor, which accordingly controls the turbine throttle valves.

³In the near future, wind farms in some European countries like Spain will be obliged to participate in the PFC. However, this is beyond the scope of this thesis, which focuses on the provision of PFC particularly by PEVs.

Figure. 3.1 presents the dynamic model of conventional generating unit for the PFC, which mainly includes the following parts (Kundur et al., 1994):

1. The PFC loop, which is typically represented by the dead-band function, which is set to avoid responding unwillingly to small frequency disturbances, and droop coefficient $R_{CGU,m}$, which controls the unit output active power according to the input frequency deviations,
2. The speed governor, which can be represented by a first order transfer function with the governor time constant (e.g., 0.5 s),
3. The turbine, which is modeled depending on the unit's type (Kundur et al., 1994). In the simplest form, the turbine can be represented by a first-order transfer function with the turbine's time constant (e.g., several seconds),
4. Depending on the power production $P_{CGU,m}$ of conventional generating unit m , it has a certain amount of power reserves to either increase or decrease. In the power systems literature, these available power reserves are called upward and downward power reserves. The upward $\Delta P_{CGU,m}^{max}$ and downward $\Delta P_{CGU,m}^{min}$ primary reserves of conventional generating unit m can be calculated as follows:

$$\Delta P_{CGU,m}^{max} = P_{CGU,m}^{max} - P_{CGU,m} \quad (3.1)$$

$$\Delta P_{CGU,m}^{min} = P_{CGU,m}^{min} - P_{CGU,m} \quad (3.2)$$

where $P_{CGU,m}^{max}$ and $P_{CGU,m}^{min}$ are the maximum and minimum power limits of the CGU m , respectively.

The output of the turbine model is the power variation of conventional generating units for the PFC. Similarly, PEVs could change their active power according to the input frequency as follows.

Decentralized PEVs from 1 to i : Figure. 3.1 shows the distributed model of PEVs (PEV 1 to i) for the PFC where each PEV responds to the system frequency. In practice, the frequency is measured at the connection point of PEVs and according to this signal, PEVs will participate in the PFC in a decentralized way. In order to evaluate the impact of PEVs on the PFC, simply all PEVs could be added to the frequency control loop.

In the next Sections, the detailed model of a single PEV is provided, and then an aggregate model of PEVs for the PFC is formulated.

3.4. Proposed Model of a Single PEV for PFC

This section proposes a new model of a single PEV for PFC studies. To this end, first according to the literature the previously developed models of a PEV for PFC

is reviewed and provided. Due to some major shortcomings of the previous model of a PEV, a new model of a PEV is proposed and developed. Later on, for this model, the total upward and downward primary reserves of a PEV are calculated.

Here, first the previously developed model of a single PEV for the PFC is described. Then, to incorporate essential characteristics of a PEV (e.g., operating modes), an enhanced model of a PEV for the PFC is proposed introducing a participation factor.

3.4.1. Previously Developed Model of a PEV for PFC

Figure. 3.2 presents the previously developed model of a single PEV for the PFC that has been extensively used in the literature (Almeida et al., 2011; Mu et al., 2013a; Pillai & Bak-Jensen, 2010b). In general, this typical model comprises the battery charger model and the primary frequency control loop (Almeida et al., 2015; Mu et al., 2013a). As comprehensively addressed in the previous chapter, the battery pack is not modeled in the PFC analysis, and the fast switching transients of the battery charger are neglected (for further information, see chapter 2).

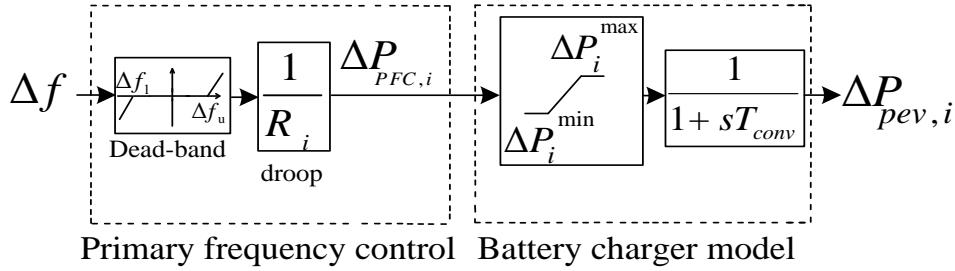


Figure 3.2.: Block diagram of the previously developed model of one single PEV for the PFC according to the literature.

On the left hand side of Figure.3.2, the PFC loop is represented by the following functions:

1. Dead-band function with the upper Δf_u and lower Δf_l limits: This function, which is employed by all generating units involved in the PFC, is set to avoid responding unwillingly to small frequency perturbations. If the units are not equipped with the dead-band function, then this might increase the “wear and tear” in the turbine, and inevitably the costs.
2. Frequency-droop coefficient R_i (corresponding to PEV i): Figure. 3.3 shows the characteristics of a droop curve which controls the PEV output active power according to the input frequency deviations. When the frequency deviates from the nominal value f_0 to another value f_1 , the PEV power accordingly changes from P_0 to P_1 . In other words, the droop control increases the PEV power by ΔP_{PFC} for the frequency drop of Δf .

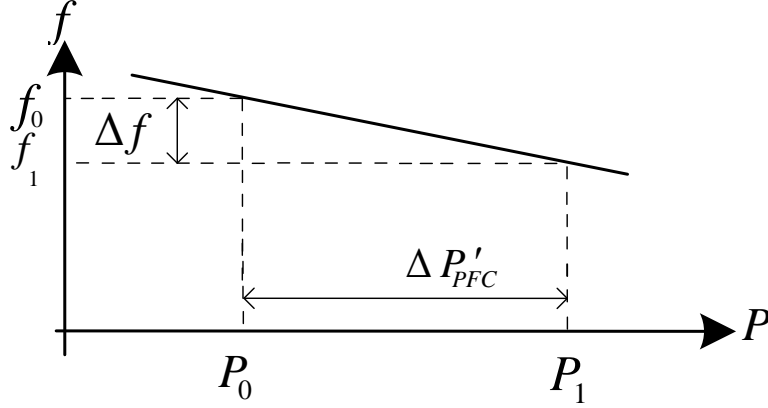


Figure 3.3.: Frequency-droop curve.

On the right hand side of Figure. 3.2, the battery charger model consists of the following elements:

1. Battery charger close-loop model: The response of the closed-loop power control system is modeled as a first-order transfer function with a small time constant (Aditya & Das, 2001; Brivio et al., 2016; Kottick et al., 1993; Zhang et al., 2012). It is worth mentioning that many fast dynamics (e.g., PWM switching patterns) of battery chargers were truly neglected in the final model. However, here the time constant of battery charger is maintained, since it has a potential to affect the PFC response within a few hundreds of milliseconds. Obviously, if the time constant has a high value, then the frequency response could be further affected. In previous research on the PFC, a wide range of values have been introduced and used for the battery charger's time constant (e.g., 15-30 ms in (Zhang et al., 2012), 26 ms in (Aditya & Das, 2001), 40 ms in (Brivio et al., 2016), 500 ms in (Kottick et al., 1993)). For instance, on the one hand, the small time constant of 5 ms might negligibly affect the frequency response. On the other hand, the large time constant of 500 ms (i.e., settling time of 2 s) could notably affect the PFC response, which ranges within hundreds of milliseconds.
2. Downward and upward primary reserves of a PEV: Figure. 3.2 shows the downward ΔP_i^{max} and upward ΔP_i^{min} primary reserves of a PEV. On the one hand, ΔP_i^{max} represents the amount of primary reserve which can be consumed when the frequency goes above the nominal value (i.e., over-frequency problem). On the other hand, ΔP_i^{min} is the amount of primary reserve which can be injected back into the grid when the frequency drops below the nominal value (i.e., under-frequency problem). ΔP_i^{max} and ΔP_i^{min} depend on the charging power $P_{c,i}$ of the PEV, which significantly varies along the day. ΔP_i^{max} and ΔP_i^{min}

are given by

$$\Delta P_i^{max} = P_i^{max} - P_{c,i} \quad (3.3)$$

$$\Delta P_i^{min} = P_i^{min} - P_{c,i} \quad (3.4)$$

where P_i^{max} and P_i^{min} are the maximum and minimum power limits of the PEV battery charger, respectively. The minimum power limit of the PEV P_i^{min} is defined according to the battery charger topology, and it can be equal to zero and minus the maximum power limit of the PEV $-P_i^{max}$ for unidirectional and bidirectional battery chargers, respectively.

As seen above, the previously developed model of a PEV for the PFC is not able to represent and reflect various essential characteristics of the PEV (e.g., operating and charging modes of a PEV). Despite the fact that in practice, these characteristics might notably affect the performance of the PEVs. Therefore, in the next section, we propose a model of PEV for the PFC in which the mentioned characteristics are included.

3.4.2. Proposed Model of a PEV for PFC

To include technical characteristics of a PEV, here an enhanced model of a PEV for PFC is formulated and developed. Figure. 3.4 shows the proposed model of a PEV for PFC in which a participation factor k_i is incorporated into the PFC loop of the PEV. Since the primary frequency loop and battery charger model were presented in detail in the previous section, here they are not described again and only the participation factor is presented and developed.

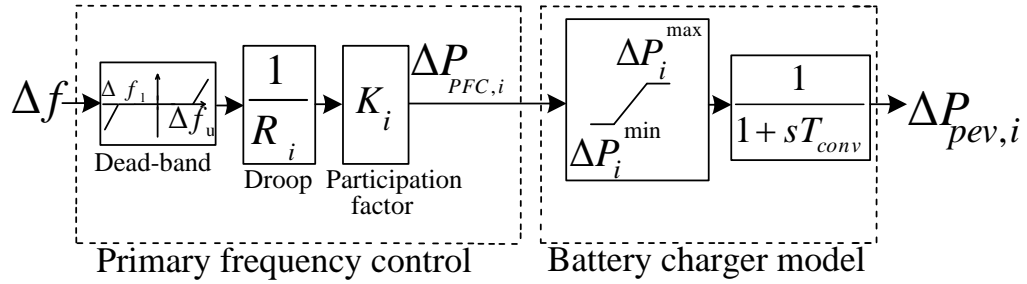


Figure 3.4.: Block diagram of the proposed model of PEVs for the PFC.

In principle, the mentioned participation factor k_i is proposed to identify the participation of each PEV in the PFC according to PEV's operating modes. Mathematically speaking, k_i varies from zero to one (that means from zero to full PFC participation) depending on the PEV i state of charge SOC_i . It is worth emphasizing that the PEV's state of charge is taken into account because it varies during the day according to the PEV's operating mode.

According to section 3.2, during the day, a PEV could take three distinct operating modes of disconnected, charging, and idle modes as follows:

Disconnected mode

The PEV, which is disconnected from the grid, is not evidently able to provide the PFC and consequently, k_i is equal to zero.

However, fortunately the vast majority of PEVs are usually connected to the grid during the day, and they are potentially able to participate in the PFC. The grid-connected vehicle could be either in the charging or idle modes as follows.

Charging mode

When in the charging mode, PEV’s state of charge dynamically changes over time. Technically speaking, according to the battery state of charge, PEVs equipped with the li-ion batteries could be in the CC or CV modes. Since the control strategies of the CC and CV modes are entirely different, thus the participation level of a PEV is affected depending on these charging modes. Note that here the li-ion battery is considered as an example of a promising technology, however the methodology remains valid and sound for other types of battery technologies as well.

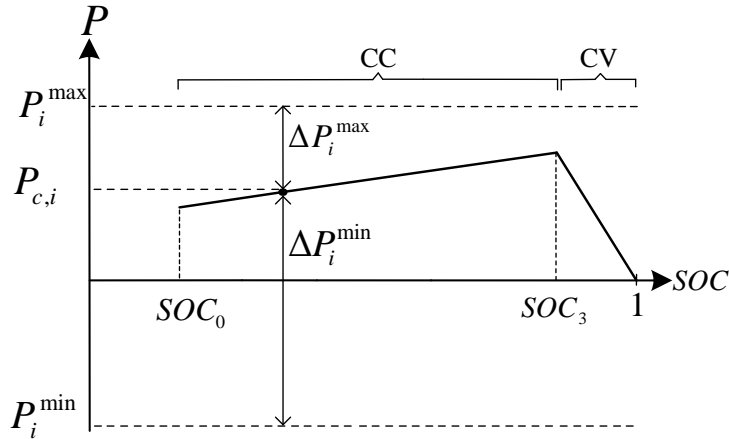


Figure 3.5.: Charging power of the li-ion battery versus SOC.

- **Constant current and constant voltage charging modes:** Figure. 3.5 shows the power variation of a PEV equipped with the li-ion battery pack in the charging mode versus the state of charge. In the first stage, the PEV is charged in the constant charging mode (between SOC_0 and SOC_3). Since the PEV charging current remains constant and the battery voltage gradually rises, the charging power of PEV steadily increases by the SOC. When the PEV voltage reaches the maximum allowable limit (at the state of charge SOC_3), then the charging mode is changed from the constant current to the constant

voltage mode. In this stage, the PEV terminal voltage remains almost constant (slightly increases), until the battery pack is fully charged ($SOC=1$). Next, we define the participation factor according to the battery charging control process.

- **Participation factor definition of a PEV in the charging mode:** Figure. 3.6 shows an example of the participation factor $k_i^C(SOC)$ versus the state of charge in the charging mode for the li-ion battery. Note that the abrupt changes of the participation factor are avoided using ramp slope when the state of charge is between SOC_0 and SOC_1 or between SOC_2 and SOC_3 . The PEV cannot provide the PFC when the battery's SOC is less than the minimum desired state of charge SOC_0 . From SOC_0 up to SOC_3 , the PEV's battery is charged in the CC charging mode in which the charging power can be fully controlled, and consequently k_i is equal to one. Then, if the SOC is more than SOC_3 , the charging control mode changes from the CC mode to the CV mode, which is configured as an open loop. This way, the control fixes the battery terminal voltage at the rated voltage until the battery is fully charged. As a result, it is assumed that the PEV does not contribute to PFC due to the open-loop nature of the control system. Consequently, k_i is equal to zero.

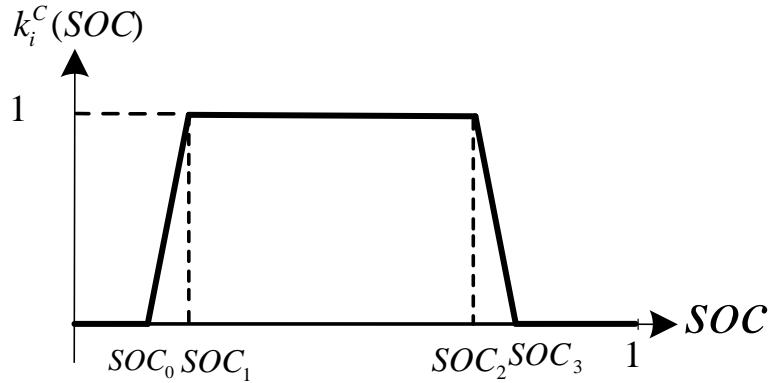


Figure 3.6.: Participation factor versus SOC in the charging mode.

Idle mode

When the PEV charging process is completed or temporarily stopped due to smart charging management strategies, the PEV could remain connected to the grid in the idle mode while the charging power remains always equal to zero. Note that during the charging mode, the PEV battery charger regulates the DC link voltage, while during the idle mode, the DC link voltage is equal to the terminal voltage of the battery. Within this mode, though the PEV charging power is zero, it is able to provide the V2G services when needed. Figure. 3.7 shows an example of the participation factor $k_i^I(SOC)$ versus the state of charge, when the PEV is in the idle mode. In order to avoid abrupt changes in the participation factor, the ramp

slope is implemented between SOC_0 and SOC_1 . In this mode, k_i is always equal to 1, unless the PEV's SOC is less than SOC_0 . Compared to the charging mode, the idle mode does not take into account the mode change between constant current and constant voltage modes and therefore the participation factor remains always equal to one when the state of charge is greater than SOC_1 .

To illustrate the impact of the participation factor on the PFC, Figure. 3.8 shows the power variation of the PEV versus the system frequency deviation $\Delta f = f_1 - f_0$. If the participation factor is equal to one ($k_i = 1$), the power variation of the PEV has a high value (i.e., ΔP_{PFC}). If the participation factor is less than one ($k_i < 1$), then the power variation of the PEV proportionally has a lower value (i.e., $\Delta P'_{PFC}$). If the participation factor has a value lower than one, then the total power reserve of the PEV can not be used for the PFC. The impact of the participation factor on the PFC loop could be interpreted as the droop value of PEVs changes over time. However in practice, the droop typically remains constant, and the PEV is not able to fully emulate the droop curve due to some technical constraints. In summary, the lower is the participation factor, the less is the participation level of a PEV in the PFC.

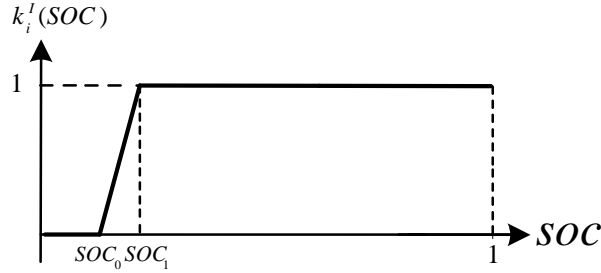


Figure 3.7.: Participation factor versus SOC in the idle mode.

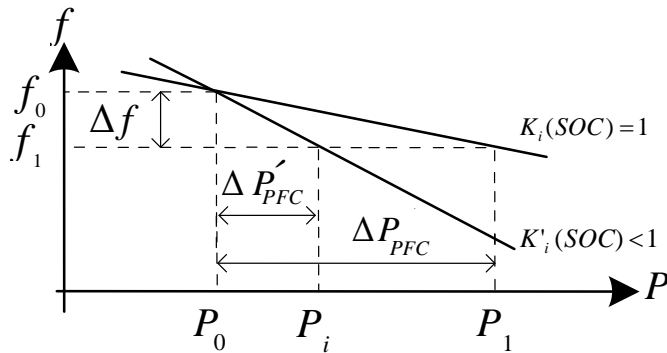


Figure 3.8.: Effect of the participation factor on the droop characteristic.

In summary, the participation factor, which was developed above, made us able to model the operating modes of a PEV that significantly vary along the day. Next, taking into account these operating modes, the upward and downward power reserves of the proposed PEV model for the PFC (shown in Figure. 3.4) are calculated.

3.4.2.1. Upward and Downward Power Reserves of a PEV

If the PEV is connected to the grid and is willing to participate in the PFC, it must be ensured that it has a sufficient power reserve for the PFC. Otherwise, the PEV is not able to satisfactorily provide the PFC service because the PEV's power might reach the maximum or minimum physical limits.

The upward and downward power reserves of the proposed PEV model, which might considerably vary during the day, are obtained in the charging and idle modes.

Upward and downward power reserves of a PEV in the charging mode As extensively described in Figure. 3.5, the PEV charging power $P_{c,i}$ changes according to the battery state of charge. In Figure. 3.5, the downward ΔP_i^{max} and upward ΔP_i^{min} power reserves of PEV i in the charging mode are given by

$$\Delta P_i^{max} = P_i^{max} - P_{c,i} \quad (3.5)$$

$$\Delta P_i^{min} = P_i^{min} - P_{c,i} \quad (3.6)$$

Thus, the PEV has the largest upward power reserve ΔP_i^{min} at the end of the constant charging mode (at SOC_2). Obviously, the PEV has the lowest upward reserve, when it is fully charged (SOC=1). Moreover, the battery charger topology is a major determinant factor in obtaining the upward power reserve of the PEV. It is important to note that P_i^{min} is equal to $-P_i^{max}$ and zero for bidirectional and unidirectional battery chargers, respectively. As a result, the upward reserve ΔP_i^{min} is obtained equal to $-(P_{c,i} + P_i^{max})$ and $-P_{c,i}$ for the bidirectional and unidirectional battery chargers, respectively.

Upward and downward power reserves of a PEV in the idle mode If the PEV is in the idle mode, then the PEV charging power $P_{c,i}$ is equal to zero. Therefore, ΔP_i^{max} and ΔP_i^{min} are written as

$$\Delta P_i^{max} = P_i^{max} \quad (3.7)$$

$$\Delta P_i^{min} = P_i^{min} \quad (3.8)$$

If the PEV is equipped with the bidirectional battery charger, the absolute values of the upward and downward reserves are the same. Otherwise, the upward reserve of a PEV equipped with bidirectional battery charger is zero.

In summary, in this section, we introduced and developed a participation factor for a PEV in various operating modes, and then the upward and downward power reserves were calculated. In the next section, the model of a PEV is generalized for the whole PEV fleet, and the aggregate upward and downward primary reserves are obtained.

3.5. Proposed Aggregate Model of PEVs

In this section, to reduce the computational complexity of decentralized models of PEVs for the PFC, we aim to introduce and propose aggregate models of PEVs. Hence, here an aggregate model for a large number of PEVs C_h (h is an index of hours) is formulated based on the arithmetic averaging technique, which is a widely known and used technique (Anton et al., 2002). To this end, first the proposed model of a PEV is generalized to the whole PEV fleet, and later on the average values of the model parameters are calculated and obtained. It is worth mentioning that here we do not model low voltage distribution networks, to which PEVs are mostly connected. In other words, PEVs within the models are assumed to be directly connected to the high voltage transmission system, and consequently the technical characteristics of distribution networks are neglected.

Figure 3.9 presents the proposed aggregate model of PEVs for the PFC that also consists of the average PFC loop and the average battery charger model. In Figure 3.9, to obtain the whole PEV fleet's power variation for the PFC, the output power of an average PEV is multiplied by the total number of grid-connected electric vehicles.

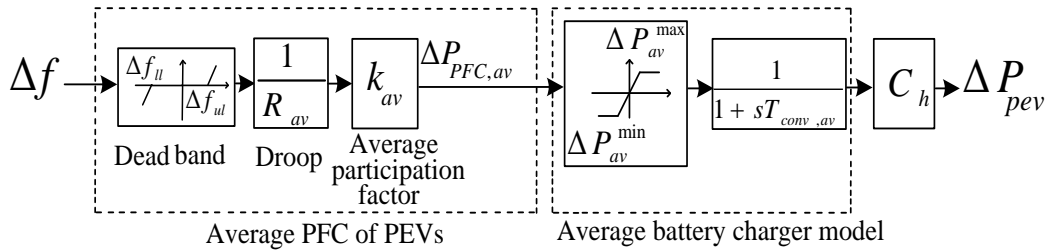


Figure 3.9.: Block diagram of the aggregate PEVs model including average participation factor.

3.5.1. Average PFC Loop of PEVs for PFC

On the left hand side of Figure 3.9, the average PFC loop comprises of the following functions:

1. Average dead-band function with the upper Δf_{ul} and lower Δf_{ll} limits: Although each PEV could be utilized by different dead-band functions, in practice this function is implemented with the same limits for all PEVs (see Section 3.2). The limits of the dead-band function are usually set by the system operators or regulatory agents. Therefore, in this formulation, the average limits are assumed equal to the upper Δf_{ul} and lower Δf_{ll} limits.
2. Average frequency-droop coefficient R_{av} : Similar to the dead-band function (see Section 3.2), the frequency-droop of PEVs is typically set to a constant value (like conventional generating units), and this value is universally adjusted by the system operators. Therefore, the average droop is assumed equal to the one of a single PEV R_i .
3. Average participation factor k_{av} : The participation factor of PEV i k_i notably varies during the day depending on the battery state of charge. Moreover, the participation factor might be notably different from one PEV to another PEV, since each PEV has a different operating point at each instant of the day. As a result inevitably, it is a challenging problem to calculate the average participation factor k_{av} according to the average state of charge at each moment of the day. To solve this problem, first we define and obtain the distribution of PEVs battery state of charge. As mentioned in Section 3.2, the battery state of charge highly varies during the day depending on many factors such as the constant current or constant voltage charging or idle mode of PEVs. An an example, the probability distribution function of PEVs state of charge $\phi_{SOC_{av}}$ can be represented by the Beta distribution function in which SOC_{av} and σ^2 are the mean value and the variance (or standard deviation) of the distribution function at a specific time of the day, as shown in Figure 3.10.

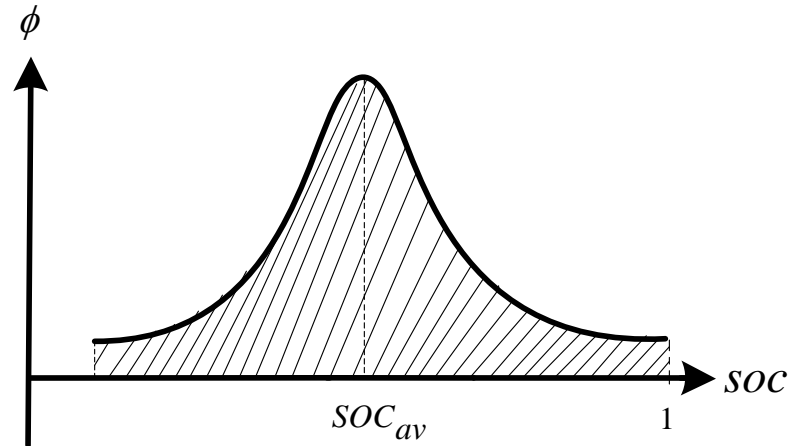


Figure 3.10.: Beta distribution function of the PEV fleet's state of charge.

Taking into account the distribution of the PEV state of charge, the average participation factor of PEVs can be separately calculated in the charging and idle modes.

Within each charging mode, the average participation factor determines the average participation level of those PEVs in the PFC.

The average participation factor in the charging mode $k_{av}^C(SOC_{av})$ over the entire range of state of charge ($0 \leq SOC_i \leq 1$) can be given by

$$k_{av}^C(SOC_{av}) = \int_0^1 k_i^C(SOC) \cdot \phi_{SOC_{av}} \cdot d(SOC) \quad (3.9)$$

where $k_i^C(SOC)$ was shown in Figure. 3.6. In a similar manner, the average participation factor in the idle mode $k_{av}^I(SOC_{av})$ over the entire range of state of charge ($0 \leq SOC_i \leq 1$) can be given by

$$k_{av}^I(SOC_{av}) = \int_0^1 k_i^I(SOC) \cdot \phi_{SOC_{av}} \cdot d(SOC) \quad (3.10)$$

where $k_i^I(SOC)$ was shown in Figure. 3.7. In both modes, since the participation factors do not remain equal to one over the entire SOC range, the average participation factors inevitably are less than one.

Finally, if α^I and α^C are defined as the share of PEVs in the idle and charging modes, then the average participation factor of the whole PEV fleet is formulated as follows

$$k_{av} = \alpha^I \cdot k_{av}^I(SOC_{av}) + \alpha^C \cdot k_{av}^C(SOC_{av}) \quad (3.11)$$

In (3.11), the average participation factor k_{av} depends on the average state of charge SOC_{av} and the probability distribution function $\phi_{SOC_{av}}$. Note that α^I and α^C were defined as the share of grid connected electric vehicles in the idle and charging modes, therefore the obtained average participation factor k_{av} represents the average participation of only PEVs, which are connected at that specific time to the grid. In other words, average participation factor k_{av} does not represent the disconnected PEVs. It is worth mentioning that the average state of charge during the day depends on the average charging power of PEVs. Despite the fact that the average SOC changes over the day, it could be assumed constant at each moment of the day for the PFC analysis. Thus, as also mentioned in the previous sections, to produce a numerical example for k_{av} , the following parameter values are considered:

- Beta distribution function $\phi_{SOC_{av}}$ with the variance $\sigma^2 = 0.0075$,
- The share of PEVs in the charging α^C and idle α^I modes are 25% and 75%, respectively, or in other words, we assume that one fourth of the connected vehicles are in charging while three fourth of them are in the idle mode at

each moment of the day. In simple words, if we assume that a PEV is mostly connected to the grid during the day and the whole charging process takes six hours, then roughly speaking 25% of the day time PEVs are in the charging mode. However, this holds true only if PEVs are homogeneously connected and charged during the day. Therefore, in practice, the share of PEVs in the idle and charging modes could also significantly vary over the day,

- To define the participation factor in the charging mode $k_i^C(SOC)$ according to Figure. 3.6, SOC_0 , SOC_1 , SOC_2 , and SOC_3 are set to 0.20, 0.25, 0.85 and, 0.90, respectively. Also, the ramp slope R is set to 20,
- To define the participation factor in the idle mode $k_i^I(SOC)$ according to Figure. 3.7, SOC_0 , and SOC_1 are set to 0.20 and 0.25, respectively. Also, the ramp slope R is set to 20.

If the above presented values are inserted into (3.11), the average participation factor is obtained versus the average state of charge. Note that as mentioned above the average participation factor at each moment of the day is obtained only for PEVs, which are connected to the electrical grid. Figure. 3.11 presents the obtained results where k_{av} notably varies between 0.4 and 1 along the day due to the following points:

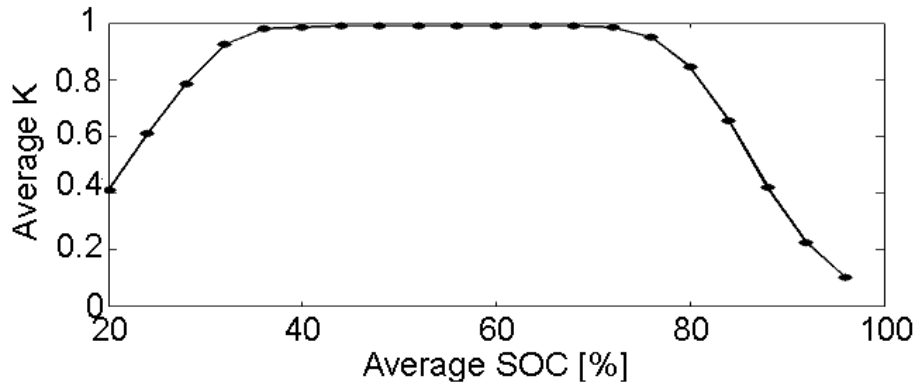


Figure 3.11.: k_{av} versus SOC_{av} .

- If the average state of charge has a low value (e.g., between 20% and 30%), then this implies that a substantial portion of the fleet do not have enough energy in their battery pack. As a result, the average participation factor is obtained below one.
- If the average state of charge has a high value (e.g., between 80% and 95%), then this implies that a substantial portion of the fleet are in the constant voltage charging mode. Therefore, the average participation factor is obtained below one.

3.5.2. Average Battery Charger Model

On the right hand side of Figure 3.9, the average battery charger model consists of the following function:

1. Average battery charger dynamic behavior: The time constant of the battery chargers of PEVs typically has a very low value (e.g., 26 ms (Aditya & Das, 2001)), since the outer power loop is relatively fast (for further information, see chapter 2). It can be assumed that all PEVs fairly have a similar power controllers, and consequently the average time constants of PEVs $T_{conv,av}$ are assumed the same.
2. Average upward and downward power reserves of PEVs: In principle, PEVs are able to quickly increase/decrease their charging power to provide downward/upward reserves. As discussed in Section 3.2, the charging power of PEVs changes during the day depending in the number of PEVs in the idle or constant current or constant voltage modes. Therefore, as the average charging power of the PEV fleet varies during the day, then inevitably the average upward and downward power reserves of PEVs will accordingly vary. The average upward ΔP_{av}^{max} and downward ΔP_{av}^{min} primary reserves of C_h number of PEVs at a specific moment of the day are calculated as follows:

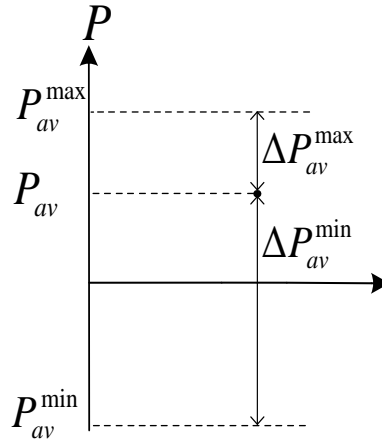


Figure 3.12.: Average upward and downward power reserves of PEVs.

$$\Delta P_{av}^{max} = P_{av}^{max} - P_{av} \quad (3.12)$$

$$\Delta P_{av}^{min} = P_{av}^{min} - P_{av} \quad (3.13)$$

where P_{av}^{max} , P_{av}^{min} , and P_{av} are the average of the maximum charger power, the minimum battery charger power, and the charging power of the PEVs, respectively.

If the average upward ΔP_{av}^{max} and downward ΔP_{av}^{min} primary reserves are multiplied by the total number of connected PEVs C_h , then the total upward ΔP_{ag}^{max} and downward ΔP_{ag}^{min} primary reserves of PEVs are obtained as follows:

$$\Delta P_{ag}^{max} = C_h \cdot \Delta P_{av}^{max} \quad (3.14)$$

$$\Delta P_{ag}^{min} = C_h \cdot \Delta P_{av}^{min} \quad (3.15)$$

In practice, it might not be necessary that PEVs provide the total upward or downward primary reserves, and this is why the droop control should be implemented in the PEVs. Besides, if the total upward or downward power reserves are necessary, PEVs might not be able to fully provide it due to a very low participation factor.

3.5.2.1. Validation of Average Model of PEVs

To validate the proposed average model of PEVs, its performance will be compared to the ones of the distributed model of PEVs for the PFC. To do so, first we show that the calculated k_{av} exactly represents the average value of participation factors considering probability distribution function of SOC of PEVs. Then, we validate the average model for 100 clusters of PEVs, which have different values of charging power as well as participation factors.

Average model performance with k_{av} considering distribution function of SOCs

For the sake of clarity, first we provide a numerical example of participation factors in both idle and charging modes. Then, we show and compare the simulation results of both models. Note that as we exactly calculate the average value of PEV participation factors, therefore the outcomes of both models are to be the same.

In previous subsection, we obtained the average participation factors considering the average SOC as well as probability distribution of SOC of PEVs, as shown in Figure.3.11. For instance, if SOC_{av} is equal to 95% (Beta function with α and β equal to 9.9 and 1.1, respectively), then the average participation factor was calculated 78.75%. Figure.3.13 shows the cumulative distribution function (CDF) for SOC_{av} of 95% as well as the participation factors of PEVs in idle and charging modes. For 25% of PEVs, which are in the charging mode, 10%, 80%, and 10%, shares have the participation of 1, 0, and 0.5, respectively. Note that the line between 0 and 1 can be exactly represented by an average value of 0.5. For 75% of PEVs, which are in the idle mode, all have the participation of 1. As a result, 77.5%, 20%, and 2.5% shares of all PEVs have the participation of 1, 0, and 0.5, respectively. The similar process can be performed for the average participation of 90%.

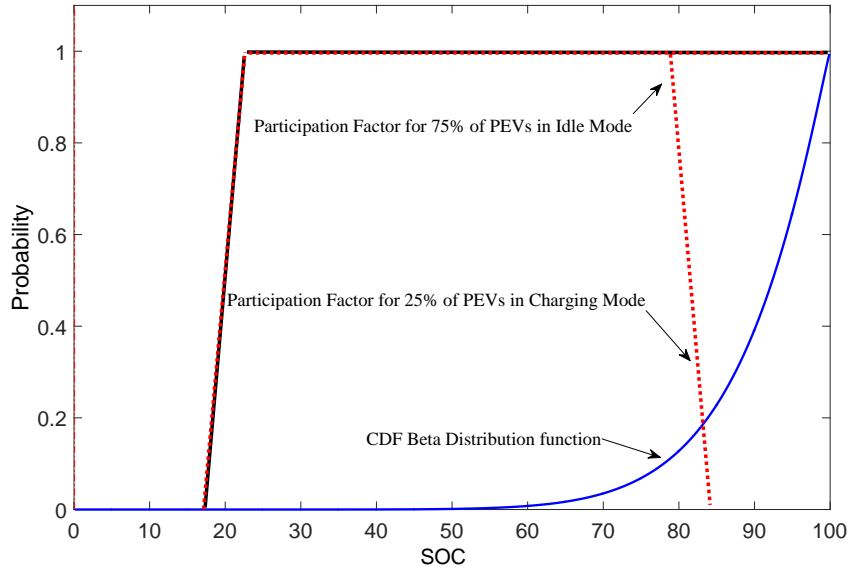


Figure 3.13.: Participation factors of PEVs in idle and charging modes considering the CDF of Beta distribution function of PEV SOC.

It is worth mentioning that the average participation factor obtained from (3.11) exactly represents the response of PEVs considering the probability distribution function of SOC. In order to create the distributed model of PEVs, three clusters of PEVs with participation factors of 1, 0.5 and 0 are considered. As shown in Figure. 3.14, the frequency response as well as PEV power variation of both detailed and average models of PEVs for PFC obtained the same for the average participation factors of 0.8 and 0.9.

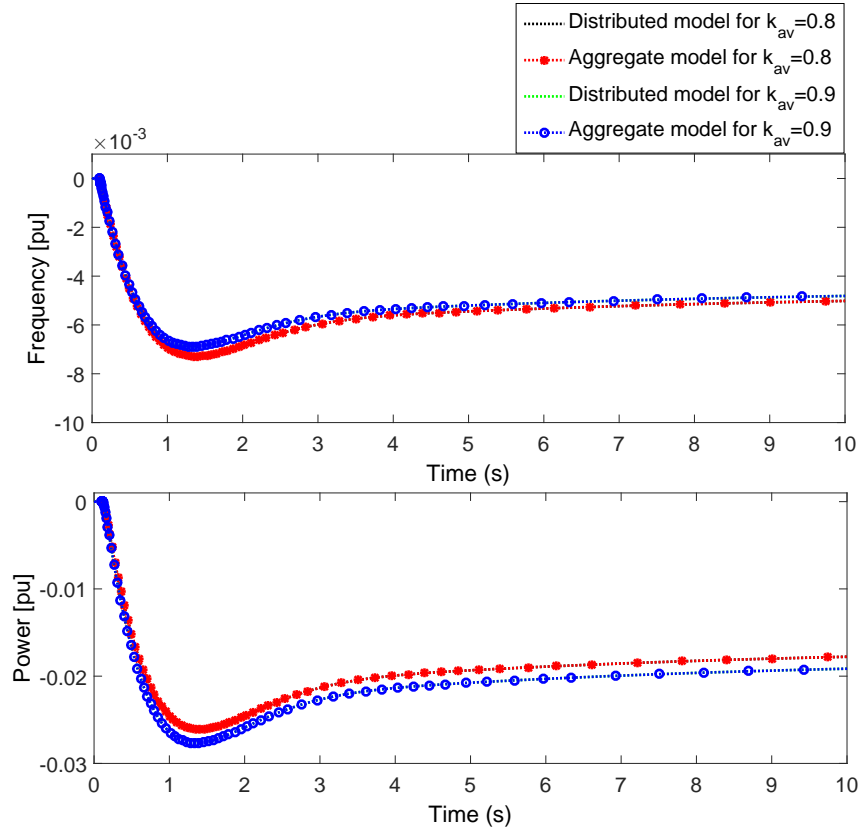


Figure 3.14.: Validation of the proposed average model in the Spanish power system model for k_{av} equal to 0.9 and 0.8. (a) frequency response of detailed and average models of PEVs. (b) PEV power variation of detailed and average models of PEVs.

Validation of average model for a PEV fleet with different charging power and participation factors

In order to test and validate the average model, we have to first build the distributed model of PEVs. As it is quite computationally complex to create such distributed model of a fleet including 2,280,000 PEVs, we divided the fleet into 100 clusters. Then, for each cluster, different charging power and participation factors were considered. While the charging power ranges from 0 to 100%, it is assumed that the participation factor lies between 0.8 and 1 (as later shown in Figure. 3.17). For the average participation of 0.9, the performance of the average model is compared to the one of distributed model in Figure. 3.15. In Figure. 3.15(a), the maximum frequency deviations after the disturbance are 0.230 Hz and 0.234 Hz for the average and detailed models of PEVs for the PFC. In Figure. 3.15(b), the maximum power variations of PEVs are 0.0365 pu and 0.0362 pu for the average and detailed models of PEVs for the PFC.

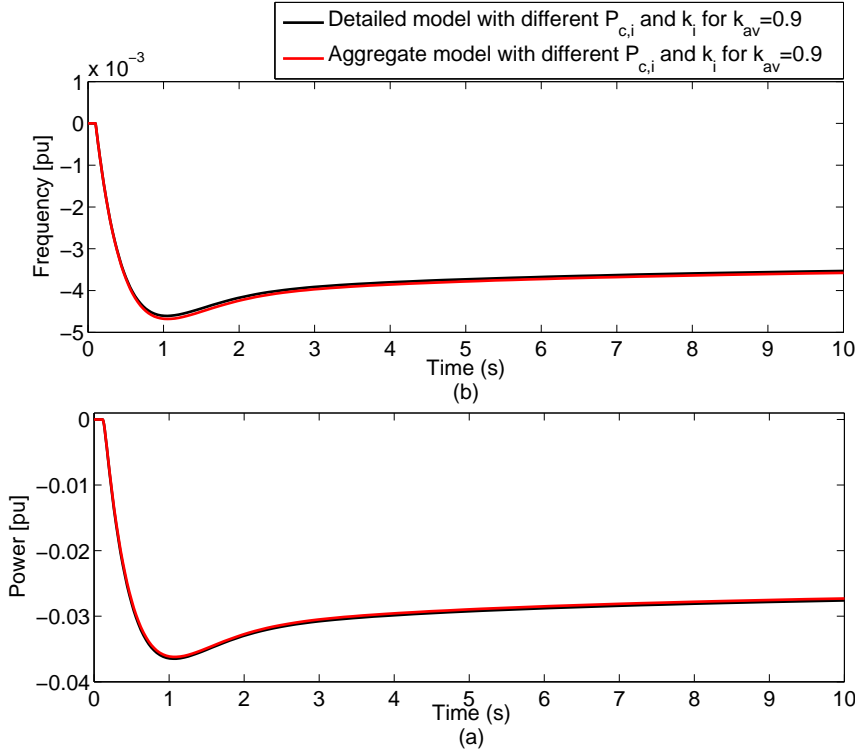


Figure 3.15.: Performance of the average and detailed models for 100 clusters of PEVs. (a) frequency response. (b) PEV power variation.

Note that the error is defined

$$Error\% = \left(\frac{|\Delta f^{DTL} - \Delta f^{AGG}|}{\Delta f^{DTL}} \right) \cdot 100 \quad (3.16)$$

where Δf^{DTL} and Δf^{AGG} are the minimum or maximum frequency deviation of the detailed and aggregate models, respectively. Thus, the error of the average model is obtained very low, e.g., 1.79%. Technically speaking, it is expected that the error of the model would be very negligible in the case that PEVs do not reach their maximum or minimum power limits. However, in the case that a number of PEVs would partly reach their maximum or minimum power limits, then the error of the model might be slightly increased. Note that the here-provided validation has been done for the model without the distribution network. In the next chapter, we validate the aggregate model of PEVs including distribution network, and moreover, the accuracy of aggregate models with and without distribution networks will be evaluated and compared.

In the next section, the proposed model of PEVs for the PFC is implemented and evaluated in the Spanish power system, to which a large number of PEVs are presumably connected.

3.6. Case Study and Simulation Scenarios

In order to evaluate the proposed aggregate model of PEVs for the PFC, a study of the impact into a real-power system (i.e., Spain) is carried out. A large number of PEVs are added to this case study in order to analyse the PFC in the target year of 2020. In particular, the Spanish power system is selected for this analysis due to the following reasons:

1. The Spanish power system is characterized by a high penetration rate of intermittent renewable energy sources such as wind and solar. Currently, the total installed capacity of solar photovoltaic and wind power in Spain are 4.33 and 22.98 GW (by 2016), respectively. Thus, the sum of wind and solar is 27.31 GW, that is a large value considering the Spanish peak power demand of 39.27 GW in 2015. In such power systems accompanied by high power fluctuations, large quantities of power reserves are required to mitigate quick power variations. In future, the required reserve can be provided not only by conventional units, but also in part by various types of distributed energy resources such as battery storage systems and PEVs. On top of this, the amount of required power reserve can be significantly reduced, if fast-response units could effectively control the power/frequency. As mentioned above, since PEVs are comparatively faster than conventional generating units, therefore in future they might be excellent options to provide the PFC in countries like Spain.
2. The Spanish power system has a limited number of cross-border transmission interconnections. Therefore, not only the Spanish power system should not heavily rely on these transmission lines (e.g., provision of automatic generation control), but also it should remain stable following the failure of these transmission lines. In other words, this means that at any time instant the Spanish power system is to be operated and controlled in the stand alone mode. In such a power system, a greater amount of power reserve is generally required that could be partly provided by PEVs in the future.

In the Spanish power system studied in this chapter, we neglected the interconnection to the European grid, to create which, we did not have enough relevant data. This could affect the accuracy of the results, as the transmission lines connected to France could also help to suppress the frequency deviations in the Spanish power system. However, hereby we clarify some additional points. First, though the accuracy of the system under study is important, our main focus in this work is on the potential impact of PEVs for the PFC. In other words, the accurate representation of real-world power system like the Spanish power system has not been/is not our main concern. Though the Spanish power system is simulated as an islanded power system, it might be suggested that the European grid is selected and analysed as the base use case. To answer this suggestion, we clarify that the simulation results of the Spanish power system are presented in per unit (pu). As a result, they can

be accurately extrapolated to the European power system assuming the following two points:

1. The generation mix of the Spanish power system is similar to the one of the European power system. This way, the dynamic behaviour of both power systems can be considered comparable.
2. In the target year 2020, we assume that the growth rate of PEV technology in Spain will be similar to the other European countries. Therefore, the penetration rates of PEVs in both power systems will be comparable, and consequently the impact of PEVs on the PFC response is very similar.

In this section, the existing Spanish power system including mainly conventional units is described for the PFC analysis. For this power system, the worst case for the PFC analysis (i.e., lowest system load) is defined and calculated. Then, relevant parameters of a fleet of PEVs for PFC are calculated and presented. Finally, several simulation scenarios are defined.

3.6.1. Modeling Conventional Power Plants

Currently, in Spain, conventional generating units are the main provider of the primary frequency control. As a result, their dynamic behaviour has a substantial impact on the frequency response of the Spanish power system. To properly represent this system, here an appropriate model of conventional generating units is provided and then simulated.

The existing Spanish power system mainly consists of various types of conventional power plants such as hydro, steam, and combined cycle gas turbines (CCGTs). Moreover, wind farms, solar units, and other generating units like biomass power plants are connected to a considerable extent to this system.

The dynamic model of conventional generating units are presented as follows:

- The dynamic models of the steam and hydro units have been extensively researched and developed in (Kundur et al., 1994). In short, the simplified model of the steam plant can be used with the governor time constant and the reheat steam turbine. Also, the hydro turbine is modeled by the governor, transient droop constant, and the hydro turbine. The gas turbine of CCGT plants has a fairly complex model (Lalor & O'Malley, 2003), and for this analysis, a simplified model of the turbine is used (Pillai & Bak-Jensen, 2011). As mentioned in the previous section, the PFC of conventional units consists of the dead-band and the droop. As addressed in chapter 2, according to the Spanish electric sector rules (REE, 2013), the dead-band function is not allowed to be implemented. Here we also assume that all units use the same frequency-droop of 5% .
- Wind farms, solar photovoltaics and other types of generating units such as biomass power plants do not participate in the PFC in this analysis, and

consequently their output power remains constant during the frequency disturbance.

- The electrical load does not support the frequency in this analysis, and therefore no demand side management schemes for the PFC support are considered. The equivalent load damping constant D , which is inherently provided by the frequency-sensitive load, is assumed equal to 1 (Mu et al., 2013a).

3.6.2. Calculation of the Inertia H for the Worst Case

In order to properly evaluate the Spanish power system, first it is required to identify the worst case associated with the frequency response. As mentioned in Section 3.2, over a year, the worst case of power systems for the PFC occurs when the load consumption level has the least value. In other words, generally speaking, the frequency response of the power system has a minimum quality when the total demand is very low. For this case, on the one hand fast-response generating units (i.e., peaking units) are not available for the dispatch when the total load consumption is low. The slow-response units (e.g., base load units like thermal) together with renewable energy power plants (that do not provide the PFC) typically are being dispatched, and they supply a large portion of the low load demand. In such conditions, the frequency deviations following a large disturbance could be very high and the frequency stability of power systems can be severely at risk.

For the Spanish power system, the total system load had a minimum value on November 3rd, 2013 at 16:50 pm. Table. 3.1 presents the generation share and power related to this case. As seen, nuclear and steam power plants supply 25.9% and 12.4% of the total load, respectively. Also, wind farms and solar photovoltaic units, which in principle do not participate in the PFC, provide 31.6% of the total load. Overall, in this case, 69.9% of the total load is provided with units that either do not provide or poorly provide the PFC. Therefore, we take this scenario as the worst-case for the simulations, where the outage of the largest generating unit (around 1 GW) could potentially put at risk the frequency stability of the Spanish power system.

Table 3.1.: Power production of generating units in Spanish power system at 16:50 pm (REE, 2013).

Power plant	H [s]	Generation share [%]	Generation power [MVA]
Hydro units	3	5.6	1,274
Nuclear power plants	7	25.9	5,846
Steam power plants	7	12.4	2,807
CCGT	4.5	5.9	1,326
Wind farms and solar	0	31.6	7,122
Other generating units	0	18.6	4,191
Total H	-	3.52 s	

In the next step, to model the Spanish power system for the worst case, it is necessary to define and calculate the equivalent system inertia H . The total system inertia is a key factor in analyzing the power system's frequency behavior, and is a measure of the total stored energy in the rotating mass of generating units connected to the power systems.

In order to calculate equivalent inertia H , first the total energy stored in the rotating mass of a power plant is given by

$$E_{m,h} = H_m \cdot S_{m,h} \quad (3.17)$$

where m , $S_{m,h}$, $E_{m,h}$, and H_m are an index for power plants, power plant installed capacity (in MVA), kinetic energy stored in the rotating mass of the power plant, and the power plant inertia, respectively.

Afterwards, the total energy stored in the rotating masses of all power plants is obtained and divided by the base power to obtain equivalent inertia as follows:

$$H_h = \frac{\sum_m E_{m,h}}{S_{sys}} \quad (3.18)$$

$$H_h = \frac{\sum_m H_m S_{m,h}}{S_{sys}} \quad (3.19)$$

Where S_{sys} is the base power for per unit system.

In order to obtain the equivalent inertia H_h of the Spanish power system, the power plants production $S_{m,h}$ and inertia H_m at 16:50 pm are used that were shown in Table. 3.1.

Thus far, the dynamic model of conventional generating units and Spanish power system were presented and obtained for the worst case, and in the next step, the parameter values of a PEV fleet are described and calculated.

3.6.3. Aggregate Model of PEV Fleet

In this section, the parameter values of the aggregate model of PEVs for the PFC are obtained. It is worth mentioning that due to lack of real historical operating data of PEVs, their data set has been inevitably collected from various sources (e.g., MERGE project (R Ball et al., 2011) and some relevant papers (Hu et al., 2010; Masuta & Yokoyama, 2012)).

According to Figure.3.9, we will calculate and provide the average values of the following functions:

1. Average battery charger model including upward and downward PEV power reserves, and charger's time constant
2. Number of grid-connected vehicles C_h

Several parameters of the PEV fleet could be assumed constant for the whole fleet at each moment. Therefore, it is not necessary to calculate the average values of the following parameters.

- Droop curves
- Charger's time constant
- Number of PEVs

On the other hand, according to the description presented in Section 3.2, the rest of the PEV fleet's parameters could vary from one PEV to another PEV, and consequently their average values should be calculated. These parameters are provided as follows:

- Average participation factor
- Average upward and downward power reserves

In conclusion, we first present the constant parameters of the PEV fleet, and later on the average values of other parameters will be calculated and described in detail.

3.6.3.1. Constant Parameters of PEVs for PFC

As mentioned, some parameters of the PEV fleet are assumed the same for all PEVs, and hence obviously the average parameter value of all PEVs is equal to the one of a single PEV. Hereby, these parameters are presented as follows:

Average frequency-droop curve of PEVs: As PEVs have not been extensively used for the PFC yet, it is a difficult task to determine the appropriate PEV droop curve, which will be used by PEVs in future power systems. However for this analysis, we assume that PEVs will have the same droop curve as the conventional generating units due to the following reasons:

1. In the Spanish power system, the PFC is an obligatory service, which must be provided by all conventional generating units such as steam and gas turbine power plants. In such power systems, all units are typically required to employ the same droop curve (e.g., 5% droop requirement in the Spanish power system). The droop of 5% means that the unit would change its total nominal active power (in MW) for the frequency deviation of 2.5 Hz. Therefore, all units provide the same amount of power reserve following the same contingency event. This is why, in a similar way in this analysis, we could assume that PEVs might utilize the same droop as conventional generating units in future.
2. Generally speaking, in practice, the droop characteristics of PEVs could be potentially set by various power system stakeholders such as system operators or PEV manufacturers. However these entities might find it extremely difficult to set different values of droop for PEVs due to their high spatial and temporal distributions. As a result, it is very likely that in future system operators consider the same droop value for all PEVs.

To sum up, in this analysis, we did assume that all PEVs use the same droop as the conventional generating units (i.e., 5% droop), though in the following chapters, we will well design the frequency-droop controller of PEVs with respect to the system frequency stability criteria.

Average charger's time constant: It is assumed that the average charger's time constant $T_{conv,av}$ is equal to 50 ms. Note that the charger's response is very fast for the PFC analysis, and consequently the frequency response might slightly change for instance when $T_{conv,av}$ increases from 35 ms to 100 ms (Mu et al., 2013a).

Number of grid-connected vehicles: According to the description presented in Section 3.2, the number of grid-connected vehicles at each hour of the day C_h could significantly vary depending on the behavior of PEV owners. Note that in this analysis we do not take into account different possible locations at which PEVs might be connected during the day. Therefore, undoubtedly, this could largely affect the performance of the PEV fleet during the day for the PFC analysis. In (Masuta & Yokoyama, 2012), the number of PEVs during the whole day have been shown in which PEVs are largely connected to grid even during the day. The obtained number of PEVs during a typical day is shown in Figure. 3.16.

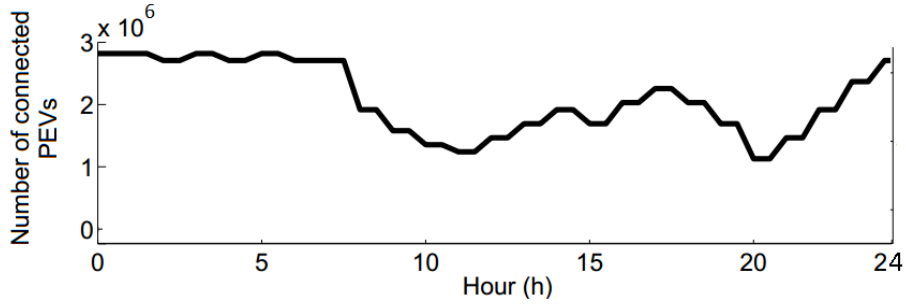


Figure 3.16.: Number of grid-connected PEVs C_h on an hourly basis.

3.6.3.2. Calculation of Average Parameters of PEVs for PFC

As mentioned before, the technical constraints of PEVs could highly affect the PFC response. To incorporate these constraints into the model, we introduced the participation factor for each PEV (see the previous section). Despite the fact that the participation factor of each PEV can be simply obtained, it was a challenging task to calculate the average participation factor of the whole PEV fleet. Moreover, it was pointed out that the available power reserves of PEVs for PFC could have significant impacts on their performance. In a similar way, the available power reserves greatly vary not only from one PEV to another PEV, but also for each specific PEV over the day.

The average values of the PEV fleet's parameters (i.e., participation factor, and maximum and minimum charger power limits), which vary from one PEV to another PEV (see also Section 3.2), are calculated and discussed in detail as follows.

Average participation factor

In order to calculate the average participation factor $k_{av,h}$ in equation 3.11, first the PEVs average state of charge SOC_{av} during the day should be known. According to Section 3.2, the state of charge of PEVs largely varies during the day depending on many factors like the idle or charging mode. Accordingly, the average state of charge of PEVs highly changes during the day depending on the behavior of PEV owners. Also, as mentioned in Section 3.2, the charging power of PEVs could be very different from one PEV to another, that additionally affects the average state of charge. Note that before, the probability distribution of state of charge of PEVs was considered and provided according to the average state of charge of PEVs. To this end, we simply took SOC_{av} from (Hu et al., 2010), as shown in Figure. 3.17. It is worth underlying that the rest of the required parameters (i.e., share of PEVs in the charging and idle modes, and the probability distribution function of PEV state of charge) were presented in detail in the previous section.

As a result, the average participation factor during the day k_{av} is calculated and presented in Figure. 3.17. As mentioned before, the average participation factor k_{av}

at each moment of the day represents only the average participation of those PEVs, which are in either idle or charging modes. In other words, the disconnected PEVs are not considered in the calculation of the average participation factor k_{av} . It was found that the availability of PEVs for the PFC k_{av} could significantly vary from 80% to almost 100% during the day. In other words, a large portion of the PEV's power reserve for the PFC might not be available due to the above-described constraints, when needed. On the one hand, the average participation factor was high when most of PEVs are in the idle or in the CC charging modes. Therefore, PEVs are able to fully provide the PFC. On the other hand, the participation factor had a low value when most of the PEVs are in the CV charging mode (at the end of their charging process). In this mode, PEVs are not able to adequately provide the PFC due to the open-loop nature of the control system. In summary, this means that the technical constraints of PEVs should be carefully taken into account especially when their available power reserve for the PFC is calculated.

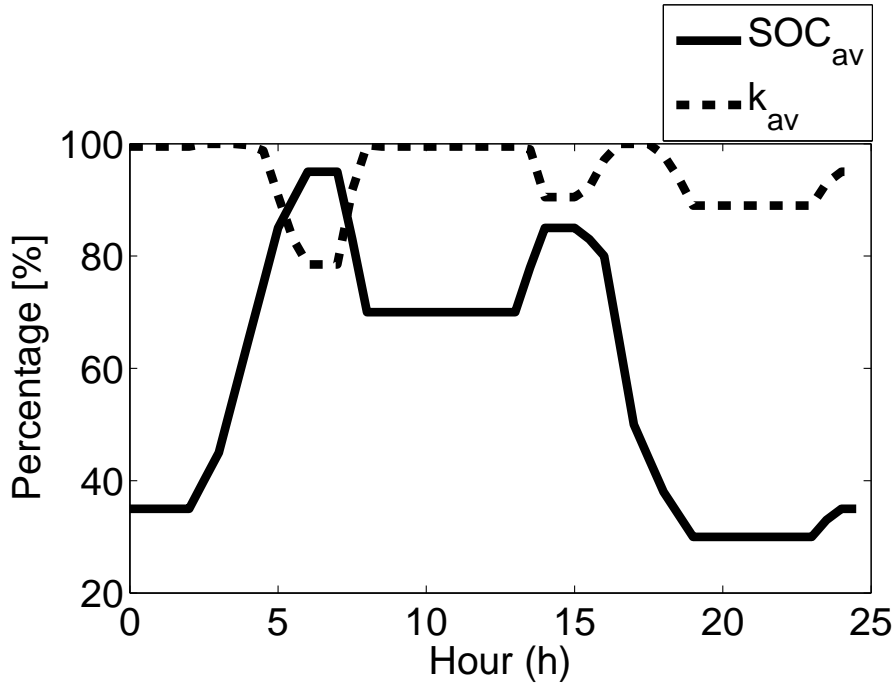


Figure 3.17.: SOC_{av} (Hu et al., 2010) and k_{av} calculated in 3.11 on an hourly basis.

Average maximum and minimum charger power limits

According to Section 3.2, the maximum and minimum power limits of battery chargers depend on both the nominal power and the topology of the battery charger. Considering equations 3.14 and 3.15, to obtain average maximum $P_{av,h}^{max}$ and minimum $P_{av,h}^{min}$ charger power limits, first the type and size (i.e., battery charger maximum power limit) of PEVs within the fleet should be described. Note that the average

maximum and minimum power values are considered only for the grid connected electric vehicles in this section, and then the total maximum and minimum average power of PEVs over the day are obtained multiplying the number of grid connected PEVs along the day by these calculated average power values.

In Section 3.2, we introduced the battery size of PEVs as an important factor for the whole charging process. Generally speaking, if the battery size is large, then accordingly the battery charger should be large enough in order to achieve a desirable total charging time. In order to define the appropriate battery charger for PEVs, first we take into account the size of different PEVs in the fleet. Generally speaking, PEVs can be categorized into four types as follows (from smallest to largest) (R Ball et al., 2011):

- 1) small goods-carrying vehicles (group identified as “L7e”),
- 2) four-seat passenger vehicles (group identified as “M1”),
- 3) medium goods-carrying vehicles (group identified as “N1”),
- 4) big goods-carrying vehicles (group identified as “N2”).

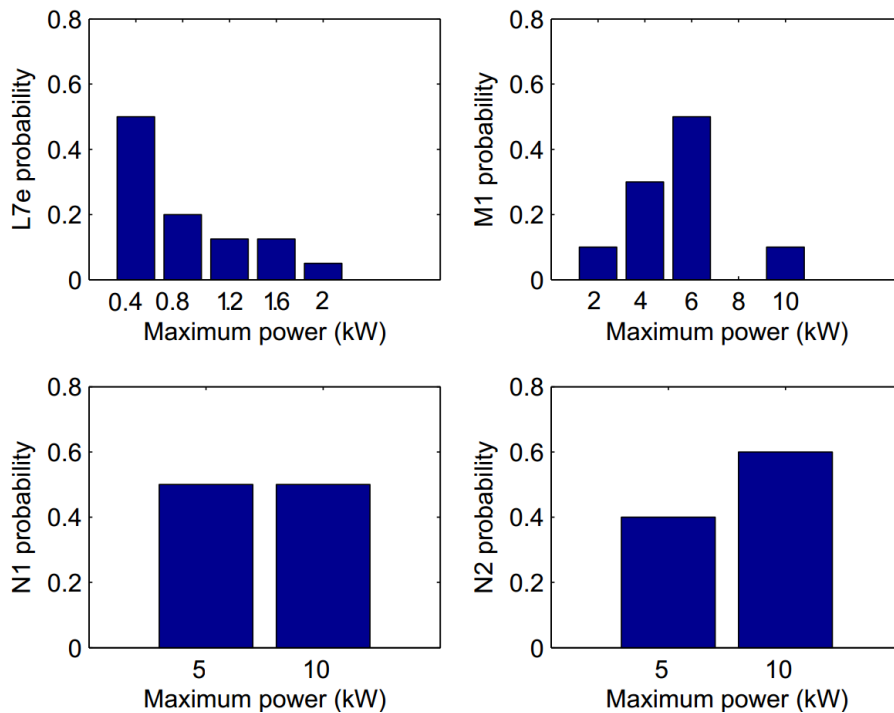


Figure 3.18.: Probability distributions of the maximum power for the four PEV groups (R Ball et al., 2011).

To define the size of PEVs, the charger power probability distributions of the above-mentioned PEV types are shown in Figure. 3.18 (R Ball et al., 2011). On the one hand, the small goods-carrying vehicles L7e typically have a low power charger (e.g., 0.4 kW). On the other hand, medium and big goods-carrying vehicles N1 & N2 are

typically equipped with a larger battery chargers (e.g, from 5 to 10 kW). Note that since these PEVs have a relatively large battery storage, their charging time can be very long using typical on-board battery chargers (e.g., 3.3 kW). Therefore, as discussed in Section 3.2, in future, they might be more connected to the fast charging stations (e.g., 11 kW) in order to largely accelerate their charging process. A single PEV might be connected to the electrical grid during the day in different locations through different battery chargers. As a result, the charging power as well as the upward and downward power reserves of the PEV for the PFC could also change over the day.

To obtain the average values of the maximum battery charger power μ , first the probability values and the maximum battery charger power of each PEV type are multiplied. As mentioned in Section 3.2, each type of PEVs might not be connected to the electrical grid through the same battery charger. Therefore, here we take into account the probability of different battery chargers, which might be utilized by each group of PEVs. This way, we could later calculate an average maximum power of various types of PEVs. Table.3.2 presents the obtained average values of the maximum battery charger power for each group. As seen, the big goods-carrying vehicles (N2) have a very large average value (i.e., 8 kW), while the small goods-carrying vehicles have a relatively low average value (i.e., 7.8 kW).

Table 3.2.: Average battery charger maximum power for four groups of PEVs.

PEV type	M1	L7e	N1	N2	Average
P_{av}^{max} [kW]	$\mu_1=5.085$	$\mu_2=7.8$	$\mu_3=7.5$	$\mu_4=8$	$\mu_{av}=5.41$
Share [%]	86.68	1.47	9.92	1.93	-

In the next step, to obtain the average maximum battery charger power of the whole PEV fleet P_{av}^{max} , we must consider the share of each PEV type. As we discussed in Section 3.2, PEVs might be connected to the electrical grid through various battery chargers, and consequently the nominal power of battery chargers connected to grid can be different. Table.3.2 shows the share of each PEV type, where 86.68% of all PEVs are considered as the four-seat passenger vehicles (R Ball et al., 2011). According to the share of PEVs, the average battery charger power of each type is weighted and then summed to obtain the average battery charger power of the whole PEV fleet P_{av}^{max} (i.e., 5.41 kW). This average power of PEV's battery chargers can be currently supplied in residential areas in many European countries (e.g., the Netherlands and Spain), and can be considered as a typical value of maximum charging power in such areas.

To obtain the average minimum battery charger power of the whole PEV fleet P_{av}^{min} , we must take into account the battery charger topology. If all PEVs are equipped with the unidirectional batter chargers, then obviously the average minimum charger power is equal to zero. However if all PEVs are equipped with bidirectional battery chargers, then the minimum battery charger power is equal to minus the average

maximum battery charger power. In such cases, the minimum battery charger power is obtain -5.41 kW. Obviously, if PEVs are equipped with both types of battery chargers, then the average minimum power lies between -5.41 and 0 kW.

As mentioned in Section 3.2, the number of grid-connected electric vehicles varies largely during the day, that could affect the performance of PEV fleet during the PFC. If the number of PEVs during the day C_h are known, then the total maximum and minimum battery charger power can be easily calculated multiplying the average battery charger power of the whole PEV fleet P_{av}^{max} (i.e., 5.41 kW) by C_h . Taking into account the number of PEVs during the day C_h shown in Figure. 3.16, Figure. 3.19 presents the total maximum and minimum battery charger power of PEVs equipped with the BBCs during the day.

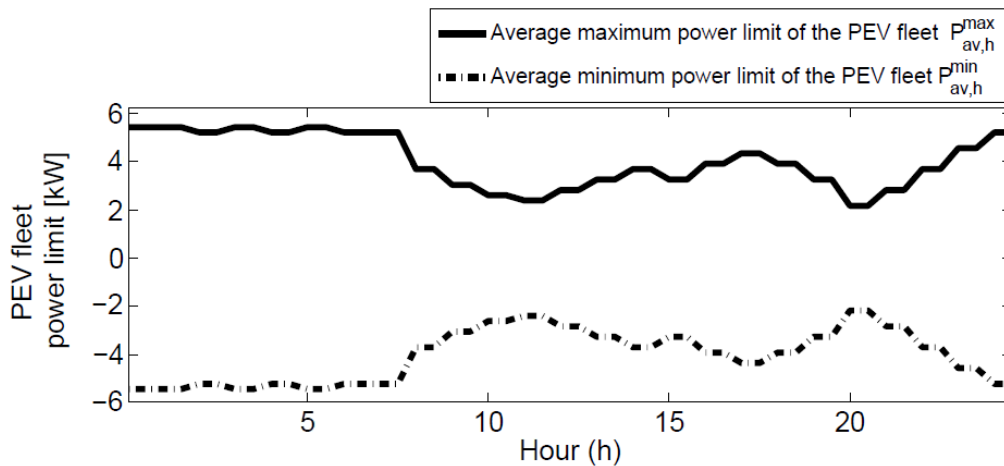


Figure 3.19.: Average minimum and maximum power ($P_{av,h}^{max}$ and $P_{av,h}^{min}$) of PEVs.

As observed above, the average values of the PEV fleet were shown and discussed over the whole day. However for this analysis, we evaluate the Spanish power system performance only for the worst case, which happens at 16:50 pm. Therefore, in the next subsection, in particular we present the average parameters of the PEV fleet for this worst case.

3.6.3.3. Average Parameters of PEVs for the Worst Case

The average parameter values of the PEV fleet are shown in Table. 3.3. Since the average state of charge has an intermediate value (i.e., 55%), the average participation factor gets a large value of 0.99. This means that most of PEVs ($\sim 2,257,200$), which are assumed in total 2,280,000 vehicles, can effectively participate in the PFC.

Table 3.3.: Average parameter values of PEVs for the worst case at 16:50 pm.

Parameter	Value
SOC_{av}	55%
k_{av}	0.99
C	2,280,000

3.6.4. Simulation Scenarios

In order to evaluate the performance of the proposed aggregate model of PEVs, two major analyses are carried out. In fact, as discussed in Section 3.2, PEVs are able to provide the PFC together with the conventional generating units, and here the impact of PEVs on the PFC is addressed and then compared to the conventional generating units. Moreover, we addressed in Section 3.2 that various relevant factors of the PEV fleet for the PFC may vary largely during the day. The upward and downward power reserves of PEVs are two important factors, which largely change during the day depending on the charging power and the topology of the battery chargers. In particular, the topology of battery chargers, which could be typically characterized by unidirectional or bidirectional battery chargers, largely affects the downward available power reserve of PEVs for the PFC. On the one hand, if PEVs are only equipped with unidirectional battery chargers, then they could only reduce their charging power to zero. On the other hand, if PEVs are equipped with bidirectional battery chargers, then they could decrease their charging power largely to minus the maximum charging power. Therefore, here the above-mentioned PEV constraints related to the topology of the battery chargers are considered and their impact on the PEV response is evaluated. Accordingly, two simulation scenarios are defined as follows:

1. Simulation scenario 1 is defined to examine the proposed aggregate PEV model, where the impact of PEVs on the frequency response of the Spanish power system is evaluated. Here, two use cases are defined and compared as follows:
 - 1.1. PEVs do not participate in the PFC using infinite droop,
 - 1.2. PEVs participate in the PFC using the droop control. Note that in both cases PEVs are equipped with the BBCs.
2. Simulation scenario 2 is defined to evaluate the PFC response of PEVs equipped either with UBCs and BBCs. This way, the upward power reserve of PEVs for the PFC will be largely different, that could affect the response of PEVs for the PFC. In other words, we evaluate the impact of the PEV's upward power reserve on the PFC response. Here, two use cases are defined and compared as follows:
 - 2.1. All PEVs are equipped with UBCs using the droop control
 - 2.2. All PEVs are equipped with BBCs using the droop control.

It is necessary to mention that in our analysis, the frequency disturbance is considered as the disconnection of the largest power plant. In the Spanish power system, the largest unit's installed capacity is equal to 1 GW, which is 0.0454 pu using the base power 22 GW. Considering that the base power S_{sys} is equal to 22 GW in (3.19), then H_h is obtained 3.52 s.

3.7. Simulation Results

In the Spanish power system, the conventional generating units mainly provide the frequency control support, which includes the PFC and load frequency control (LFC). Then, PEVs are added to this power system, and their performance is compared to the conventional generating units. Though PEVs are able to provide the LFC together with the PFC, here it is assumed that they only participate in the PFC. This way, the minor impact of the LFC signal on the PFC analysis is neglected in this analysis. The dynamic simulations are carried out through Matlab / Simulink on the worst case of the Spanish power system. Note that the simulations are only carried out for under-frequency events, however in a similar way, they can be implemented for over-frequency events.

3.7.1. Simulation Results of PEV's Participation in the PFC

Simulation results of scenario 1 are carried out and presented for the worst case of the Spanish power system. If PEVs do not provide the PFC, then this equally means that they are equipped with an infinite droop. On the other hand, if PEVs participate in the PFC, the value of their droop is set to 0.05, which is typically provided by conventional generating units. In this analysis, the disturbance of 1 GW (or 0.0454 pu) is applied to the power system at $t=0$ s.

Figure. 3.20.(a) shows the frequency response following the frequency disturbance for scenarios 1.1 and 1.2. In scenario 1.1, PEVs do not participate in the PFC and consequently only conventional generating units support the PFC. As a result, the maximum frequency deviation for scenario 1.1 is 0.33 Hz that exceeds the allowed frequency deviation limit 0.20 Hz. However, in scenario 1.2, PEVs are successfully able to keep the frequency deviation within allowable limits using droop coefficient 5%, where the maximum frequency deviation is obtained 0.19 Hz. As a result, PEVs could significantly improve the minimum frequency response by 42.42%.

Figure. 3.20.(b) shows the power variation of PEVs for the PFC in scenarios 1.1 and 1.2 following the disturbance. Obviously, the PEVs power variation remains zero for scenario 1.1. However in scenario 1.2, PEVs provide a large quantity of power reserve (i.e., 0.036 pu) for the PFC taking into account the disturbance of 0.0454 pu. As seen, PEVs not only provide a large amount of power, but also they inject the power into the grid very fast within 0.52 s. As shown in Figure. 3.20.(c), conventional

generating units provide the power reserve within 1.50 s, which is 300% slower than the one of PEVs. Moreover, Figure. 3.20.(c) shows that the required primary reserve from conventional generating units is decreased by 57.14%, when PEVs additionally participate in PFC.

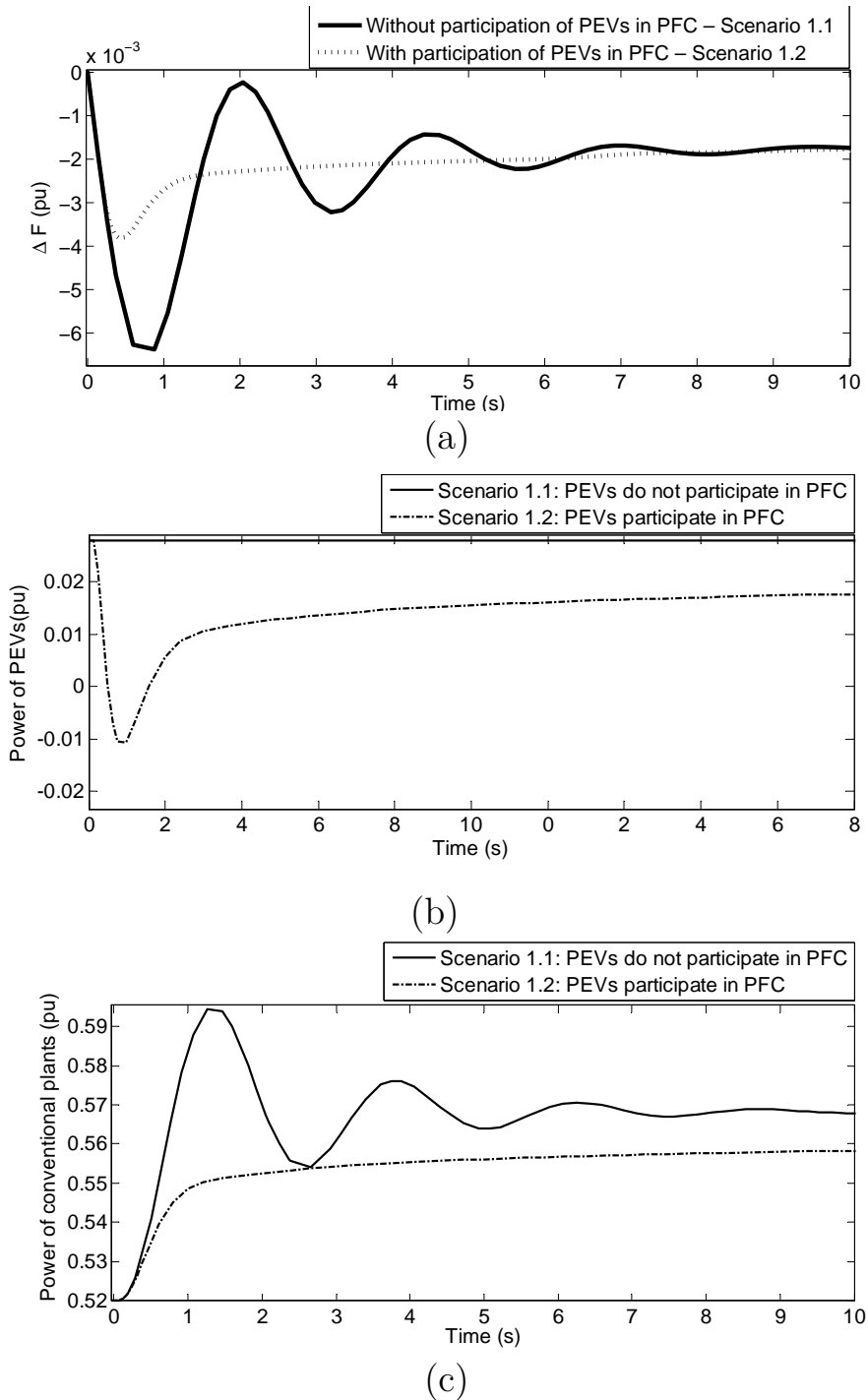


Figure 3.20.: Simulation results of scenarios 1.1 and 1.2. (a) System frequency response. (b) PEVs power, and (c) Conventional power plants power.

In summary, it was demonstrated that PEVs have a great potential to provide a large amount of power reserve for the PFC (e.g., 0.036 pu for the frequency disturbance of 0.0454 pu). Therefore, the power reserve of conventional generating units is less used for the PFC (e.g., by 57.14%). Moreover, PEVs could inject their active power very fast (e.g., 0.52 s), which helped considerably improve the frequency response.

3.7.2. Simulation Results of the Impact of PEV's Upward Power Reserve on the PFC

In scenarios 2.1 and 2.2, the performance of the PEVs equipped with various battery charger topologies (i.e., BBC and UBC) are evaluated for the worst case of the Spanish power system at 16:50 pm. As seen in Figure. 3.20.(b), the active power of PEVs got a negative value when they participated in the PFC. In fact this happened because we assumed that all PEVs in scenario 1 were equipped with the bidirectional battery chargers. Therefore, PEVs had the capability to inject the power into the grid. However, if PEVs are only equipped with the unidirectional battery chargers, then the PEV's power could not get negative values in Figure. 3.20.(b) (fixed at zero). This could notably affect the performance of PEVs for the PFC that will be shown below. It is worth mentioning that in both scenarios, the power response rates of PEVs either with BBC or UBC are the same, since the droop is fixed at 0.05. Therefore, the key difference between scenarios 2.1 and 2.2 is the amount of PEV's upward reserve available for the PFC.

Figure. 3.21.(a) shows the frequency response for scenarios 2.1 and 2.2 where the frequency disturbance of 0.0454 pu is applied to the Spanish power system at $t=0$ s. The minimum frequency response of PEVs equipped with the UBC is obtained 0.175 Hz, which is higher than 0.15 Hz for PEVs equipped with BBC. The results are obtained in accordance with the expectations that PEVs equipped with the BBCs have a better performance (i.e., 14.28 % improvement in the minimum frequency) compared to the ones equipped with the UBCs.

Figure. 3.21.(b) presents the power variation of PEVs in scenarios 2.1 and 2.2. As expected, PEVs with the BBCs inject a higher amount of the power reserve (i.e., 0.038 pu) that is large compared to PEV's power equipped with UBC (i.e., 0.028 pu). In other words, PEVs with the BBCs provided 35.71% more power active reserve for the PFC.

Figure. 3.21.(c) illustrates the power variation of conventional generating units for scenarios 2.1 and 2.2. At $t=0.52$ s, when the frequency reaches the minimum value, the power variation of conventional generating units for scenarios 2.1 and 2.2 are 0.031 and 0.37 pu, respectively. Therefore, if PEVs are equipped with the BBCs instead of the UBCs, they could reduce the need for the conventional generating unit's power reserve by 19.35%.

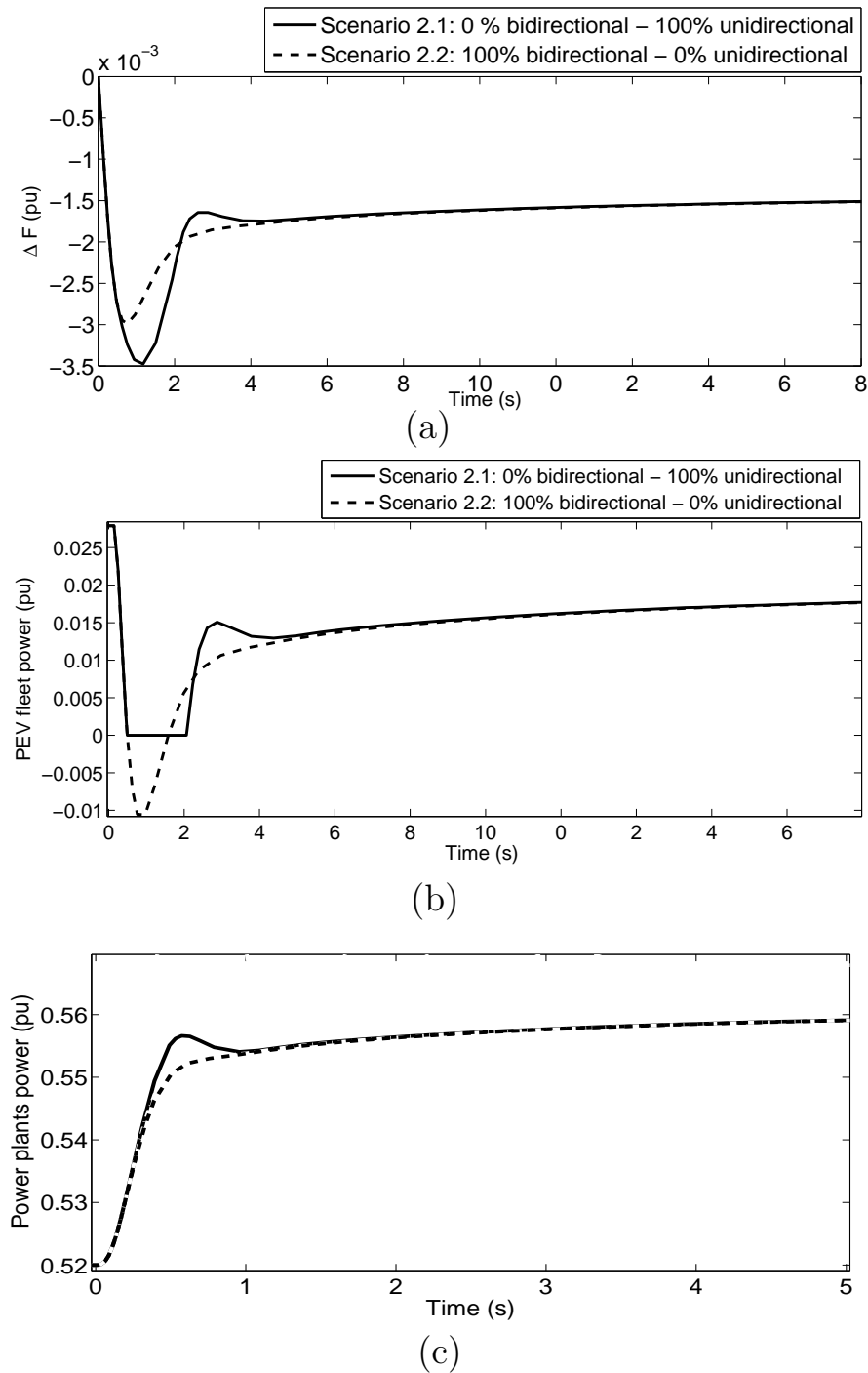


Figure 3.21.: Simulation results of Scenarios 2.1 and 2.2. (a) System frequency response. (b) Total PEVs power. (c) Conventional generating unit power.

In summary, as expected, PEVs with the BBCs had a better performance (e.g., 14.28% improvement in the minimum frequency) compared to the ones with the UBCs. Moreover, the power reserve of conventional generating units is less used for the PFC (e.g., 19.35%).

3.8. Conclusions and Out-Look

This chapter proposed an aggregate model of PEVs for the PFC. In summary, we addressed in detail the provision of PFC by PEVs, where various essential characteristics of PEV fleets were considered and analyzed. To this end, a participation factor was introduced through which the provision level of each PEV was taken into account. The obtained participation factor of PEVs could notably vary during the day from a very low value (i.e., 79%) up to almost 100%. In other words, this means that a large portion of PEV power reserve might not be available during the day for the PFC service. Moreover, the upward and downward primary reserves of PEVs for the PFC were calculated. It was found that the available power reserves of PEVs could significantly change according to the number of PEVs connected to the grid along the day. Moreover, the upward power reserves of PEVs were calculated and obtained for PEVs equipped with either bidirectional or unidirectional battery chargers. It was shown that PEVs largely improve the PFC if they could also inject the power back into the grid using the bidirectional battery chargers rather than unidirectional battery chargers.

Moreover, on the first attempt, an aggregate model of PEVs for the PFC was developed and formulated using the arithmetic averaging technique. Later on, the model was created and tested for a case study of the Spanish power system using Matlab / Simulink. Also, the fleet's essential characteristics such as the PEV's operating modes (i.e., disconnected, idle, or charging modes) and the constant voltage and constant charging modes were successfully incorporated into the model calculating the average participation factor. It was shown that PEVs are able to effectively improve the system frequency response following the contingency events. Note that here we evaluated the impact of PEVs on a large-scale power system (i.e., Spanish power system), later in chapter 5, assesses and compare the techno-economic performance of PEVs in both large-scale and islanded networks.

In this chapter, it was assumed that PEVs within the model are directly connected to the high-voltage transmission system. Therefore low-voltage distribution systems, to which PEVs are mostly connected, were neglected. In spite of this fact, there are several technical characteristics of distribution networks that could notably affect the dynamic response of PEVs for the PFC. Therefore, in the next Chapter, various characteristics of distribution network such as power consumed in the network and maximum allowed current of the distribution lines and transformers are incorporated into the previously-developed aggregate model of PEVs for PFC.

4. An Aggregate Model of PEVs Including Distribution Networks

Contents

4.1. Introduction	74
4.2. Context of PFC by PEVs Within Distribution Networks Over Time	77
4.3. Equivalent Model of A Single PEV for PFC in a Radial Distribution Network	79
4.3.1. Power Consumed in Distribution Network	80
4.3.2. Maximum Allowed Current of A Single PEV for PFC	89
4.3.3. PEV Equivalent Model for PFC Including Proposed Distribution Network and Transformer Limit	91
4.4. Aggregate Model of a Large-scale PEV Fleet in a Radial Distribution Network for PFC	95
4.4.1. Aggregate Fleet's Instantaneous Power Including Power Consumption in the Network During PFC	95
4.4.2. Maximum Allowed Current of Average PEV for PFC	99
4.4.3. Aggregate Model of PEVs for PFC Including Distribution Network and Transformer Limit	100
4.5. Case Study and Simulation Scenarios	102
4.5.1. Case Study	102
4.5.2. Simulation Scenarios and Sensitivity Analysis	109
4.6. Simulation Results	111
4.6.1. Simulation Results of the Case Study for Scenario 1	111
4.6.2. Simulation Results of the Case Study for Scenario 2	113
4.6.3. Validation of Aggregate Models With And Without Network & Sensitivity Analysis Results &	116
4.6.4. Discussion	117
4.7. Conclusions and Out-Look	118

In the previous chapter, an aggregate model of PEVs for the PFC was developed. Despite the fact that the aggregate model was able to represent the behaviour of PEV fleets for the PFC, it was not able to represent either the electrical distribution network or the location of PEVs for the PFC. Thus, in this chapter, we provide an aggregate model of PEVs that could additionally incorporate essential characteristics of distribution networks such as electric power consumed in the network and maximum allowed power of distribution lines and transformers. To represent the dynamic behaviour of distribution networks, first the variation of power consumed in the network with respect to the current deviation of the lines is calculated in the dq reference frame. Then, the calculated variation of power consumed in the network is added to the model of a single PEV. Also, the maximum allowed currents of the lines and transformers are calculated and added as an additional power limit to the model of a PEV. Later on, an aggregate model of PEVs for the PFC is proposed, where the power consumed in distribution network and maximum allowed power of the lines and transformers are implemented. The aggregate model is simulated and tested in a CIGRE benchmark and simulation results will be presented. Finally, the main conclusions are drawn.

4.1. Introduction

In the previous chapter, the characteristics of PEVs, which are required to properly analyse the PFC, were implemented and extensively studied. In spite of this, to model the PEVs, we assumed that all PEVs were unrealistically connected to the high-voltage transmission network. In other words, for the sake of simplification, we neglected the distribution networks, to which PEVs will be mostly connected in the near future.

In this chapter, in particular distribution network characteristics are considered and incorporated into the previously developed model of PEVs for the PFC. The main research questions, which will be addressed in this chapter, are posed as follows:

- *Does the dynamic behaviour of distribution networks have an impact on the performance of the aggregate model of PEVs for the PFC?*
- *Which characteristics of distribution networks have a significant impact on the provision of PFC by PEVs?*
- *How would the characteristics of distribution networks be formulated and then incorporated into the aggregate model of PEVs for the PFC studies?*

In order to properly address the above mentioned questions, first we provide an overview of the aggregation of distributed energy resources in power systems. In previous research, to efficiently study the dynamic behavior of a large number of DERs, their aggregate models have been extensively proposed and developed. In

fact, in the past, these aggregate dynamic models were mainly utilized either for transient stability or frequency stability analyses, which were classified and described in (Kundur et al., 1994).

To study the transient stability, aggregate models of wind farms or induction machines in power systems have been developed and studied (Conroy & Watson, 2009; Fernandez et al., 2008; Nozari et al., 1984; Taleb et al., 1994). In fact, these models have been highly required in order to significantly reduce not only the simulation time, but also the computational complexity of modeling a large number of units. While aggregate models of wind farms have been developed at the high-voltage transmission side, the aggregate models of induction machines have been proposed at the low-voltage distribution side as follows:

- At the high-voltage transmission side, in (Akhmatov, 2004; Conroy & Watson, 2009; Mercado-Vargas et al., 2015), aggregate models of wind turbines have been proposed either for fixed-speed or variable-speed wind turbines. In (Conroy & Watson, 2009), the transient behavior of a wind farm including full-converter wind turbine generators has been analyzed. In (Mercado-Vargas et al., 2015), three aggregate models of a wind farm have been developed by adapting various aggregation criteria that exist in the technical literature.
- At the low-voltage distribution side, aggregate models of induction machines have been developed for transient stability studies (Nozari et al., 1987, 1984). In (Nozari et al., 1987), a technique has been developed to obtain an equivalent model of induction machines, where the most important parameters of the motor have been calculated from standards. In (Taleb et al., 1994), a method for the aggregation of induction motor loads has been proposed where their equivalent transient characteristics have been calculated using Thevenin theorem.

To study the frequency stability, aggregate models of PEVs have been proposed and developed in previous research (Galus et al., 2011; Mu et al., 2013a; Pillai & Bak-Jensen, 2011; Ulbig et al., 2010). While in (Galus et al., 2011; Pillai & Bak-Jensen, 2011; Ulbig et al., 2010), aggregate models of PEVs for the load frequency control have been provided, a preliminary aggregate model of PEVs for the PFC has been developed in (Mu et al., 2013a). In (Mu et al., 2013a), a preliminary aggregate model of PEVs for the PFC has been developed. The PEV charging power based on the statistical behavior of PEVs has been initially estimated, and then according to the battery state of charge of PEVs, the aggregate primary reserve of PEVs for PFC has been obtained. To obtain this preliminary aggregate model of PEVs, the sum of the output charging power of all PEVs was calculated. Note that in this model, no dynamic frequency-droop controller was implemented, as PEVs are abruptly disconnected following the disturbance (zero droop).

Despite the fact that the above-mentioned models have represented the behavior of PEVs for the frequency control, these models have not taken into account distribution networks, to which PEVs will be mostly connected in the future. The dynamic

response of distribution networks might largely affect the performance of PEVs for the PFC, and consequently it can not be simply neglected due to the following reasons. First, a substantial amount of the power losses in present-day power systems occurs in low-voltage distribution networks. Since PEVs mostly participate in the PFC at the low-voltage grids, the power consumed in the network definitively varies during the PFC that might considerably affect the dynamic behavior of power systems (e.g., 15%). On top of this, PEVs might largely change the current of the distribution lines and transformers during the PFC, and therefore the protection devices installed on the distribution networks might be unexpectedly activated. In conclusion, if the distribution networks are neglected in the aggregate model of PEVs for the PFC, then this might result in a serious error in the PFC studies. As a result, in this chapter, we make the previous aggregate models of PEVs for PFC more accurate by additionally taking into account the distribution networks. To this end, first the most relevant characteristics of distribution networks for the PFC analysis are to be identified and justified. It is worth underlying that though these characteristics are particularly considered for aggregate models of PEVs for the PFC, they remain valid and relevant for other types of DERs, which also participate in the PFC together with PEVs at the low-voltage distribution networks.

To identify proper distribution network characteristics for the PFC analysis, in the beginning, all possibly related characteristics of distribution networks to the PFC study are listed. These characteristics include power consumed in the network, maximum allowed current of the lines and transformers, voltage levels, voltage regulators, and capacitor banks. In principle, since the distribution network will be modelled in per unit, the voltage levels are implicitly considered. Moreover, we assume that PEVs only change their active power in order to provide the PFC (or in other words, PEVs do not provide reactive power support), and consequently voltage regulators and capacitor banks could be neglected in this analysis. Thus, from the above provided list, the most relevant characteristics of distribution networks, which must be taken into account for the PFC by PEVs, are as follows:

1. Distribution network power consumption (DNPC): The DNPC significantly characterizes the dynamic behavior of distribution networks. Since for the PFC, PEVs largely vary their active power from the bottom of the distribution network, undoubtedly they highly affect the level of power consumed in all lines of the distribution network. This is why, it is expected that the large variation of power consumed in the network during the PFC service could highly impact the performance of the previously-developed aggregate models of PEVs for the PFC.
2. Maximum current limit of the distribution transformers and lines: In present-day power systems, the transformers and lines are to be protected using over-current relays /or fuses. Depending on the level of the current, these protection devices are typically activated after a certain period of time, and consequently disconnect the line or transformer. For the PFC service, in the case of over-frequency problems, PEVs immediately increase their charging power following

a contingency event. Therefore, the current of the lines and transformers might largely increase, and unexpectedly the over-current /or fuse protection would be activated. To avoid such problems in the future distribution networks, it is very relevant to take into account this characteristic of the network for the PFC analysis.

This chapter comprises of the following seven Sections:

- Section 4.2 generally describes the provision of PFC by PEVs within the electrical distribution networks over time.
- Section 4.3 presents the proposed model of a single PEV for the PFC which takes into account the above-mentioned distribution network characteristics. It is worth mentioning that here a simplified radial distribution network including only a PEV is considered and analyzed. Therefore, the proposed formulation can be more easily followed and understood.
- Section 4.4 proposes an aggregate model of PEVs for the PFC, in which the dynamic behavior of distribution networks is incorporated. Therefore, in this section, the proposed model of a single PEV is easily generalized to a large-scale distribution network due to its linear structure.
- Section 4.5 presents the low-voltage CIGRE benchmark, which is particularly created to evaluate the performance of the aggregate model of PEVs in low-voltage distribution networks. Moreover, this section describes the simulation scenarios and sensitivity analyses.
- Section 4.6 compares simulation results obtained from the detailed model and the proposed aggregate model of PEVs. Moreover, the results of the sensitivity analysis are provided and then discussed.
- Section 4.7 concludes this chapter and the outlook of the next chapter is presented.

4.2. Context of PFC by PEVs Within Distribution Networks Over Time

As mentioned above, various characteristics of distribution networks are to be considered especially when the provision of PFC by electric vehicles connected to the distribution network is studied and evaluated. To this end, we identified two key network's characteristics, i.e., power consumed in the network¹ and maximum current limit of the distribution transformers and lines, which might greatly affect the participation of PEVs in the PFC over time. In order to be able to properly evaluate

¹In this section, we mainly address the power consumed in the low-voltage distribution networks because typically a considerable portion of power consumption occurs at the low voltage side. However, the same formulation and considerations will hold true at the medium voltage side.

the dynamic behavior of distribution networks including PEVs, first it is of great importance to introduce the most relevant parameters of PEV fleets, which largely vary over time. In the previous section, a number of important PEV fleet's parameters such as battery state of charge, number of grid-connected PEVs, upward and downward power reserves were introduced and thoroughly described. However in the previous section, the spatial distribution of PEVs throughout the network were neglected or in other words, PEVs were assumed to be connected at the high voltage transmission level in the model. Despite this fact, low voltage distribution networks might highly affect the dynamic response of distributed PEVs that is reflected from the low voltage side to the high voltage side. In summary, here we mainly introduce and address the impact of the location of PEVs across the network on their performance during the PFC.

In fact, PEVs could be charged and connected to the electrical grid in different locations during the day. This undoubtedly affects the dynamic behavior and operational characteristics of distribution networks like the power consumed in the network along the day. For instance, if a large number of PEVs are connected at the very end of the distribution feeder, then the level of power consumed in the network may obtain a higher value compared to the case, in which a large number of PEVs are connected at the head of the distribution feeder. Since PEVs dynamically change their active power during the PFC, the level of power consumed in distribution networks will accordingly vary during the PFC taking into account the spatial distribution of PEVs along the distribution feeder. Moreover, if PEVs are mostly connected to the very end of the distribution feeder, then a greater number of distribution lines might be congested or reach the maximum limits of overcurrent relay protection. Note that during the over-frequency problems, PEVs increase their charging power during the PFC, and as a result, some distribution lines might reach their maximum limits depending on the location, in which PEVs are connected to the electrical grid.

Besides, obviously the number of PEVs connected to each specific bus bar might largely vary during the day, as PEVs are connected to and disconnected from the grid in various bus bars along the day. For instance, on the one hand, at a workplace, a large number of PEVs are connected to the bus bar in the morning and are disconnected from the bus bar in the afternoon. Therefore, while a large number of PEVs are connected during day at the workplace, a very low number of PEVs might be connected to that bus bar over night. On the other hand, a larger number of PEVs might be connected to the low-voltage residential bus bars over night especially when PEVs arrive at home after the work. In summary, during the day, PEVs could provide the PFC from various locations, because of which the dynamic response of distribution networks including PEVs might be very different.

Also, as comprehensively mentioned in the previous chapter, the available power reserve of PEVs depends on both the actual charging power as well as the maximum /and minimum battery charger power limits. Regarding the charging power of PEVs, this highly depends on the idle or charging mode, and if in charging, depends

on the constant current or constant voltage mode of PEVs during the day. Additionally, since PEVs could be charged using different battery chargers at a specific location, then the total charging power at each specific bus bar could accordingly vary during the day. In conclusion, at each specific bus bar, the total upward and downward power reserves of PEVs might significantly vary during the day depending on the above mentioned parameters (i.e., number of PEVs, charging power of PEVs, maximum /and minimum power of battery chargers).

Finally, it is worth underlying that not only the location of PEVs could be an essential factor, but also the spatial distribution of distributed generation units and loads along the network is a significant feature to represent the dynamic behavior of the network during the PFC. In fact, on the one hand, if the loads are mostly connected at the end of the distribution feeder then generally the total power consumed in the network would largely increase. On the other hand, if the distributed generation are mostly connected at the end of the distribution feeder then generally the total power consumed in the network would largely decrease. Nonetheless, obviously the impact of distributed generation and loads on the power consumed in the network might be negligible when they are connected the the head of the distribution feeder. In addition, the number of distribution lines, which might reach their maximum power limit during the PFC, might greatly depend on the spatial distribution of distributed generation units and loads. Therefore, in the next section, we will simultaneously take into account the spatial distribution of not only PEVs, but also the distributed generation units and loads.

Taking into account the above-mentioned factors, next we will formulate and develop an equivalent model of a single PEV for the PFC within a radial distribution network. To this end, first we introduce the simplified network including a PEV, and provide some reasonable simplifying assumptions. Then, we formulate the equivalent model of a PEVs considering the dynamic behavior of the distribution network.

4.3. Equivalent Model of A Single PEV for PFC in a Radial Distribution Network

First of all, distribution network characteristics such as power consumed in the network and maximum allowed current of the lines and transformers are calculated and obtained. The power consumed in the network is calculated in the two-axis dq reference frame. Moreover, the maximum allowed currents of the lines are taken into consideration, and accordingly a new power limit for the PFC loop of PEVs is proposed. Finally, we incorporate the already calculated characteristics of distribution networks into the model of a single PEV for the PFC.

4.3.1. Power Consumed in Distribution Network

In this subsection, our aim is to calculate the instantaneous power consumed at medium voltage (MV) level, when a single PEV participates in the PFC at the end of a low-voltage distribution feeder. To more easily express the dynamic model of the network, here a two-axis dq reference frame is utilized where the current of lines and voltage of buses are represented in this reference frame using the power-invariant park transformation. Then, the power consumption associated with the distribution network is calculated.

First of all, it is necessary to introduce both steady-state and dynamic modes of the distribution network in this formulation. Before the frequency disturbance, the distribution network is in the steady state, and consequently the current of lines as well as the power consumed in the network can be assumed constant. While, during the frequency disturbance, the distribution network is undergoing a transient state, and therefore the power consumed in the network vary according to the dynamic model of the network.

4.3.1.1. Voltages and Currents in the dq Reference Frame

Figure. 4.1 shows a multi-feeder distribution network with a radial configuration, which has a single PEV participating in the PFC. The distribution network is simply represented by feeder 1 including Load 1 and PEV 1, and also other feeders including Load 2. In general, within the rotating dq reference frame, the choice of the dq reference is arbitrary even though it is typically aligned with the voltage reference. This way, it will be easier to obtain the active and reactive power, which can be calculated by $v_d \cdot i_d$ and $v_d \cdot i_q$, respectively. To do so, here the d -axis is aligned with the voltage vector, thus the q -axis voltage V_q can be assumed equal to zero.

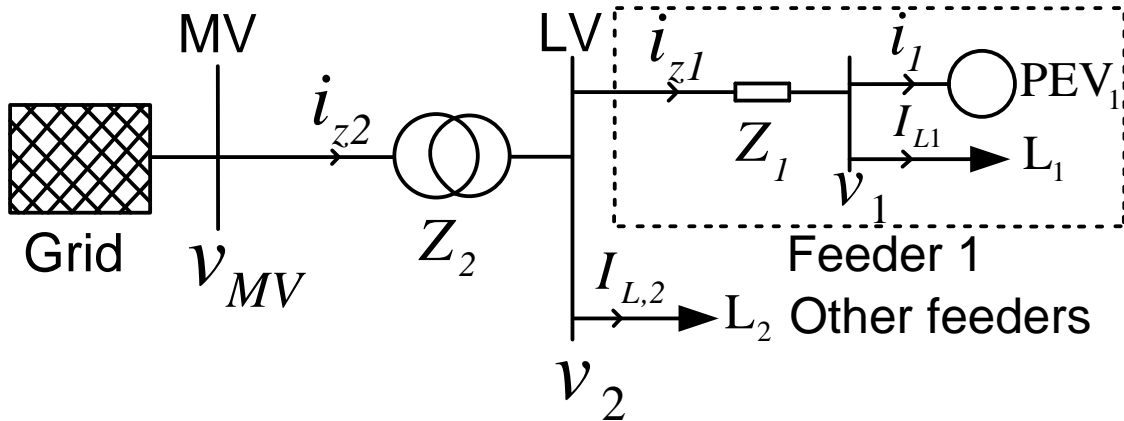


Figure 4.1.: Distribution network representation in a radial configuration including a single PEV model and loads.

The current of PEV in the dq reference frames $i_1 = i_{d,1} + j \cdot i_{q,1}$ can be given by:

$$i_{d,1} = I_{d,1} + \Delta i_{d,1} \quad (4.1)$$

$$i_{q,1} = I_{q,1} + \Delta i_{q,1} \quad (4.2)$$

where $I_{d,1}$, $I_{q,1}$, $\Delta i_{d,1}$, and $\Delta i_{q,1}$ are the d - and q - axis currents of the PEV before the disturbance and the d - and q - axis current increment of the PEV during the disturbance, respectively.

Similarly, the current of impedance 1 in the dq reference frames $i_{z1} = i_{d,z1} + j \cdot i_{q,z1}$ and the current of impedance 2 in the dq reference frames $i_{z2} = i_{d,z2} + j \cdot i_{q,z2}$ can be written as

$$i_{d,z1} = I_{d,z1} + \Delta i_{d,z1} \quad (4.3)$$

$$i_{q,z1} = I_{q,z1} + \Delta i_{q,z1} \quad (4.4)$$

$$i_{d,z2} = I_{d,z2} + \Delta i_{d,z2} \quad (4.5)$$

$$i_{q,z2} = I_{q,z2} + \Delta i_{q,z2} \quad (4.6)$$

Since the dynamic behavior of the distribution network is highly complex, inevitably for this formulation, some simplifying assumptions are made that are presented in the next subsection.

4.3.1.2. Simplifying Assumptions

The provision of PFC by PEVs at the low-voltage distribution side affects the voltage of buses and current of the lines. However, this might have negligible impact on the performance of other electrical components like loads. Moreover, since for the PFC service, it is required that PEVs inject active power into the grid, their reactive power variation could be assumed zero. Therefore, reactive power flows could be basically assumed constant for this analysis.

In summary, some simplifying assumptions of this formulation for the PFC analysis are made as follows:

- The PEV changes its power only for PFC, and consequently the d -axis charging current varies during the frequency disturbance. In other words, during the PFC, the PEV does not simultaneously provide dynamic reactive power/voltage support. As a result, $\Delta i_{q,1}$ is equal to zero.
- The current of loads 1 and 2 are assumed constant during the PFC (i.e., during the disturbance, the loads current variations Δi_{L1} and Δi_{L2} are equal to zero). However, in practice some loads respond to the frequency deviations. For instance, dynamic loads such as induction machines also respond to the frequency deviations, however their participation in the PFC is typically much lower than the one of PEVs. Hence, the power variation of induction machines compared to PEVs has been neglected. In spite of this, it is important to point out that later the case studies will include the detailed model of the loads consisting of both static and dynamic loads (e.g., heating systems and induction machines).
- According to the previous assumption, since the current of load 2 remains constant during the PFC, the current variation of impedance 2 remains equal to the current variation of impedance 1.
- Small voltage variations during the frequency disturbance are neglected ($v_d = V_d + \Delta v_d \simeq V_d$). In fact it is assumed that the PEV largely changes the current for the PFC, and the absolute value of the reference voltage is negligibly affected by the PEV current injection.
- The main focus of this study will be on the distribution networks, where the power consumed in the network has a high value. We assume that the voltage at HV transmission line is not affected by the disturbance. If the voltage at the HV transmission side is affected by the disturbance, then the load power at HV side might vary as well. This potential problem at HV transmission side is outside the scope of this analysis, and is included as a relevant future research.

Next, the power consumed in the distribution network lines is formulated.

4.3.1.3. Instantaneous Power Consumption in a Radial Distribution Network Including a Single PEV

Technically speaking, for the PFC analysis, the non-linear components of power systems (e.g., turbine governor models) are to be always linearized around their operating mode (Kundur et al., 1994). Though this might obviously cause an error, the computational effort and complexity can be significantly reduced. Note that the power consumed in the network is a non-linear function of the line current that can not be directly used for the PFC analysis.

The total consumed power variation during the disturbance is the sum of the power consumed in the resistances Δp_R and the power consumed in the inductances Δp_L

of impedances 1 and 2 in Figure. 4.1. In fact, the inductance has already stored a certain amount of energy according to the absolute value of the current, and when its current varies during the PFC, the level of the stored energy in the inductance start to largely vary. This way, the inductance consumes a certain amount of active power, and therefore an amount of active power would be provided or dissipated in the inductance of each line. Therefore, here we calculate the power consumption increment of the resistances and inductances with respect to the current variation of a single PEV during both steady-state (i.e., before the disturbance) and dynamic modes (during the disturbance).

Variation of power losses in the resistance during PFC

The power losses in the resistance R_1^L of impedance 1 during the disturbance (p_{R1}) is written as:

$$p_{R1} = R_1^L \cdot [i_{d,z1}^2 + i_{q,z1}^2] \quad (4.7)$$

Taking into account the following equations

$$i_{d,z1} = I_{d,z1} + \Delta i_{d,z1} \quad (4.8)$$

$$\Delta i_{q,z1} = 0 \quad (4.9)$$

Equation (4.7) is rewritten as follows:

$$p_{R1} = R_1^L \cdot [\Delta i_{d,z1}^2 + 2\Delta i_{d,z1} \cdot I_{d,z1} + I_{d,z1}^2 + I_{q,z1}^2] \quad (4.10)$$

Then, the increment of power losses in resistance 1 during the disturbance (Δp_{R1}) is given by:

$$\Delta p_{R1} = R_1^L \cdot [\Delta i_{d,z1}^2 + 2\Delta i_{d,z1} \cdot I_{d,z1}] \quad (4.11)$$

Similarly, the increment of power losses in resistance 2 during the disturbance (Δp_{R2}) is written as

$$\Delta p_{R2} = R_2^L \cdot [\Delta i_{d,z2}^2 + 2\Delta i_{d,z2} \cdot I_{d,z2}] \quad (4.12)$$

where R_2^L is the resistance of impedance 2 (Z_2). Therefore, the total increment of power losses in resistances 1 and 2 (Δp_R) can be given by

$$\Delta p_R = R_1^L \cdot \Delta i_{d,z1} \cdot [\Delta i_{d,z1} + 2 \cdot I_{d,z1}] + R_2^L \cdot \Delta i_{d,z2} \cdot [\Delta i_{d,z2} + 2 \cdot I_{d,z2}] \quad (4.13)$$

For the sake of simplification, we might be able to neglect $\Delta i_{d,z1}$ against $2 \cdot I_{d,z1}$, which is twice the sum of both d -axis currents of load 1 and PEV 1 (see the discussion below). If so, (4.13) can be simplified as follows:

$$\Delta p_R = 2 \cdot R_1^L \cdot \Delta i_{d,z1} \cdot I_{d,z1} + 2 \cdot R_2^L \cdot \Delta i_{d,z2} \cdot I_{d,z2} \quad (4.14)$$

Discussion on potential limitations of the above simplification

First of all, we consider a generic electrical network, which is shown in Figure. 4.2. The electrical network consists of generators and grids, each of which has a number of feeders including loads and PEVs. Generally speaking, three types of disturbances may occur in this network as follows: 1) trip of one feeder (i.e., low disturbance), 2) trip of one grid (i.e., high disturbance), and 3) trip of one generator. Then, the following observations can be taken into account:

- As the total power generation increases in an electrical network, the size of the disturbance increments. For instance in Figure. 4.2, the trip of one feeder or one grid would be obviously larger, if the total power consumption was higher. Similarly, each generator is to inject more active power when the total load is higher. Therefore, the previous assertion can also be applied for the loss of generation.
- In future electrical networks, it can be assumed that PEVs are distributed all over the network. In such context, it is sensible to consider the correlation, in each grid, between the current consumed and the current variation of PEVs.

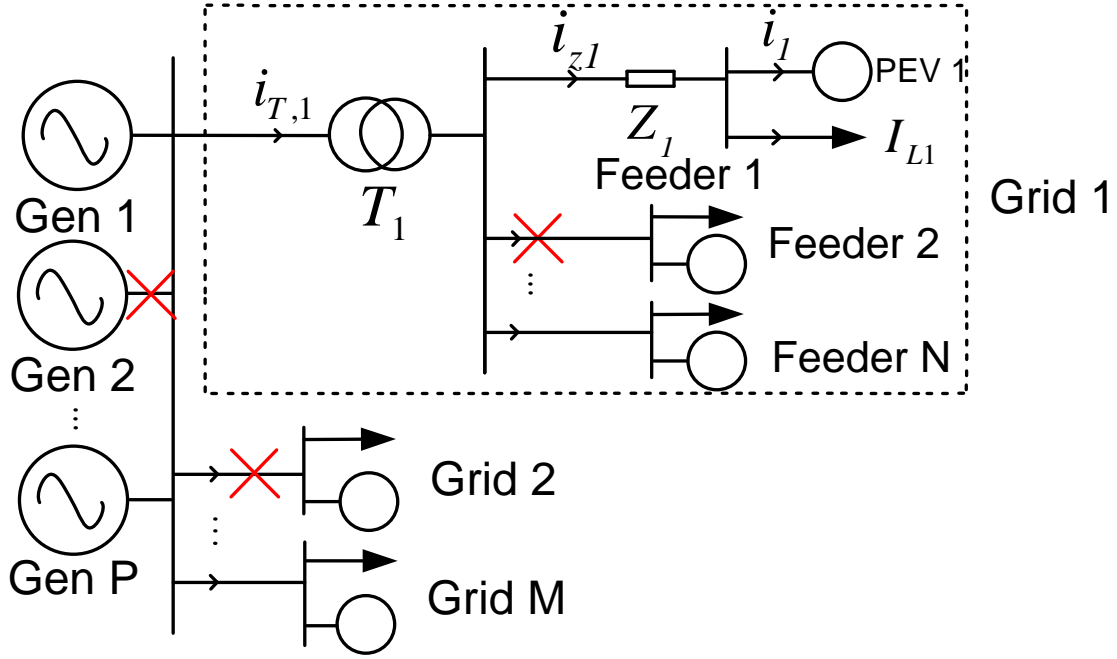


Figure 4.2.: Possible types of disturbances in the electrical network under study.

Taking into account two above-mentioned observations, we can conclude that there is a correlation between the disturbance and the participation from each grid/feeder in the PFC. Thus, if the relative size of the disturbance has a large value (i.e., context of very small grid including few lines), then the simplification might cause an error. However, if the relative size of the disturbance has a medium or low value, then the simplification may have a negligible error. This thesis mainly addresses medium or large-scale electrical networks, which are typically subject to the medium (e.g., up to 20%) or low values (e.g., up to 5%) of the disturbance, respectively. As a result, it is reasonable and almost accurate to apply this simplification here within the scope of this research work.

Variation of power consumed in the inductance during PFC

Since the current of the line inductance changes during the frequency disturbance, inevitably the energy stored in inductance 1 (e_{L1}) varies. As a result, a certain amount of active power (p_{L1}) could be provided or consumed in the inductance of each line during the frequency disturbance as follows

$$p_{L1} = \frac{de_{L1}}{dt} \tag{4.15}$$

$$p_{L1} = \frac{d\left(\frac{1}{2} \cdot L_1^L \cdot [i_{d,z1}^2 + i_{q,z1}^2]\right)}{dt} \quad (4.16)$$

where L_1^L is the inductance of line 1. As $i_{q,z1}$ remains constant during the PFC, then

$$p_{L1} = \frac{1}{2} \cdot L_1^L \frac{d(i_{d,z1}^2)}{dt} \quad (4.17)$$

deriving and simplifying,

$$p_{L1} = i_{d,z1} \cdot L_1^L \frac{d(i_{d,z1})}{dt} \quad (4.18)$$

Finally, using (4.8) and simplifying, the increment of inductance power Δp_{L1} during PFC can be written as:

$$\Delta p_{L1} = L_1^L \cdot (I_{d,z1} + \Delta i_{d,z1}) \cdot \frac{d(\Delta i_{d,z1})}{dt} \quad (4.19)$$

Similarly, the increment of power in inductance 2 (Δp_{L2}) during PFC is equal to

$$\Delta p_{L2} = L_2^L \cdot (I_{d,z2} + \Delta i_{d,z2}) \cdot \frac{d(\Delta i_{d,z2})}{dt} \quad (4.20)$$

where L_2^L is the inductance of line 2. Therefore, the total increment of power in inductances 1 and 2 (Δp_L) during PFC is equal to

$$\Delta p_L = L_1^L \cdot (I_{d,z1} + \Delta i_{d,z1}) \cdot \frac{d(\Delta i_{d,z1})}{dt} + L_2^L \cdot (I_{d,z2} + \Delta i_{d,z2}) \cdot \frac{d(\Delta i_{d,z2})}{dt} \quad (4.21)$$

If the assumptions in previous subsection will hold, Δp_L can be also simplified as follows:

$$\Delta p_L = L_1^L \cdot I_{d,z1} \cdot \frac{d(\Delta i_{d,z1})}{dt} + L_2^L \cdot I_{d,z2} \cdot \frac{d(\Delta i_{d,z2})}{dt} \quad (4.22)$$

Total power consumption increment in the line impedances

The total power consumption increment is the sum of the power consumption increment of resistances and inductances, which were obtained in the previous steps. The variation of the total power consumed during the disturbance Δp_{DNPC} , which is the sum of power variation in resistances Δp_R in (4.11) and inductances Δp_L in (4.19), is given by:

$$\Delta p_{DNPC} = \Delta p_R + \Delta p_L \quad (4.23)$$

$$\begin{aligned} \Delta p_{DNPC} = & R_1^L \cdot [\Delta i_{d,z1}^2 + 2\Delta i_{d,z1} \cdot I_{d,z1}] + L_1^L \cdot (I_{d,z1} + \Delta i_{d,z1}) \cdot \frac{d(\Delta i_{d,z1})}{dt} \\ & + R_2^L \cdot [\Delta i_{d,z2}^2 + 2\Delta i_{d,z2} \cdot I_{d,z2}] + L_2^L \cdot (I_{d,z2} + \Delta i_{d,z2}) \cdot \frac{d(\Delta i_{d,z2})}{dt} \end{aligned} \quad (4.24)$$

The PEV current variation Δi_d is relatively small compared to the total impedance current $I_{d,z}$, which includes the power consumption of both PEVs and large loads within the area. Thus, Δp_{DNPC} can be given by:

$$\begin{aligned} \Delta p_{DNPC} = & 2 \cdot \left(R_1^L + \frac{L_1^L}{2} \cdot s \right) \cdot \Delta i_{d,1} \cdot I_{d,z1} \\ & + 2 \cdot \left(R_2^L + \frac{L_2^L}{2} \cdot s \right) \cdot \Delta i_{d,2} \cdot I_{d,z2}. \end{aligned} \quad (4.25)$$

In order to further elaborate the (4.24), it is possible and required to neglect the small voltage variation during the frequency disturbance ($v_d = V_d + \Delta v_d \simeq V_d$). Therefore, a low value term $\Delta v_d \cdot \Delta i_{d,1}$ from the power consumption equation could be neglected. Taking into account two previous assumptions, (4.24) is multiplied by

d -axis voltages V_d , and then Δp_{DNPC} is given by:

$$\Delta p_{DNPC} = \underbrace{\frac{2 \cdot P_{z1}}{V_{d,1}^2} \cdot \left(R_1^L + \frac{L_1^L}{2} \cdot s \right)}_{LF_1} \cdot \Delta p_1 + \underbrace{\frac{2 \cdot P_{z2}}{V_{d,2}^2} \cdot \left(R_2^L + \frac{L_2^L}{2} \cdot s \right)}_{LF_2} \cdot \Delta p_{z1} \quad (4.26)$$

$$\Delta p_{z1} = \underbrace{\frac{2 \cdot P_{z1}}{V_{d,1}^2} \cdot \left(R_1^L + \frac{L_1^L}{2} \cdot s \right)}_{LF_1} \cdot \Delta p_1 \quad (4.27)$$

$$\Delta p_{z2} = \underbrace{\frac{2 \cdot P_{z2}}{V_{d,2}^2} \cdot \left(R_2^L + \frac{L_2^L}{2} \cdot s \right)}_{LF_2} \cdot \Delta p_{z1} \quad (4.28)$$

$$\Delta p_{DNPC} = \Delta p_{z1} + \Delta p_{z2} \quad (4.29)$$

where P_{z1} , P_{z2} , $V_{d,1}$, $V_{d,2}$, Δp_1 , Δp_{z1} , and Δp_{z2} are the three-phase active power of impedances 1 and 2 before the disturbance, the d -axis voltage in buses 1 and 2 before the disturbance, the power variation of the single PEV and impedances 1 and 2 during the disturbance, respectively. Δp_1 , Δp_{z1} and Δp_{z2} are shown in Figure 4.3.

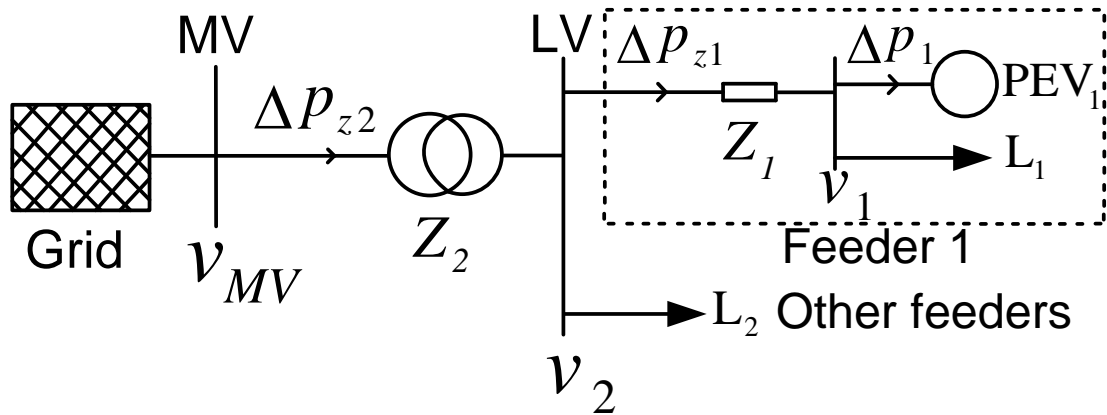


Figure 4.3.: Distribution network representation in a radial configuration including a single PEV model and loads.

As seen in (4.26), a new parameter LF has been proposed and introduced that stands for the line factor. In simple words, the line factor represents the power consumption variation of each line according the power variation of its corresponding bus bar. In (4.26), LF_1 and LF_2 are the constant line factors of impedances 1 and 2, respectively. Therefore, Δp_{DNPC} is re-written as:

$$\Delta p_{DNPC} = LF_1 \cdot \Delta p_1 + LF_2 \cdot \Delta p_{z1}. \quad (4.30)$$

where in a similar way, the power variation of impedance 1 Δp_{z1} is given by

$$\Delta p_{z1} = \Delta p_1 + LF_1 \cdot \Delta p_1. \quad (4.31)$$

By substituting Δp_{z1} according to (4.30) and (4.31), Δp_{DNPC} is finally formulated as:

$$\Delta p_{DNPC} = (LF_1 + LF_2 + LF_1 \cdot LF_2) \cdot \Delta p_1 \quad (4.32)$$

Equation (4.32) clearly shows that the total power consumption variation in a simplified distribution network can be easily obtained according to the power variation of a single PEV. Since (4.32) has a linear structure, it is possible to flexibly extend our proposed formulation to other large-scale distribution networks.

Next, another essential characteristic of distribution networks, i.e., maximum allowed current of the lines and transformers, is addressed and calculated.

4.3.2. Maximum Allowed Current of A Single PEV for PFC

In the existing power systems, the transformers and lines are to be protected by over-current relays or fuses. Depending on the current value, these protection devices are typically activated after a certain period of time, and consequently disconnect the line or transformer. In fact the provision of PFC by PEVs might unexpectedly activate the protection devices, and this is why here the current variation of lines and transformers during the PFC by PEVs is further analyzed.

Typically, during the over-frequency problems, the PEV participates in the PFC by increasing its charging current. As mentioned, this might get the transformer or the line overloaded during the PFC. To avoid this, the PEV active current for PFC should be calculated and later on should be compared to the maximum allowed current of transformer I_{z2}^{max} . If the current of the transformer in the dq reference

frame is $I_{d,z2} + j \cdot I_{q,z2}$, then the current variation of the PEV due to the transformer limit ΔI_{z2}^{max} is written as

$$\Delta I_{z2}^{max} = \sqrt{(I_{z2}^{max})^2 - I_{q,z2}^2} - I_{d,z2}. \quad (4.33)$$

Equation (4.33) demonstrates that the PEV should not increase its charging current during the frequency disturbance more than the obtained ΔI_{z2}^{max} . Note that the maximum current of transformer is to be selected according to the nominal power of transformer (e.g., 1.1 times of the nominal value), in such a way that the over-current protection would not be activated over time and consequently would not trip the whole feeder.

In order to properly implement the current limit in a single PEV, the following points must be taken into consideration:

- It is worth mentioning that the calculated limit is not a dynamic limit (i.e., is a static limit), or in other words, it does not change during the PFC. The limit is calculated in the steady-state (before the disturbance), and then remains constant during the frequency disturbance. This way, it is possible to calculate and periodically update this limit in practice over a certain period of time (e.g., every 10 minutes).
- In the previous chapter, the upward and downward power reserves of a single PEV were calculated and shown. However these power limits were calculated while the configuration of the electrical grid was totally neglected. Technically speaking, though PEVs are able to completely provide their upward or downward power reserves, this might have severe impacts on the operation of electrical grids. Therefore in future, some additional power/current limits associated with the network might be highly required to be implemented in PEVs, when they provide the PFC.
- In practice, PEV owners do not generally have access to the operational data of the electrical grids. Therefore, they are not able to calculate and implement appropriate current limits for PEVs in order to mitigate their serious impacts on the electric grids. As an alternative, to implement this limit in the PEV fleet, an aggregating entity, e.g., the so-called aggregator of PEVs, might be envisioned in the future. This entity might have access to some operational data of the electrical grids, and consequently might be able to calculate the current limit of each PEV for PFC on a time basis, e.g., a quarter-hour basis, according to (4.33). Then, the aggregator can send these current limit signals to the corresponding PEVs. This way, the system operators could ensure that the provision of PFC by PEVs do not substantially put at risk the safe operation of distribution networks.

In the next step, an equivalent model of a single PEV for the PFC is proposed, into which the two above-mentioned characteristics are further incorporated.

4.3.3. PEV Equivalent Model for PFC Including Proposed Distribution Network and Transformer Limit

In the previous steps, two important characteristics of distribution networks were formulated and obtained in a linear fashion. This helps us in this section to flexibly add these characteristics to the aggregate model of PEVs for the PFC, which also has a linear structure. Figure. 4.4 shows an equivalent model of a single PEV connected to the MV feeder of a radial distribution network. The proposed equivalent model of a single PEV that takes into account the yield DNPC calculation together with the maximum allowed current of PEV due to the transformer is presented in Figure. 4.5. It is important to note that compared to the previous aggregate model presented in chapter 3, here we model and simulate the distribution network in more detail, and as a result the voltage and current signals are available. However, in the previous chapter, we employed the typical frequency control scheme of power systems that is only based on the variation of the frequency according to the active power variations (no current or voltage signals exist in that models). Since in this formulation, the voltage signals are available when the power flow is carried out, therefore the current signals can be accordingly calculated and used. Then, as the distribution lines as well as IGBT switches are rated based on the current, here the static limits of the battery charger and transformer can be precisely represented by the d - axis current rather than the active power.

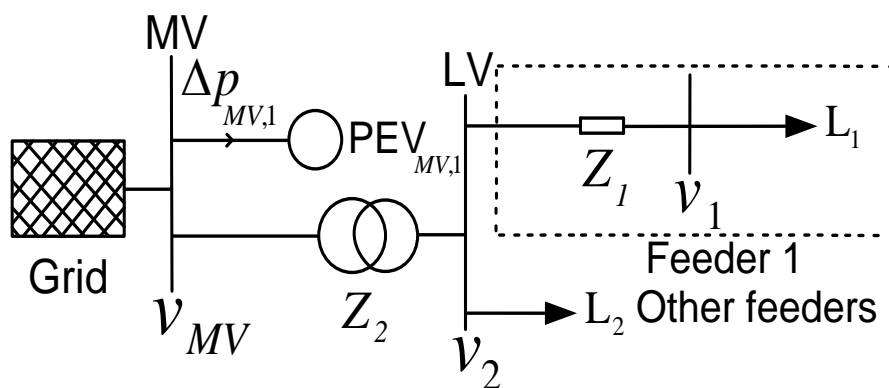


Figure 4.4.: Distribution network representation in a radial configuration including loads and an equivalent model of PEV.

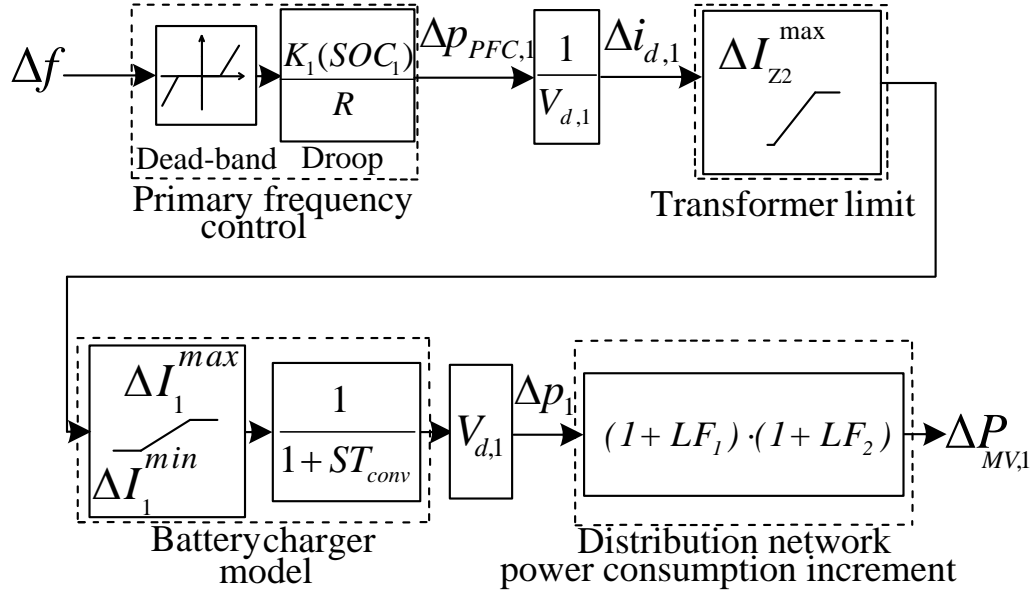


Figure 4.5.: Proposed aggregate model of a single PEV in a radial distribution network.

The equivalent model of PEV consists of the following functions:

1. Primary frequency control (for further information, also see the aggregate model of PEVs in chapter 3)
2. Proposed maximum allowed current of PEV
3. Closed-loop battery charger model (for further information, also see the aggregate model of PEVs in chapter 3)
4. Proposed distribution network power increment

The primary frequency control and the closed-loop battery charger model were formulated and extensively addresses in the previous chapter. However the previous models of PEVs for the PFC were only a function of PEV active power, where the distribution networks were not considered. In this formulation, it is highly required to take into account current signals due to the following reasons:

- As mentioned, the distribution lines and transformers are typically rated based on their current,
- The power consumed in the network is more easily calculated according to the line current,
- The protection devices like over-current relays operate according to the measured line currents,
- The fast switches (e.g., IGBT based switches) of battery chargers are typically protected against excessive currents.

As a result, the previous model has been further improved by introducing the voltage and current signals. Note that the voltage and current signals are considered as static parameters. Therefore, they are once obtained in steady-state before the frequency disturbance, and then remain constant during the frequency disturbance.

Next, we present the equivalent model of a single PEV for the PFC. As extensively discussed in the previous chapter, here the primary frequency control and battery charger model are shortly reviewed. However, the distribution network power increment and maximum allowed current of PEVs for PFC, which are the main contribution of this chapter, are presented in detail.

4.3.3.1. Primary Frequency Control Loop

The primary frequency control loop was extensively explained in chapter 3, as also shown in Figure.4.5. Note that due to the above-mentioned reasons, the charging current variation of a single PEV $\Delta i_{d,1}$ is to be calculated instead of its power variation. To this end, the output power of the PFC loop $\Delta p_{PFC,1}$ is divided by the PEV d -axis voltage before the disturbance $V_{d,1}$, and as a result the charging current variation of a single PEV $\Delta i_{d,1}$ is obtained. Then, the current variation of a single PEV is constrained according the maximum allowed current of distribution line and transformer.

4.3.3.2. Proposed Maximum Current of a PEV due to Transformer Limit

In order to take into account the maximum current limits of distribution lines and transformers, a new limit for PEVs was proposed and introduced in this section. In fact this limit has been introduced to control the severe impacts of PEVs on the normal operation of distribution networks during the PFC. The maximum allowed current of the PEV for PFC was obtained in (4.33) and described in detail. This additional limit means that the PEV, which participates in the PFC, should not increase its charging current more than the maximum allowed limit ΔI_{z2}^{max} . On the one hand, if the maximum allowed current limit ΔI_{z2}^{max} is greater than the PEV's maximum upward current ΔI_1^{max} , then the PEV is not able to affect the operation of the network due to the battery charger's current limit. On the other hand, if the maximum allowed current limit ΔI_{z2}^{max} is lower than the PEV's maximum upward current ΔI_1^{max} , then the PEV's current variation for PFC should be limited though the PEV's current has not reached the maximum current limit of the battery charger. In other words, the maximum allowed current of PEV can be defined as the minimum of ΔI_{z2}^{max} and ΔI_1^{max} .

4.3.3.3. Closed-loop Battery Charger Model

The battery charger was extensively explained in chapter 3, as also shown in Figure. 4.5. Also, due to above-mentioned reasons, we calculate and obtain the PEV's maximum

downward ΔI_1^{max} and upward ΔI_1^{min} currents. These limits specify to what extent the PEV is able to increase/decrease its charging current during over/under frequency problems.

The downward ΔI_1^{max} and upward ΔI_1^{min} power reserves of a single PEV are given as follows:

$$\Delta I_1^{max} = I_1^{max} - I_{d,1} \quad (4.34)$$

$$\Delta I_1^{min} = I_1^{min} - I_{d,1} \quad (4.35)$$

where I_1^{max} and I_1^{min} are the maximum and minimum current limits of the battery charger, respectively. As discussed in the previous chapter, I_1^{min} typically depends on the topology of the battery charger. It is equal to zero and $-I_1^{max}$ for unidirectional and bidirectional battery chargers, respectively. Since the impact of the battery charger topologies of PEVs on their response was studied in detail in the previous chapter, here we do not further address and evaluate them.

The input of the battery charger model in Figure. 4.5 is the current signal. However to obtain the variation of power consumed in the network according to (4.32), it is necessary to calculate PEV power. Therefore, after the battery charger model in Figure. 4.5, the power variation of the PEV is obtained, where the charging current variation of PEV's battery charger is multiplied by $V_{d,1}$. Thus, the output current of the battery charger is used to obtain the PEV's power variation in Figure. 4.5, which is later fed into the distribution network block.

4.3.3.4. Distribution Network Power Increment

As shown in Figure. 4.1, a single PEV participates in the PFC at the very end of the distribution feeder, and our aim is to obtain the increment power of the distribution network at the medium voltage line. Therefore, the distribution network power consumption increment Δp_{DNPC} should be calculated according to the PEV power variation shown in (4.32). Figure. 4.4 clearly shows that the equivalent model of a single PEV at the medium voltage level not only should represent the power variation of the PEV, but also the variation of power consumed in the network during the PFC. Therefore, the power variation of the proposed equivalent model of a single PEV $\Delta p_{ag,MV}$ is equal to the sum of PEV power variation and DNPC increment Δp_{DNPC} in impedances 1 and 2. In simple terms, $\Delta p_{ag,MV}$ in Figure. 4.5 is given as follows:

$$\Delta P_{ag,MV} = \Delta p_1 + \Delta p_{DNPC} \quad (4.36)$$

By substituting Δp_{DNPC} according to (4.32),

$$\Delta P_{ag,MV} = \Delta p_1 \cdot (1 + LF_1) \cdot (1 + LF_2). \quad (4.37)$$

Equation (4.37) illustrates that the variation of power consumed in the network according to the PEV power variation can be flexibly implemented by introducing the line factors in a linear fashion. This important flexibility can be effectively employed, when a large-scale distribution network including a large number of PEVs is taken into account. Therefore, next, we generalize the here-presented equivalent model of a single PEV to a large-scale PEV fleet using mainly the line factors.

4.4. Aggregate Model of a Large-scale PEV Fleet in a Radial Distribution Network for PFC

In this section, the equivalent model of a single PEV, which was calculated in (4.37), is generalized to a large scale PEV fleet. Similar to the previous model, the arithmetic averaging technique is essentially employed and applied to the proposed model that is a widely known technique. Two essential characteristics of the distribution networks for the PFC analysis, which are the power consumed in the network and the maximum current limit of the lines and transformers, are first calculated and incorporated into the proposed model of PEVs for the PFC in the following two subsections. In the end, the aggregate model of PEVs for the PFC will be proposed and described. As mentioned above, in the here-developed formulation, the variation of power consumed in the network during the PFC has a linear structure that provides a large amount of flexibility and extensibility in this section. This way, the formulation can be straightforwardly applied to a large number of PEVs, which are distributed along the distribution network.

4.4.1. Aggregate Fleet's Instantaneous Power Including Power Consumption in the Network During PFC

In order to formulate the aggregate model of PEVs, first it is required to calculate the aggregate instantaneous power at the head of the distribution network. To this end, we describe a typical distribution network, in which PEVs and loads² are distributed. Figure. 4.6 presents a radial distribution network that includes a feeder

²As mentioned before, for the sake of simplicity, in this formulation, other distributed generation units such as wind turbines and PV systems were neglected. In other words, we did not consider the dynamic behavior of other electronically-interfaced generating units connected to the low voltage distribution network during the PFC.

with the loads L_n and PEVs PEV_n connected to bus n . Note that n is an index for buses and impedances. In this feeder, different number of PEVs are connected to various bus bars, and all PEVs are potentially able to participate in the PFC. It is assumed that the loads do not participate in the PFC and consequently their currents remain constant during the frequency disturbance.

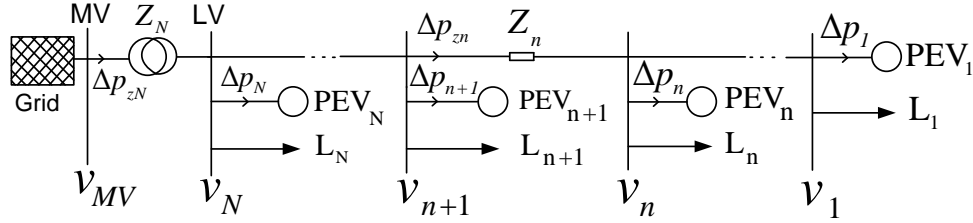


Figure 4.6.: Distribution network representation in a radial configuration including loads and a large scale distributed PEV fleet.

In Figure. 4.7, the aggregate model of PEVs is connected to the MV bus. The power variation of this aggregate model mainly includes the total power variation of PEVs as well as the variation of the power consumed along the distribution feeder during the frequency disturbance. It is important to point out that here we only aggregate PEVs for the PFC and the loads are not aggregated in this analysis.

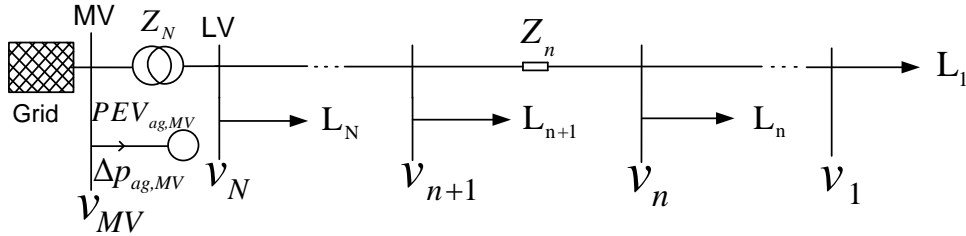


Figure 4.7.: Distribution network representation in a radial configuration including loads and an aggregate model of PEVs.

To obtain the aggregate model of the PEVs, the aggregation of distribution network is carried out bus-to-bus from PEV_1 in bus 1 up to PEV_N in bus N , as shown in Figure. 4.6 and Figure. 4.7. This way, PEVs connected to bus 1 are aggregated into bus 2, and so on. The resulting aggregate model, which is presumably connected to bus 2, not only incorporates the power variation of PEVs Δp_1 in bus 1, but also the power consumption increment Δp_{z_1} of impedance 1. As a result, the aggregate

power variation of PEVs $\Delta p_{2,1}$ in bus 2 with respect to the PEV power variation in bus 1 is obtained according to (4.32):

$$\Delta p_{2,1} = (1 + LF_1) \cdot \Delta p_1. \quad (4.38)$$

In a similar way, the aggregate power variation of PEVs $\Delta p_{3,1}$ in bus 3 with respect to the PEV power variation in bus 1, that incorporates both $\Delta p_{2,1}$ and power variation in impedance 2, is obtained in bus 3 as follows:

$$\Delta p_{3,1} = (1 + LF_2) \cdot \Delta p_{2,1} \quad (4.39)$$

$$\Delta p_{3,1} = (1 + LF_1) \cdot (1 + LF_2) \cdot \Delta p_1. \quad (4.40)$$

By generalizing (4.40) to all buses, the power variation of PEVs in MV bus $\Delta p_{MV,1}$ with respect to the PEV power variation in bus 1 is given by:

$$\Delta p_{MV,1} = (1 + LF_N) \cdots (1 + LF_1) \cdot \Delta p_1 \quad (4.41)$$

$$\Delta p_{MV,1} = \Delta p_1 \cdot \prod_{n=1}^N (1 + LF_n). \quad (4.42)$$

Thanks to the linear structure of our formulation, we could straightforwardly obtain the total instantaneous power variation at the medium voltage with respect to the power variation of PEVs connected to bus 1. Needless to say, LF_n , which was extensively discussed in the previous section, is the line factor in bus n as follows:

$$LF_n = \frac{2 \cdot P_{zn}}{V_{d,n}^2} \cdot \left(R_n^L + \frac{L_n^L}{2} \cdot s \right) \quad (4.43)$$

where R_n^L , L_n^L , P_{zn} , and $V_{d,n}$ are the resistance, the inductance, and the three-phase active power of impedance n before the disturbance, and d -axis voltage of bus n before the disturbance, respectively.

In the previous step, the power consumption in all distribution lines was calculated when PEVs connected to bus 1 participated in the PFC. In a similar way to (4.42),

the power variation of PEVs in MV bus $\Delta p_{MV,n}$ with respect to the PEV power variation Δp_n in bus n can also be formulated as follows:

$$\Delta p_{MV,n} = \Delta p_n \cdot \prod_{j=n}^N (1 + LF_j) \quad (4.44)$$

where j is an auxiliary index for buses. In other words, if PEVs connected to n participate in the PFC, the power reflected to the medium voltage bus is equal to the power variation of PEVs and the variation of power consumed in the network.

Finally, we can simply generalize (4.44) to the whole distribution feeder by adding the power variation of all PEVs. Hence, the aggregate power variation of PEVs in MV bus Δp_{ag} with respect to the PEV power variation in all buses is given according to (4.42) :

$$\Delta p_{ag} = \sum_{n=1}^N \Delta p_{MV,n} \quad (4.45)$$

$$\Delta p_{ag} = \left[\prod_{n=1}^N (1 + LF_n) \quad \cdots \quad \prod_{n=N}^N (1 + LF_n) \right] \cdot \begin{bmatrix} \Delta p_1 \\ \vdots \\ \Delta p_N \end{bmatrix} \quad (4.46)$$

where Δp_n is the power variation of PEVs in bus n . The power variation of PEVs at each bus depends not only on the number of PEVs connected to the bus, but also on the participation factor of each PEV. If the number of PEVs connected to each bus is vary large, then it is very complex to individually take them into account. As a solution, in the previous chapter, we proposed to employ the arithmetic averaging technique in order to represent the behavior of PEVs. Similarly, here we calculate the average power variation of PEVs at each bus by which the formulation is considerably simplified. Therefore, (4.46) can be rewritten as follows:

$$\Delta p_{ag} = \left[\prod_{n=1}^N (1 + LF_n) \quad \cdots \quad \prod_{n=N}^N (1 + LF_n) \right] \cdot \begin{bmatrix} C_1 \cdot \Delta p_{av,1} \\ \vdots \\ C_N \cdot \Delta p_{av,N} \end{bmatrix} \quad (4.47)$$

where C_n and $\Delta p_{av,n}$ are the estimated number and the charging power variation of PEVs connected to bus n , respectively. Though we simplified the formulation using average values of PEVs, there are various reasons because of which in future system operators might also use these values. Ideally speaking, if the perfect real-time data

of the PEV fleet is available, then the PEV aggregator can utilize equation (4.46) to obtain an aggregate dynamic response of the PEV fleet. However in future, the real-time charging power data of PEVs is not likely to be available and provided to either the PEV aggregator or the system operators. In such cases, to evaluate the dynamic performance of the distribution network including PEVs, an average charging power of PEVs Δp_{av} at each time of the day or night shall be considered. In the end, by employing the simplifying assumption that the average power variation of PEVs Δp_{av} is provided, Δp_{ag} in (4.47) can be reformulated as follows:

$$\Delta p_{ag} \approx \Delta p_{av} \cdot \sum_{j=1}^N \left[\prod_{n=j}^N (1 + LF_n) \cdot C_j \right]. \quad (4.48)$$

Equations (4.47) and (4.48) indicate that the total PEV power variation Δp_{ag} , which is reflected in the upstream HV transmission system, depends on both the calculated line factors and the spatial distribution of PEVs in the distribution network. For instance in (4.48), C_1 estimated number of PEVs, which are located very far from HV transmission network, incorporate a high coefficient of LF, i.e., $C_1 \cdot \prod_{n=1}^N (1 + LF_n)$. Therefore, the active power variation during the PFC disturbance in the HV line is comparatively higher than the total PEV fleet active power variation for PFC due to the variation of power consumed in the network. On the other hand, C_N estimated number of PEVs, which are located very close to the HV transmission network, incorporate very low coefficient of LF, i.e., $C_N \cdot (1 + LF_N)$. Thus, both the topology of the distribution network and the location of PEVs and loads are implicitly included in (4.48).

4.4.2. Maximum Allowed Current of Average PEV for PFC

In the previous section, it was shown that a new maximum current limit might be necessary for PEVs when their PFC provision violates the current limits of the lines and transformers. Here, this new limit can be calculated for a distribution feeder to which a large number of PEVs are connected. If it is assumed that the transformer at the medium voltage level is protected at a specific maximum current, then the total current of PEVs connected to the feeder should not exceed this limit. The maximum allowed current variation of the transformer $\Delta I_{ag,MV}^{max}$ with respect to the maximum current of transformer I_{zN}^{max} is given by:

$$I_{zN}^{max} = \sqrt{(I_{zN,d} + \Delta I_{ag,MV}^{max})^2 + I_{zN,q}^2} \quad (4.49)$$

$$\Delta I_{ag,MV}^{allwd} = \sqrt{(I_{zN}^{max})^2 - I_{zN,q}^2} - I_{zN,d} \quad (4.50)$$

where $I_{zN,d}$ and $I_{zN,q}$ are the d - and q -axis currents of impedance n , respectively. Equation (4.50) is the maximum amount of current that can be provided by all PEVs during the PFC. If the total number of PEVs is known, then it is possible to obtain the average maximum current of each PEV that could be provided for the PFC. Note that in the above-developed equation, only the reference frame of the bus voltage of the transformer has been considered, and therefore the reference frame of other PEVs connected to different buses were not taken into account to obtain the proposed transformer limit. The average maximum allowed current of each PEV $\Delta I_{z,av}^{max}$ is written as follows:

$$\Delta I_{Z,av}^{max} = \frac{\Delta I_{ag,MV}^{max}}{\sum_{n=1}^N C_n}. \quad (4.51)$$

Equation (4.51) demonstrates that the average current of PEVs should not exceed $\Delta I_{z,av}^{max}$. To implement the limit of (4.51) in practice, this additional limit might be calculated by an aggregator for each PEV and then be provided in coordination with the TSO to each PEV. The implementation of this limit for PEVs could be crucial in future in order to ensure safe and reliable operation of distribution grids.

4.4.3. Aggregate Model of PEVs for PFC Including Distribution Network and Transformer Limit

So far, in this section, we proposed an aggregate model of PEVs in which the variation of power consumed in the network as well as the maximum current of the lines and transformers were considered and formulated. Since (4.48) and (4.51) have a linear fashion, they can be straightforwardly added to the aggregate model of PEVs for the PFC. Figure 4.8 presents the proposed aggregate model of a large scale PEV fleet for PFC. The aggregate model of PEVs consists of the following blocks:

1. Primary frequency control,
2. Proposed allowed current limit of PEV fleet
3. Average battery charger model (see chapter 3),
4. Simplified distribution network.

It is worth mentioning that the average of primary frequency control was formulated and obtained in the previous chapter, while the new contributions of this chapter such as the average values of both simplified distribution network model and the proposed allowed current of PEV were formulated and obtained here. In short, the average primary frequency control includes an average participation factor of PEVs $K_{av}(SOC_{av})$ and the typical droop characteristics R according to the previous chapter.

To apply the maximum allowed current limit of an average PEV according to (4.51), first the average charging current variation of PEVs $\Delta I_{d,av}$ is to be obtained. As mentioned before, the output signal of the PFC loop represent the average power variation of PEVs for the PFC, despite the fact that in the above mentioned formulation, the average current variation of PEVs is required. Therefore, the average PFC power variation of PEVs $\Delta p_{PFC,av}$ is divided by the weighted average d - axis bus voltage $V_{d,av}$, which is given by:

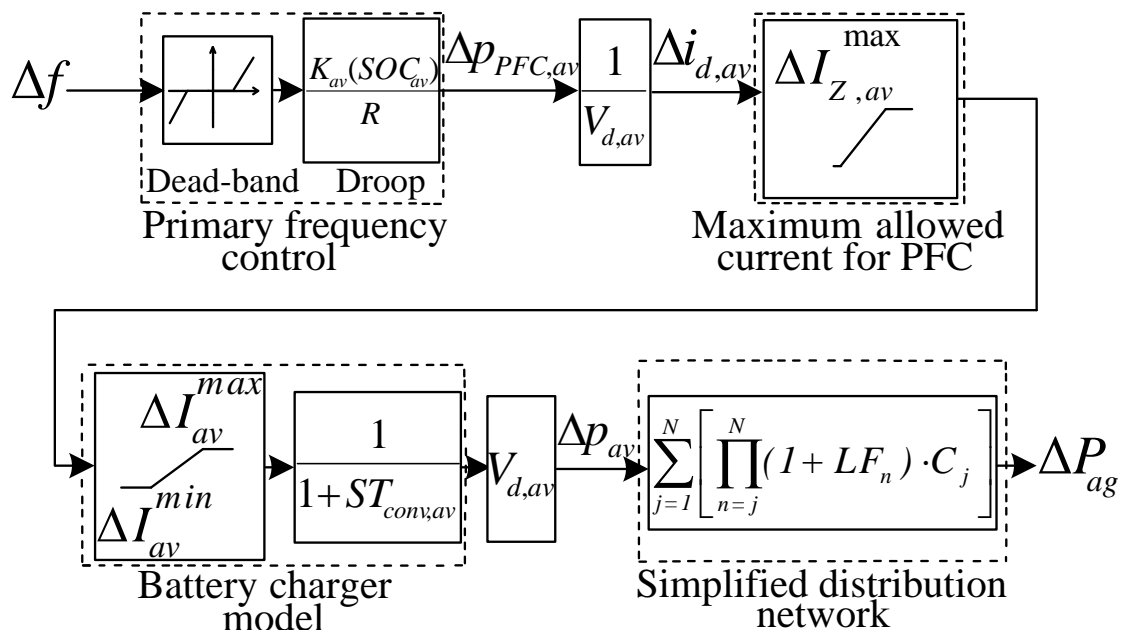


Figure 4.8.: Proposed aggregate model of a large scale PEV fleet in a radial distribution network.

$$V_{d,av} = \frac{\sum_{n=1}^N C_n \cdot V_{d,n}}{\sum_{n=1}^N C_n} \quad (4.52)$$

where $V_{d,n}$ is the d - axis voltage in bus n . It is worth emphasizing that the weighted average d - axis bus voltage $V_{d,av}$ is a static parameter (i.e., constant) which can be calculated before the disturbance. Thus, the value of $V_{d,av}$ does not change during the frequency disturbance. Moreover, generally speaking, despite the fact that using the weighted average value of voltage might cause a slight error, we have used it as the most appropriate representative of the voltage of buses. However in future, appropriate techniques could be developed in order to more accurately obtain the d - axis bus voltage value.

As broadly addressed in the previous and current chapter, the downward and upward current limits of PEVs could have a significant impact on their performance during

the PFC studies. In order to complete the here-presented aggregate model of PEVs for the PFC, we calculate the values of upward and downward available current of PEVs. The average downward PEV current ΔI_{av}^{max} and the average upward PEV current ΔI_{av}^{min} are given as follows:

$$\Delta I_{av}^{max} = \frac{\sum_{n=1}^N I_n^{max} - \sum_{n=1}^N I_{d,n}}{\sum_{n=1}^N C_n} \quad (4.53)$$

$$\Delta I_{av}^{min} = \frac{\sum_{n=1}^N I_n^{min} - \sum_{n=1}^N I_{d,n}}{\sum_{n=1}^N C_n} \quad (4.54)$$

where I_n^{max} and I_n^{min} are the cumulative maximum and minimum current limits of PEVs in bus n , respectively. As seen, this value was obtained according to the total number of PEVs connected to the distribution feeder.

In the end, in Figure. 4.8, the battery charger current variation is multiplied by the average d - axis bus voltage $V_{d,av}$ to obtain the average power variation of PEVs Δp_{av} . Therefore, instead of the current signal of PEVs, the average power variation of PEVs could be provided into the simplified distribution network model. In fact as shown in (4.48), the total power variation at the medium voltage has been simplified as a linear function of the power variation of PEVs. This way, the distribution network model incorporates the DNPC variation according to (4.48). In conclusion, the active power output in Figure. 4.8 not only includes the power variation of PEVs but also takes into account the distribution network characteristics such as power consumed in the network and maximum current of the lines and transformers.

4.5. Case Study and Simulation Scenarios

In order to evaluate the performance of the above mentioned aggregate model of PEVs for the PFC, a low-voltage CIGRE benchmark is considered and described. This benchmark consists of three subnetworks (i.e., industrial, residential, and commercial), among which PEVs are sporadically distributed. After the base case study is presented, a number of relevant simulation scenarios are provided.

4.5.1. Case Study

As mentioned, the low-voltage CIGRE benchmark is considered and described in detail in this section. In fact this case study has been selected due to some reasons as follows:

- Since PEVs will be mostly connected to the low voltage distribution networks, it is required to provide a case study which represents in detail a low voltage distribution network. The CIGRE benchmark contains a number of detailed subnetworks, each of which provides various specifications of the lines/conductors and loads. Therefore, it is possible to calculate the power consumed in the low-voltage feeders,
- In this benchmark, the transformer connected to the medium voltage bus bar has been equipped with an over-current relay. Therefore, it is possible to evaluate the performance of the above presented limit of PEV's current for the PFC.

First of all, it is important to point out that the here-used CIGRE benchmark has a relatively limited-scale. In other words, the grid, PEV fleet, and frequency disturbance are scaled down in size, therefore, the system under study represents a small-scale power system or more likely an islanded system. This has been taken into account in order to facilitate understanding of the formulation and performance of the proposed aggregate model. Nonetheless, the described power system and the proposed model can be easily replicated and extended into a large-scale power system.

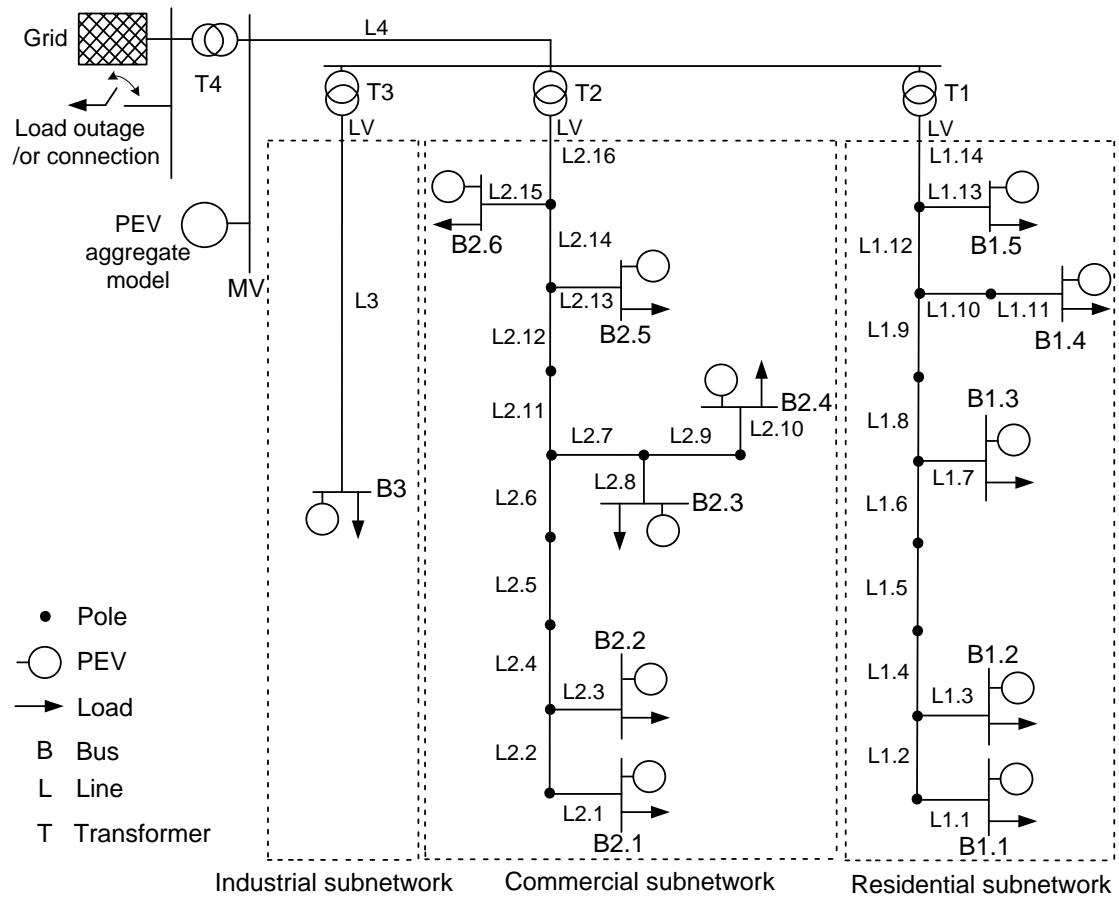


Figure 4.9.: Power system under study including the CIGRE multi-feeder benchmark LV network including residential and commercial subnetworks.

The CIGRE benchmark consists of various essential components of electrical grids. Figure.4.9 presents the power system under study which consists of the following five essential components. Note that here we do not take into account some characteristics of the network that do not typically affect the dynamic response of distribution networks for the PFC. For instance, the type of transformers, capacitor banks, grounding schemes, and unbalanced flows are not presented in this case study.

4.5.1.1. Electrical Grid

The external grid has been considered in order to represent the behavior of centralized conventional generating units. Therefore, the grid is represented as an equivalent model of a conventional generator, a HV transmission line, and a HV/MV substation. In this case study, the MV and LV are set to 20 kV and 0.4 kV, respectively (Papathanassiou et al., 2005). The equivalent model of the conventional generator has the droop value of 0.05 for the PFC (Kundur et al., 1994).

4.5.1.2. Frequency Disturbance

The frequency disturbance can be the trip or connection of a large load that creates the over frequency or under frequency problem, respectively. Technically speaking, for the PFC analysis the amount of the disturbance is considered equal to the largest generating unit connected to the grid. Since the here-presented case study has been scaled down, proportionally the amount of the disturbance could be reduced as well. For this case study, the connection/disconnection of a large load is considered as the frequency disturbance to create under/over voltage problems. The power consumption of this load is 600 kW.

4.5.1.3. LV Distribution Network

The LV distribution network is created according to the CIGRE multi-feeder benchmark network (Papathanassiou et al., 2005), as shown in Figure.4.9. The whole PEV fleet is either represented by an aggregate model in MV bus or by the distributed model of PEVs, which are connected to the LV distribution network. This includes the industrial, the residential and the commercial subnetworks, in which PEVs and loads are distributed. The residential subnetwork includes five bus bars from $B1.1$ to $B1.5$, and fourteen lines from $L1.1$ to $L1.14$. Besides, the commercial subnetwork includes six bus bars from $B2.1$ to $B2.6$, and sixteen over-head lines from $L2.1$ to $L2.16$, whereas the industrial subnetwork only includes the bus bar $B3$ and the under-ground line $L3$. To present the LV distribution network, first, the load and PEV fleet characteristics before and during the disturbance are presented and accordingly, the total power consumption at each bus is obtained. Then, the parameters of the lines are presented and LF of each line is calculated according to (4.43).

The loads are represented by a combination of the static and dynamic loads. Here, while dynamic loads are mainly modelled as induction machines, static loads are represented as constant power (CP) and constant impedance (CI). The static load is represented as a polynomial “ZIP” load model (Bokhari et al., 2014), consisting of constant impedance (Z), constant current (I), and constant power (P). In general, the load active power consumption is written as:

$$P_{Load} = P_0 \cdot \left[a_1 \cdot \frac{|V_{d,Load} + j \cdot V_{q,Load}|^2}{V_0^2} + a_2 \cdot \frac{|V_{d,Load} + j \cdot V_{q,Load}|}{V_0} + a_3 \right] \quad (4.55)$$

where a_1 , a_2 , and a_3 are the corresponding coefficients of constant impedance, constant current, and constant power terms of the load model, respectively. Also, P_0 and V_0 are the rated power and voltage of the load, respectively. In Table.4.1, the ratio of dynamic and static loads for the residential, commercial, and industrial

subnetworks are presented that applies to the load consumption at each bus, as presented in Table. 4.2. Dynamic loads represent induction motors connected to 400 V, which are modelled as different units of rated power from 5 hp to 150 hp with inertia in the range of 0.1 to 2 kgm^2 . All loads and PEVs only have the balanced three phase connections.

Table 4.1.: Ratio of dynamic and static loads in the residential, commercial, and industrial subnetworks.

	Dynamic load [%]	Static load [%]	
		CI [%]	CP [%]
Residential subnetwork	25	25	50
Commercial subnetwork	35	25	40
Industrial subnetwork	50	25	25

Before the frequency disturbance, the load consumption S^L in each bus is shown in Table. 4.2. To obtain the number of loads in each bus, as shown in Table. 4.2, on the one hand it is assumed that the average load consumption in the commercial and residential areas are 6 kVA and 3 kVA with the power factor of 0.95, respectively. Then, PEVs are dispersed along the feeders according to the number of loads at each bus. On the other hand, the industrial load only consists of a workshop load. Besides, before the disturbance, the PEV consumption S^{PEV} in each bus shown in Table. 4.2 depends on the number of PEVs and the average charging power of PEVs. To obtain the number of PEVs, it is assumed that the number of loads in the commercial and residential areas are equal to the number of PEVs. Also, five PEVs are considered for the industrial area. The total number of PEVs is obtained 198. This number of PEVs is reasonable for the small scale distribution network under study. Moreover, a gravity index G , which accounts for the average distance of the PEV fleet from MV bus, is given by:

Table 4.2.: Active and reactive power of loads and PEVs in each bus.

Bus	1.1	1.2	1.3	1.4	1.5	2.1	2.2	2.3	2.4	2.5	2.6	3
Case study												
$S^L(kVA)$	150	30	150	342	34.2	66	82.8	53.2	26.4	99	175	210
$S^{PEV}(kW)$	21	4.2	21	48.3	4.9	4.2	5.6	3.5	2.1	7.7	12.6	3.5
# Loads	30	6	30	69	7	6	8	5	3	11	18	5
#PEVs C_j	30	6	30	69	7	6	8	5	3	11	18	5
$P^B(kW)$	163	32.7	163	373	37.3	70	84.2	54	26.8	102	179	203
$Q^B(kVar)$	46.8	9.3	46.8	106	10.6	20.6	25.8	16.6	8.24	30.9	54.6	117
SA II												
$I_{av}(A)$	2	0.5	1.5	0.35	0.7	3	2.5	1.7	0.2	0.3	0.4	3

$$G = \frac{\sum_{n=1}^N C_n \cdot D_n}{\sum_{n=1}^N C_n} \quad (4.56)$$

where D_n is the distance to MV bus from bus n . To obtain the average charging current of PEVs, it is assumed that 10% of the total number of PEVs are in the charging mode and 90% of the total number of PEVs are in the idle mode. If in the charging mode, the PEV charging power is 6.92 kW, thus, the average charging power of PEVs is 0.69 kW. Table.4.2 shows the charging power of PEVs in each bus. Finally, the total active power consumption in each bus P^B and total reactive power consumption in each bus Q^B are shown in Table.4.2.

During the frequency disturbance, it is assumed that the loads do not participate in the PFC, although the active power consumption of induction machines and constant impedance loads might vary during the frequency disturbance due to the voltage and frequency variations. PEVs can participate in the PFC by changing their charging power with respect to the frequency deviation. To this end, the PFC loop is incorporated into the PEV charger control system, which consists of fast inner current control loops and outer power control loops. It is assumed that all PEVs connected to the distribution network can provide PFC, and the average PFC characteristics of PEVs at each bus is equal to the average of the whole PEV fleet. While the number of PEVs at each bus C_j is presented in Table.4.2, Table.4.3 presents calculated parameters of an average PEV with respect to Figure.4.8 such as $K_{av}(SOC_{av})$, dead-band range, droop value R , ΔI_{av}^{max} , ΔI_{av}^{min} , $\Delta I_{PFC,av}^{allwd}$, $V_{d,av}$, and G . In primary frequency control, the dead band range and the inverse of droop coefficient are ± 10 mHz and 100. $K_{av}(SOC_{av})$ is 0.9 when the average state of charge SOC_{av} is assumed 76%. In battery charger model, $T_{conv,av}$ and $V_{d,av}$ are 50 ms and 391.2 V, respectively. In addition, to calculate ΔI_{av}^{max} and ΔI_{av}^{min} , it is assumed that PEVs are equipped with bidirectional chargers with maximum current limit of 10 A. According to the average charging current of 1 A, ΔI_{av}^{max} and ΔI_{av}^{min} are obtained 9 A and -11 A, respectively. Finally, the gravity of PEV fleet G is equal to 1250.5 m .

Table 4.3.: Parameters of an average PEV for PFC.

Primary frequency control				Battery charger model				Gravity
Dead-band [mHz]	$1/R$	SOC_{av} [%]	$K_{av}(SOC_{av})$	$T_{conv,av}$ [ms]	ΔI_{av}^{max} [A]	ΔI_{av}^{min} [A]	$V_{d,av}$ [V]	G [m]
± 10	100	76	0.9	50	10	-11	391.2	1250.5

According to Table.4.2, the LF of the lines of Figure.4.9 can be calculated. First, to obtain the impedance of each line, the resistance and reactance of conductor in Ω/km , and the line's length are presented. The over-head lines of the commercial

and residential subnetworks are equipped with the typical LV cables of PRYSMIAN group with the impedance of $0.242 + j0.096 \Omega/km$, while the under-ground line of the industrial subnetwork is equipped with UL 150 mm^2 XLPE cable with the impedance of $0.264 + j0.071 \Omega/km$. The pole-to-pole distance of residential subnetwork is 50 m , while the pole-to-pole distance of the commercial subnetwork is 45 m . The length of industrial under-ground cable is 200 m . Then, to obtain LF_n according to (4.43), first it is required to calculate the load flow in power system. In other words, before running the dynamic model of the network, the static model of the network before the disturbance must be solved to obtain LF_n . The load flow results are shown in Table.4.2 and accordingly LF of the LV distribution network lines from L1.1 up to L3 can be obtained.

4.5.1.4. MV Distribution Network,

As mentioned, our formulation could be flexibly adapted to various voltage levels. Therefore for this analysis, not only low-voltage distribution networks could be incorporated into the model of PEVs for the PFC, but also in a similar manner the power consumed in medium voltage lines could be also taken into account. The medium voltage distribution network consists of a cable line $L4$, a MV transformer, and three LV transformers as shown in Figure. 4.9. According to the standard ratings of transformers and the peak power consumption of each network, the size of T_1 , T_2 , T_3 , and T_4 are 1000 kVA, 430 kVA, 250 kVA, and 1750 kVA with the impedance of $0.001 + j0.03$ pu, respectively. The MV cable line $L4$ has $0.1509 + j0.094 \Omega/km$ impedance and 1000 m length. Similar to LV distribution network, LF of $L4$ is obtained.

4.5.1.5. PEV Aggregate Model.

In order to obtain an aggregate model of PEVs, first we had to add a certain number of PEVs to the CIGRE benchmark. Since the size of the benchmark is small, accordingly a low number of PEVs are assumed for this benchmark. Note that the original LV benchmark does not include the charging power of PEVs, and consequently has a lower level of power losses. By the way, if we include the total charging power of PEVs in the LV benchmark under study, then the level of power losses would become higher compared to the original benchmark. In the here-provided results, the variation of power consumed in the network during PFC is relatively large, because some lines are notably loaded. Nonetheless, if the level of power consumed in the network would be lower, still its impact on the PFC could be high. To roughly justify this, we plug our statement into an estimated numerical example. If 1) only the power loss variation in resistance is considered and even the power consumed in the inductance is neglected, 2) 20% and 80% of total power passing through lines are reactive and active power (power factor=0.8), 3) total disturbance and the power losses are 5% and 7%, respectively, and 4) PEVs and CGUs compensate active power of 3%

and 2% of total 5% disturbance, respectively, then in such network, the variation of power losses is roughly obtained around 0.503% ($= (\frac{[83^2+20^2]}{[80^2+20^2]} - 1) \cdot 7\%$). Compared to the size of disturbance 5%, the neglect of power loss variation of 0.503% could roughly produce an error of 10%. As mentioned, in general, it is expected and makes sense that the impact of variations of power consumed in the network on the PFC by PEVs would be considerable, even at lower levels of power consumed in the network.

A PEV aggregate model, which represents 198 number of PEVs in the LV distribution network, is connected to the medium voltage busbar. Two aggregate models of PEVs are defined and compared that are the previous aggregate model of PEVs provided in the previous chapter, and the proposed aggregate model of PEVs. The previous aggregate model neglects the distribution network, and consequently the overall LF in (4.48) is equal to zero. The previous aggregate model of PEVs is called the primitive aggregate model of PEVs. On the other hand, the proposed aggregate model of PEVs incorporates the characteristics of distribution network using (4.46), as shown in Table. 4.3.

In this subsection, the low-voltage CIGRE benchmark was presented in detail that will be used later for the simulations. However, beforehand, some simulation scenarios and sensitivity analyses are defined and presented to further evaluate the impact of various PEV fleet parameters on the proposed aggregate model of PEVs for the PFC.

4.5.2. Simulation Scenarios and Sensitivity Analysis

Our here-proposed model of PEVs for the PFC has two additional characteristics compared to the primitive aggregate model of PEVs. Therefore, two simulation scenarios are defined in order to evaluate the impact of these characteristics on the performance of PEVs model. These two simulation scenarios are defined to achieve two objectives:

1. To validate the proposed aggregate model of PEVs and later on, to compare three models of the PEV fleet for PFC,
2. To evaluate and validate the proposed PFC limit of PEVs.

Note that three models of PEVs include are as follows:

1. Distributed model of PEVs,
2. Primitive aggregate model of PEVs provided in the previous chapter,
3. Here proposed aggregate model of PEVs.

In summary, taking into account the above mentioned-objectives, two simulation scenarios including several parts for each scenario are presented as follows:

In scenario 1, the under-frequency disturbance is applied on the power system when the load is connected at $t=0$ s to the grid. scenario 1 comprises three parts as follows:

- Scenario 1.1) the distributed model of PEVs provides the PFC where $1/R$ set 100,
- Scenario 1.2) the primitive aggregate model of PEVs provides the PFC where the distribution network characteristics are neglected,
- Scenario 1.3) the proposed aggregate model of PEVs provides the PFC where the distribution network characteristics are considered.

Note that in the case study, the average model is used for each PEV in both the distributed model of PEVs and the aggregate models of PEVs.

In scenario 2, the over-frequency disturbance is applied on the power system when the load is disconnected at $t=0$ s from the grid. scenario 2 comprises five parts as follows:

- Scenario 2.1) the distributed model of PEVs provides the PFC where $1/R$ set 100,
- Scenario 2.2) the primitive aggregate model of PEVs provides the PFC where the distribution network characteristics are neglected,
- Scenario 2.3) the proposed aggregate model of PEVs provides the PFC where the distribution network characteristics are considered.

Note that in scenarios 2.1, 2.2, and 2.3, the proposed limit for PEVs has not been applied, therefore to evaluate and validate the proposed PFC limit for PEVs, scenarios 2.4 and 2.5 are defined as follows:

- Scenario 2.4) the distributed model of PEVs provides the PFC where the proposed PFC limit for PEVs is considered,
- Scenario 2.5) the proposed aggregate model of PEVs provides the PFC where the PFC limit for PEVs is considered.

Note that $\Delta I_{PFC,av}^{allwd}$ in (4.51) and $\Delta I_{ag,MV}^{allwd}$ in (4.50) are the proposed maximum current limit of an average PEV in Scenario 2.4 and the maximum current limit of the proposed aggregate model in scenario 2.5, respectively.

Taking into account that the average charging current of the whole PEV fleet I_{av} and the gravity index G in the case study are 1 A and 1250.2 m , respectively, then three sensitivity analyses (SAs) are presented to investigate the proposed model performance as follows:

- SA I) the average charging level of all PEVs in the base case study increases from 1 A to 3 A,
- SA II) since in the case study, all PEVs have identical average charging current of 1 A, an in-homogeneous PEV fleet is evaluated according to Table. 4.2, while PEVs in each bus have different charging levels, the PEV fleet average charging current is still equal to 1 A,

- SA III) the gravity index of the whole fleet in the base case study increases from 1250.5 m to 1432 m , where PEVs of the residential and commercial subnetworks are totally moved and connected to buses 1.1 and 2.1, respectively.

In this section, two simulation scenarios including several sub-scenarios were defined in order to evaluate the impact of distribution network characteristics on the aggregate model of PEVs for the PFC.

4.6. Simulation Results

The dynamic simulations are carried out through Matlab / Simulink on the CIGRE benchmark. In order to evaluate scenarios 1 and 2, the presented power system including PEVs is simulated, and later on, the results of the case study as well as the sensitivity analysis are presented. Finally, the simulation results are discussed. Note that in scenarios 1 and 2 as well as the sensitivity analysis, the loads in each bus are modelled as static loads (i.e., constant power and constant impedance loads) and dynamic loads (i.e., induction machines) taking into account their corresponding ratios in Table. 4.1.

4.6.1. Simulation Results of the Case Study for Scenario 1

Figure. 4.10 shows the simulation results for scenario 1 in which a load of 600 kW is connected to the grid at $t=0$ s. As a consequence, the frequency starts to drop following the disturbance, as shown in Figure. 4.10(a). Note that the system frequency is the frequency of center of inertia at the conventional generating units.

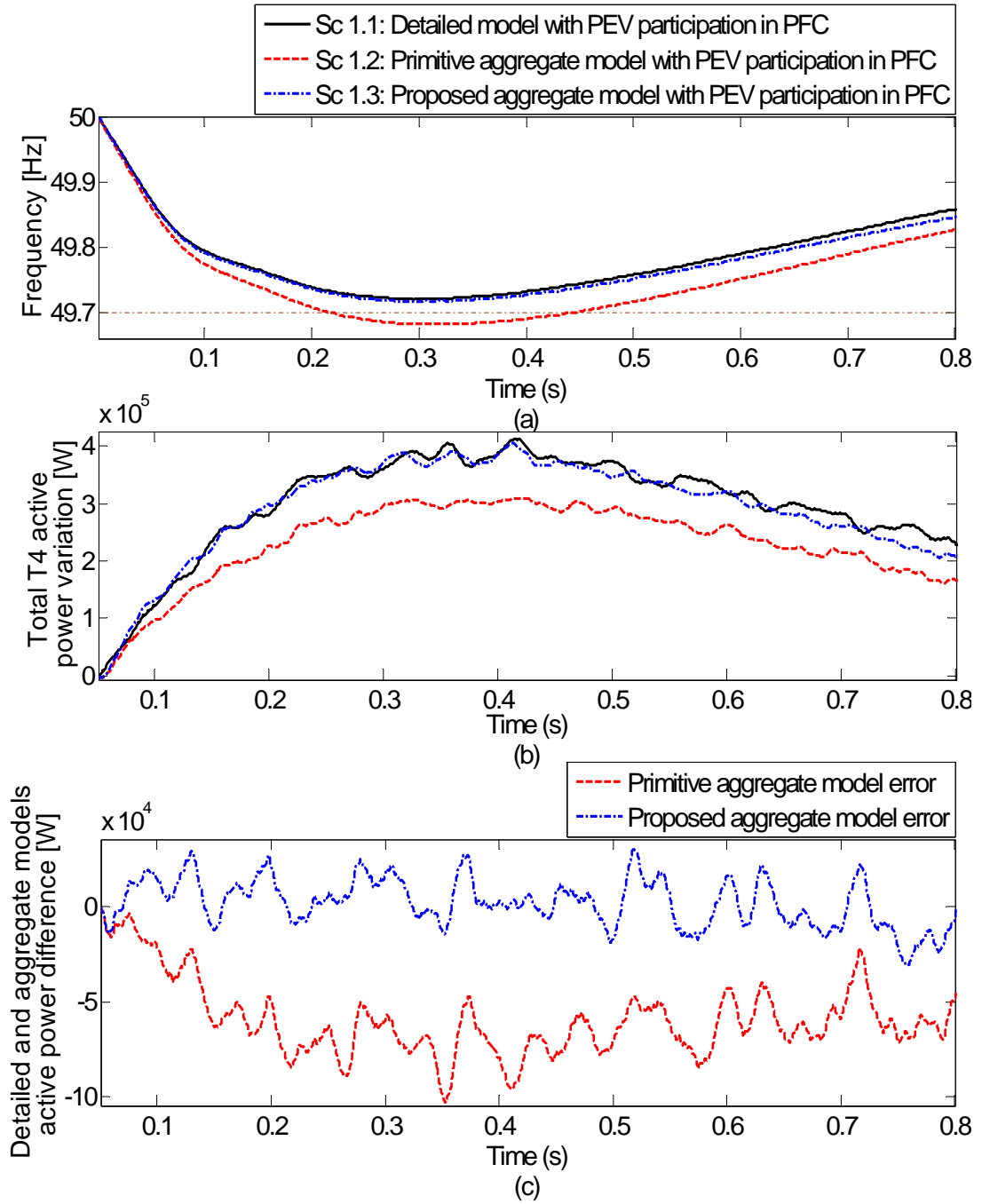


Figure 4.10.: Simulation results for scenario 1 (a) frequency; (b) total T4 active power variation; (c) detailed and aggregate models active power difference.

To compare the distributed model of PEVs with the aggregate models of PEVs, scenario 1.1 is contrasted with scenarios 1.2 and 1.3. According to Figure 4.10(a), the minimum frequency for scenarios 1.1, 1.2, and 1.3 are 49.72 Hz, 49.714 Hz, and 49.681 Hz, respectively. If the allowable frequency range is ± 0.3 Hz, then

the frequency deviation for scenario 1.2 in the previous aggregate model is out of range, although in reality the frequency is within the allowable range in scenario 1.1. Scenarios 1.2 and 1.3 in comparison to scenario 1.1 have the accuracy of 98.58% and 88.90%, respectively. To quantify numerical accuracy of the primitive and proposed aggregate models with respect to the detailed model, the following formula is used:

$$Accuracy\% = \left(1 - \frac{|\Delta f^{DTL} - \Delta f^{AGG}|}{\Delta f^{DTL}}\right) \cdot 100 \quad (4.57)$$

where Δf^{DTL} and Δf^{AGG} are the minimum or maximum frequency deviation of the detailed and aggregate models, respectively. Thus, the proposed model appreciates 9.68% higher accuracy for the under-frequency problem than the primitive model due to incorporation of power consumed in the network. In Figure. 4.10(b), the power variation of the proposed aggregate model of PEVs is close to the power variation of distributed model of PEVs at T4 in Figure. 4.9. However the power variation of the primitive aggregate model of PEVs is different from the power variation of distributed model of PEVs following the disturbance. In the end, Figure. 4.10(c) shows the active power error of the primitive and proposed aggregate models with respect to the detailed model.

4.6.2. Simulation Results of the Case Study for Scenario 2

Figure. 4.11 shows the simulation results for scenario 2 in which a load of 600 kW is disconnected from the grid at $t=0$ s. As a consequence, the frequency increases following the disturbance, as shown in Figure. 4.11(a).

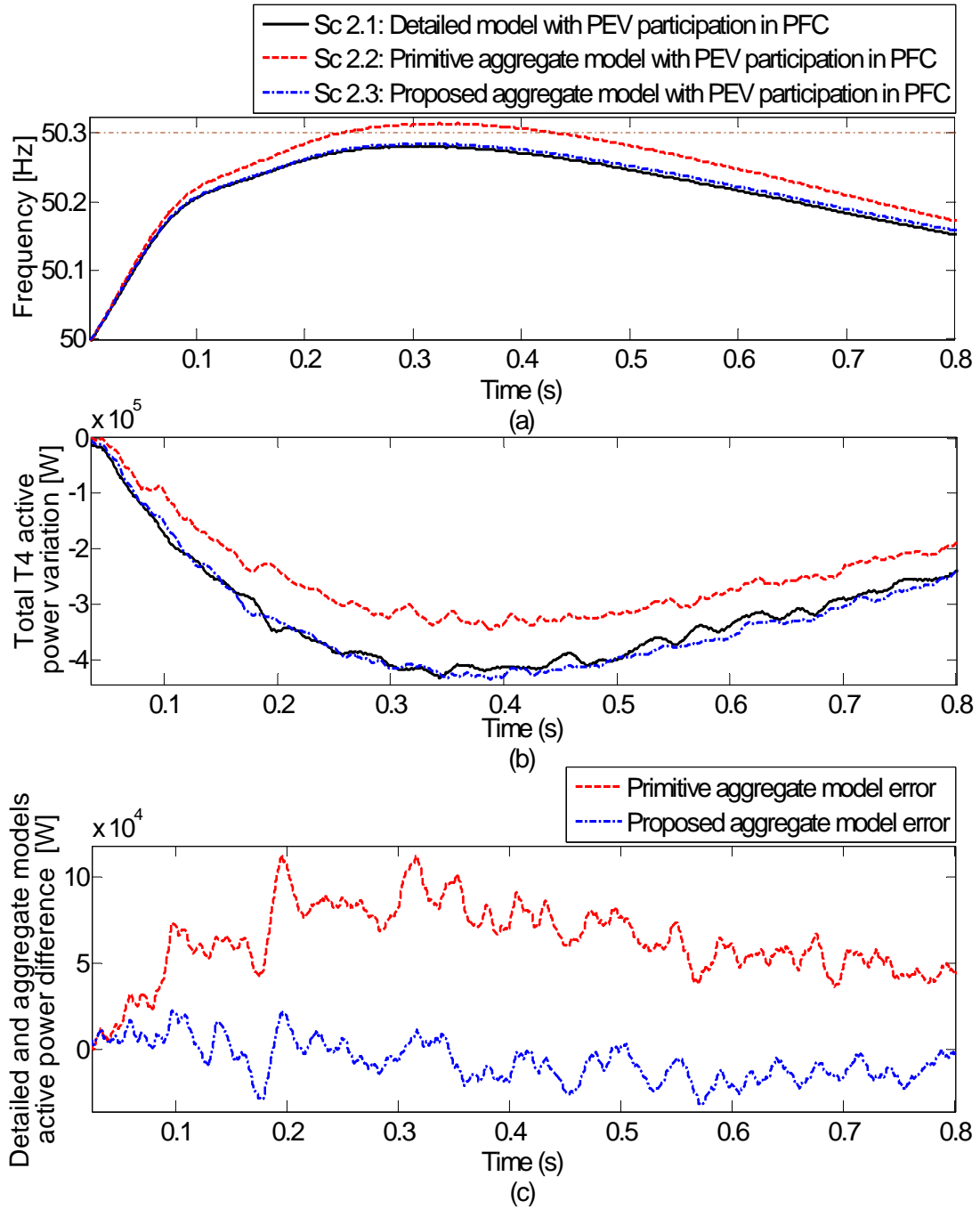


Figure 4.11.: Simulation results for scenario 2 (a) frequency; (b) total T4 active power variation; (c) detailed and aggregate models active power difference.

To compare distributed model of PEVs with the aggregate models of PEVs, scenario 2.1 is contrasted with scenarios 2.2 and 2.3. According to Figure. 4.11(a), the maximum frequency for scenarios 2.1, 2.2, and 2.3 are 50.280 Hz, 50.313 Hz, and 50.285 Hz, respectively. This indicates that scenarios 2.2 and 2.3 in comparison to

scenario 2.1 in terms of the minimum frequency have the accuracy of 98.21% and 88.21%, respectively. Thus, the proposed model appreciates 10% higher accuracy than the primitive model due to incorporation of power consumed in the network. In Figure. 4.11(b), the power variation of the proposed aggregate model of PEVs is close to the power variation of distributed model of PEVs at T4 in Figure. 4.9, however the power variation of the primitive aggregate model of PEVs is different from the power variation of distributed model of PEVs following the disturbance. Finally, Figure. 4.11(c) shows the active power error of the primitive and proposed aggregate models with respect to the detailed model.

To evaluate the effect of the proposed PFC limit, scenario 2.1 is compared with scenario 2.4 and scenario 2.5 in Figure. 4.12(a) and (b). In Figure. 4.12(a) for scenario 2.1, the current of T4 at the MV level reaches 1.2 times of the nominal current of MV transformer that might activate the operation of MV transformer fuse/ or over current relay. However by calculating and applying the proposed PFC limit for PEVs according to (4.51) in scenario 2.5, the current of grid does not exceed 1.04 times of the transformer nominal current. Moreover in Figure. 4.12(a), the aggregate model current in scenario 2.5 properly follows the distributed model of PEVs in scenario 2.4. In Figure. 4.12(b), the maximum frequency in scenario 2.4 and scenario 2.5 are 50.513 Hz and 50.52 Hz, that shows the accuracy of 98.63%. This indicates that the accuracy of the aggregate model of PEVs even increases when PEVs reach their maximum or minimum limits.

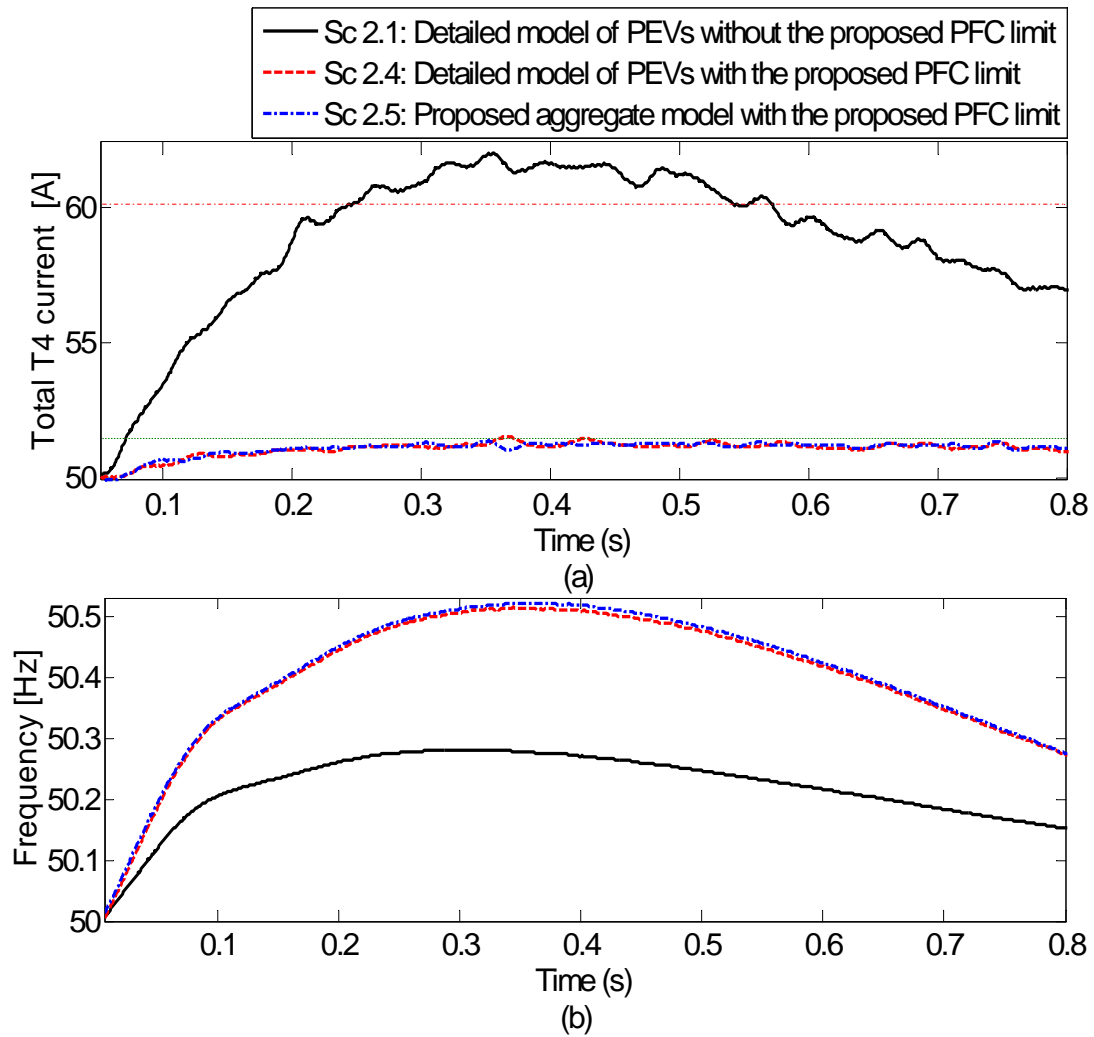


Figure 4.12.: Simulation results of the PEV proposed limit for scenarios 2.1, 2.4, and 2.5 (a) total T4 current at the MV level; (b) frequency.

4.6.3. Validation of Aggregate Models With And Without Network & Sensitivity Analysis Results &

Table.4.4 presents the results of the case study as well as the sensitivity analysis mainly for the under-frequency events. However, the results of the sensitivity analysis remain also valid for the over frequency events. In SA I, since the average PEV fleet charging current increases from 1 A to 3 A, the level of power consumed in the distribution network has higher value. This generally improves the maximum frequency deviation of SA I compared to the case study because the power consumed in the network further reduces during the under frequency disturbance. As can be seen in SA I, the aggregate model without network has the low accuracy of 81.81%, because the impact of power consumed in the network becomes higher in SA

I compared to the base case study. However of SA I, the proposed aggregate model have the accuracy of 97.72%, which is slightly lower than the accuracy of the case study. In SA II, as shown in Table. 4.2, the accuracy of proposed aggregate model decreases compared to the case study. In fact the selected in-homogeneous PEV fleet has 1.11% lower accuracy in scenarios 1 compared to the homogeneous PEV fleet. In the case the the charging power of PEVs has been in-homogeneously distributed among the fleet, similarly, the accuracy of the aggregate model without the network become lower from 88.9% in base case to 84.83% in SA II. Finally in SA III, since all PEVs are connected at the end of the feeders, the level of power consumed in the network remarkably increases. In fact, PEVs consume a notable amount of power at the very end of the feeder, therefore the power losses as well as power consumption in the network have the largest value compared to other scenarios. This notably improves the frequency response of both detailed and proposed aggregate models compared to the case study, however the accuracy of the proposed aggregate model is moderately reduced from 98.58% to 94.75% compared to the case study. Also, due to the very extreme impact of power losses on the results, the accuracy of the aggregate model without the network dramatically decreases from 88.9% in the base case study to 65.50% in SA III. Thus, the proposed model in SA III has 3.83% lower accuracy in comparison to the case study. This is not only due to the non-linear behavior in the power consumed in the network, but also in the dynamic and static loads which respond to the voltage and frequency variations during the frequency disturbance.

Table 4.4.: Accuracy of the proposed model for the case study and sensitivity analysis in scenario 1.

		Case study Homogeneous $I_{av}=1 A$ $G=1.25 km$	SA I Homogeneous $I_{av}=3 A$ $G=1.25 km$	SA II In-homogeneous $I_{av}=1 A$ $G=1.25 km$	SA III Homogeneous $I_{av}=1 A$ $G=1.43 km$
Detailed model	Min. freq. [Hz]	49.72	49.731	49.723	49.771
Agg. mdl. without ntwk	Min. freq. [Hz]	49.681	49.683	49.681	49.692
	Accuracy [%]	88.9%	81.81%	84.83%	65.50%
Agg. mdl. with ntwk	Min. freq. [Hz]	49.714%	49.725	49.716	49.759
	Accuracy [%]	98.58%	97.72%	97.47%	94.75%

4.6.4. Discussion

As seen, a number of simulations and sensitivity analyses results were presented regarding the performance of the aggregate model of PEVs for the PFC. Generally, it was shown that the here proposed aggregate model of PEVs for the PFC has a better performance compared to the previous models of PEVs for the PFC. However,

there are still several points that could be further detailed. Here, we have selected three very relevant points, which are further discussed in detail as follows

1. The fuse / or the over-current relay rating of the transformer in scenario 2: Although only 32.43% of the total PEV available upward reserve is allocated for the over-frequency problem in Figure. 4.12(a), the current of transformer exceeds 1.2 times the nominal current from 0.25 s to 0.55 s. The fuse /or the over-current relay setting of the distribution transformer typically set between 1.2 - 1.5 times the nominal current with the operation time between 0.3 s and 0.6 s. Thus in scenario 2.1, the over current protection might disconnect the transformer from the grid, which results in the black out of the distribution area. To solve this, in scenarios 2.4 and 2.5 with the proposed PFC limit, it was shown that the proposed control limit of PEVs can help avoid such incidents. Nonetheless, as shown in Figure. 4.12(b), the maximum frequency response in scenarios 2.4 and 2.5 considerably have higher maximum frequency than scenario 2.1. Hence, although PEVs have a high value of the upward primary reserve for PFC, the proposed control only allocates an allowed amount of upward primary reserve by which the over-current protection limits are not violated.
2. Accuracy of simulation results: Many factors can affect the result accuracy such as the topology of the distribution networks, the reactive power and voltage control strategy in the distribution network, the load models, e.g., constant power or constant impedance loads, and the level of power consumed in the distribution network.
3. Simulation time reduction: The proposed aggregate model of PEVs for PFC reduces the computational complexity of distributed PEV models including twelve bus bars in scenario 2.1 to an aggregate model in MV bus bar in scenario 2.3. On top of this, the simulation time in scenario 2.3 compared to scenario 2.1 is reduced from 47 minutes 45 s to 7 minutes 40 s in Matlab / Simulink using Quad-Core processors clocking at 2.93 GHz and 4 GB of RAM.

Finally, in practice the proposed aggregate model of PEVs could be used by different entities in the power systems, for instance network operators or PEV aggregators. Under a regulated vertically integrated system, the unique energy service provider (ESP) or the TSO will have access to all data needed to evaluate to what extent PEVs could contribute to the PFC. On the other hand, in an unbundled power sector, aggregators could evaluate the available primary control reserves of their PEV fleet, that could be offered as an ancillary service to system operators.

4.7. Conclusions and Out-Look

In this chapter, to particularly improve the accuracy of previous PEV models for the PFC, and notably reduce the simulation time and computational complexity

of modeling a large number of PEVs, we proposed an aggregate model of PEVs for the PFC. In comparison to previous models of PEVs, the proposed model of PEVs additionally included the distribution network characteristics, i.e., the power consumed in the distribution network and the maximum allowed current of the lines and transformers.

To dynamically incorporate the variation of power consumed in the network for the proposed model, a line factor (LF) for each line or transformer was introduced. The LF of each line was obtained with respect to the line impedance, and the power consumption and the location of PEVs and loads, which were distributed in different buses of the distribution feeder. Moreover, the maximum allowed current of the lines and transformers was incorporated into the proposed aggregate model of PEVs by an additional PFC limit for PEVs that later was calculated. Then, a small-scale CIGRE multi-feeder benchmark network was considered and created. To this end, 262 PEVs were distributed throughout buses according the total load consumption at each bus. At the first stage, in the steady state, the load flow analysis was performed to obtain the active power of lines and voltage of buses, and later on line factors were calculated according to the line impedance, the active power of lines and voltage of buses. Afterwards, dynamic simulations were carried out in order to evaluate the performance of the following models:

1. Detailed model of PEVs,
2. Previous aggregate model of PEVs in which distribution network characteristics were not included,
3. Proposed aggregate model of PEVs in which distribution network characteristics were included.

To obtain the accuracy of the previous and here-presented aggregate models of PEVs for PFC, they were compared to the detailed model of PEVs. In general, it was shown that the frequency deviation of power systems following a large disturbance was notably suppressed when PEVs participated in the PFC. Moreover, in comparison to the distributed model of PEVs, the previous aggregate model of PEVs had a low accuracy of 88.21% in terms of the minimum frequency due to the neglect of the distribution network, whereas the proposed aggregate model of PEVs had an excellent degree of accuracy of 98.21% due to inclusion of the distribution network dynamics. Importantly, it was shown that without the proposed PFC limit, the MV distribution transformer heavily got overloaded for the over-frequency problem, and consequently the over-current protection could be activated. Thus in future, to avoid the operation of the fuse/or over current relay of distribution lines and transformers, the implementation of the proposed PFC limit for PEVs might be absolutely necessary.

In the next chapter, a strategy will be described to design the frequency-droop controller of plug in electric vehicles for primary frequency control. This strategy will be based on the proposed aggregate model of PEVs, which was presented in detail in this chapter. In fact, in our analysis so far, the droop coefficients were

arbitrarily used for the PFC by PEVs, though these droop curves were not necessarily well-designed or fine-tuned with respect to the overall system stability criterion. Therefore we design the droop such that it always guaranties the same stability margin for the control system with and without PEVs, therefore both strategies can be properly compared. Two main contributions, which are addressed in detail in the next chapter are as follows:

1. We will demonstrate that PEVs improve the PFC performance reducing significantly the frequency deviations.
2. A method will be proposed to evaluate the positive economic impact of PEVs participation in PFC.

5. Design of PEVs Frequency-Droop Controller for PFC and Economic Performance Assessment

Contents

5.1. Introduction	122
5.2. Technical Implementation: Strategy to Design Frequency-Droop Controllers of PEVs	125
5.2.1. System Stability Margin Analysis	128
5.2.2. Design of the Overall Controller Gain of PEVs	133
5.2.3. Design of the Frequency-Droop Controller of Individual PEVs	137
5.2.4. Replacement of PEV's reserve by CGU's reserve during PFC	140
5.3. Case Studies and Simulation Scenarios	142
5.3.1. Base Case Study of Small-Scale Distribution Network	142
5.3.2. Simulation Scenarios	143
5.4. Simulation Results	147
5.4.1. Results of Scenario A for Different PEV Penetration Rates	147
5.4.2. Results of Scenario B For Different PEV Penetration Rates	150
5.4.3. Results of Scenarios A and B With and Without Maximum Power Limits of PEVs for PFC	152
5.4.4. PEV's Power Reserve Release Moments After the Disturbance	153
5.5. Brief Description And Discussion On Economic Evaluation of PEVs for PFC (Outside the Scope of This Technical Research)	155
5.5.1. Introduction To Economic Value Of PFC In Power Systems	155
5.5.2. Economic Evaluation of PFC Including PEVs	162
5.5.3. UFLS Scheme For Previous Case Study And Simulation Scenarios	166
5.5.4. Results	167

5.6. Discussion 170
5.7. Conclusions and Out-Look 170

Within both previously-developed aggregate models of PEVs for PFC in chapters 3 and 4, the frequency-droop controller was not necessarily chosen in an optimal way, and in fact the desirable value of the droop controller was not basically known. In previous simulations, it was observed that on the one hand, the power response of PEVs for PFC has a very low value when the droop is large. On the other hand, the response of PEVs during the PFC could become very oscillatory, when the droop has a very low value. In simple words, due to a relatively fast response, PEV’s participation in the PFC could highly affect the frequency stability of power systems. Thus, in this chapter, we describe a strategy to design the frequency-droop controller of PEVs for PFC. The design guaranties the same stability margin for the control system with and without PEVs, therefore both strategies can be properly compared. The proposed control strategy is simulated and evaluated using Matlab / Simulink, and the simulation results will be presented and discussed. Finally, the main conclusions will be drawn. Besides, since we mainly discussed the technical performance of PEVs for the PFC (outside the scope of this technical research), their economic performance will be also addressed and assessed in brief at the end of this thesis research.

5.1. Introduction

In the previous two aggregate models of PEVs for the PFC in chapters 3 and 4, the value of PEV’s frequency droop was chosen according to the one of conventional generating units or taken from other research works, and consequently the PEV’s droop controller was not optimally selected. Despite this fact, the droop controller of PEVs could have significant impacts on the frequency stability of power systems. Therefore, there is a critical need for innovative strategies to properly design and adjust the frequency droop controller of PEVs. Moreover, to evaluate the previously-proposed aggregate models of PEVs for the PFC, we compared the minimum /or maximum frequency response of power systems, despite the fact that beforehand, we first should have checked and ensured the frequency stability of the power system.

- The main research questions are posed as follows:
 - To what extent the participation of PEVs in the PFC affects the frequency stability of power systems? To what extent a trade-off does exist between the frequency stability and performance of power systems including PEVs?
 - What is the best value of PEV’s droop controller for the PFC considering the frequency stability criteria? How shall the PEV’s droop controller be

well designed taking into account the highest expected penetration rate of PEVs?

In order to properly address the above mentioned questions, first the previous research works on the provision of PFC by PEVs are reviewed. In fact, in the past, the frequency droop controller has been the most widely used approach in order to make PEVs able to provide the PFC (Almeida et al., 2011, 2015; Mu et al., 2013a; Pillai & Bak-Jensen, 2010b). In particular, these research works have mainly compared the minimum frequency response of power systems with and without PEVs. In (Mu et al., 2013a), PEVs effectively participated in the PFC by immediately disconnecting (0% droop) from the Great Britain power system in the target year of 2020. In (Pillai & Bak-Jensen, 2010a,b), PEVs were employed to enhance the frequency response of an islanded Danish distribution network, where they are equipped with 4% droop coefficient. In (Almeida et al., 2011), the frequency response of an isolated network was improved by PEVs using 2% droop coefficient (i.e, the nominal PEV power for a frequency deviation of 1 Hz). Also, the same droop coefficient (i.e., 2%) was used in (Almeida et al., 2015), where additionally the emulated inertia controller was implemented. In (Liu et al., 2013; Ota et al., 2010), the droop curve of PEVs has been continuously adjusted between 1% and infinity over a long period of time to maintain the battery energy close to the desired value. Moreover, in chapters 3 and 4, the droop coefficients of 5% and 1% were not optimally chosen and used within the proposed aggregate models of PEVs for the PFC.

Though, a great deal of previous research has been conducted on the provision of PFC by PEVs, some important aspects of the frequency stability in electric power systems have not been adequately and properly addressed and ensured yet. In fact, PEVs are able to provide the PFC service relatively fast, and consequently they have a great potential to severely affect the frequency stability of power systems. Undoubtedly, the previous research falls short in properly addressing the following points:

- Without first investigating the system frequency stability, in previous research, the minimum frequency value during PFC was considered as the main performance index for the PFC including PEVs. However from the control theory point of view, the minimum frequency of systems with and without PEVs for the PFC could be properly compared only if beforehand the frequency stability of two systems is checked and guaranteed. In other words, the frequency response of the power system with PEVs has a similar curve shape to the one without PEVs. If in future PEVs put at risk the overall frequency stability of power systems (oscillatory response), system operators might not entirely use their capability, even though they largely improve the minimum frequency of power systems. So far, little research attention has been paid to this important aspect in the literature, as the penetration rates of PEVs have been typically considered very low. As a result, PEVs had a negligible impact on the frequency stability of power systems. Despite this fact, as reported in (Mu

et al., 2013a), the frequency stability could be seriously deteriorated when the high penetration rate of PEVs attains higher values.

- As mentioned, the droop coefficients have not been optimally chosen for the PFC by PEVs, and therefore these droop curves were not necessarily well-designed or fine-tuned with respect to the overall system stability criterion. On the one hand, if PEVs have a very low droop coefficient, as considered in (Mu et al., 2013a), they could quickly provide a large amount of active power reserve following a frequency disturbance. This way, a large number of PEVs could potentially put at risk the system frequency stability, as reported in (Mu et al., 2013a). On the other hand, if PEVs have a large droop coefficient, then they do not sufficiently support the frequency during the disturbance. Therefore, for instance in (Pillai & Bak-Jensen, 2010a,b), the available primary power reserves of PEVs have been very slowly utilized using a typical droop coefficient of 4%, while the frequency stability was still ensured. In summary, if the PEV's droop is not properly designed according to the system frequency stability criterion, the provision of PFC by PEVs might have serious consequences (e.g., oscillatory modes or frequency instability) for the system operation.

To shed light on the above-stated shortcomings, this chapter describes a strategy to design the frequency-droop controller of PEVs for PFC. From a technical point of view, we demonstrate that PEVs improve the PFC performance by reducing significantly the frequency deviations. To this end, a novel design of PEV's frequency-droop controllers for PFC is proposed while maintaining the overall stability margins of systems with and without PEVs. In fact, the PEV's participation in the PFC might notably degrade the system frequency-response stability (e.g., a very oscillatory response), although the frequency response in terms of the minimum frequency is improved by PEVs utilizing the typically used droop curves. The PEV's droop controller is well designed for the worst-case operating mode for the greatest future expected penetration of PEVs using LINMOD function / Simulink (Matlab/LINMOD, 2015) such that the overall stability margin of the system including PEVs is guaranteed to be always equal to or greater than the one without PEVs. Then by simulating the original non-linear system, the system performance improvements, which result from PEVs, in terms of the minimum frequency response are assessed. Besides, since the fast response of PEVs may cause to mask the response in conventional units, a novel control scheme is developed to replace some portion of PEV's reserve after a certain time by the reserve of conventional units during PFC,

This chapter comprises of the following seven Sections:

- Section 5.2 presents the technical implementation of the previously developed aggregate models of PEVs for the PFC. In this section, a strategy is described to design the frequency droop controller of PEVs for the PFC.
- Section 5.3 describes the case study of CIGRE low voltage distribution network, which was presented in detail in the previous section. Moreover, simulation scenarios for a large-scale power system and an islanded network are

provided.

- Section 5.4 presents the simulation results of power systems with and without PEVs using the well designed droop controller. Also, the economic impact of PEVs participation in the PFC will be briefly described, evaluated and discussed.
- Section 5.5 concludes this chapter and the outlook of the next chapter is presented.

5.2. Technical Implementation: Strategy to Design Frequency-Droop Controllers of PEVs

This section presents a strategy to design the frequency droop controller of PEVs for PFC is proposed and described. As discussed above, PEVs have a large potential to affect the frequency stability of power systems due to their relatively fast response. In fact, the currently used droop curves of PEVs are not necessarily well-designed or fine-tuned with respect to the overall system stability criteria. As a result, from a technical point of view, there is a need for investigating the frequency stability of power systems, while PEVs participate in the PFC. On top of this, the frequency droop controller of PEVs shall be well designed according to the frequency stability criteria. To check this criteria, the frequency stability is usually measured by the stability margins such as phase or gain margins, while the original nonlinear system has to be linearized around the operating point. In summary, the design will be performed in this section mainly in the following three steps:

1. *System stability margin analysis:* The stability margins (i.e., gain and phase margins) of power systems with and without PEVs are obtained for various values of PEV's gain for the PFC. It is worth mentioning that the overall PEV's gain is a function of both frequency droop curve and penetration rates of PEVs. Therefore, when the desired gain of a single PEV is obtained, then the droop curve can be designed for the penetration rate of PEVs. To properly compare systems with and without PEVs, the system stability margin is to be preserved using the desired gain of PEV droop controller. The results, which are analyzed in this step, are only for the system's worst case that beforehand has been identified through extensive sensitivity analyses on various sets of system's parameters (see step 2).
2. *Design of the overall gain of PEVs:* The overall gain of PEVs is obtained for the worst case of power systems (see below), for which the stability margin has a very low value. To identify the worst case of power systems, extensive sensitivity analyses are carried out on a considerable number of sets of system's parameters.
3. *Design of the frequency droop controller of individual PEV:* As the overall gain of PEVs is obtained in the previous step, we obtain the frequency droop control

of each individual PEV for the worst case scenario (see below), i.e., highest future expected penetration rate of PEVs. According to the penetration rate of PEVs, we will design and obtain the desired droop coefficient of a single PEV.

The well-designed droop could have a low value compared to the one of CGUs, and therefore PEVs using well-designed droop are able to cover a large portion of the disturbance during the PFC. If PEVs reject a high portion of the power mismatch just after the disturbance, CGUs with a relatively slow response might negligibly participate in the PFC. After step 3, we propose an effective and simple control scheme to release some portion of the reserve of PEVs by the one of CGUs. As a result, it is ensured that CGUs have also covered some portion of the disturbance during the PFC.

Second, we address in brief how the performance of the proposed design strategy could be tested and evaluated through dynamic simulations. As mentioned above, during the three design steps, the original non-linear system should have been linearized around the operating point. However, in order to evaluate the design strategy, we create a detailed and realistic non-linear model of the power system, and then this model is evaluated and verified through dynamic simulations.

Technically speaking, if the participation of fast-controlled PEVs in the PFC puts the frequency-response stability of the system at risk using improper PEV droop coefficient, even though they improve the minimum frequency following the disturbance. In other words, though the minimum frequency following the disturbance is improved by the PEV's participation, the obtained frequency response curve by PEVs might not be feasible and acceptable with respect to the system stability criterion (e.g., a highly oscillatory response). By continuously checking and monitoring the phase margins and crossover frequency of power systems with and without PEVs, we will be able to design the frequency droop controller of PEVs while safely preserving the frequency stability. To describe our proposed design strategy, first we have to determine the worst case for which the phase margin of the control system has the lowest value. To this end, we qualitatively describe the worst cases associated with power systems and PEVs as follows:

- *Worst case of power systems:* Technically speaking, to identify the worst case of power systems, sensitivity analyses are carried out on various sets of system parameters such as equivalent inertia, damping ratio, turbine time constants, PEV time constants, and secondary frequency controllers. Importantly, the frequency stability of power systems highly depends on the equivalent system inertia¹. If the overall system inertia has a low value, then the rate-of-change-of-frequency following a contingency event could be very large, and as

¹As presented in chapter 2, the overall power system inertia can be described as the rate of change of the conventional generator's kinetic energy according to the time. In other words, it can be also interpreted as the ability of power systems to suppress frequency deviations following either small or large mismatch between the total generating power and load power consumption.

a result the frequency might reach the maximum /or minimum limits. The phase margin of power systems is gradually reduced when the system inertia steadily decreases. In present-day power systems, the overall system inertia still has a very satisfactory value because of which system operators are not currently required to ensure a certain amount of inertia. However, in the near future, as the penetration level of renewable energy sources like wind and solar largely increases, system operators might need to determine the unit commitment schedules in such a way that always a certain amount of inertia would be maintained. This way, they could ensure the frequency stability of power systems following the large disturbances by preserving the system inertia. In summary, the worst case of power systems for frequency stability could occur when the inertia has the lowest value. Thus, we will perform our design strategy for the frequency-droop controller of PEVs based on this worst case scenario. In a similar manner, other system parameters are also evaluated in such a way that the worst case scenario of power systems is defined.

- *Worst case of PEV fleets:* In the near future, a significant increase in the number of PEVs is expected. If a large number of PEVs participate in the PFC, then they could largely affect the frequency stability of power systems because they are able to quickly provide the PFC service. From a control theory point of view, this makes the closed-loop of frequency control very fast, and consequently the stability margin can be greatly degraded (i.e., very oscillatory or even unstable). As might be expected, the higher the number of PEVs, the lower is the frequency stability margin. To describe an appropriate design strategy for the frequency droop controller of PEVs, we have to determine the worst case of PEV fleets, that could the highest future expected penetration rate of PEVs.

In a nutshell, once the design strategy is properly performed according to the above-determined worst cases, then we could ensure the frequency stability of power systems with and without PEVs for all other possible scenarios as well. As a result, in the next stage, it would be possible to surely compare the minimum frequency response of both systems during the PFC through dynamic simulations. As mentioned, in previous research, the frequency stability of power systems has not been primarily checked and ensured, since the penetration rate of PEVs mostly had a very low value. However, undoubtedly, this is an important process that can not be simply neglected especially for scenarios with moderate or high penetration rates of PEVs. As in this thesis research, we evaluated a wide range of PEV's penetration rates for the PFC analysis, inevitably we have to check and ensure the system's frequency stability beforehand. Therefore, we could properly compare the performance of power systems with and without PEVs during the PFC.

To obtain the above mentioned stability margins, first the non-linear model of the network for the PFC is to be linearized around the operating point. Therefore, the frequency control's non-linear functions such as the dead-band, maximum and

minimum power limits, and ramp rates² of the generating units as well as PEVs are to be neglected. Then, the bode plots of the open loop control system can be obtained (e.g., in Matlab/Simulink using LINMOD function), as shown in Figure 5.1 (for further information on the models of governor-turbines depicted in Figure 5.1, see Appendix B).

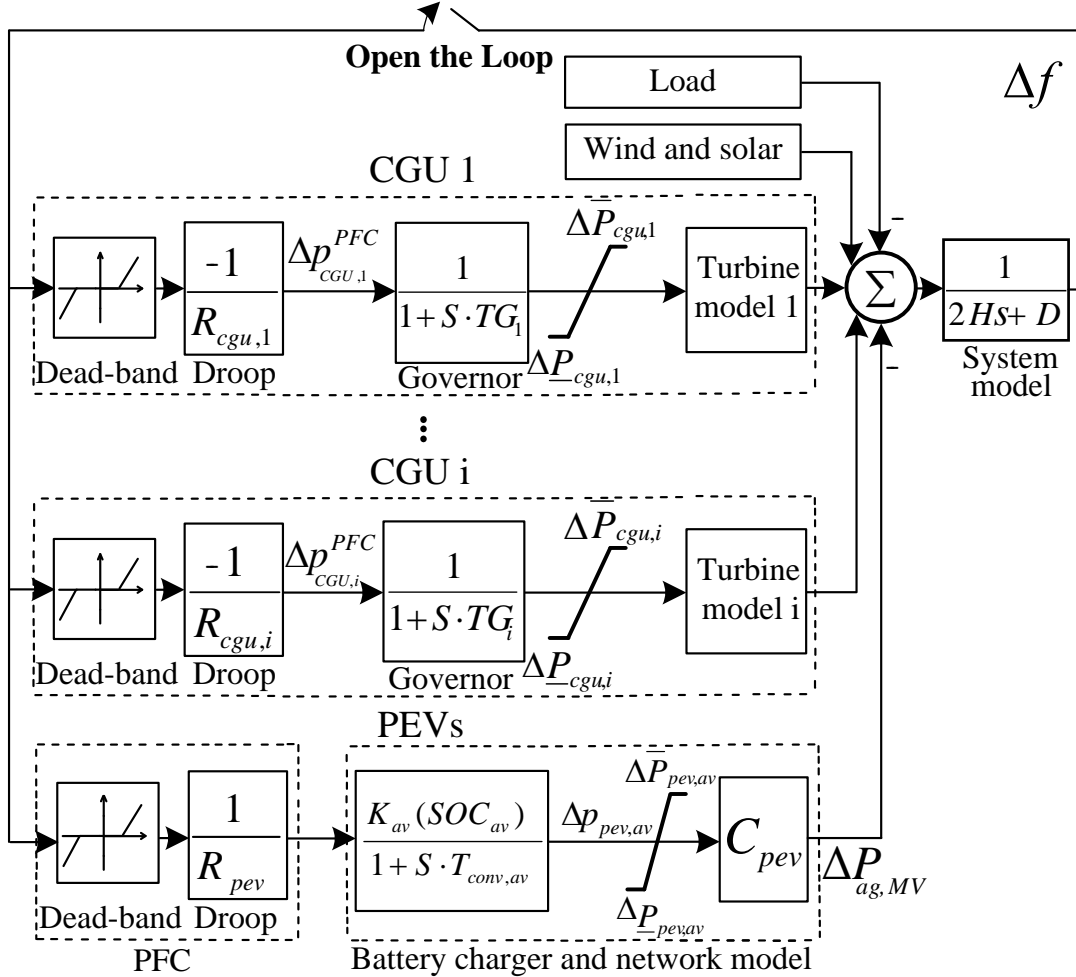


Figure 5.1.: Frequency control system including aggregate PEVs, and the point where the loop is opened.

5.2.1. System Stability Margin Analysis

In the first step, our aim is to obtain the phase margin and crossover frequency of power systems with and without PEVs. If PEVs do not participate in the PFC, then their overall gain in the model could be considered as zero. Therefore, the

²Here, ramp rate is defined as the change in the power of generating units over time. It is the maximum rate at which conventional generating units could vary their active power within a certain period of time.

phase margin and crossover frequency of power systems will uniquely depend on the dynamic behaviour of conventional generating units³. If PEVs are added to the power system for the PFC, then this means that their overall controller gain should be increased. The overall controller gain of PEVs K_{pev} can be given by

$$K_{pev} = \frac{K_{av}(SOC_{av}) \cdot \sum_{j=1}^N \left[\prod_{n=j}^N (1 + LF_n) \cdot C_j \right]}{R_{pev}} \quad (5.1)$$

As observed, the overall gain of PEVs depends on both the effective number of PEVs for PFC as well as the droop characteristics. Therefore, to perform our proposed design strategy, first our aim is to determine the appropriate overall gain of PEVs for the PFC according to the phase margin and crossover frequency obtained from the bode diagrams. Then, once the overall gain was found, then the droop of PEVs could be adjusted according to the effective number of PEVs for the PFC. Note that in this step, only the results of the worst case of the power system are analyzed, and in the second step, the worst case will be identified conducting sensitivity analyses on various sets of system parameters. In other words, here only the results of the previously identified worst case will be given and analyzed.

To obtain the bode diagrams and then stability margins, we shall draw the following considerations:

1. *Frequency control loop linearization:* In fact, the precise dynamic model of power systems including PEVs has a highly nonlinear character. For instance, many components such governors and turbines of conventional generating units have a very nonlinear behavior. Also, the power conversion system of PEVs (i.e., battery charger system) has a nonlinear feature. On top of this, the frequency control loop has a number of nonlinear functions, which should be linearized around the operating point according to the classic control. In this analysis, as mentioned above, the nonlinear components have already been linearized, and furthermore, the non-linear terms such as dead-band and maximum /or minimum power limits can be simply neglected.
2. *Open-loop frequency control loop:* In order to obtain the bode diagrams, the closed loop frequency control should be obviously opened. In fact, the feedback of the PFC loop is considered in the whole open-loop system including CGUs and PEVs, and the bode diagrams of amplitude and phase of the linearized system is obtained using LINMOD function / Simulink.

³In this chapter, we assume that renewable energy sources like wind and solar as well as the demand do not actively participate in the PFC. As a consequence, their power variation during the PFC is assumed zero and moreover, they do not affect the stability margins obtained from the frequency control loop.

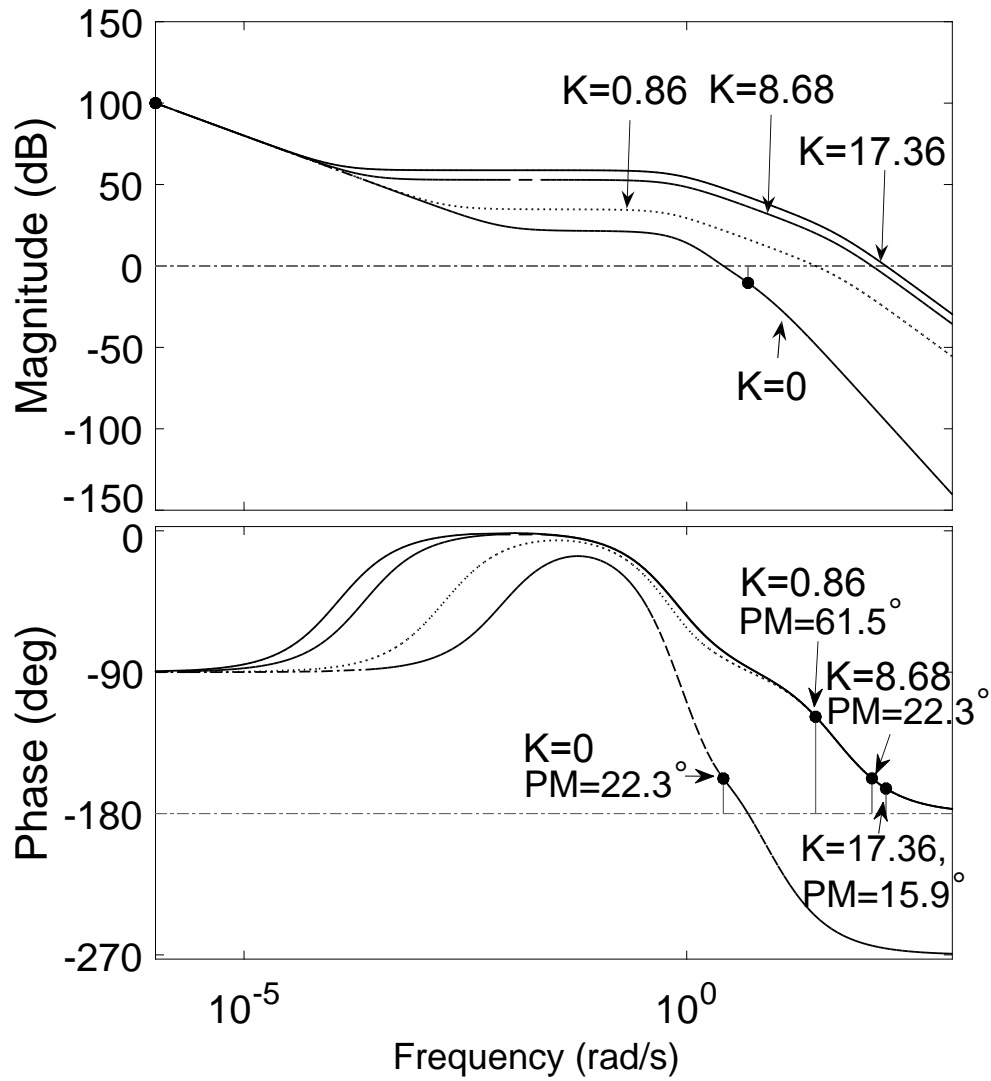


Figure 5.2.: Open-loop bode diagrams of amplitude and phase for various values of the PEVs overall gain K_{peg} .

In summary, we will be able to obtain the bode plots and then phase margin of power system including PEVs, where K_{peg} changes from 0 to a high value (i.e., 17.36). Figure. 5.2 presents the open-loop bode diagrams of amplitude and phase for various values of K_{peg} .

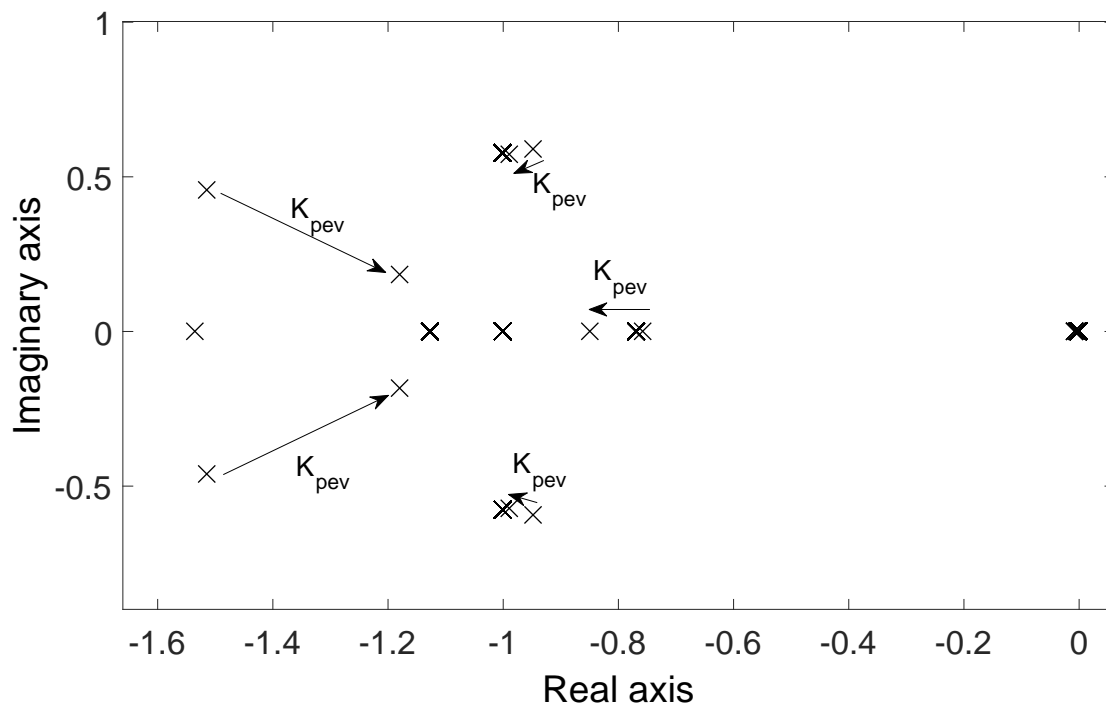


Figure 5.3.: Trace of closed loop eigenvalues for K_{peg} from 0 to 8.68

To further evaluate the frequency stability, the well-established eigenvalue analysis is performed on the power system's dynamic model presented in Figure. 5.3. Figure. 5.3 shows the trace of closed loop eigenvalues where K_{peg} increases from zero to the desired value, i.e., 8.68. As expected, the phase remains very similar in both cases.

As t K_{peg} increased from zero to a high value, we observed that initially the phase margin was improved by PEVs (until K_{peg} equal to 0.868). Then however the phase margin started to decrease until the stability margin of systems with and without PEVs becomes the same (K_{peg} equal to 8.68). To analyze the obtained stability margin according to K_{peg} , first it is worth underlying that the average converter time constant $T_{conv,av}$ of PEVs (e.g., a few fundamental cycles or a few tens of milliseconds) is relatively very low compared to the governor TG_i and turbine TR_i time constants of CGUs (e.g., several seconds). Therefore, the introduction of PEVs into the PFC system generally leads to a comparatively fast response of the control system (providing a lower delay), and consequently both phase margin and system crossover frequency at 0 dB gain initially increase by K_{peg} in the bode diagrams (for further details of the typical system under study, see section 5.5).

Figure. 5.4 illustrates the phase margin and crossover frequency versus K_{peg} . For higher values of K_{peg} , the phase margin steadily degraded. As a result, we could identify three distinct phases as follows, as shown in Figure. 5.4:

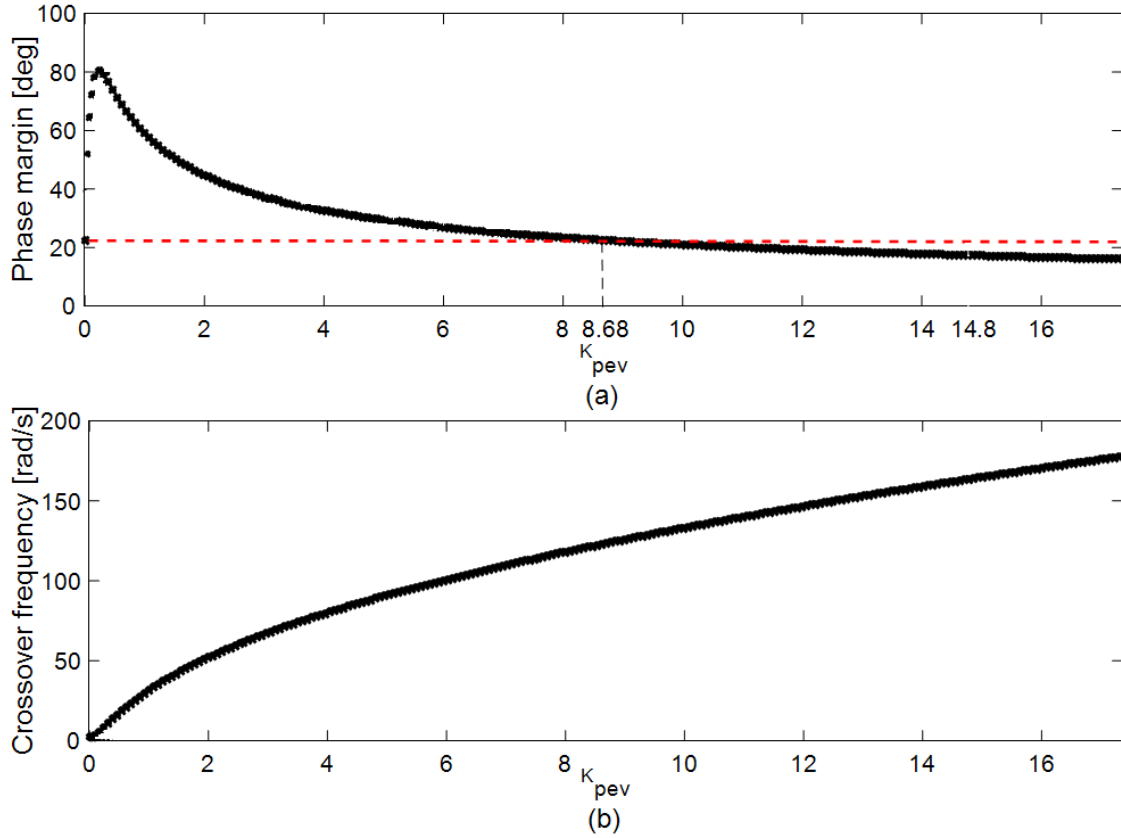


Figure 5.4.: Phase margin and crossover frequency of the frequency control scheme versus K_{peg} for worst case.

1. K_{peg} between 0 to 0.868: If K_{peg} is equal to zero, then this means that PEVs do not participate in the PFC or are not connected to the power system. According to the case study defined in section 5.5, the phase margin and crossover frequency of power system are 22.3° and 2.59 rad/s, respectively. When K_{peg} increases from 0 to 0.868, the overall system phase margin is initially improved from 22.3° to 28.7° . Also, the crossover frequency largely increases from 2.59 to 61.5 rad/s. This illustrates that PEVs have a great potential to make the frequency control loop fast.
2. K_{peg} between 0.868 and 8.68: For K_{peg} greater than 0.868, the stability margin starts to progressively decrease until at a certain value of $K_{peg}^{desired}$ equal to 8.68, it reaches the same stability margin as the system without PEVs (i.e., $K_{peg} = 0$). Also, the crossover frequency largely increases from 28.70 to 124 rad/s.
3. K_{peg} greater than 8.68: For K_{peg} greater than 8.68, the stability margin is highly degraded compared to the one of the system without PEVs. For instance, when K_{peg} increases from 8.68 to 17.36 (two times), the overall system

⁴In this chapter, the overall gain of PEVs at which the stability margin of power systems with and without PEVs become the same is called $\kappa_{peg}^{desired}$.

phase margin reduces from 22.3° to 15.9° . Also, the crossover frequency largely increases from 124 to 179 rad/s.

Our aim in this step was to evaluate the impact of PEVs on the frequency stability of power systems. As observed, for a lower penetration rate of PEVs, they initially improved the phase margin. However, for higher penetration rates of PEVs, the stability margin started to steadily reduce until it reached the same value as the system without PEVs (e.g., at $K_{pev}^{desired}$ equal to 8.68). On the one hand, in order to ensure the stability of the system, this means that the overall gain of PEVs should not be set greater than the obtained value. On the other hand, if the overall gain of PEVs is set lower than the obtained value, then the available fast response of PEVs might not be sufficiently employed, and as a consequence, the crossover frequency obtained a lower value.

In conclusion to this design step, we generally identified and demonstrated a clear trade-off between the frequency stability and performance of power systems including PEVs. Accordingly the optimal value of the overall gain of PEVs was obtained where PEVs could support the frequency response at the optimal rate, while preserving the frequency stability.

It is worth noting that the above-mentioned analysis was performed only for a predefined case study of power systems, despite the fact that the dynamic behavior of power systems could significantly change over time. Thus, in the next design phase, we identify and evaluate the worst case of power systems for the frequency stability problem.

5.2.2. Design of the Overall Controller Gain of PEVs

In this design step, we identify and evaluate the worst case of power systems for the frequency stability problem. In practice, the share and type of conventional generating units committed to the system highly change over time based on the outcome of the unit commitment schedules. As a result, the overall inertia of power systems could largely vary over time that considerably affects the overall stability margin of power systems. According to the classic control, in the frequency control loop, the overall stability margin is expected to have the lowest value when the overall inertia is minimum. In other words, we expect that the worst case of power systems occurs at the minimum level of overall system inertia. In order to support this statement, Figure 5.5 shows the phase margin and crossover frequency of the open-loop control system versus K_{pev} for various shares and types of conventional generating units with different total inertia. Note that here to evaluate the stability margins for low, medium, and high values of the system inertia, we considered 1.3, 3.9, and 7.8 s, respectively. Then, the stability of power systems with and without PEVs for different values of inertia (i.e., 1.3, 3.9, and 7.8 s) are analyzed as follows:

- *Stability of power systems without PEVs:* At K_{pev} equal to zero, Figure. 5.5 shows the overall system stability margin of power systems including only CGUs. As seen, when the system inertia increases from 1.3 to 7.8 s, the phase margin largely varies from 22.3° to 43.9° . Also, at K_{pev} equal to zero, the crossover frequency reduces from 2.59 to 0.89 rad/s. This obviously demonstrates that the overall stability increases by the system inertia. Therefore, the worst case of power systems might be the case for which the inertia has the minimum value. In order to further ensure this, next we evaluate the stability margins of different systems when PEVs are added to them.
- *Stability of power systems with PEVs:* If PEVs are added to provide the PFC, different optimal values of K_{pev} might be obtained according to the overall inertia of power systems. As mentioned in the previous step, PEVs initially improve the stability margin and later for their higher penetration rates, the stability margin was highly degraded, as shown in Figure. 5.5. In Figure. 5.5, the phase margin and crossover frequency versus the overall gain of PEVs is illustrated for different values of inertia (i.e., 1.3, 3.9, and 7.8 s). On the one hand, at each value of K_{pev} in Figure. 5.5(a), the overall stability margin of the system with inertia equal to 1.3 s always remains low compared to the one with the inertia equal to 7.8 s. On the other hand, at each value of K_{pev} in Figure. 5.5(b), the crossover frequency of the system with inertia equal to 1.3 s remains large compared to the one with the inertia equal to 7.8 s. As shown, if K_{pev} is obtained and designed at 8.68 for the lowest level of inertia equal to 1.3 s, then always the stability margin safely remains at higher values for other shares of CGUs with the higher total inertia. As a result, it can be concluded that the worst case of power systems is always associated with the minimum total inertia of the system, and for this worst case of power systems, $K_{pev}^{Desired}$ was obtained equal to 8.68.

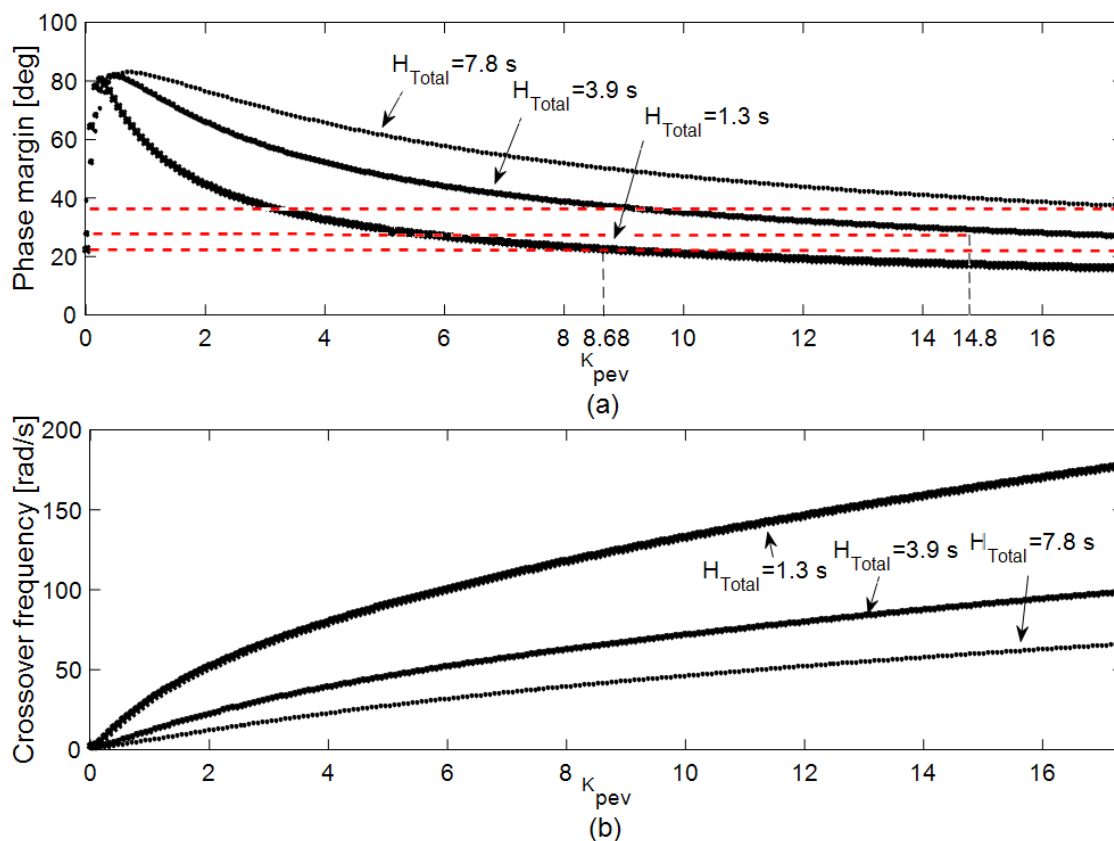


Figure 5.5.: Phase margin and crossover frequency of the frequency control scheme versus K_{pegv} for various shares and types of conventional units with different total inertia of the system.

It is worth mentioning that if the design strategy is performed for the minimum value of $K_{pegv}^{desired}$, then as shown, the system's stability is successfully preserved for higher values of $K_{pegv}^{desired}$. Nonetheless, $K_{pegv}^{desired}$ does not only depend on the overall inertia, but also on various sets of parameters of power system's dynamic models, given in Figure 5.6. Therefore, to represent the minimum desired value of $K_{pegv}^{desired}$, an extensive sensitivity analysis similar to the above-obtained inertia is performed on the relevant parameters of the dynamic model. Figure 5.6(a) shows $K_{pegv}^{desired}$ obtained for various ratios (i.e., 1 (Kundur et al., 1994; Pillai & Bak-Jensen, 2011), 1.25, 1.5, and 2 times) of the nominal turbines time constants. Here it is reasonably assumed that the turbine time constants could range up to two times of the nominal turbines time constants. As expected, the minimum $K_{pegv}^{desired}$ of 8.68 is obtained for the lowest turbine's time constant for which the CGU's behavior becomes relatively fast. Figure 5.6(b) shows that the minimum $K_{pegv}^{desired}$ of 8.68 is obtained when the PEV time constant $T_{conv,av}$ has a high value. If the time constant changes from 30 ms (Zhang et al., 2012), to one time constant period (i.e., 20 ms). Similarly, Figure 5.6(c) illustrates that the minimum $K_{pegv}^{desired}$ of 8.68 is obtained when the load damping had a high value. It is assumed that the load damping ranges between 0.5

(Nguyen et al., 2015) and 1 (Kundur et al., 1994; Mu et al., 2013a). Last but not least, Figure 5.6(d) clearly shows that the impact of load frequency controller (i.e., principally integral controller) (Kundur et al., 1994) is relatively low on $K_{pev}^{desired}$. In fact, for this design strategy, the secondary frequency controllers have a negligible impact, since they have a very slow response compared to the PFC controllers. In summary, $K_{pev}^{desired}$ is obtained for the lowest possible inertia and turbine time constant and the highest possible PEV time constant and load damping. Note that though the above mentioned ranges of parameters were taken from the relevant literature (Kundur et al., 1994; Mu et al., 2013a; Nguyen et al., 2015; Pillai & Bak-Jensen, 2011; Zhang et al., 2012), in practice these ranges might still change from one network to another. Nonetheless, the aim of the here-presented sensitivity analysis was to particularly demonstrate to what extent each dynamic model's parameter affects the stability margins as well as $K_{pev}^{desired}$ within a realistic range.

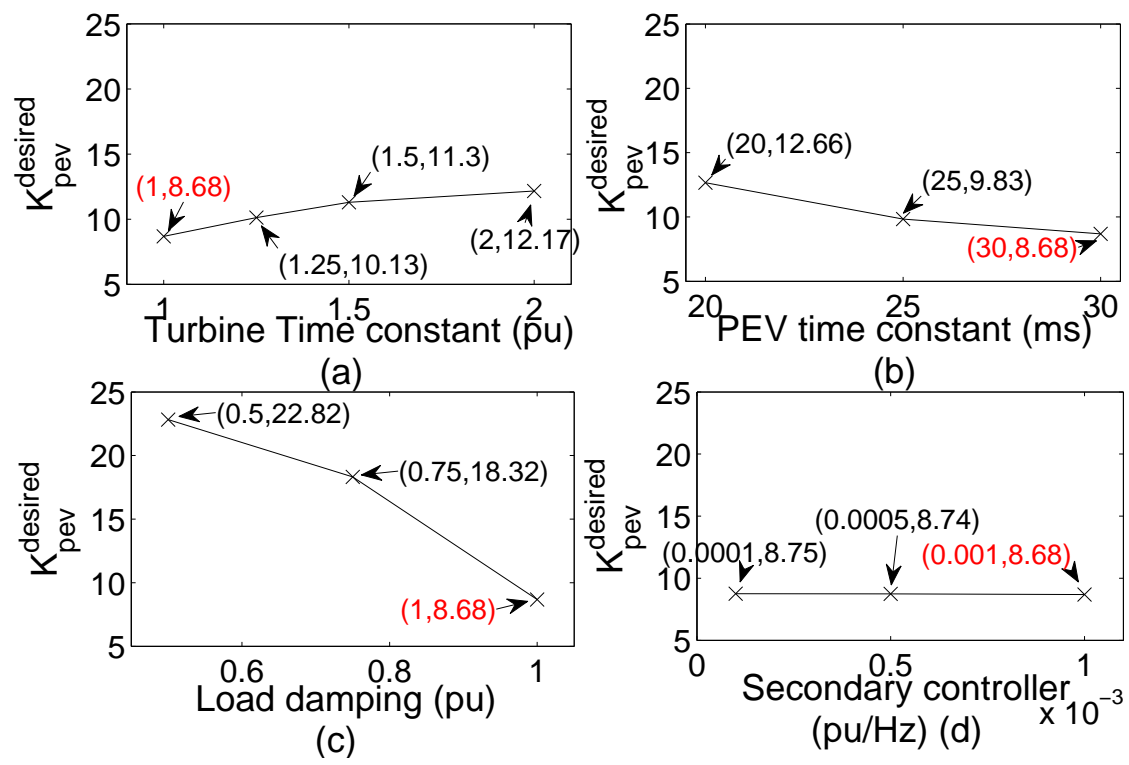


Figure 5.6.: $K_{pev}^{desired}$ for various sets of parameters, i.e., turbine time constant (pu), PEV time constant, load damping, and secondary controller

Our aim in this step was to identify the worst case of power systems for the frequency stability problem, and it was concluded that the worst case occurred when the overall inertia had its minimum value. For this worst case of power systems, $K_{pev}^{Desired}$ was obtained equal to 8.68. In order to complete the proposed strategy, next we calculate and design the frequency droop controller of a single PEV taking into account the above-obtained gain of all PEVs as well as the highest future expected penetration rate of PEVs.

5.2.3. Design of the Frequency-Droop Controller of Individual PEVs

In the last design step, the droop controller of a single PEV is designed such that the overall stability margin of the linearized system is not degraded by PEVs for the worst-case design condition, i.e., greatest future expected penetration of PEVs. To define this worst case scenario, we show that if the PEV droop is properly designed for the highest expected penetration rate of PEVs, then using this droop value, also the system stability margin safely remains high for the lower penetration rates of PEVs.

According to 5.1, K_{pev} depends on three parameters of $K_{av}(SOC_{av})$, R_{pev} , and C_{pev} . Taking into account $K_{pev}^{Desired}$ obtained in the previous design step, various values of PEV droop R_{pev} should be obtained according to the values of $K_{av}(SOC_{av})$ and C_{pev} as follows:

- Average participation factor $K_{av}(SOC_{av})$: As described in chapter 3, the participation factor was introduced for PEVs in order to determine the participation level of each PEVs in the PFC. Afterwards, the average participation factor of PEVs was obtained that depends on the probability density function of PEV's state of charge. Note that for this analysis, all PEVs are considered to have the maximum participation ($K_{av}(SOC_{av})$ is equal to one) and later it will be shown that the stability will be ensured for lower values of $K_{av}(SOC_{av})$.
- Effective number of PEVs C_{pev} according to the number of PEVs as well as distribution network characteristics: In the near future, the number of PEVs is expected to highly increase, and consequently their penetration rate in electric power systems will increment. To calculate the penetration rate of PEVs $\rho_{pev}\%$, it can be obtained according to the effective number of PEVs considering the distribution network C_{pev} , maximum average power limit of PEVs $\bar{p}_{pev,av}$, and total base power S_{base} as follows:

$$\rho_{pev}\% = 100 \cdot \frac{\bar{p}_{pev,av} \cdot C_{pev}}{S_{base}}. \quad (5.2)$$

In fact, we formulate the droop of PEVs in such a way that the effective number of PEVs is taken into account. Since a wide range of penetration rates of PEVs could be expected in the future, here we evaluate the PEV penetration rates of 2%, 5%, and 30%.

Our aim here is to demonstrate that if the design strategy is performed for the highest future penetration rate of PEVs (i.e., last scenario of PEVs), then the system stability is straightforwardly assured for the lower penetration rates of PEVs as well. As mentioned, $K_{pev}^{desired}$ was obtained equal to 8.68 for the worst case of power system in the previous step. For this $K_{pev}^{desired}$ in Figure 5.7, the PEV droop percent $R_{pev}\%$ is obtained equal to 0.07% for the penetration rate of 30%. Note that in Figure 5.7, the PEV droop percent was calculated as follows

$$R_{pev}\% = 100 \cdot \frac{\Delta f}{f_{nom}} \cdot \frac{P_{nom}^{PEV}}{\Delta P_{pev,av}} \quad (5.3)$$

$$R_{pev}\% = 100 \cdot \frac{P_{nom}^{PEV}}{S_{base} \cdot f_{nom}} \cdot \frac{\sum_{j=1}^N \left[\prod_{n=j}^N (1 + LF_n) \cdot C_j \right]}{\kappa^{PEV}}. \quad (5.4)$$

Finally, the well-designed droop is obtained 0.07%, which relatively lower than the droop value of the CGUs (e.g., 5%). However, it is worth mentioning that in practice the droop value might be calculated at higher values due to various reasons. First of all, we did not take into account measurements, computational delays, communication networks, etc, which might affect the stability of the control loop and consequently, in practice the well designed droop might be calculated higher than 0.07%. Secondly, non-linear functions, which could typically have an adverse impact on the frequency stability, were not obviously included (e.g., dead-bands, power limits, or ramp rates). Third, the abrupt power variation of PEVs especially in weak distribution grids might result in severe voltage deviations. As a result, in practice, the droop values higher than 0.07% might be implemented in PEV in future.

At $R_{pev}\%$ equal to 0.07%, for the penetration rates of 2% and 5% in Figure Figure. 5.7 on page 139, κ_{pev} is obtained equal to 0.5 and 1.4, respectively. This way, as shown in Figure Figure. 5.5 on page 135(a), the stability margin safely remains higher for the values of κ_{pev} below 8.68, e.g., 0.5 and 1.4 for the penetration rates of 2% and 5%, respectively. In conclusion, the desired PEV droop controller is obtained 0.07%, for which the system stability margin is securely preserved for a wide range of PEV penetration rates.

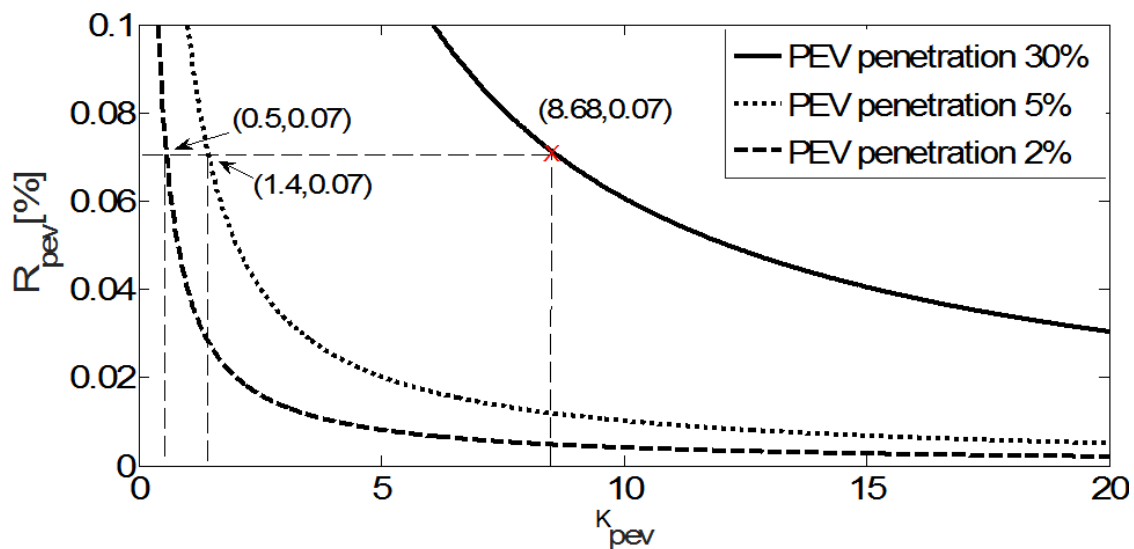


Figure 5.7.: PEV frequency-droop percent versus k_{pev} for PEV penetration rates of 2%, 5%, and 30%.

In conclusion to this design strategy, first we could successfully identify the worst cases of both power systems and PEVs for the design according to the phase margin and crossover frequency from the bode diagrams. Then, we could obtain the optimal value of frequency droop controller for each individual PEV while the frequency stability was checked and maintained. To illustrate this statement, Figure. 5.8 shows the frequency response of control system with and without PEVs using the here well designed droop controller, where they have similar curve shapes. This way, the maximum frequency deviations of both systems can be properly compared.

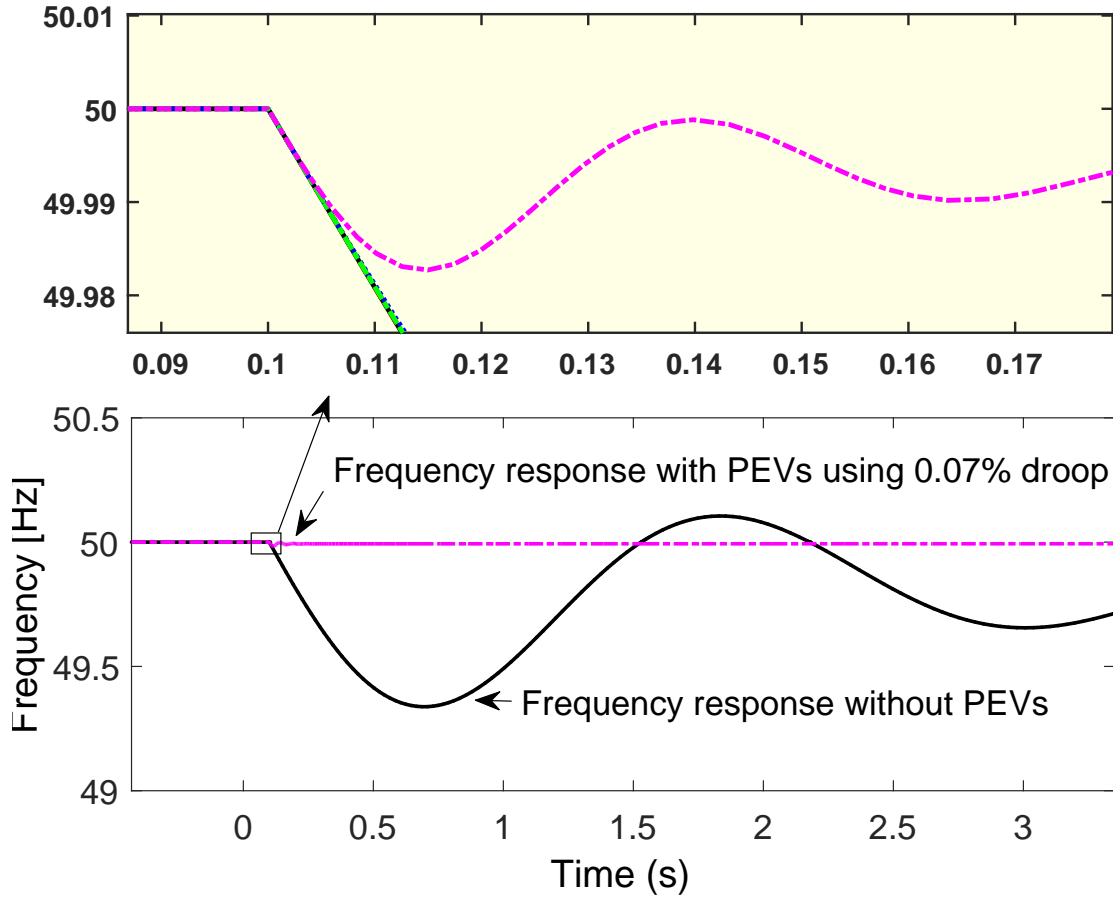


Figure 5.8.: PEV frequency-droop percent versus κ_{pev} for PEV penetration rates of 2%, 5%, and 30%.

5.2.4. Replacement of PEV's reserve by CGU's reserve during PFC

If PEVs use lower values of droop and their available reserve for PFC would be close to the amount of disturbance, then due to their superior fast response, they greatly reject the disturbance during PFC. This might undesirably mask the governor-turbine response in CGUs, and consequently CGUs might negligibly participate in PFC. To avoid this problem, PEVs reserve can be distributed among CGUs some moments after the disturbance. This has three major benefits for the PFC in power systems as follows:

1. The superior fast response of PEVs is effectively used right after the frequency disturbance. One of most important goal of the design was to avoid the underutilization of fast response of PEVs for the PFC just after the disturbance. However, when PEVs effectively suppress the frequency deviations, then the PEV's reserve can be released some moments after the disturbance.

2. The response of CGUs is not covered by the fast response of PEVs, so they also reject some portion of the disturbance during PFC. In practice, the fast superior response of PEVs using lower values of droop (e.g., 0.07%) mitigates the frequency disturbance in such a way that CGUs might negligibly participate in the PFC. During the time scale of PFC, if some portion of PEV's reserve is released, then CGUs could increase their participation in the PFC.
3. The reserve capacity of PEVs is partly released for the possible subsequent disturbances. If PEV's reserve for the PFC would be close to the size of disturbance in power systems, then it is crucial to improve the frequency response at any time of the day. If PEVs use most of their reserve for the PFC after a disturbance, then the power system might not have enough reserve for the PFC during the possible subsequent disturbances. Therefore, when PEVs improve the frequency deviations after the first disturbance, it will be essential to replace their fast reserve with the relatively slow reserve of CGUs during the PFC.

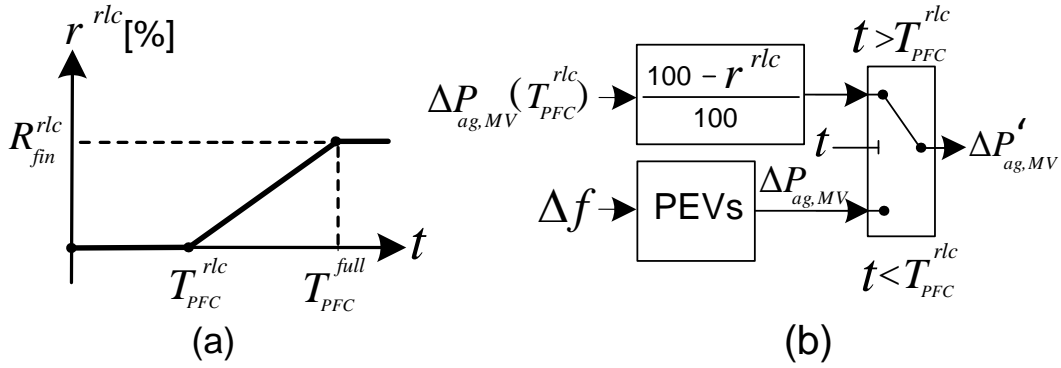


Figure 5.9.: Proposed PEV reserve replacement scheme after T_{rlc} PFC during PFC. (a) percentage of PEV reserve r^{rlc} replaced by CGU's reserve after disturbance over time. (b) proposed control scheme for PEV reserve replacement.

Figure. 5.9 presents the proposed replacement scheme of PEV's reserve by CGU's reserve. Figure. 5.9(a) shows the percentage of PEV reserve replaced r^{rlc} by CGU's reserve after disturbance. At t equal to zero, the disturbance is applied to the network. When the time is between zero and T_{PFC}^{rlc} , PEVs fully participate in PFC, and consequently do not release their reserve. After the time equal to T_{PFC}^{rlc} , PEVs start to release their reserve in a linear manner until the final PEV reserve release R_{fin}^{rlc} is obtained at T_{PFC}^{full} . To achieve this, PEVs during this period should not temporarily respond to the frequency deviations, therefore only CGUs respond to frequency changes and substitute their reserve. After T_{PFC}^{full} , which is the full deployment time of PFC, the PEV reserve replacement remains constant equal to R_{fin}^{rlc} . Figure. 5.9(b) shows the proposed control scheme for PEV reserve replacement, which is activated after T_{PFC}^{rlc} . The PEV's output power $\Delta P'_{ag,MV}$ after T_{PFC}^{rlc} is given by

$$\Delta p'_{ag,MV} = \Delta P_{ag,MV}(T_{PFC}^{rlc}) \cdot \left(\frac{100 - r^{rlc}}{100} \right) \quad (5.5)$$

where r^{rlc} , $\Delta P_{ag,MV}(T_{PFC}^{rlc})$ and $\Delta p'_{ag,MV}$ are the percentage of PEV's reserve replaced by CGU's reserve over time, the aggregate PEV power variation at T_{PFC}^{rlc} and the aggregate output power of PEVs during PFC, respectively. Note that this proposed scheme is implemented within the time scale of PFC (e.g., several seconds up to one minute), and therefore it is independent of the load frequency control which may last up to several minutes.

In order to evaluate the above-proposed technical implementation procedure, next we describe case studies of a large-scale power system and an islanded network.

5.3. Case Studies and Simulation Scenarios

The performance of a large-scale power system and an islanded network including PEVs during the PFC could be very different. This is why, this section describes case studies and simulation scenarios for both networks, i.e., a large-scale power system and an islanded network. To this end, we first present and analyze a base case study, which is a small-scale distribution network including PEVs. Then, this small-scale network will be replicated and scaled up to create an islanded network and a large-scale power system, which will represent simulation scenarios A and B, respectively.

Note that on a per unit basis, the dynamic model of an islanded network or a large-scale power system could be very similar in general, nonetheless in this thesis, two networks are distinguished due to the following reasons: 1) in an islanded network, a low number of CGUs supply the load, and as a consequence, the outage of a large generating unit could create a large disturbance (e.g., 0.1-0.25 pu) compared to the one of large-scale power systems (e.g., 0.02-0.05 pu), 2) as the UFLS scheme is considered for the economic evaluation (see section 5.5), different UFLS frequency thresholds as well as load amounts could be taken into account in an islanded network or a large-scale power system that finally results in different UFLS costs. In islanded network, UFLS can be triggered at higher values (Vrakopoulou & Andersson, 2010).

5.3.1. Base Case Study of Small-Scale Distribution Network

Technically speaking, the proposed strategy can be applied to both large scale power systems and islanded networks in a scalable and flexible way. Therefore, the small-scale distribution network, which mainly comprises of industrial, residential, and commercial areas, can be first considered and analyzed and then this small-scale

network could be scaled up to create the desired networks (for further information, see chapter 4).

Here, our aim is to obtain the total power variation of small-scale network for the PFC when PEVs participate in the PFC. To this end, in addition to the power variation of PEVs for the PFC, we should take into account the characteristics of the distribution network. As described in detail in chapter 4, the small scale network consisted of several distribution lines, which were characterized by the line's power and impedance, line factors LF_n . Afterwards in chapter 4, using the obtained LF_n and the number of PEVs C_j in each bus, the effective number of PEVs C_{pev} were calculated. The effective number of PEVs for the PFC C_{pev} was obtained 1.14 times of the total number of PEVs. Finally, by employing the simplifying assumption that $\Delta p_{pev,av}$ is already known about the PEV fleet, the aggregate power of PEVs $\Delta p_{ag,MV}$ was approximated in chapter 4.

The obtained aggregate power of PEVs $\Delta p_{ag,MV}$ includes both the power variation of PEVs and the variation of power consumed in the network during the PFC at the head of the distribution network. In the next step, this exemplary distribution network will be scaled up and replicated in order to create simulation scenarios for a large-scale power system and an islanded network.

5.3.2. Simulation Scenarios

To create the islanded network and large-scale power system, the previously presented small-scale distribution network, is replicated and scaled up. To this end, some parameters are to be adjusted according to the context of the large-scale power systems (i.e., scenario A) or islanded network (i.e., scenario B). However, a number of parameters will remain the same for both scenarios, and before presenting them, these common parameters such as the total system inertia, and operating characteristics of an average PEV for PFC are addressed as follows:

- *Total system inertia and load equivalent damping:* As mentioned in the previous section, the total inertia of the system depends on the type and share of the generating units committed to the system at each moment of the day. In this analysis, we could assume the same minimum inertia for both scenarios A and B, and therefore both networks could experience the same worst case of the system. This way, we could later properly compare the performance of both systems during the PFC. Generally speaking, the total system inertia H of a large number of generating units can be given by (see Table. 5.1)

$$H = \frac{\sum_m H_m S_m}{S_{base}} \quad (5.6)$$

where S_m , m , and H_m are the power produced by CGU m , an index for power plants, and the equivalent inertia of CGU m , respectively. The inertia of conventional generating units highly depends on the type of the units. While

large-scale thermal units could have a very large inertia (e.g., 7 s), gas turbines might have a relatively low inertia (e.g., 2 s). As stated above, the worst case for $K_{pev}^{desired}$ was obtained for the large values of load damping, e.g., 1.

Table 5.1.: CGUs and frequency control system in scenarios A & B.

	Scenario A		Scenario B
Power plant	H [s]	Generating power [MVA]	
Steam plants	3	30	3,000
CCGT	2	20	2,000
Wind and solar	-	50	5,000
System parameter	Value		
S_{base} [MVA]	100		10,000
Largest disturbance	10 MW - 0.10 pu		500 MW - 0.05 pu
Total equivalent H	1.3 s		
Load damping	1		

- *Average PEV for the PFC:* The average PEV for the PFC could be essentially the same for both scenarios A and B. Table. 5.2 mainly presents an average PEV for the PFC analysis, where the PEV model for the PFC has been comprehensively presented in chapter 4. The average nominal power of the battery charger P_{nom}^{PEV} and the average charging power of PEVs are assumed 3 kW and 1 kW, respectively. Also, the dead-band limit and the average time constant $T_{conv,av}$ of battery chargers are typically 10 mHz and 30 ms, respectively. It is assumed that all PEVs are equipped with bidirectional battery chargers, therefore they are able to inject the active power back into the grid during the PFC.

Table 5.2.: Average parameter values of PEVs for PFC.

Parameter	Value
$\rho_{pev}\%$	2%, 5%, or 30%
$T_{conv,av}$ [ms]	30
$\bar{P}_{pev,av}$ [kW]	3
$\underline{P}_{pev,av}$ [kW]	-3
$R_{pev}\%$	0.07%, 5%
Dead-band [mHz]	± 10

Next, we separately describe scenarios A and B, where the specific characteristics of such networks will be taken into account.

5.3.2.1. Simulation Scenario A for an Islanded Network

There are a number of justifiable reasons why an islanded network is evaluated and tested in this analysis. First, typically the frequency stability has a relatively lower level in islanded networks compared to the large scale power systems. Second, the amount of the largest disturbance has a comparatively high value in such networks. Table. 5.2 presents the power production of various generating units such as steam power plants, CCGT, wind farms and solar plants within an islanded network. To define the worst case scenario for this islanded network, it is assumed that the total power produced by wind and solar has a very high value, i.e., 50 MW or 50% of the total consumption⁵. From (5.6), if the base power of the islanded network S_{base} is 100 MVA, the total system inertia is obtained 1.3 s. As shown in Table. 5.1, the size of the disturbance is equal to 10 MW or 0.10 pu.

5.3.2.2. Simulation Scenario B for a Large-scale Power System

In the near future, the influence of PEVs on the frequency response of networks might be more significant in the islanded networks. However, to additionally compare the performance of PEVs in islanded networks and large scale power systems, we present scenario B for a large scale power system. Table. 5.1 presents the power produced by various generating units such as steam power plants, CCGTs, wind farms and solar plants. Compared to the islanded network, it is assumed that the large-scale power system is 100 times larger, although for the sake of simplification, the dynamic models of two systems are assumed the same. In order to represent the worst case scenario for the low inertia, it is assumed that the total power produced by wind and solar has a large value, i.e., 5,000 MW or 50% of the total consumption. From (5.6), if the base power of a large scale power system S_{base} is 10 GVA, then the total system inertia is obtained 1.3 s. Note that typically the overall inertia of power systems with a low penetration rate of RESs has a higher value than 1.3 s, however here to characterize the future possible worst case, the power system with a relatively large penetration of RESs of 50% and a very low inertia is considered. As shown in Table. 5.1, the size of the disturbance is equal to 500 MW or 0.05 pu.

Next, to evaluate various parameters of the proposed design strategy, we provide sensitivity analyses for both scenarios A and B.

5.3.2.3. Sensitivity Analyses of Scenarios A and B

In this subsection, we define a number of sensitivity analyses not only to evaluate the performance of the design strategy for each separate scenario, but also to jointly compare the performance of PEVs for the PFC in both large-scale and islanded networks. To evaluate the frequency response improvement obtained by PEVs using the well designed droop, sensitivity analyses are performed on the following parameters:

⁵In this analysis, wind farms and PV units are assumed that they do not provide the PFC support.

Table 5.3.: Sensitivity analyses for scenarios A and B.

	$R_{pev}[\%]$	ρ [%]	PFC LIMIT	PEV RESERVE RELEASE
Sc.A.1 /OR Sc.B.1	-	0	-	-
Sc.A.2.1 /OR Sc.B.2.1	5%	2	YES	-
Sc.A.2.2 /OR Sc.B.2.2	0.07%	2	YES	-
Sc.A.3.1 /OR Sc.B.3.1	5%	30	YES	-
Sc.A.3.2 /OR Sc.B.3.2	0.07%	30	YES	-
Sc.A.4 /OR Sc.B.4	0.07%	2	NO	-
Sc.A.5.1 /OR Sc.B.6.1	0.07%	10	YES	ABRUPT
Sc.A.5.2 /OR Sc.B.6.2	0.07%	10	YES	SMOOTH

1. *PEV frequency droop controller:* In order to compare the performance of PEVs with conventional droop or the here well designed droop, various simulation scenarios are defined, as shown in Table. 5.3. For the penetration rate of 2%, in scenarios A.2.1 and B.2.1, PEVs are equipped with 5% droop, while in scenarios A.2.2 and B.2.2, PEVs use the here well designed droop. Similarly, for the penetration rate of 30%, in scenarios A.3.1 and B.3.1, PEVs are equipped with 5% droop, while in scenarios A.3.2 and B.3.2, PEVs use the here well designed droop.
2. *PEV penetration rate:* Undoubtedly, the performance of PEVs for the PFC highly depends on the number of electric vehicles connected to the electrical grid and available to provide the service. In other words, the penetration rate of PEVs (with respect to the size of the network under study) is a determinant factor, and here we carry out sensitivity analysis on various penetration rates of PEVs for the PFC. Thus, Table. 5.3 presents the defined scenarios A.1-3 and B.1-3, where the penetration rate of PEVs varies from 0% to 30%, while the maximum power limit of PEVs for PFC is applied. On the one hand, in scenarios A.2.1, A3.1, B.2.1, and B.3.1, the PEV droop is set the same as the typical droop of CGU's that has a large value of 5%. for the penetration rates of 2% and 30%. This improper droop value later results in the under-utilization of fast-controlled PEVs for the PFC and consequently poor frequency response. On the other hand, in scenarios A.2.2, A3.2, B.2.2, and B.3.2, the proposed well-designed frequency droop controller is used for the penetration rates of 2% that lead to a significantly improved frequency response. In order to compare the response of systems with and without PEVs using 0.07%, the damping ratio ζ is chosen as a quantitative index.
3. *Available upward or downward power reserves of PEVs for PFC:* Not only the penetration rate of PEVs could highly determine the performance of PEVs, but also the available upward and downward power reserves of PEVs for the

PFC could have a significant impact on the frequency response. In particular, with respect to the upward power reserve of PEVs, the topology of the battery chargers (i.e., unidirectional or bidirectional chargers) has an essential factor where PEVs equipped with bidirectional battery chargers typically has at least twice power reserve of PEVs equipped with unidirectional battery chargers. In summary, in Table. 5.3, to evaluate the impact of non-linear terms of PEVs on the PFC, the response of the frequency-control loop is tested with power limits for PFC in scenarios A.4 and B.4. Then, these are compared to the response of the frequency-control loop without power limits for PFC in scenarios A.2.2 and B.2.2, respectively. Note that it is assumed that all PEVs are equipped with bidirectional battery chargers, therefore they are able to inject the active power back into the grid.

4. *Release of PEV's reserve during PFC and replace it by the reserve of CGUs:* In order to address the replacement of PEV's reserve by CGU's reserve after the disturbance, scenarios B.5 and B.6 are defined for R_{fin}^{rlc} of 50% and 25%, respectively. In scenarios B.5.1 and B.6.1, we evaluate the frequency response, if PEVs abruptly release their replacement reserve R_{fin}^{rlc} at T_{PFC}^{rlc} equal to 10 s. In scenarios B.5.2 and B.6.2, the PEV's reserve is smoothly released in a linear way from T_{PFC}^{rlc} to T_{PFC}^{full} , which is equal to 30 s (Bevrani, 2009).

5.4. Simulation Results

The dynamic simulations are carried out on the worst case of both power systems and PEVs where the well design droop controller of PEVs is implemented and used. To achieve the desirable results, the original non-linear system including PEVs is simulated in Matlab / Simulink, where the frequency disturbance is applied to the system at $t=0.1$ s. Later on, the sensitivity analysis results of both technical implementation are presented. It is worth mentioning again that the base power ratings for per unit calculations are 100 MVA and 10 GVA in scenarios A and B, respectively. Also, the sizes of the disturbances in scenarios A and B are 10 MW (0.1 pu) and 500 MW (0.05 pu), respectively, where the largest generating unit is suddenly disconnected.

5.4.1. Results of Scenario A for Different PEV Penetration Rates

For scenarios A.1-A.3 of the islanded network, the frequency response following the disturbance of 0.10 pu is evaluated for various penetration rates of PEVs using either the droop value of CGUs, i.e., 5% or the proposed well-designed droop, i.e., 0.07%. In Figure. 5.10(a), for scenario A.2.2, the PEV power reaches the maximum limits of 2% using 0.07% droop, however in scenario A.2.1 for the PEV penetration of

2%, the maximum PEV power variation is relatively low, i.e., 0.01, using 5% droop. Since PEVs effectively participate in the PFC using 0.07% droop in scenarios A.2.2-A.3.2, consequently in Figure. 5.10(b), the CGU's participation in the PFC notably decreases. In particular, in Figure. 5.10(b), the need for CGU's power reserve during the PFC is remarkably reduced from scenario A.3.1 to A.3.2. In fact, the CGU's power variation highly decreases from 0.065 to 0.003 pu, while still the stability margins are successfully preserved. In Figure. 5.10(c), it is shown that the minimum frequency in scenario A.1 without PEV's participation in the PFC has a low value, i.e., 48.68 Hz, while the minimum frequency is notably improved in scenarios A.2-A.3, where PEVs together with the CGUs participate in the PFC. Compared to scenario A.2.1, in scenario A.2.2, the minimum frequency is highly improved from 48.78 to 48.94 Hz using the designed droop curve. Also, compared to scenario A.3.1, in scenario A.3.2, the frequency is outstandingly improved from 49.45 Hz to 49.96 Hz, when the well designed droop is used for the highest penetration rate of PEVs, i.e., 30%.

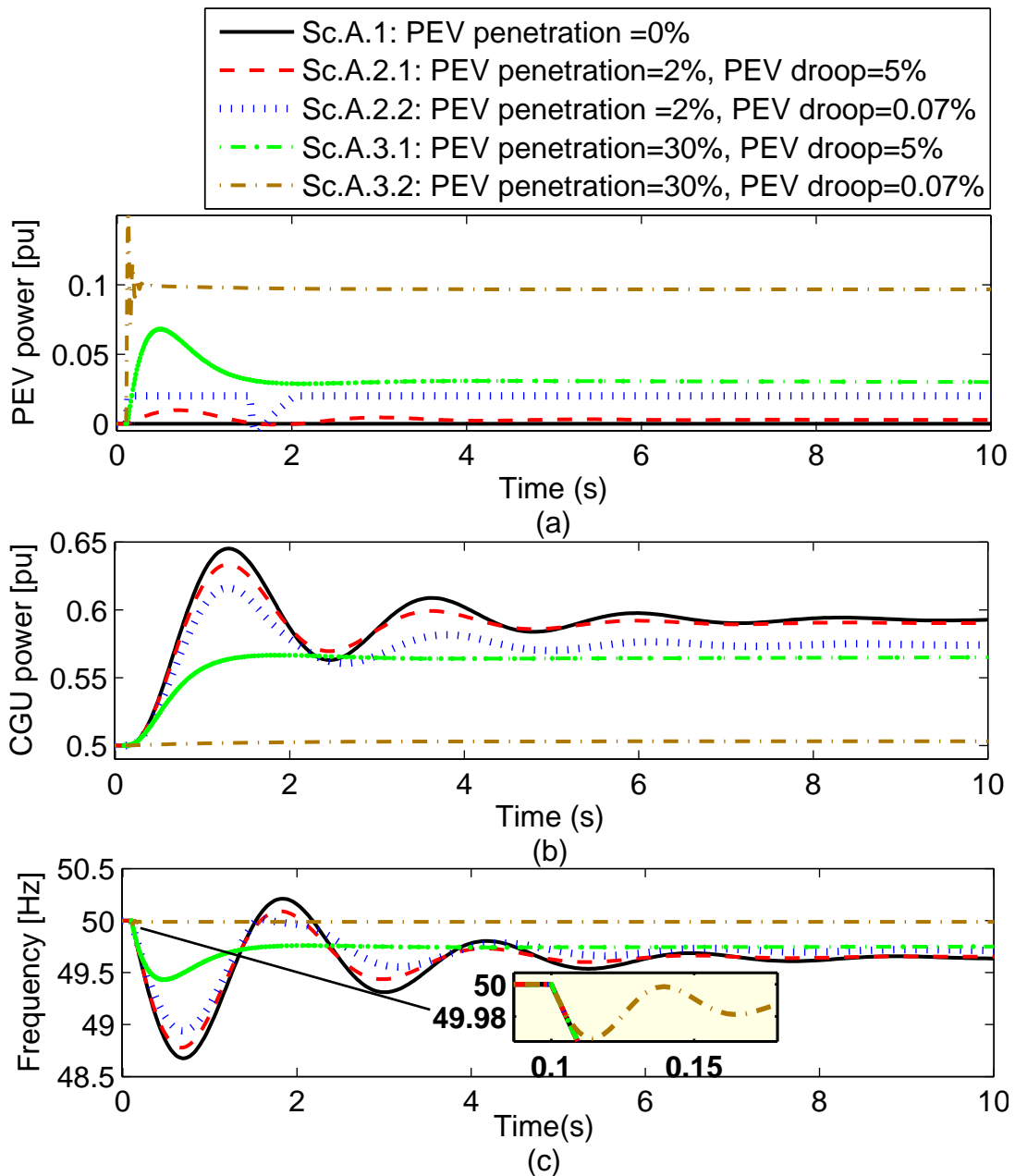


Figure 5.10.: Simulation results of scenario A for the islanded network. (a) PEV active power. (b) CGU active power. (c) System frequency.

In order to compare the networks without PEVs and with 30% penetration rate of PEVs in scenarios A.1 and A.3.2, the percentage overshoot as well as damping ratio ζ are obtained. In both systems, as expected, the percentage overshoot and damping ratio ζ are obtained very similar close to 56% and 0.78, respectively. Note that as the overall stability margins in scenarios A.1 and A.3.2 were obtained the same in Section 3 of this chapter, our design approach is well validated when the frequency

curve shapes of scenarios A.1 and A.3.2 are achieved very similar in Figure. 5.10(c). In other words, this demonstrates that the stability margin of the systems have been safely checked and ensured within our proposed design strategy, and this way we have properly compared the frequency response of systems with and without PEVs.

In a similar way, next, we evaluate and simulate a large scale power system including PEVs where the designed droop controller has been implemented in the PEVs.

5.4.2. Results of Scenario B For Different PEV Penetration Rates

For scenarios B.1-B.3 of the large-scale power system, the frequency response following the disturbance of 0.05 pu is assessed for various penetration rates of PEVs using either the droop value of CGUs, i.e., 5% or the proposed well designed droop, i.e., 0.07%. In Figure. 5.11(a), for scenarios B.2.2, the PEV power reaches the maximum limits of 2%, however in scenario B.2.1 for the PEV penetration of 2%, the maximum PEV power variation is very low, i.e., 0.005 pu, using 5% droop. Since PEVs effectively participate in the PFC in scenarios B.2-B.3, consequently in Figure. 5.11(b), the CGU's participation in the PFC considerably decreases. In particular, in Figure. 5.11(b), the need for CGU's power reserve during the PFC is remarkably reduced from scenario B.3.1 to B.3.2. In fact, the CGU's power variation highly decreases from 0.053 to 0.0016 pu, while still the stability margins are effectively maintained. In Figure. 5.11(c), it is shown that the minimum frequency in scenario B.1 without PEV's participation in the PFC has a low value, i.e., 49.34 Hz, while the minimum frequency is notably improved in scenarios B.2-B.3, where PEVs together with the CGUs participate in the PFC. Compared to scenario B.2.1, in scenario B.2.2, the minimum frequency is highly improved from 49.39 to 49.60 Hz using the proposed droop controller. Compared to scenario B.3.1, in scenario B.3.2, the minimum frequency is highly improved from 49.72 to 49.98 Hz, when the well designed droop is used for the highest penetration rate of PEVs, i.e., 30%.

In order to compare the networks without PEVs and with 30% penetration rate of PEVs in scenarios B.1 and B.3.2, the percentage overshoot as well as damping ratio ζ are obtained. In both systems, the percentage overshoot and damping ratio ζ are similarly obtained close to 56% and 0.78, respectively. Note that as the overall stability margins in scenarios B.1 and B.3.2 were obtained the same in Section 3, it is further validated when the frequency curve shapes of scenarios B.1 and B.4 are achieved very similar in Figure. 5.11(c). Moreover, in scenario B.2.2, for which the overall stability margin of the system was obtained at a high value, clearly the frequency responses have lower amplitude oscillations compared to scenarios B.1 and B.3.2.

Here in scenarios A.3.2 and B.3.2, the aim was to mainly demonstrate the effectiveness and accuracy of the proposed design strategy for PEV's frequency droop controller. However in practice, such an improvement in the frequency response

might not be achieved due to various reasons such as measurement and computational delays and large prespecified dead bands.

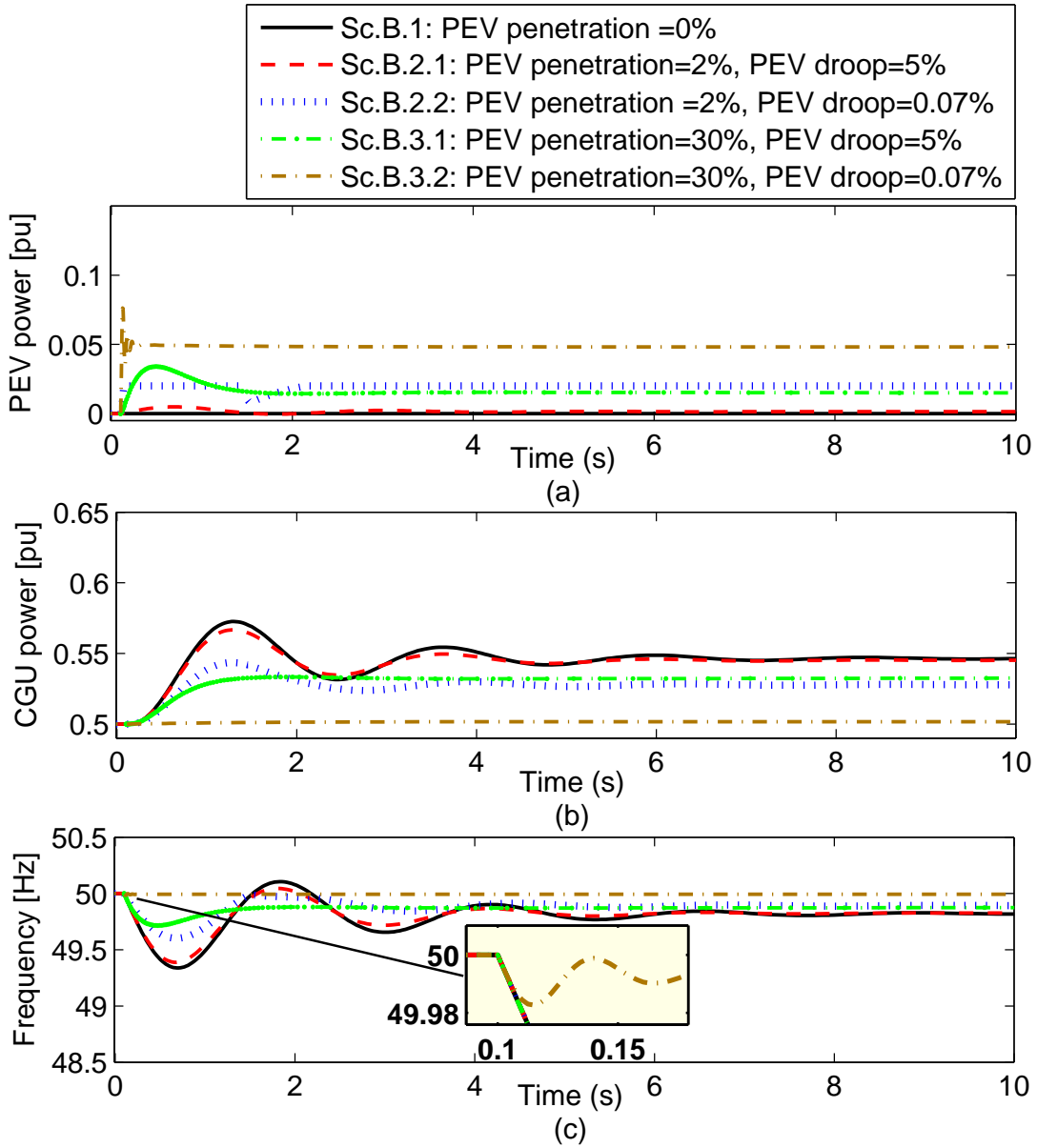


Figure 5.11.: Simulation results of scenario B for the large-scale power system. (a) PEV active power. (b) CGU active power. (c) System frequency.

In both large-scale power system and islanded network, it was demonstrated that the designed PEV’s droop controller has a satisfactory performance. Thus, on the one hand, the available fast power reserve of PEVs are effectively and sufficiently utilized during the PFC, because of which the minimum frequency is remarkably improved. On the other hand, it was shown that the frequency stability of the

system is not put at risk as the frequency responses of systems with and without PEVs in scenarios 1 and 3 have similar curve shapes.

5.4.3. Results of Scenarios A and B With and Without Maximum Power Limits of PEVs for PFC

As described in section 5.3, to obtain the bode plots and then stability margins, the frequency control loop should have been linearized around the operating point, and to this end, we neglected a number of non-linear functions of PEVs for the PFC. Despite this fact, in this subsection, we aim at evaluating and validating the following points:

- *Non-linear terms of PEVs for the PFC:* To analyze the impact of the non-linear terms of the PFC such as the maximum power limits of PEVs on the frequency response, here in scenarios A.4 and B.4, the maximum PEV power limits are not considered for the PEV penetration rate of 2%, as presented in Table. 5.3. Figure. 5.12 shows the simulation results of the PEV power, the CGU power, and the system frequency for these four scenarios. In Figure. 5.12(a), from scenario A.2.2 to A.4, the maximum PEV power notably increases from 0.02 to 0.98 pu, and consequently in Figure. 5.12(b), the CGU's participation in the PFC remarkably decreases. In Figure. 5.12(c) from scenario A.2.2 to A.4, the frequency response is greatly improved from 49.94 to 48.82 Hz when the power limit of PEV for PFC is neglected. Similarly from scenario B.2.2 to B.4, the frequency response is highly improved from 49.60 to 49.90 Hz by neglecting the power limit of 0.02 pu.
- *Comparing the frequency response of islanded system to large-scale power system:* To be able to properly compare two scenarios, we show the simulation results of scenarios 1, 2, and 5 within the same figure. As can be seen in Figure. 5.12(c), the frequency deviations in scenarios A.1 and A.2 have larger values compared to scenarios B.1 and B.2, as the islanded network is subject to a larger disturbance.

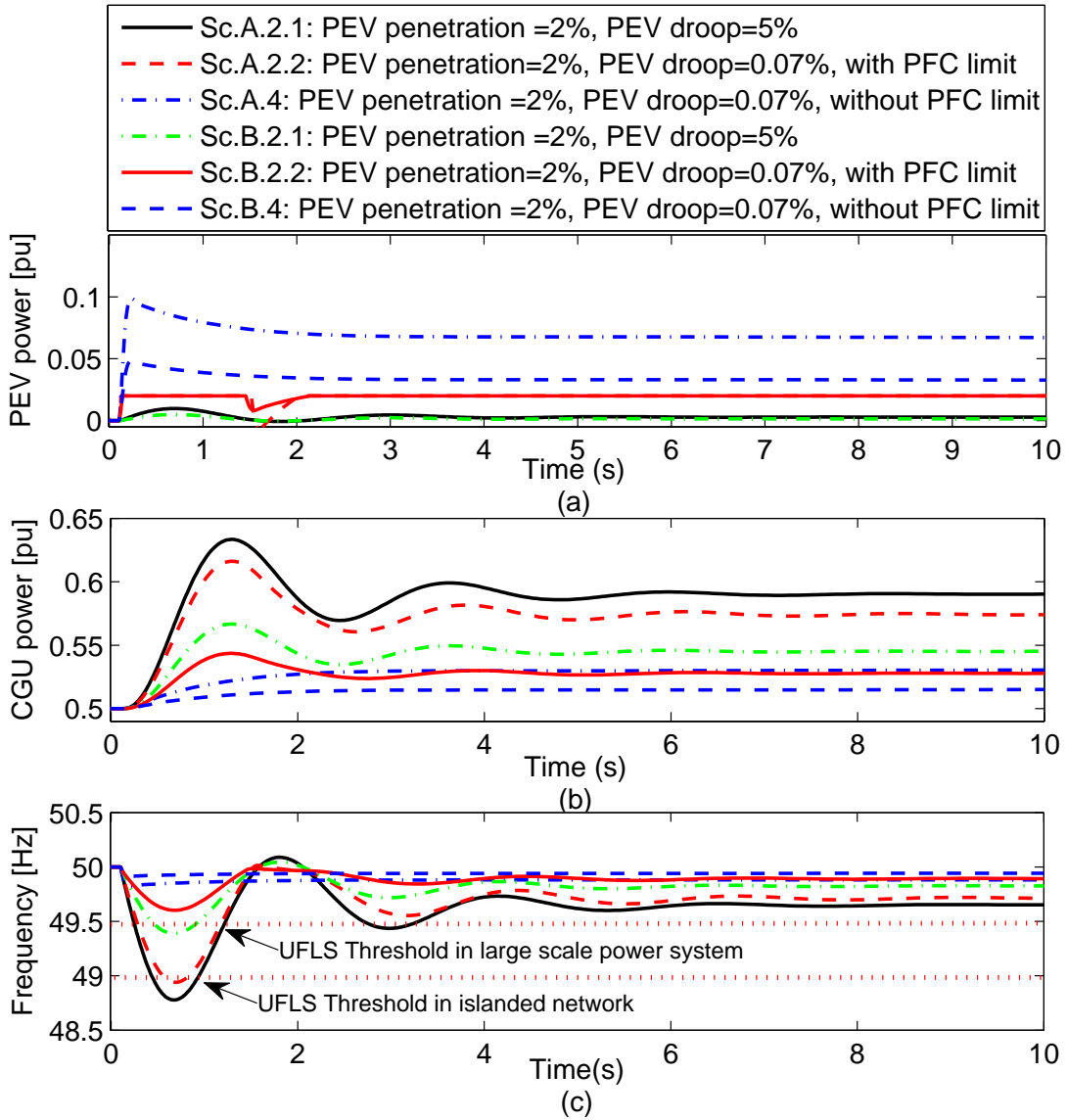


Figure 5.12.: Simulation results of scenarios A and B with and without the PFC power limits for PEVs. (a) PEV active power. (b) CGU active power. (c) System frequency.

5.4.4. PEV’s Power Reserve Release Moments After the Disturbance

Figure. 5.13(a) presents the PEV power variation during the PFC in scenarios B.5 and B.6. Right after the disturbance (0.05 pu), PEVs almost cover the whole required reserve within the first second. To later replace the PEV’s reserve by CGU’s reserve during PFC, the PEV’s reserve can be released from 10.1 to 30.1 s either abruptly or in a linear fashion. Figure. 5.13(b) shows the power variation of CGUs

during PFC. After the disturbance, CGU's participation in PFC is negligible (0.004 pu), as PEVs cause to mask CGU's turbine-governor response. Later on, if the reserve of PEVs is abruptly released at 10.1 s, then as expected, the CGU's power exhibits high-amplitude oscillations. In Figure. 5.13(c), when 50% and 25% of total PEV's reserve are suddenly released, the minimum frequencies after $t = 10.1$ s for scenarios B.5.1 and B.6.1 have large values of 49.59 and 49.78 Hz, respectively. Whereas using the proposed reserve replacement scheme, the minimum frequencies after $t = 10.1$ s for scenarios B.5.2 and B.6.2 are greatly improved to 49.90 and 49.94 Hz, respectively.

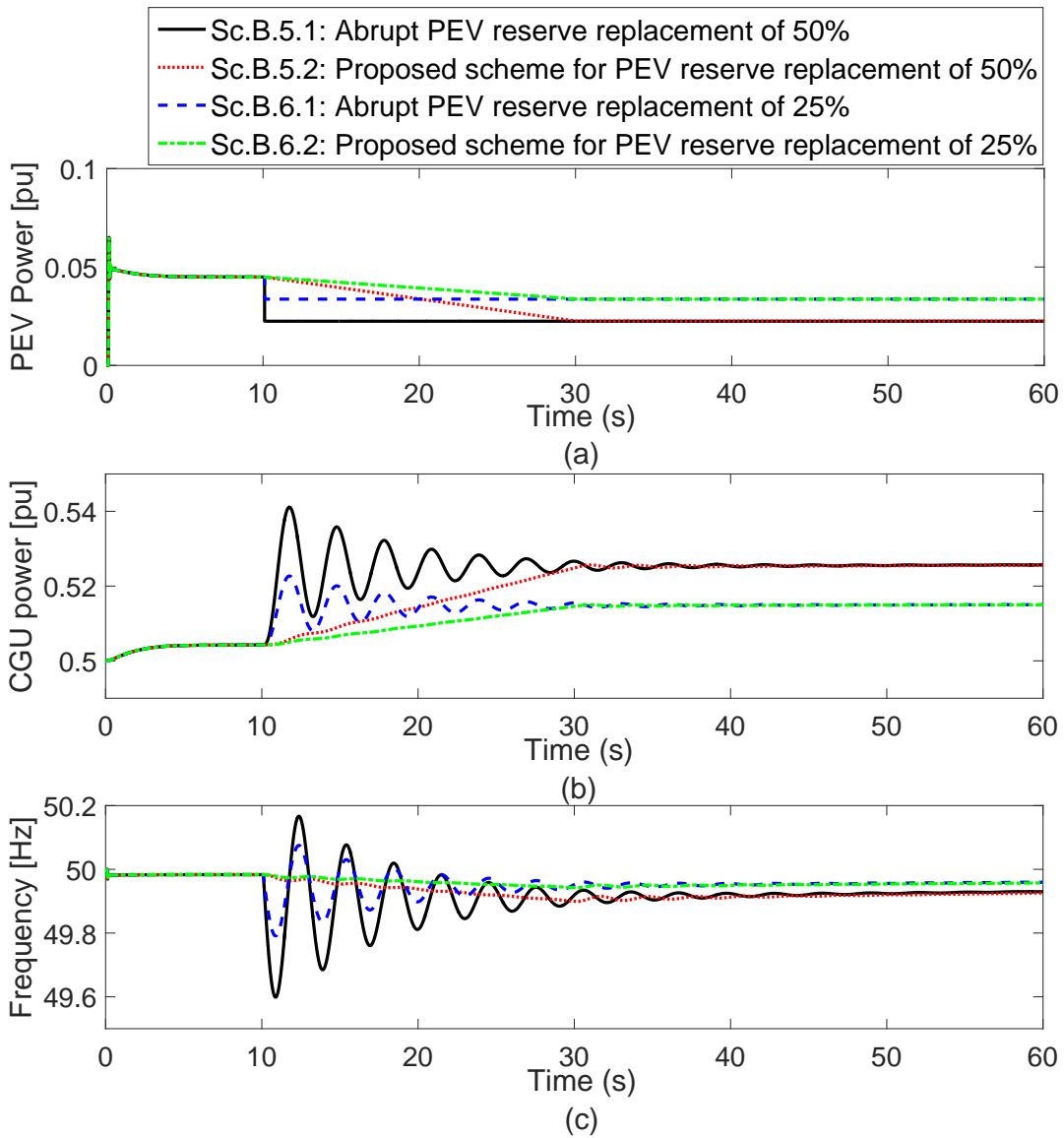


Figure 5.13.: Simulation results of replacement of PEV's reserve with CGU's reserve 10 s after the disturbance until 30 s. (a) PEV active power. (b) CGU active power. (c) System frequency.

In this technically-oriented thesis research, so far we did not have the opportunity to sufficiently cover and address the economic aspects of the provision of the PFC by PEVs. Despite this fact, they are briefly considered and assessed in the future research together with the technical aspects. Therefore, we provide an introduction of economic evaluation and benefits, which could potentially result from PEVs due to their participation in the PFC. Nonetheless, note that the below-provided economic evaluation of PEVs is outside the scope of this technical research.

5.5. Brief Description And Discussion On Economic Evaluation of PEVs for PFC (Outside the Scope of This Technical Research)

Undoubtedly, the provision of PFC by PEVs has a significant impact on the economic operation of power systems. In spite of the importance, the economic impact of the participation of PEVs in the PFC on the system costs associated with the PFC service has been rarely reported.

- The main research questions related to the economic evaluation are posed as follows:
 1. What are the total costs associated with the PFC either in large-scale power systems or islanded networks?
 2. To what extent the total costs associated with the PFC could be reduced when PEVs additionally participate in the PFC?
 3. In which type of networks, i.e., large-scale power systems or islanded networks, PEVs have a more positive impact on the costs of the PFC?

To shed light on the above-stated shortcomings, this subsection assesses the economic impact of PEVs on the PFC. First, an introduction to the economic value of PFC in power systems is given. Then, from an economic point of view, a method is proposed to evaluate the positive economic impact of PEVs participation in PFC. To this end, the system PFC cost savings mainly through the avoidance of under frequency load shedding (UFLS) are calculated.

5.5.1. Introduction To Economic Value Of PFC In Power Systems

Generally speaking, both availability and provision of primary control reserves by the conventional generating units imposes substantial costs to the power systems. If PEVs quickly provide the PFC, then in future there could be a significantly lower need for the power reserve of the conventional generating units. In order to properly

address the economic aspects of the PFC in electric networks, first it is required to distinguish two major power system structures as follows (Holttinen et al., 2012):

- Non-competitive vertically integrated power industry structure: Within the regulated monopoly framework, the traditional vertically integrated utility consisting of generation, transmission, distribution zones, and retailing is the main responsible for the operation and planning of the whole electricity supply. In this context, a unique electric service provider, who maintains the instantaneous power balance between supply and demand, is to ensure the provision of power system's ancillary services by all the conventional generating units. Typically speaking, ancillary services like the PFC are seen as mandatory services, which are to be provided by all the conventional generating units.
- Competitive power market structures (unbundled power industry structure): Unlike to the unique electric service provider, in an unbundled power market, independent system operators (ISOs) or TSOs are the main responsible for ensuring and maintaining the instantaneous power balance between supply and demand. Typically speaking, ancillary services like the PFC are provided through the electricity markets, in which conventional generating units compete to provide services.

In brief, generally speaking, the provision of ancillary services like the PFC could be mandatory (e.g., Spain) or optional (e.g., Germany and the Netherlands) (Brivio et al., 2016; Rebours et al., 2007b). In this subsection, we try to also address and assess the economic aspects of the provision of the PFC by PEVs. To achieve this goal, the three above-posed questions are first discussed in detail in the following three subsections:

5.5.1.1. Total Costs Associated With PFC in Electrical Networks Addressed in Research Question 1

In both vertically integrated and unbundled power industries, the provision of PFC imposes substantial costs on the power system. Technically speaking, power system operators are always required to maintain a certain amount of the power reserve of the conventional generating units to cope up with the contingency events (Ela et al., 2014a,b; Rebours et al., 2007a). As a result, the power system could remain stable and safe even after the largest possible disturbance. This permanent availability of the reserve for the PFC will impose significant costs (Rebours et al., 2007b), which are the PFC reserve capacity costs. Moreover, during the contingency event, if the frequency drops below a certain value, then a portion of the load might be shed. This results in some additional costs, which are the UFLS costs (Ruiz & Sauer, 2008).

Here, these two major costs associated with the PFC during the normal operating conditions and the frequency disturbance are described and discussed in detail as follows:

PFC reserve capacity cost

As mentioned, during normal operating conditions, the system must always secure and maintain sufficient primary power reserve to cope up with critical unexpected contingencies. On the one hand, under regulated environment, the PFC service is mandatory, and all CGUs are obliged to allocate a minimum percentage of their total installed generating capacity for the PFC. Since this power capacity percentage can not be sold or offered through energy or other ancillary services, CGUs incur service availability costs⁶ as well as lost opportunity costs⁷ (Hirst & Kirby, 1997; Singh & Papalexopoulos, 1999). On the other hand, as mentioned, under deregulated market environment, CGUs are able to compete and participate in the ancillary service markets such as the PFC market. Over the past years, PFC markets have been implemented in various countries such as the New Zealand, Germany, and the Netherlands. In New Zealand⁸, the operator co-optimizes the CGU's energy and instantaneous reserve offers in order to obtain the least cost schedule. In Germany and the Netherlands, CGUs submit bids into an auction on the primary reserve through PFC markets. Then, as shown in Table.5.4, all winning CGUs in the auction are paid according to either their actual bid offered to the PFC market (e.g., pay-as-bid in New Zealand, Germany and the Netherlands) or the marginal price of the primary reserve (i.e., unified PFC market clearing price in Australia). Moreover, as shown in Table.5.4, CGUs are remunerated for their availability for the PFC in Germany, the Netherlands, and Australia, whereas in New Zealand, they are only remunerated when the PFC service is utilized.

Table 5.4.: Remuneration methods and structures for PFC in various countries (Rebours et al., 2007b).

Remuneration methods	
Single clearing price	Pay as bid price
Australia	Germany Netherlands New Zealand
Remuneration structures	
Availability	Utilization frequency
Australia Netherlands Germany	New Zealand

⁶The availability cost refers to the payments to those conventional generating units, which are available to provide the spinning reserve.

⁷The opportunity cost refers to the potential value or power production lost, when an alternative service is provided.

⁸In the New Zealand's electricity market, the primary frequency control service is called "Instantaneous reserve".

UFLS cost

As mentioned, system operators incur significant costs to provide an adequate level of the PFC at each moment of the day (Ruiz & Sauer, 2008). This way, they could avoid excessive costs associated with the power system stability issues such as the UFLS or blackouts. In fact, if the amount of the provided PFC is not sufficient and the frequency disturbance is relatively large, then the frequency might drop below the minimum prespecified threshold⁹ following the contingency event. In these cases, the UFLS scheme curtails a portion of the load consumption during the frequency disturbance (Sigrist et al., 2010). Undoubtedly, this imposes some additional costs to both system operators and end-use customers, who are accidentally deprived from the electricity supply for a certain period of time. For instance, in Europe, according to ENTSO-E¹⁰, 15% and 50% of the total load are to be shed when the frequency reaches 49 and 48 Hz, respectively. If a certain portion of the load is shed during the frequency disturbance, then the associated costs mainly depend on the value of the lost load (VOLL). The VOLL depends on many factors such as the type of the load (i.e., residential commercial, or industrial), the energy not served, the time at which the load is shed, and the geographical attributes.

In this subsection, we mainly answered the question of “how much does the provision of the PFC service cost in power systems”. To this end, we addressed two major costs associated with the PFC in power systems so far without the presence of distributed energy resources like PEVs. Next, we address the question of “To what extent the total costs associated with the PFC could be reduced when PEVs additionally participate in the PFC?”.

**5.5.1.2. Potential PFC Cost Savings by PEVs Addressed in Research
Question 2**

As mentioned, over the past years, the PFC has been mainly provided by conventional generating units in electric power systems. However, other types of DERs like PEVs are able to compete with the conventional generating units, and provide the PFC service. Thanks to the energy storage of the PEV’s battery as well as the fast-controlled battery charger, PEVs are able to very quickly provide the PFC service compared to the conventional generating units. To be able to compete with the conventional generating units, small-scale PEVs are required to be efficiently aggregated by new profit-seeking agents, the so-called aggregators (Gonzalez Vaya & Andersson, 2014; Momber et al., 2016). For instance, in the existing German PFC market, the minimum acceptable bid is 1 MW, which is obviously much higher

⁹A similar scheme might be implemented when the frequency goes above the maximum prespecified threshold. In such cases, distributed generation units like PV systems might curtail a certain amount of their output power or even become disconnected from the electrical grid.

¹⁰ENTSO-E stands for the European Network of Transmission System Operators.

than the power capacity of a single PEV. Therefore, to meet this minimum requirement, in the near future, PEV aggregators might be absolutely required to make PEVs able to participate in the German and Dutch PFC market. This way, if PEVs effectively participate in the PFC in an aggregated and coordinated manner, then they might largely reduce both PFC reserve capacity and UFLS costs. However, on the one hand, compared to the CGUs, aggregators might have very low operating costs, that mainly depend on the battery degradation of PEVs (Sarker et al., 2015a). On the other hand, in the near future there will be a need for additionally investing in the telecommunication infrastructure, as PEV aggregators are to be able to effectively communicate with PEVs. In conclusion, PEVs shall be able to sufficiently reduce the total PFC costs in the near future, therefore the extra costs associated with their aggregation in power systems could be effectively covered.

In previous research, the economic aspects of the PFC in power systems mainly including CGUs have been analyzed and evaluated (Aguero et al., 2000; Dai et al., 2010, 2007; Ela et al., 2014a,b; Rebours et al., 2007a,b; Ruiz & Sauer, 2008; Soler et al., 2010). In (Ruiz & Sauer, 2008), it was discussed that the value of spinning contingency reserve depends on various characteristics of electric power systems such as reliability, dynamic behavior, regulatory and economic aspects. Then, the value of CGU's spinning contingency reserve was approximated where a number of reserve demand functions were created and formulated. In addition, the costs for under frequency load shedding (UFLS) were partly addressed in (Ruiz & Sauer, 2008). In (Dai et al., 2010), a control scheme was proposed in a multi-area power system to control the power injections. It was concluded that larger power systems have a lower costs associated with the primary frequency control reserve, as they typically experience lower frequency deviations. In (Dai et al., 2007), the PFC capabilities of conventional generating units within a three-area power system was investigated where the impact of dead band and load disturbance were evaluated. In (Aguero et al., 2000), a method was applied to calculate the costs for the PFC based on a redistribution of the income which is collected by the conventional generating units for energy by pricing the reserve according to the energy cost in the system. It was found out that the contribution of conventional generating units to primary frequency control provide some economic benefits without affecting the total income collected for the energy by the generators. In (Ela et al., 2014a,b), a much more advanced analysis was made where a PFC market was implemented in competitive pool-based market co-optimizing the energy and PFC service. It is worth mentioning that over the past years, the PFC markets have been recently implemented in various countries such as the New Zealand, Germany, and the Netherlands. In New Zealand, the operator co-optimizes the conventional generating unit's energy and instantaneous reserve offers in order to obtain the least cost schedule. In Germany and the Netherlands, conventional generating units submit bids into an auction on the primary reserve through PFC markets. Also, in (Soler et al., 2010), the costs for frequency control were calculated under a deregulated market environment, where conventional generating units were penalized when the frequency deviated from the

nominal value.

As extensively reviewed, the economic aspects of the PFC in power systems including only conventional generating units have been analyzed and investigated in previous research. It was mentioned that the system operators might incur some costs associated with the PFC for both availability of the power capacity reserve (during normal operating conditions) and the activation of under frequency load shedding (UFLS) (during the frequency disturbance). In particular, in (Ela et al., 2014a,b), it was shown if the PFC response of power systems only including CGUs is improved reducing the CGU's droop coefficient from 5% to 4%, then the total profits increases by 57%. Nonetheless, since the topic of PEVs for the PFC has been recently discussed, a few (or to the best of our knowledge, almost no previous research work) works have investigated in detail the economic aspects of the provision of PFC by PEVs. For power systems including PEVs, similarly it needs to be evaluated to what extent the PFC costs could be reduced when PEVs participate in the PFC using a well-designed droop rather than an arbitrarily selected one.

The two previously-mentioned major costs of the PFC could be potentially reduced by the introduction of PEVs into power systems as follows.

PFC reserve capacity cost savings by PEVs

According to the National Household Travel Survey (Krumm, 2012), PEVs are parked more than 90% of the time and are likely connected to the grid most of the time. As the number of grid-connected electric vehicles could be large in the near future, they have a great potential to provide a large amount of PFC reserve. In this context, PEVs might potentially reduce the average price of primary reserve in the PFC market, and consequently the total PFC reserve capacity costs. For the sake of illustration, Figure. 5.14 presents the aggregate demand-supply curves of systems with (blue curve) and without (green curve) PEVs in the PFC market. In such market, the marginal prices of the PFC market is determined by the intersection of primary reserve demand set via the operator¹¹ and primary reserve supply offered by the CGUs and PEVs. So far, as far as we know, no PEVs have participated in practice in the PFC market. Therefore, it is not known about what price PEVs will bid into the PFC market in the future. However, if PEVs would be able to bid a lower price compared to the CGUs, then they could effectively reduce either the marginal or the average PFC price, as shown in Figure. 5.14. In other words, it is assumed that the PEV bid is equal to the lowest bid offered by generating units. As a real life example, if the charging power of PEVs is assumed only equal to 3.3 kW, then 236,363 PEVs will be sufficient to provide 780 MW primary power reserve of the German and Dutch PFC markets.

¹¹In Europe, the total PFC demand is annually determined by ENTSO-E (i.e., around 3,000 MW), out of which around 780 MW is provided by the German and Dutch PFC markets.

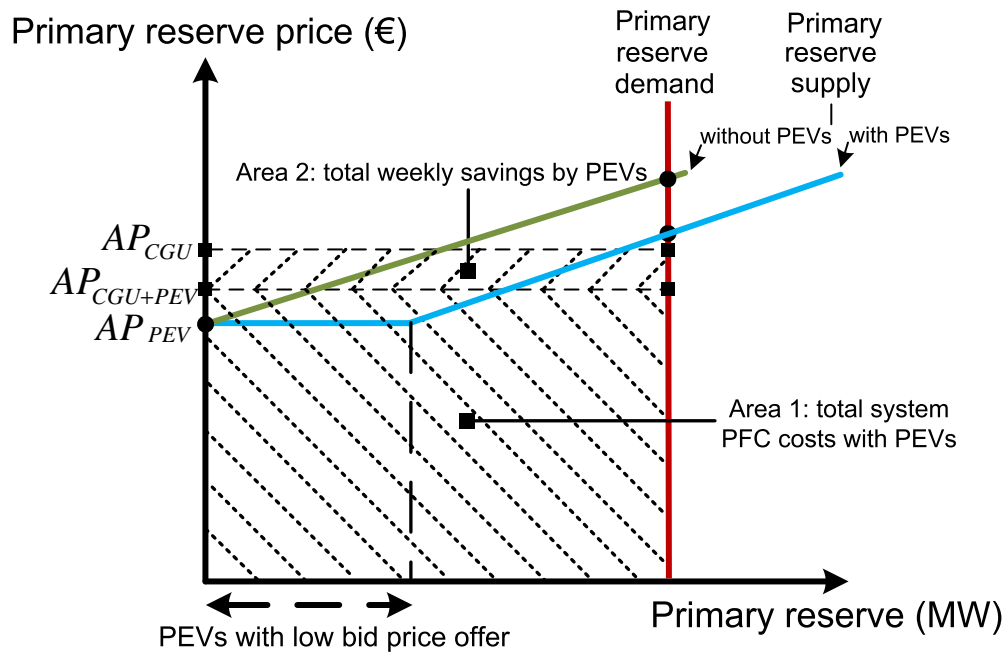


Figure 5.14.: Demand-supply curves of systems with and without PEVs in the PFC market in the Netherlands and Germany.

UFLS cost savings by PEVs

Thanks to the fast-controlled battery charger of PEVs, they are able to quickly provide the PFC following a contingency event compared to the CGUs (Almeida et al., 2015; Baboli et al., 2010). This way, if fast-controlled PEVs participate in the PFC using the well-designed droop, then the frequency might not reach the minimum allowable limits, and consequently a lower portion of loads will be shed due to the activation of the UFLS schemes. In conclusion, some important costs associated with the UFLS could be saved using effectively PEVs during the PFC.

In this subsection, we briefly addressed the potential PFC cost savings, which might come from the provision of PFC by PEVs. Next, we address the third research question “In which type of networks, i.e., large-scale power systems or islanded networks, PEVs have a more positive impact on the costs of the PFC?”.

5.5.1.3. PFC Cost Reduction in Large-scale Power Systems and Islanded Network Addressed in Research Question 3

From both technical and economic points of view, the type of the electrical grid under study (i.e., large scale power system and islanded network) is of great importance. In fact, there are major differences between the large scale power system and islanded network for the PFC analysis, that might highly affect the here-proposed technical implementation and economic evaluation for the PFC by PEVs.

With respect to the technical aspects, the overall inertia is much higher in the large-scale power systems compared to the one in the islanded network (compared with the base power of total load in per unit). In other words, the frequency stability of islanded networks is much lower, and consequently PEVs might severely affect the frequency response of islanded networks during the frequency disturbance. On top of this, typically a limited number of conventional generating units supply the whole islanded area, and generally the loss of a generating unit creates a relatively large disturbance. As a result, our proposed design strategy might be more effective and required for islanded networks in the near future. This is why, in this subsection, we evaluate and compare both large scale power system and islanded network for the PFC using PEVs.

In the next subsection, we provide the technical implementation of the previous aggregate models of PEVs for the PFC, where a strategy will be described to design the frequency-droop controller of PEVs for PFC. As comprehensively addressed in the previous chapters, there are a number of practical reasons why here the aggregate models of PEVs for PFC are used and preferred over the distributed model of PEVs for the PFC. Next, these valid reasons will be presented and discussed in brief as well. In the subsequent subsection, a method is proposed to evaluate the positive economic impact of PEVs participation in PFC.

Next, we address in brief the economic evaluation of PFC including PEVs.

5.5.2. Economic Evaluation of PFC Including PEVs

This subsection provides the economic assessment of the PFC including PEVs. The total costs associated with the PFC in electric power systems can be divided into two major parts. Regarding the first part, the total PFC reserve costs are typically imposed to the power system during the normal operating conditions. Therefore, system operators are to determine the unit commitment schedules in such a way that a certain amount of upward and downward power reserves would be always available. As this thesis research mainly focuses on the performance of power systems including PEVs only following contingency events for a short period of time, here we briefly address only how these costs could be calculated. Note that no simulation or numerical results will be provided for these costs, as they are fairly outside of the scope of this technical research. Regarding the second part, system operators might have to shed a portion of the total demand when the frequency drops below a prespecified threshold. PEVs have a great potential to reduce the frequency deviations and consequently they might effectively avoid the costs associated with the under frequency load shedding scheme.

5.5.2.1. PFC Costs Associated With PFC Reserve Capacity Cost

In practice, the total costs associated with the PFC reserve capacity depend on the regulatory framework under which the electrical network is operated. Technically speaking, the calculation of total PFC costs could be very complex and computationally intensive. However, as we reviewed the existing literature, a number of very simplified formulations were found that could be used for the calculation of the total PFC costs. Thus here, we aim at very briefly addressing how these costs could be addressed under various regulatory frameworks.

As mentioned before, under vertically integrated electric utility, the conventional units are obliged to provide the PFC service. Thus, not only the conventional generating units are to be available to provide the spinning reserve along the day, but also they incur the opportunity costs of not procuring other electricity services. As a result, the total PFC costs C_{PFC}^{COST} including both availability costs $C_{PFC,A}^{COST}$ and opportunity costs $C_{PFC,O}^{COST}$ can be given by:

$$C_{PFC}^{COST} = C_{PFC,A}^{COST} + C_{PFC,O}^{COST} \quad (5.7)$$

Under deregulated electricity market environment, a number of models could be formulated and developed. For instance, if it is assumed that CGUs are penalized due to the frequency deviations, then the penalty associated with frequency deviations is considered as a quadratic cost function C_{PFC}^{PNL} as follows (Soler et al., 2010):

$$C_{PFC}^{PNL} = PF_{PFC} \cdot \int_{t=t_0}^{t=t_1} [f(t) - F^{nom}]^2 \cdot dt \quad (5.8)$$

where PF_{PFC} , $f(t)$, t_0 , t_1 , and F^{nom} are the frequency penalty factor, the frequency, time of the disturbance, time associated with the frequency nadir of the system without PEVs, and the nominal frequency, respectively. In this case, if PEVs could improve the frequency deviations, then obviously the total penalties could be largely reduced.

As another example, if PEVs participate in the PFC market shown in Figure. 5.14, then they could potentially reduce the average price of primary reserve, and consequently the total PFC reserve capacity costs. Therefore, the PFC reserve capacity cost savings with PEVs ΔC_{PFC} are given by (see area 2 in Figure. 5.14):

$$\Delta C_{PFC} = D_{PFC} \cdot (AP^{CGU} - AP^{CGU+PEV}) \quad (5.9)$$

where D_{PFC} , AP^{CGU} , and $AP^{CGU+PEV}$ are the total primary reserve demand, average price of primary reserve of systems with and without PEVs, respectively. As addressed before, PEVs could decrease the total PFC costs of the market, only if they could bid at a lower price compared to the conventional generating units (in

other words, $AP^{PEV} < AP^{CGU}$). This way, they could effectively reduce the average price from AP^{CGU} to $AP^{CGU+PEV}$, as shown in Figure. 5.14.

Nonetheless, these costs are not addressed in this thesis, which mainly evaluates the dynamic performance of the systems with and without PEVs using well designed droop controller only following a contingency event (not during the normal operating conditions). We rather evaluate the dynamic performance of the systems with and without PEVs using well designed droop controller only following a contingency event (not during the normal operating conditions). Here, we are able to evidently assume that the total amount of the PFC reserve costs of PEVs as well as installation costs remain the same for any value of droop during normal operating condition. In other words, regardless of PEV's droop value, PEVs anyway incur some costs for making their primary reserve available over time. Therefore, the PFC cost difference between PEVs using the proposed well-designed droop and an arbitrarily selected droop could be mainly the UFLS costs during dynamic conditions.

5.5.2.2. PFC Costs Associated With UFLS

As stated, during the frequency disturbance, if the frequency drops below the minimum prespecified threshold, then after an intentional delay (e.g., 18 cycles or 0.36 s), the UFLS scheme curtails a portion of demand. For the sake of illustration, Figure. 5.15 shows the frequency response before and during the disturbance for power systems with and without PEVs. For the case of power systems without PEVs, the frequency reached the first minimum prespecified threshold f_{min1} , and consequently a portion of the load will be shed. For the case of power systems with PEVs, though the frequency reached the first minimum prespecified threshold f_{min1} , it recovered very soon (less than the intentional delay t_{int}) and the UFLS scheme is not activated. If fast-controlled PEVs participate in the PFC using the well-designed droop, then the frequency might not reach the minimum allowable value, and consequently the load might not be shed.

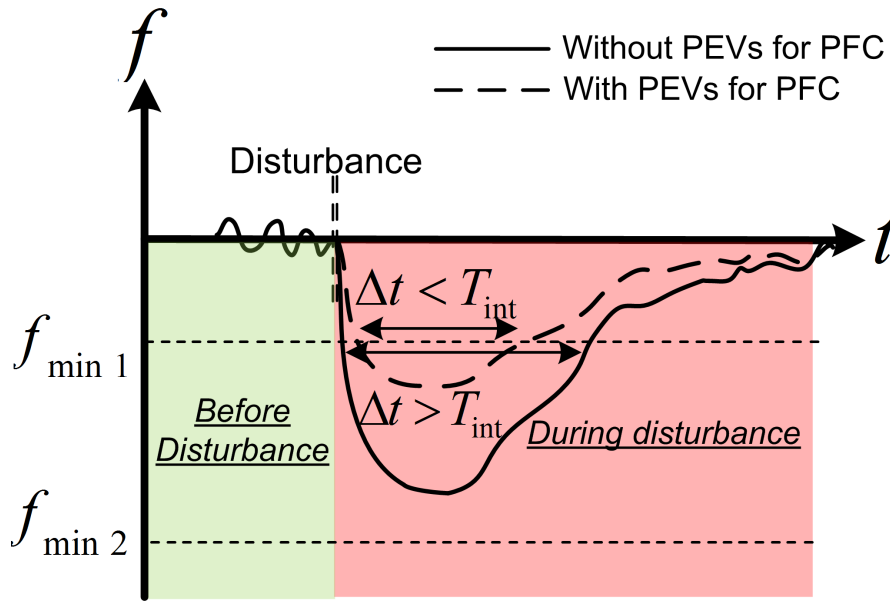


Figure 5.15.: Frequency of power systems with and without PEVs.

The UFLS cost savings ΔC^{UFLS} during a year depends on a number of factors such as:

- Estimated number of event occurrences for a given year PR^{DST} : In practice, large disturbances such as the loss of large-scale generating units might occur a few times per year. This can be taken into account using some historical values. It can be assumed that a certain portion of load would not be shed during these event occurrences using PEVs, while these loads would have been shed without the presence of PEVs.
- Energy not served ENS : When the UFLS scheme disconnects a number of loads during the frequency disturbance, these loads are typically connected again after a certain period of time. As a result, the loads are deprived from the electrical energy for that period of time which are introduced and defined as energy not served. To calculate the energy not served ENS , the amount of shed load SL is to be multiplied by the time duration of ENS .
- Value of lost load $VOLL$: The value of lost load can be defined as the willingness of the end-use customers to pay in order to avoid the process of load shedding. In practice, this value highly depends on the type and activity of end-use costumers that highly vary from one country to another.

As PEVs could largely improve the frequency response in term of the minimum frequency, it could be realistically expected that they effectively avoid a large portion of the costs associated to the UFLS scheme. Taking into account the above mentioned parameters, the cost savings ΔC^{UFLS} through the avoidance of the UFLS for

a given year can be given by

$$\Delta C^{UFLS} = PR^{DST} \cdot ENS \cdot VOLL \quad (5.10)$$

As mentioned in the previous subsection, it is worth adding that here to accurately assess the frequency response improvement of the original systems with and without PEVs, dynamic simulations for the PFC are to be performed considering the non-linear terms of system. Then, it is possible to check whether the frequency has been remained below the prespecified threshold more than the intentional delay (e.g., 18 cycles or 0.36 s). If the frequency is recovered in less than the duration time of the intentional delay, then it is very likely that the UFLS scheme would not be activated. However, if the frequency remains below the prespecified threshold more than the duration time of the intentional delay, then the UFLS would disconnect a certain portion of the load from the electrical grid. We will check the activation of UFLS scheme, when later the simulation results are provided, though the UFLS scheme would not be implemented in the dynamic model (or in other words no load would be shed during the simulations).

5.5.3. UFLS Scheme For Previous Case Study And Simulation Scenarios

In order to calculate the UFLS cost, several parameters such as VOLL, time duration of ENS, minimum prespecified frequency, and the amount of shed load SL , i.e., 5% of the total load, are to be considered. In summary, Table. 5.5 presents these parameters for both scenarios A and B. As seen, except the minimum frequency f^{min} and the shed load SL , the rest of the parameters are considered the same or both scenarios A and B. The value of the lost load is assumed equal to €5000 /MWh¹² according to the RCP energy market report (Lucia & Kong, 2012). Also, the duration of load shedding is assumed one hour, which notably varies in practice from one country to another. The estimated number of event occurrences for a given year PR^{DST} is assumed one. Moreover, the intentional delay is assumed equal to 0.36 s. As stated before, in this analysis the UFLS scheme is not implemented in the control system, however the activation of the UFLS can be identified according to the frequency response obtained from dynamic simulations, when the frequency drops below the prespecified threshold for more than the intentional delay, i.e., 0.36 s. It is worth mentioning that for the UFLS scheme, the minimum prespecified threshold in the islanded network (i.e., 49 Hz) is assumed low compared to the one in the large-scale power system (i.e., 49.50 Hz), as shown in Table. 5.5.

As the frequency deviations could be much higher in the islanded network compared to the large-scale power systems, it is expected that a larger portion of the total

¹²For the sake of simplicity, here we assumed €1=\$1.

Table 5.5.: UFLS in scenarios A & B.

	Scenario A	Scenario B
UFLS parameter	Value	
f^{min} [Hz]	49.00	49.50
Shed load SL	5 MW - 0.05 pu	500 MW - 0.05 pu
VOLL [€/MWh]	500, 5000, 10,000	
Duration of ENS [h]	1	
Intentional delay [s]	0.36	
PR^{DST} [$year^{-1}$]	1	

load will be shed during the PFC. This apparently imposes more costs associated with the UFLS to the islanded networks compared to the large scale power systems. As a result, PEVs are very likely to be more effective in islanded networks, in which they could largely reduce the frequency deviations and consequently the PFC costs. The total PFC costs are calculated for various contexts: 1) VOLL is currently equal to €5000 /MWh, 2) If the value of the VOLL increases to €10,000 /MWh, 3) in the context of rural villages, the VOLL might have a very low value, e.g., €500 /MWh. Moreover, the sensitivity analyses are carried out for various values of the intentional delay of the UFLS scheme (i.e., 0.05 s, 0.36 s, and 1 s).

Next, we create the above-described case studies and simulation scenarios, and then provide the results of the UFLS scheme.

5.5.4. Results

PEVs have a great potential to avoid the costs associated with the UFLS. To this end, here we evaluate to what extent PEVs are able to avoid the activation of the UFLS scheme and consequently provide some cost saving to power system operators. Therefore, we carefully look into the dynamic simulation results obtained from the previously mentioned scenarios A and B, and see whether the UFLS scheme is already activated or not. In summary, Table. 5.6 shows the results of sensitivity analyses for scenarios A and B, that are the maximum power variation of PEVs $\Delta P_{av,ag}^{max}$, minimum frequency Δf^{min} , total annual UFLS costs C^{UFLS} , UFLS scheme activation, and total UFLS cost reduction ΔC^{UFLS} per year. Note that in this analysis the same amount of load shedding has been considered for both cases according to the standard though in practice different UFLS schemes might be applied.

Table 5.6.: Sensitivity analyses results for scenarios A and B.

	$\Delta P_{av,ag}^{max}$ [PU]	Δf^{min} [Hz]	C^{UFLS} [K€]	$UFLS$	ΔC^{UFLS} [K€]
Sc.A.2.1	0.01	48.68	24	1	-
Sc.A.2.2	0.02	48.94	24	1	0
Sc.A.3.2	0.3	49.94	0	-	24
Sc.B.2.1	0.005	49.34	2520	1	-
Sc.B.2.2	0.02	49.60	0	-	2520
Sc.B.3.2	0.3	49.98	0	-	2520

As shown in Table. 5.6, in scenario A.2.1, PEVs using 5% droop are not able to adequately mitigate the frequency deviations, and consequently, the UFLS is activated. For scenario A.3.2 in the islanded network, PEVs using the well designed droop are able to successfully avoid the activation of the UFLS, and consequently the UFLS costs could be successfully avoided per year. However in Figure. 5.12(c) for scenario A.2.2, PEVs even using the well designed droop are not able suppress the frequency deviation due to the low PEV penetration of 2%. Therefore, the UFLS is activated and consequently the UFLS costs are not successfully reduced.

It is worth mentioning that in scenarios A.2 and A.3, the power variation of PEVs reaches the maximum power limits if 2% and 5%, respectively. However, in the islanded network, the maximum power variation of 2% of PEVs in scenario A.2 is not sufficient to avoid the activation of the UFLS scheme. As a result, the frequency drops to a low value of 48.94 Hz and the due to the activation of the UFLS, the total costs of k€24 were imposed to the operator of the islanded area. However, in scenario A.2, the power variation of 5% of PEVs was sufficient to avoid the activation of the UFLS scheme, and as a result the total costs of k€24 were avoided. In the context of the islanded network, the total PFC costs were equal to k€24, which obviously is significantly lower than the total PFC costs of the large-scale power systems, i.e., k€2,520.

As shown in Figure. 5.12(c) and Table. 5.6, in scenario B.2.1, PEVs using 5% droop are not able to sufficiently reduce the frequency deviations, and consequently, the UFLS is activated. For scenario B.2.2 in the large-scale power system, PEVs are able to successfully avoid the activation of the UFLS even for the low PEV penetration rate of 2%, and consequently the UFLS costs could be successfully avoided per year. Obviously for the fixed PEV penetration rate of 2%, PEVs are able to further improve the frequency response of the large-scale power system under the disturbance of 5% rather than the islanded network under the disturbance of 10%

Table. 5.7 briefly show the sensitivity analyses results for various values of the VOLL. As can be seen, the VOLL could have a very low value in the context of rural villages, and consequently the total PFC costs are equal to k€2.4 and k€252 for the islanded system and large-scale power systems, respectively. Also, as mentioned

5.5 Brief Description And Discussion On Economic Evaluation of PEVs for PFC (Outside the Scope of This Technical Research)

in (Lucia & Kong, 2012), the VOLL could potentially increase to €10,000/MWh. For this scenario, the total PFC costs will be two times and increase to k€48 and k€5040 for the islanded system and large-scale power systems, respectively. As seen, in conclusion, in most of the scenarios, PEVs could effectively avoid the costs associated with the UFLS.

Table 5.7.: Sensitivity analyses results for scenarios A and B for various VOLL values.

	C^{UFLS} [k€]	C^{UFLS} [k€]	C^{UFLS} [k€]
	VOLL 5000 [€/MWh]	VOLL 500 [€/MWh]	VOLL 10,000 [€/MWh]
Sc.A.2.1	24	2.4	48
Sc.A.2.2	24	2.4	48
Sc.A.3.2	0	0	0
Sc.B.2.1	2,520	252	5040
Sc.B.2.2	0	0	0
Sc.B.3.2	0	0	0

Table. 5.8 shows the total costs for scenarios A and B, where the intentional delay of the UFLS scheme varies from 0.05 s to 1 s. As seen, if the intentional delay has a very low value, in both islanded and large-scale power systems, the UFLS scheme is activated in scenarios A.2.2 and B2.2. However, if the intentional delay increases to 1 s, then the UFLS is not activated either in the islanded network or in the large scale power system in any scenario.

Table 5.8.: Sensitivity analyses results for scenarios A and B for various intentional delays of the UFLS scheme.

	C^{UFLS} [k€]	C^{UFLS} [k€]	C^{UFLS} [k€]
	$T_{int} = 0.36s$	$T_{int} = 0.05s$	$T_{int} = 1s$
Sc.A.2.1	24	24	24
Sc.A.2.2	24	24	0
Sc.A.3.2	0	0	0
Sc.B.2.1	2,520	2,520	2,520
Sc.B.2.2	0	2,520	0
Sc.B.3.2	0	0	0

5.6. Discussion

In this chapter, in order to ensure the frequency stability for the worst case scenario, the droop for individual PEVs was designed equal to 0.07%. Then, the techno-economic impact of PEVs on the PFC was evaluated in a large-scale power system and an islanded network. As addressed before in section 5.2, the value of the designed droop was obtained relatively low compared to the one of conventional generating units (e.g., droop of 5%), therefore here some considerations are further discussed.

From a technical point of view, though the value of 0.07% droop was obtained fairly low, still we shall differentiate it from 0% droop for PEVs. As illustrated and discussed in (Mu et al., 2013b), if PEVs (with 0% droop) are abruptly disconnected from the electrical grid following the disturbance, then they could largely deteriorate the frequency response and put at risk the frequency stability. Similarly, in the analysis of this chapter, the phase margin became extremely low (close to zero), when the PEV droop tended to zero. As a result, the implementation of droop even with a low value seems necessary in the future to avoid the frequency instabilities. The current simulation results revealed that PEVs using 0.07% quickly participate in the PFC, therefore the frequency response was remarkably improved. However, if some other factors such as measurements, computational delays, communication networks, non-linear blocks are also taken into account, then the PEV droop would be designed at a higher value. Also, in practice, aforementioned factors might highly decrease the abrupt power variation of PEVs during the PFC. In conclusion, though the droop of 0.07% was truly designed and tested for the worst case of a fairly ideal power system, in real-power networks, a higher value of droop would be designed and implemented in PEVs.

From an economic point of view, PEVs provided an excellent response by which the costs of UFLS were avoided. However, due to the above mentioned factors. in practice, PEVs using a higher droop value might not provide very fast response to avoid the UFLS costs (especially in islanded networks with a low penetration rate of PEVs).

5.7. Conclusions and Out-Look

This chapter described a strategy to design the frequency droop controller of PEVs for the PFC. In order to design the strategy, we defined and performed the three following steps:

1. Obtain and evaluate the phase margin and crossover frequency from the bode diagrams, which resulted from the linearized open-loop of the frequency control
2. Achieve the overall gain of PEVs for the worst case of power systems through extensive sensitivity analyses (e.g., minimum equivalent inertia, maximum

damping ratio, lowest turbine time constants, highest PEV time constants, etc)

3. Design the frequency droop controller of each individual PEV according to the worst case of PEVs (i.e., highest future expected penetration rate of PEVs)

In the next stage, the base case study for a small-scale distribution network including PEVs was defined and afterwards, this small-scale network was replicated and scaled up to create an islanded network and a large-scale power system. Then, dynamic simulations in Matlab / Simulink was carried out to obtain the frequency response improvement by PEVs using the designed droop in both islanded and large-scale power systems Accordingly, sensitivity analyses were performed on the following parameters:

1. For the sake of comparison, PEVs equipped with either conventional droop or here well-designed droop curves,
2. PEV penetration rate,
3. Maximum power limit of PEVs for PFC.

From a technical perspective, the well-designed droop controller of PEVs had a satisfactory performance in terms of effectively and quickly utilizing the PEVs power reserve for the PFC, while at the same time successfully preserving the overall system stability. Despite the fact that the PFC non-linear terms such as the maximum power limit of PEVs had a detrimental influence on the PEV performance for the PFC, PEVs using the designed droop could remarkably improve the minimum frequency response of either islanded networks (e.g., by 19.69%) or large-scale power systems (e.g., by 39.39%) following the largest anticipated disturbance, even for low penetration rates of PEVs, e.g., 2%. Note that in this analysis, PEVs and CGUs were principally considered for the PFC, however in the future wind farms and solar power plants could further improve the frequency response within large scale power systems.

Besides, fairly outside the scope of this technical research, the economic aspects of the provision of PFC by PEVs were briefly reviewed and evaluated. From an economic perspective, it was shown that PEVs using the designed droop controller had a considerable potential to highly reduce the system PFC costs associated with the UFLS. In fact, PEVs had a great potential to suppress the frequency deviations following a contingency event, and consequently the UFLS scheme were not activated (no loads were shed).

In the next final chapter, we will summarize the conclusions drawn from this chapter and earlier chapters together with the suggestions for future research.

6. Conclusions and Future Work

Contents

6.1. Conclusions	172
6.2. Future Work	175
6.3. List of Thesis-Related Publications in Prestigious (JCR) Journals & International Conferences	176

In this thesis research, we first provided an overview of the provision of PFC by PEVs in electric power systems in chapter 2. In addition, we reviewed the state-of-the-art in detail, where we could clarify and identify the existing research gaps related to the overarching research questions. According to the identified research gaps, on the first attempt, in chapter 3, we formulated and developed an aggregate model of PEVs for the PFC using the arithmetic averaging technique. Since the distribution networks, to which PEVs will be mostly connected in the near future, were neglected in the previous model of PEVs, a novel aggregate model of PEVs including the distribution network for the PFC was formulated in chapter 4. Finally in chapter 5, in order to technically implement evaluate the previously developed aggregate models of PEVs for the PFC, we described a strategy to design the frequency droop controller of PEVs. Besides, outside the scope of this technical research, the economic performance of PEVs for the PFC was briefly reviewed and assessed. Here, in this last chapter of the thesis, the main conclusions are drawn and summarized, and some directions for future work are provided.

6.1. Conclusions

With respect to the research gaps identified in chapter 2, this thesis proposes advanced aggregate models of PEVs for the PFC. Chapter 3 develops an aggregate model of PEVs, which successfully incorporates essential technical characteristics of PEV fleets for the PFC studies. As the distribution networks, to which PEVs are mostly connected, were neglected in the previous model of PEVs, chapter 4 formulates and proposes a sophisticated aggregate model of PEVs in which technical characteristics of distribution networks are properly addressed and incorporated. Finally, to technically implement and economically evaluate our proposed aggregate models of PEVs for PFC, chapter 5 describes a strategy to well design the frequency

droop controller of PEVs and evaluates the economic performance of PEVs for the PFC.

According to the above-reported research works, the main conclusions of this thesis can be listed and divided into the following three parts:

Aggregate Model of PEVs Including PEV Fleet Characteristics for PFC

On the first attempt, an aggregate model of PEVs for the PFC is formulated and developed using the arithmetic averaging technique. According to the previously surveyed state-of-the-art, several PEV fleet characteristics such as PEV's charging modes (i.e., constant current or constant voltage), PEV's operating modes (i.e., disconnected, idle, or charging), and battery charger topologies (i.e., unidirectional battery chargers or bidirectional battery chargers) are incorporated into the PEV model for the PFC introducing a participation factor. The charging power and operating modes of PEVs could highly change during the day, and as a result the average state of charge of PEVs will accordingly change. Thus, to obtain the average participation factor of PEVs for PFC, the probability density function of PEV's state of charge is defined and considered over the course of the day. It is demonstrated that a large portion of PEV fleet's power reserve might not be available for the PFC during the day due to the PEV fleet's technical restrictions. In spite of these technical limits, PEVs equipped either with the unidirectional battery chargers or bidirectional battery chargers have a great potential to improve the frequency response of power systems following a contingency event. In fact, thanks to the fast-controlled battery chargers, PEVs have a very satisfactory performance during the PFC compared to the conventional generating units. As expected, PEVs equipped with the bidirectional battery chargers show a better performance in term of minimum frequency response compared to the ones equipped with the unidirectional battery chargers.

The original contribution of this part is to devise an aggregate model of PEVs for the PFC where the essential operating modes as well as relevant technical constraints of PEV fleets could be effectively included by introducing the participation factor (also see Izadkhast et al. (2015)).

Nonetheless, in the here proposed model of PEVs, electrical distribution networks, to which PEVs are mostly connected, are neglected and undoubtedly this makes the previous model of PEVs in accurate.

Aggregate Model of PEVs Including Distribution Characteristics for PFC

The previously developed aggregate model of PEVs for PFC could become even more accurate, if the technical characteristics of distribution network such as the power consumed in the network and maximum current limit of the distribution lines and transformers are taken into account. To achieve this goal, the power consumed in distribution lines are linearised around the operating point, and then incorporated

into the previous model of PEVs for the PFC. To include the maximum current limit of lines and transformers, an additional limit is introduced and implemented in the PFC loop of each PEV. Compared to the previous model of PEVs, this aggregate model of PEVs for PFC has a relatively better accuracy and precision due to the inclusion of distribution networks. Moreover, the implementation of the additional current limit in the PFC loop of PEVs might be absolutely necessary in the near future, when a large number of PEVs notably increase their charging power for the PFC. Otherwise, distribution lines and transformers might become heavily overloaded during the over-frequency problem, and consequently the over-current protection could be improperly activated.

The original contribution of this part is to incorporate the technical characteristics of distribution networks (i.e., power consumed in the network and maximum power/current limits) into the previous aggregate model of PEVs for PFC, in which distribution networks were neglected (also see Izadkhast et al. (2014, 2016)).

In the two previously proposed aggregate models of PEVs for the PFC, the minimum frequency response is considered as the primary performance indicator, while in reality the frequency stability of power systems including PEVs shall be checked and ensured in advance. On top of this, the frequency droop controller of PEVs was arbitrarily set. Thus, we describe a strategy to well design the frequency droop of PEVs and additionally assess the economic performance of PEVs for the PFC.

Technical Implementation and Economic Evaluation of Aggregate Models of PEVs for PFC

The technical implementation of the previously-developed aggregate models of PEVs for PFC are addressed.

From a technical point of view, first a novel design of PEV's frequency-droop controller for PFC is provided considering the overall system stability margins. To obtain the well-designed droop, first bode plots as well as eigenvalue analysis are performed. Second, the worst case of the power system is identified through an extensive sensitivity analyses on a large number of sets of system parameters. Then the overall droop of PEVs is calculated for the worst case scenario of PEVs in the future. The well-designed droop controller of PEVs has a satisfactory performance in terms of effectively and quickly utilizing the PEVs power reserve for the PFC, while at the same time successfully preserving the overall system stability. Firstly, despite the fact that the non-linear terms of the PFC such as the maximum power limit of PEVs has a detrimental influence on the PEV performance for the PFC, PEVs using the designed droop could remarkably improve the minimum frequency response of either islanded networks or large-scale power systems following the largest anticipated disturbance.

Besides, from an economic point of view, fairly outside the scope of this technical research, the impact of PEVs on the PFC costs is touched upon. To assess the

performance improvements, which come from PEVs, the total system costs associated with the PFC is evaluated mainly calculating the normal operation PFC costs as well as the emergency UFLS costs. It is shown that PEVs using the designed droop controller has a considerable potential to highly reduce the system PFC costs associated with the UFLS.

The original contribution of this work is to describe a strategy to well design the frequency droop controller of PEVs for the PFC where the system's stability criterion is always respected. Outside the scope, also the economic performance of PEVs for the PFC is briefly reviewed and evaluated (also see Izadkhast et al. (2017)).

6.2. Future Work

A number of directions for future work in this area are suggested and listed below:

Variable Frequency-Droop Controller

In the aggregate model of PEVs including PEV fleet characteristics, the frequency droop controller of PEVs is assumed constant and the same for the whole PEV fleet. However in future, PEVs might adjust the droop characteristics depending on the PEV operating conditions, e.g., battery state of charge. Therefore, it is interesting to further develop the aggregate model of PEVs where PEVs have different droop curves.

Dynamic Voltage Support by PEVs

In the aggregate model of PEVs including distribution network characteristics, it is assumed that PEVs do not provide dynamic voltage support before or during the frequency disturbance for the distribution networks. However in practice, distribution system operators can make the most of PEV grid support capability not only for PFC support but also simultaneously for voltage support. It is interesting to evaluate the accuracy and performance of the model, when PEVs do provide both frequency and voltage support.

Unbalanced Flow Events

In the aggregate model of PEVs including distribution network characteristics, a balanced three-phase radial distribution network is considered and evaluated. However in reality, distribution networks are inherently unbalanced not only due to unequal single-phase loads, but also due to other single-phase units like PEVs. Therefore, it is important to carry out more research to evaluate the performance of the PEV aggregate model for the PFC during the unbalanced flow events.

Load Power Variation Due to Voltage Variation At Transmission After Large Disturbances

The aggregate model of PEVs including the network mainly focused on the distribution side, where PEVs are connected. It will be interesting to consider the load power variations due to voltage changes at HV transmission after a large disturbance.

Aggregation of PV Units and Wind Farms for PFC (Next to PEVs)

Next to PEVs, technically speaking, other DERs like PV units and wind farms have a potential to provide the PFC. As the main focus of this thesis was on the aggregation of PEVs for the PFC, technical characteristics of other types of DERs for the PFC were not adequately addressed. The here developed aggregate models of PEVs could be flexibly extended and used for other types of DERs, and consequently it will be interesting to additionally evaluate these aggregate models taking into account various technical constraints of other types of DERs.

Economic Evaluation of PFC Including PEVs

In chapter 5, where the total system PFC costs are calculated, for the sake of simplification the PFC reserve capacity costs are neglected. However to comprehensively evaluate the economic impact of PEVs on the system costs associated with the PFC, a PFC market should be implemented in competitive pool-based electricity markets co-optimizing the energy and PFC service and adopting novel pricing designs. To achieve this goal, the following steps could be suggested:

1. It will be interesting to incorporate PEVs in the security-constrained unit commitment (SCUC) model, where the dynamic behaviour of PEVs during both PFC and SFC will be formulated.
2. A process could be developed to further ensure the required speed for the PFC through dynamic simulations.
3. A proper pricing scheme might be designed to quantify both energy and ancillary services in pool based markets.

Also, outside the scope of this PhD project, the provision of islanding and emergency back-up by PEVs was partly evaluated within the framework of GRID4EU project and this will surely remain an interesting direction for future research.

6.3. List of Thesis-Related Publications in Prestigious (JCR) Journals & International Conferences

- **S. Izadkhast**, P. Garcia-Gonzalez, and P. Frías, “An aggregate model of plug-in electric vehicles for primary frequency control,” *IEEE Transactions on*

Power Systems, vol. 30, no. 3, pp. 1475–1482. May 2015.

- **S. Izadkhast**, P. Garcia-Gonzalez, and P. Frías, L. Ramirez-Elizondo, and P. Bauer, “An aggregate model of plug-in electric vehicles including distribution network characteristics for primary frequency control,” *IEEE Transactions on Power Systems*, vol. 31, no. 4, pp. 2987–2998. Jul 2016.
- **S. Izadkhast**, P. Garcia-Gonzalez, P. Frías, and P. Bauer, “Design of plug-in electric vehicle’s frequency-droop controller for primary frequency control and performance assessment,” *IEEE Transactions on Power Systems*, accepted and to be published.
- **S. Izadkhast**, P. Garcia-Gonzalez, and P. Frías, L. Ramirez-Elizondo, and P. Bauer, “Aggregation of plug-in electric vehicles in distribution networks for primary frequency control,” in *IEEE International Electric Vehicle Conference*, Dec. 2014 Florence, Italy.
- **S. Izadkhast**, P. Garcia-Gonzalez, and P. Frías, “An aggregate model of plug-in electric vehicles for primary frequency control,” *Power & Energy Technology Systems (PES) General Meeting*, Jul. 2016 IEEE Boston, Massachusetts, USA.
- **S. Izadkhast**, P. Garcia-Gonzalez, and P. Frías, L. Ramirez-Elizondo, and P. Bauer, “An aggregate model of plug-in electric vehicles including distribution network characteristics for primary frequency control,” *Power & Energy Technology Systems (PES) General Meeting*, Jul. 2016 IEEE Boston, Massachusetts, USA.
- **S. Izadkhast**, “Plug-in electric vehicle participation in primary frequency control considering characteristics of distribution networks,” in *Young Energy Engineers & Economists Seminar*, Nov. 2014 KU Leuven, Belgium.

A. Review on Regulation- and Market-Oriented Aggregation Approaches

Contents

A.1. Regulation-Oriented Approach	180
A.1.1. Aggregation Provision Under the Regulatory Framework .	180
A.2. Market-Oriented Approach	181
A.2.1. Aggregation Provision Under the Competitive Electricity Market Environment	181

This appendix presents a more detailed overview of the aggregation approaches in electric power systems, as shown in Figure A.1 and Figure A.2. In chapter 2, our main focus was devoted to the technically-oriented approach. However to give a higher-level background of DER aggregation in electric power systems research, in brief here we additionally review the state-of-the-art in DER aggregation concerned with the regulation-oriented (Armbrust et al., 2010; Borenstein & Bushnell, 2015; Codognet, 2004; Defeuilley, 2009; Littlechild & others, 2000; Markovic et al., 2013; Teece, 1980; Williamson, 1985) and market-oriented (Bessa et al., 2012; Foster & Caramanis, 2013; Gonzalez Vaya & Andersson, 2014; Momber et al., 2015, 2014; Ortega-Vazquez et al., 2013; Sarker et al., 2015b).

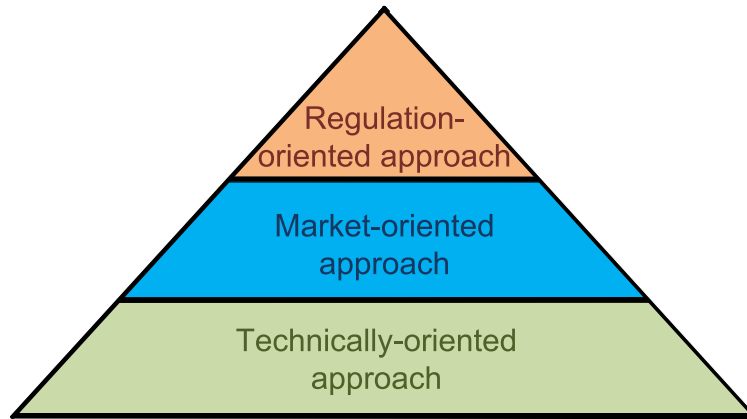


Figure A.1.: DER aggregation approaches in electric power systems.

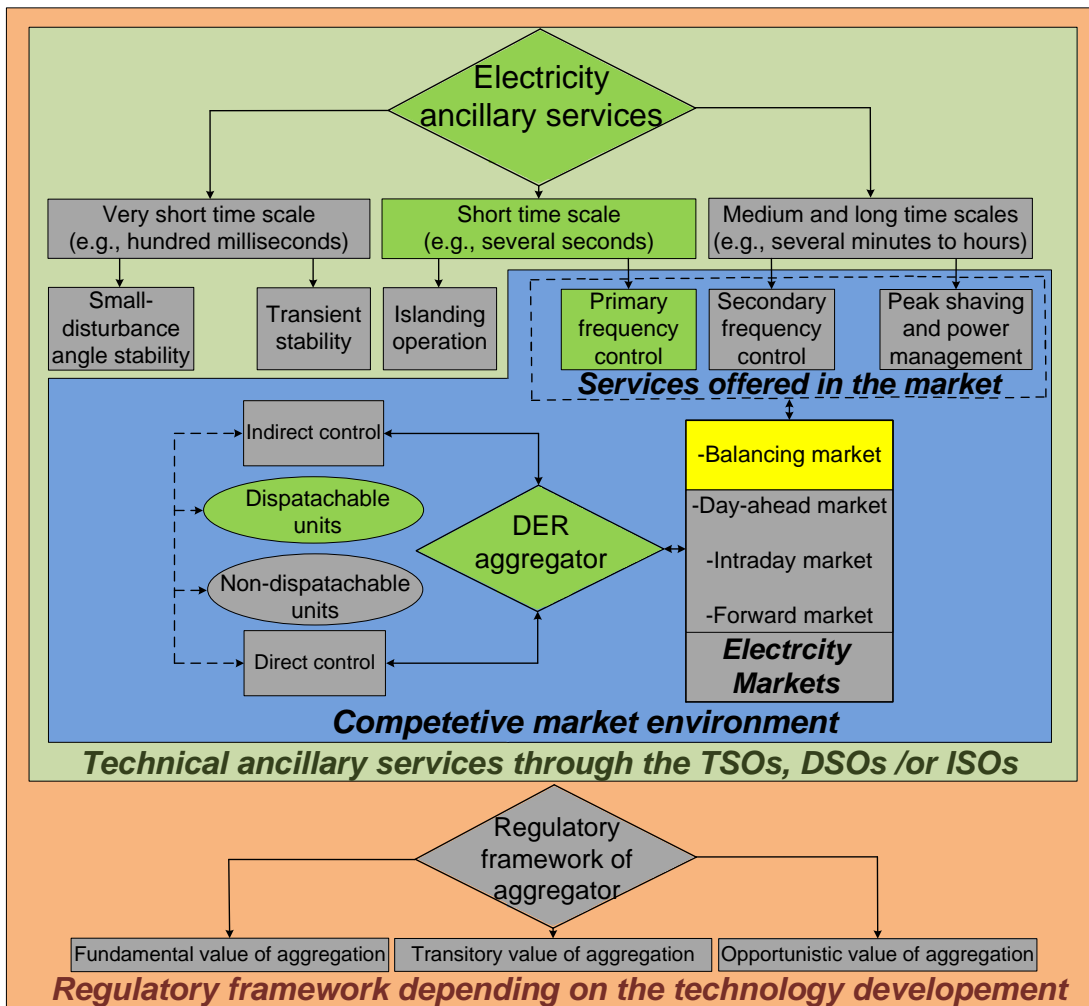


Figure A.2.: Classification of DER aggregation based on the regulation-oriented, market-oriented, and technically-oriented approaches (Green blocks were mainly addressed and evaluated in this thesis research).

A.1. Regulation-Oriented Approach

A.1.1. Aggregation Provision Under the Regulatory Framework

Generally speaking, aggregation of small-scale DERs is required to potentially bring some additional benefits to the economic system that in essence can not be practically provided by each individual small-scale DER. To this end, on a universal level, an appropriate regulatory framework depending on the technological development is required to effectively facilitate the coordination between the various electric power industry actors such as utility companies, manufacturers, market operators, system operators, aggregators, and small-scale DER owners.

A.1.1.1. Value of Aggregation

Within the existing electricity systems, the DER Aggregation might result in either system or private value. On the one hand, aggregation may contribute to the system value if it increases the overall static and dynamic economic efficiency of the power system (Nordhaus, 1969). Nowadays many electricity industry actors believe that the aggregation of small-scale DERs may efficiently provide an economic value to the system (Asmus, 2010; Braun & Strauss, 2008). On the other hand, the private value may not be necessarily aligned with the system value, while the economic value of some agents is raised, the one of other agents might be decreased. In summary, the value of small-scale DER aggregation based on the either system value (e.g., fundamental or transitory value) or private value (e.g., opportunistic value) can be divided into the following three parts:

- *Fundamental or intrinsic value of aggregation:* This value results inherently from the kinetics of aggregation itself, and it does not depend on any either specific regulatory action or policy decision. Therefore it will remain approximately permanent and stable over time. In general, the fundamental value could be created through capitalizing on economies of scale (Armbrust et al., 2010; Markovic et al., 2013) and scope (Codognet, 2004; Teece, 1980), managing various uncertainties (Littlechild & others, 2000), and spurring competition and innovation (Borenstein & Bushnell, 2015; Defeuilley, 2009; Littlechild & others, 2000).
- *Transitory value of aggregation:* This value typically leads to a better system performance only at the present and near future, however as soon as some technological norms, market dynamics, or regulatory conditions become favourable in the future, the transitory value might be lost. To create transitory value (Codognet, 2004), aggregators can act as the interface between the utility grid and DERs in helping them coordinate via information exchange.
- *Opportunistic value of aggregation:* This value mainly results from some regulatory pressures, institutional and market imperfections, and technological

flaws, because of which the opportunistic behaviour of aggregating agents, i.e., aggregators, is likely to occur.

This opportunism might impede the efficient and fair competition between individuals especially small-scale DERs. Despite this fact, if properly controlled and supervised, regulators or policy makers might be able to effectively remove some barriers (Williamson, 1985) depending on the future technological development such that the aggregation of small-scale DERs creates fundamental or transitory value. Next according to the literature, the aggregation of small-scale DERs in electricity markets is addressed.

A.2. Market-Oriented Approach

A.2.1. Aggregation Provision Under the Competitive Electricity Market Environment

In the last few years, small-scale DERs have been increasingly connecting to the electric power grids to such extent that their aggregate installed capacity may even become comparable to the installed capacity of several conventional generating units, which operate and participate in various electricity markets. In a similar manner to the conventional generating units, if properly integrated, DER units could also participate in numerous electricity markets. Undoubtedly, this large-scale integration of small-scale DERs could potentially bring numerous economic challenges and opportunities regarding the short-term operation and long-term planning of electricity markets.

In this context, to effectively facilitate the small-scale DER participation in the market in the near future, the aggregation of small-scale DER is likely to be greatly required due to the following reasons:

- *Very low installed power capacity and energy content of small-scale DERs:* Since in deregulated electricity markets, the submitted bids of producers must typically comply with rules such as minimum power installed capacity and minimum energy volume for the bids, small-scale DERs are not mostly able to enter the market on their own. In such cases, aggregation of DER units is highly required in order to facilitate the electricity market entry and make them able to enter and effectively participate in the market.
- *Low operational efficiency of small-scale DERs in electricity markets:* Generally, small-scale DER operators are not adequately trained and prepared to effectively formulate a market entry strategy. On top of this, the power forecast error of each individual small-scale DER could be significant along the day or night. This automatically results in a lower efficiency and profits of small-scale DERs in the market, where they might also be penalized for their

generation deviations. Aggregation of DERs could help minimize the total power forecast error in such a way that positive forecast errors are likely to be compensated by negative forecast errors. In summary, while aggregation of small-scale DERs in a coordinated way could notably help not only ensure an efficient market outcome for them, but also reduce the total power forecast error.

- *Annual fees for market participants including small-scale DERs:* As a matter of fact, all market participants are required to pay annual capacity and membership fees, which may be a significant barrier to market entry of an individual small-scale DER due to a relatively low annual income (Faria et al., 2014, 2012).
- *Data exchange barriers between distribution system operators (DSOs), transmission system operators (TSOs), and DERs:* In present day power systems, unlike conventional generating units interfaced with real-time data acquisition systems, the real-time operational data of DERs like PV systems and PEVs at the LV side are not adequately available to either TSOs or DSOs. In this context, aggregation of small-scale DERs could help facilitate the data exchange based on an effective communication infrastructure between TSOs, DSOs, and DERs.

A.2.1.1. Aggregator As An Intermediary Between the Electricity Market and DER Units

As shown in Figure A.2, the aggregator can act as an intermediary between the electricity markets (e.g., real-time balancing markets) and DER units. On the one hand, aggregators act in the market by offering the energy and power capacity, which are essentially provided by DER units. On the other hand, aggregators are required to control the power produced by DER units using various control schemes.

Aggregator and DER Units

To effectively participate in the market, aggregators should be able to either partially or completely operate and control the power produced by DER units. As shown in Figure A.2, generally, aggregators can make use of the DER units either via direct or indirect control as follows (Momber et al., 2016; Pinson et al., 2014; Ruiz et al., 2015):

- *Direct control:* In this control scheme, the detailed information of DER units is provided via a direct communication link to one aggregating agent. Accordingly, this agent is able to centrally control the power set-points of DERs, which are practically interfaced to a fixed volumetric energy pricing. Since aggregators must instantaneously and optimally provide a large number of DERs with their corresponding power set-points, the direct control scheme might be

highly computationally intensive and time-consuming. Nonetheless, using this control scheme, aggregators are less likely to be penalized in the electricity markets because they are able to precisely calculate and immediately use the power reserve of DER units.

- *Indirect control:* In this control scheme, a relatively limited information of DER units is provided to various aggregation agents in a distributed manner. Therefore, aggregators are subject to a much higher uncertainty and risk associated with the scarcity of data. To make use of DER units, aggregators have to provide proper economic incentives (e.g., price signals) to DER owners, and accordingly DER owners respond to the aggregator's signal. Then aggregators are able to approximately estimate the available power reserve of DERs with respect to the DER owners signal sensitivity that highly varies depending on a compromise between the potential economic rewards and owners living comfort. Using this control scheme, aggregators are more likely to be penalized in the electricity markets because they are not able to precisely calculate and determine the available power reserve of DER units.

To implement either direct or indirect control schemes, remote real-time data acquisition together with advanced information and communication infrastructure shall be developed and established to facilitate the interaction between the aggregator and the DER units. To this end, the aggregator might send the charging control or incentive signal over the communication network to DER units, and accordingly DERs respond to the signal provided.

Regardless of whether the aggregator employs the direct or indirect control, all types of DER units might not be able to provide the aggregator with the required power capacity or energy due to the technical and practical constraints. In Figure A.2, DER units are divided into two major categories as follows:

- *Dispatchable DER units:* Technically speaking, the output power of dispatchable DERs such as battery energy storage systems, PEVs, combined heat and power (CHP), fuel cells, micro-turbines, and small-scale hydro can be increased or decreased by the aggregator for a certain period of time. Therefore, potentially aggregators can rely mainly on these units, when they offer the available power capacity or the deliverable energy of dispatchable DERs into the electricity markets.
- *Non-dispatchable DER units:* Unlike dispatchable DERs, the output power of non-dispatchable DERs such as wind generation, tidal stream turbines, and solar cells cannot be reliably and readily called upon by the aggregator. In other words, non-dispatchable DERs mostly generate not in accordance with the aggregator needs, but rather inherently according to the availability of intermittent energy sources. In such cases, the aggregator might be able to partially participate in the market using non-dispatchable resources by only curtailing their power production. This might not be attractive and desirable from an economic point of view due the loss of green energy.

Aggregator's Participation in the Market

Generally speaking, the proper integration of DER units into the electricity markets via the aggregator might remarkably bring financial benefits not only to the final consumers (Momber et al., 2016), but also to the system as a whole in an efficient manner. To achieve this goal, undoubtedly the aggregator plays a key role in facilitating the participation of DER units in various short-term electricity markets such as day-ahead, intra-day, and real-time balancing markets, as shown in Figure A.2. On the one hand, with respect to the energy content, the aggregator can take part in the day/hour ahead energy market by submitting offers and bids for the energy based on the day/hour ahead forecasts of the available energy of DER units. On the other hand, with respect to the power content, the aggregator can provide various ancillary services over a short time horizon in the real-time balancing market by employing the estimated available power capacity of DER units (Han et al., 2011).

Over the past years, in particular, PEV aggregation in electricity markets has gained increasing importance because firstly PEVs have both high power and high stored energy capability to provide various system ancillary services due to their flexibility (Yilmaz & Krein, 2013), and furthermore they have a high potential to bring new challenges and opportunities in either day-ahead (Bessa et al., 2012; Foster & Caramanis, 2013; Gonzalez Vaya & Andersson, 2014) or balancing markets (Gonzalez Vaya & Andersson, 2015; Sarker et al., 2015a). Therefore, in the near future, it is very likely that profit-seeking agents, so-called PEV aggregators, serve as a commercial middleman between the electricity market, DSOs, TSOs, and PEV owners. As shown in Figure A.2, PEV aggregators are going to be the main provider and controller of vehicle-to-grid (V2G) technical ancillary services, e.g., primary frequency control, secondary frequency control, peak shaving, voltage control, and power management, which are addressed in detail as follows.

B. Models of Governor-Turbine

Figure B.1 shows a simplified GAST model representing the dynamic behavior of the gas governor-turbine. To evaluate the frequency control loop, in this analysis, the temperature control loop was neglected. The value of parameters are as follows: fuel system lag time 1 $T_1= 1.5$ s, fuel system lag time 2 $T_2= 0.1$ s, maximum value position $V_{MAX}= 1$, minimum value position $V_{MIN}= -0.02$, and turbine damping $D_{turb}= 0$.

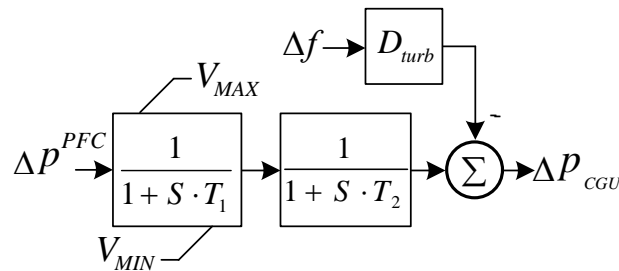


Figure B.1.: Simplified GAST model to represent the gas governor-turbine (Nagpal et al., 2001).

Figure B.2 shows the generic IEEE1 governor-turbine model of steam plant. The value of parameters are as follows: governor time constant $T_G^{Steam}= 0.25$ s, high pressure turbine time constant $T_3= 0.6$ s, intermediate pressure turbine time constant $T_4= 8$ s, medium pressure turbine time constant $T_5= 0.6$ s, high pressure turbine gain $G_1= 0.3$, intermediate pressure turbine $G_3= 0.4$, medium pressure turbine gain $G_5= 0.3$, and the rest of parameters are zero.

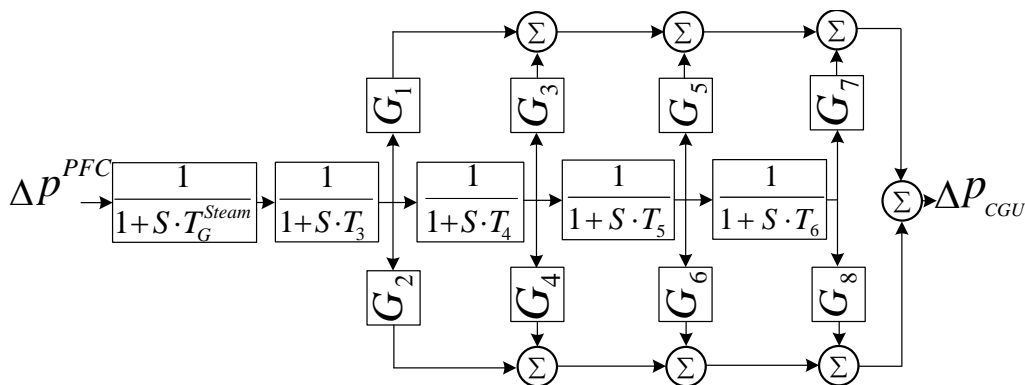


Figure B.2.: Generic IEEE1 governor-turbine model of steam plant (Kundur et al., 1994).

Bibliography

- ACEA, E. A. M. A. (2014). *New electric vehicle registrations in the European Union 2013 / 2014*. Technical report.
- ACEA, E. A. M. A. (2015). *New electric vehicle registrations in the European Union 2014 / 2015*. Technical report.
- Aditya, S. K. & Das, D. (2001). Battery energy storage for load frequency control of an interconnected power system. *Electric Power Systems Research*, 58(3), 179–185.
- Adrees, A. & Milanovic, J. V. (2016). Study of frequency response in power system with renewable generation and energy storage. In *2016 Power Systems Computation Conference (PSCC)* (pp. 1–7).: IEEE.
- Aghamohammadi, M. R. & Abdolahinia, H. (2014). A new approach for optimal sizing of battery energy storage system for primary frequency control of islanded Microgrid. *International Journal of Electrical Power & Energy Systems*, 54, 325–333.
- Agüero, J. L., Beroqui, M., & Molina, R. (2000). Economic transactions due to primary and secondary regulation of frequency in Argentina, methods and experience. In *Power Engineering Society Summer Meeting, 2000. IEEE*, volume 1 (pp. 325–330).: IEEE.
- Akhmatov, V. (2004). An aggregated model of a large wind farm with variable-speed wind turbines equipped with doubly-fed induction generators. *Wind Engineering*, 28(4), 479–486.
- Akhmatov, V. & Knudsen, H. (2002). An aggregate model of a grid-connected, large-scale, offshore wind farm for power stability investigations—importance of windmill mechanical system. *International Journal of Electrical Power & Energy Systems*, 24(9), 709–717.
- Almeida, P., Pecos Lopes, J., Soares, F., & Seca, L. (2011). Electric vehicles participating in frequency control: Operating islanded systems with large penetration of renewable power sources. In *PowerTech, 2011 IEEE Trondheim* (pp. 1–6).
- Almeida, P. R., Soares, F. J., & Pecos Lopes, J. (2015). Electric vehicles contribution for frequency control with inertial emulation. *Electric Power Systems Research*, 127, 141–150.
- Anton, H., Bivens, I., & Davis, S. (2002). *Calculus*, volume 2. Wiley Hoboken.
- Armbrust, M., Fox, A., Griffith, R., Joseph, A. D., Katz, R., Konwinski, A., Lee, G., Patterson, D., Rabkin, A., Stoica, I., & others (2010). A view of cloud computing. *Communications of the ACM*, 53(4), 50–58.
- Asmus, P. (2010). Microgrids, virtual power plants and our distributed energy future. *The Electricity Journal*, 23(10), 72–82.

- Automotive, I. (2015). *Norway leads global electric vehicle market*. Technical report.
- Baboli, P. T., Moghaddam, M. P., & Fallahi, F. (2010). Utilizing Electric Vehicles on Primary Frequency Control in Smart power Grids.
- Battistelli, C., Baringo, L., & Conejo, A. J. (2012). Optimal energy management of small electric energy systems including V2g facilities and renewable energy sources. *Electric Power Systems Research*, 92, 50–59.
- Beck, F. & Martinot, E. (2004). Renewable energy policies and barriers. *Encyclopedia of energy*, 5(7), 365–383.
- Bessa, R., Matos, M., Soares, F., & Pecos Lopes, J. (2012). Optimized Bidding of a EV Aggregation Agent in the Electricity Market. *IEEE Transactions on Smart Grid*, 3(1), 443–452.
- Bevrani, H. (2009). *Robust power system frequency control*, volume 85. Springer.
- Bokhari, A., Alkan, A., Dogan, R., Diaz-Aguilo, M., De Leon, F., Czarkowski, D., Zabar, Z., Birenbaum, L., Noel, A., & Uosef, R. (2014). Experimental Determination of the ZIP Coefficients for Modern Residential, Commercial, and Industrial Loads. *IEEE Transactions on Power Delivery*, 29(3), 1372–1381.
- Borenstein, S. & Bushnell, J. (2015). *The US Electricity Industry After 20 Years of Restructuring*. Technical report, National Bureau of Economic Research.
- Braun, M. & Strauss, P. (2008). A review on aggregation approaches of controllable distributed energy units in electrical power systems. *International Journal of Distributed Energy Resources*, 4(4), 297–319.
- Brivio, C., Mandelli, S., & Merlo, M. (2016). Battery energy storage system for primary control reserve and energy arbitrage. *Sustainable Energy, Grids and Networks*, 6, 152–165.
- Chen, M. & Rincon-Mora, G. A. (2006). Accurate electrical battery model capable of predicting runtime and I-V performance. *IEEE Transactions on Energy Conversion*, 21(2), 504– 511.
- Codognet, M.-K. (2004). *The shipper as the architect of contractual relations in access to natural gas networks*. Technical report, Working Papers du Groupe RÅlseaux Jean Monnet.
- Company, M. . (2014). *Electric vehicles in Europe: gearing up for a new phase?* Technical report.
- Conroy, J. & Watson, R. (2009). Aggregate modelling of wind farms containing full-converter wind turbine generators with permanent magnet synchronous machines: transient stability studies. *IET Renewable Power Generation*, 3(1), 39.
- Costanzo, G. T., Kheir, J., & Zhu, G. (2011). Peak-load shaving in smart homes via online scheduling. In *Industrial Electronics (ISIE), 2011 IEEE International Symposium on* (pp. 1347–1352).: IEEE.
- Dai, J., Phulpin, Y., Sarlette, A., & Ernst, D. (2010). Impact of delays on a consensus-based primary frequency control scheme for AC systems connected by a multi-terminal HVDC grid. In *Bulk Power System Dynamics and Control (iREP)-VIII (iREP), 2010 iREP Symposium* (pp. 1–9).: IEEE.

- Dai, Y., Zhao, T., Tian, Y., & Gao, L. (2007). Research on the primary frequency control characteristics of generators in power system. In *2007 2nd IEEE Conference on Industrial Electronics and Applications* (pp. 569–574).: IEEE.
- Dees, D. W., Battaglia, V. S., & Baba, J. langer, A. (2002). Electrochemical modeling of lithium polymer batteries. *Journal of power sources*, 110(2), 310–320.
- Defeuilley, C. (2009). Retail competition in electricity markets. *Energy Policy*, 37(2), 377–386.
- Ela, E., Gevorgian, V., Tuohy, A., Kirby, B., Milligan, M., & O'Malley, M. (2014a). Market designs for the primary frequency response ancillary service-Part I: Motivation and design. *Power Systems, IEEE Transactions on*, 29(1), 421–431.
- Ela, E., Gevorgian, V., Tuohy, A., Kirby, B., Milligan, M., & O'Malley, M. (2014b). Market designs for the primary frequency response ancillary service-Part II: Case Studies. *Power Systems, IEEE Transactions on*, 29(1), 432–440.
- Estebanez, E. J., Moreno, V. M., Pigazo, A., Liserre, M., & others (2011). Performance evaluation of active islanding-detection algorithms in distributed-generation photovoltaic systems: Two inverters case. *Industrial Electronics, IEEE Transactions on*, 58(4), 1185–1193.
- Faria, P., Soares, T., Vale, Z., & Morais, H. (2014). Distributed generation and demand response dispatch for a virtual power player energy and reserve provision. *Renewable Energy*, 66, 686–695.
- Faria, P., Vale, Z., Soares, T., & Morais, H. (2012). Energy and reserve provision dispatch considering distributed generation and demand response. In *Innovative Smart Grid Technologies (ISGT Europe), 2012 3rd IEEE PES International Conference and Exhibition on* (pp. 1–7).: IEEE.
- Fernandez, L. M., Jurado, F., & Saenz, J. R. (2008). Aggregated dynamic model for wind farms with doubly fed induction generator wind turbines. *Renewable Energy*, 33(1), 129–140.
- Foster, J. & Caramanis, M. (2013). Optimal Power Market Participation of Plug-In Electric Vehicles Pooled by Distribution Feeder. *IEEE Transactions on Power Systems*, 28(3), 2065–2076.
- Galus, M. D., Koch, S., & Andersson, G. (2011). Provision of Load Frequency Control by PHEVs, Controllable Loads, and a Cogeneration Unit. *IEEE Transactions on Industrial Electronics*, 58(10), 4568–4582.
- Garcia, C. A., Fernandez, L. M., & Jurado, F. (2015). Evaluating reduced models of aggregated different doubly fed induction generator wind turbines for transient stabilities studies. *Wind Energy*, 18(1), 133–152.
- Gonzalez Vaya, M. & Andersson, G. (2014). Optimal Bidding Strategy of a Plug-In Electric Vehicle Aggregator in Day-Ahead Electricity Markets Under Uncertainty. *IEEE Transactions on Power Systems*, PP(99), 1–11.
- Gonzalez Vaya, M. & Andersson, G. (2015). Self Scheduling of Plug-In Electric Vehicle Aggregator to Provide Balancing Services for Wind Power. *IEEE Transactions on Sustainable Energy*, PP(99), 1–14.

- Haghbin, S., Khan, K., Lundmark, S., Alakala, M., Carlson, O., Leksell, M., & Wallmark, O. (2010). Integrated chargers for EV's and PHEV's: examples and new solutions. In *Electrical Machines (ICEM), 2010 XIX International Conference on* (pp. 1–6).: IEEE.
- Haghbin, S., Lundmark, S., Alakala, M., & Carlson, O. (2011). An isolated high-power integrated charger in electrified-vehicle applications. *Vehicular Technology, IEEE Transactions on*, 60(9), 4115–4126.
- Han, S., Han, S., & Sezaki, K. (2011). Estimation of Achievable Power Capacity From Plug-in Electric Vehicles for V2g Frequency Regulation: Case Studies for Market Participation. *IEEE Transactions on Smart Grid*, 2(4), 632–641.
- Hentunen, A., Lehmuspelto, T., & Suomela, J. (2011). Electrical battery model for dynamic simulations of hybrid electric vehicles. In *2011 IEEE Vehicle Power and Propulsion Conference (VPPC)* (pp. 1–6).: IEEE.
- Hirst, E. & Kirby, B. (1996). *Electric-power ancillary services*. Oak Ridge National Laboratory.
- Hirst, E. & Kirby, B. (1997). *Creating competitive markets for ancillary services*. Oak Ridge National Laboratory.
- Holtinen, H., Cutululis, N. A., Gubina, A., Keane, A., & Van Hulle, F. (2012). *Ancillary services: technical specifications, system needs and costs. Deliverable D 2.2*. Technical report.
- Hu, W., Chen, Z., & Bak-Jensen, B. (2010). Optimal operation strategy of battery energy storage system to real-time electricity price in Denmark. In *Power and Energy Society General Meeting, 2010 IEEE* (pp. 1–7).: IEEE.
- Huang, C. C. & Lu, C. N. (2009). Peak load shaving system with voltage sag mitigation capability. In *Sustainable Alternative Energy (SAE), 2009 IEEE PES/IAS Conference on* (pp. 1–7).: IEEE.
- Ingleson, J. & Allen, E. (2010). Tracking the Eastern Interconnection frequency governing characteristic. In *2010 IEEE Power and Energy Society General Meeting* (pp. 1–6).
- IRF (2009). International rectifier bulletin.
- Izadkhast, S., Garcia-Gonzalez, P., & Frias, P. (2015). An Aggregate Model of Plug-In Electric Vehicles for Primary Frequency Control. *Power Systems, IEEE Transactions on*, 30(3), 1475–1482.
- Izadkhast, S., Garcia-Gonzalez, P., Frias, P., & Bauer, P. (2017). Design of Plug-in Electric Vehicle's Frequency-droop Controller for Primary Frequency Control and Performance Assessment. *Power Systems, IEEE Transactions on*, *accepted for publication*.
- Izadkhast, S., Garcia-Gonzalez, P., Frias, P., Ramirez-Elizondo, L., & Bauer, P. (2014). Aggregation of plug-in electric vehicles in distribution networks for primary frequency control. In *International Electric Vehicle Conference (IEVC), 2014 IEEE* (pp. 1–7).
- Izadkhast, S., Garcia-Gonzalez, P., Frias, P., Ramirez-Elizondo, L., & Bauer, P. (2016). An Aggregate Model of Plug-in Electric Vehicles Including Distribution Network Characteristics for Primary Frequency Control. *Power Systems, IEEE Transactions on*, 31(3), 2987–2998.

- Kisacikoglu, M. C., Ozpineci, B., & Tolbert, L. M. (2010). Examination of a PHEV bidirectional charger system for V2g reactive power compensation. In *Applied Power Electronics Conference and Exposition (APEC), 2010 Twenty-Fifth Annual IEEE* (pp. 458–465).: IEEE.
- Kottick, D., Blau, M., & Edelstein, D. (1993). Battery energy storage for frequency regulation in an island power system. *IEEE Transactions on Energy Conversion*, 8(3), 455–459.
- Kroeze, R. C. & Krein, P. T. (2008). Electrical battery model for use in dynamic electric vehicle simulations. In *IEEE Power Electronics Specialists Conference, 2008. PESC 2008* (pp. 1336–1342).: IEEE.
- Krumm, J. (2012). How people use their vehicles: Statistics from the 2009 national household travel survey. In *Society of Automotive Engineers (SAE) 2012 World Congress*.
- Kundur, P., Balu, N. J., & Lauby, M. G. (1994). *Power system stability and control*, volume 7. McGraw-hill New York.
- Kwon, J., Yoon, S., & Choi, S. (2012). Indirect current control for seamless transfer of three-phase utility interactive inverters. *Power Electronics, IEEE Transactions on*, 27(2), 773–781.
- Lalor, G. & O'Malley, M. (2003). Frequency control on an island power system with increasing proportions of combined cycle gas turbines. In *Power Tech Conference Proceedings, 2003 IEEE Bologna*, volume 4 (pp. 7–pp).: IEEE.
- Littlechild, S. C. & others (2000). *Why we need electricity retailers: A reply to Joskow on wholesale spot price pass-through*. Judge Institute of Management Studies.
- Liu, H., Hu, Z., Song, Y., & Lin, J. (2013). Decentralized vehicle-to-grid control for primary frequency regulation considering charging demands. *Power Systems, IEEE Transactions on*, 28(3), 3480–3489.
- Liu, H., Hu, Z., Song, Y., Wang, J., & Xie, X. (2015). Vehicle-to-Grid Control for Supplementary Frequency Regulation Considering Charging Demands. *IEEE Transactions on Power Systems*, PP(99), 1–10.
- Louie, K. W., Marti, J. R., & Dommel, H. W. (2007). Aggregation of induction motors in a power system based on some special operating conditions. In *Electrical and Computer Engineering, 2007. CCECE 2007. Canadian Conference on* (pp. 1429–1432).: IEEE.
- Lucia, L. & Kong, P. P. L. (2012). Review of the value of lost load (VoLL). *Energy Market Company, Paper No. EMC/RCP/60/2012/CP38*.
- Markovic, D. S., Zivkovic, D., Branovic, I., Popovic, R., & Cvetkovic, D. (2013). Smart power grid and cloud computing. *Renewable and Sustainable Energy Reviews*, 24, 566–577.
- Masuta, T. & Yokoyama, A. (2012). Supplementary load frequency control by use of a number of both electric vehicles and heat pump water heaters. *Smart Grid, IEEE Transactions on*, 3(3), 1253–1262.
- Matlab/LINMOD (2015). Extract continuous-time linear state-space model around operating point - MATLAB linmod - MathWorks Benelux.

- Meng, J., Mu, Y., Wu, J., Jia, H., Dai, Q., & Yu, X. (2015). Dynamic frequency response from electric vehicles in the Great Britain power system. *Journal of Modern Power Systems and Clean Energy*, 3(2), 203–211.
- Mercado-Vargas, M. J., Gomez-Lorente, D., Rabaza, O., & Alameda-Hernandez, E. (2015). Aggregated models of permanent magnet synchronous generators wind farms. *Renewable Energy*, 83, 1287–1298.
- Momber, I., Siddiqui, A., Gomez San Roman, T., & Soder, L. (2015). Risk Averse Scheduling by a PEV Aggregator Under Uncertainty. *IEEE Transactions on Power Systems*, 30(2), 882–891.
- Momber, I., Wogrin, S., & Gomez, T. (2014). An MPEC for electricity retail alternatives of plug-in electric vehicle (PEV) aggregators. In *Power Systems Computation Conference (PSCC), 2014* (pp. 1–7).
- Momber, I., Wogrin, S., & Roman, T. G. S. (2016). Retail Pricing: A Bilevel Program for PEV Aggregator Decisions Using Indirect Load Control. *IEEE Transactions on Power Systems*, 31(1), 464–473.
- Morel, J., Obara, S., & Morizane, Y. (2015). Stability Enhancement of a Power System Containing High-Penetration Intermittent Renewable Generation. *Journal of Sustainable Development of Energy, Water and Environment Systems*, 3(2), 151–162.
- Moreno, R., Chamorro, H., & Izadkhast, S. (2013). A framework for the energy aggregator model. In *2013 Workshop on Power Electronics and Power Quality Applications (PEPQA)* (pp. 1–5).
- Morren, J., De Haan, S. W., Kling, W. L., Ferreira, J. A., & others (2006). Wind turbines emulating inertia and supporting primary frequency control. *IEEE Transactions on Power Systems*, 21 (1).
- Mu, Y., Wu, J., Ekanayake, J., Jenkins, N., & Jia, H. (2013a). Primary frequency response from electric vehicles in the Great Britain power system. *Smart Grid, IEEE Transactions on*, 4(2), 1142–1150.
- Mu, Y., Wu, J., Ekanayake, J., Jenkins, N., & Jia, H. (2013b). Primary frequency response from electric vehicles in the Great Britain power system. *Smart Grid, IEEE Transactions on*, 4(2), 1142–1150.
- Nagpal, M., Moshref, A., Morison, G. K., & Kundur, P. (2001). Experience with testing and modeling of gas turbines. In *IEEE Pow. Eng. Soc. Winter Meeting, 2001*, volume 2 (pp. 652–656 vol.2).
- Nguyen, N., Almasabi, S., & Mitra, J. (2015). Estimation of penetration limit of variable resources based on frequency deviation. In *North American Power Symposium (NAPS), 2015* (pp. 1–6).: IEEE.
- NHTS (2009). National household travel survey, u.s. department of transportation. washington, dc.
- Nordhaus, W. (1969). *Innovation, growth, and welfare*. Cambridge, Mass.: MIT Press.
- Nozari, F., Kankam, M. D., & Price, W. W. (1987). Aggregation of induction motors for transient stability load modeling. *IEEE Transactions on Power systems*, 4(2), 1096–1103.

- Nozari, G. R., Manno, J., & Alden, R. T. H. (1984). An Aggregate Induction Motor Model for Industrial Plants. *IEEE Transactions on Power Systems*, 103(4).
- Office of Energy Efficiency & Renewable Energy, U. S. (2015). *Over one million in plug-in vehicles sales worldwide in 2015*. Technical report.
- Ortega-Vazquez, M., Bouffard, F., & Silva, V. (2013). Electric Vehicle Aggregator/System Operator Coordination for Charging Scheduling and Services Procurement. *IEEE Transactions on Power Systems*, 28(2), 1806–1815.
- Ota, Y., Taniguchi, H., Nakajima, T., Liyanage, K. M., Baba, J., & Yokoyama, A. (2010). Autonomous distributed V2g (vehicle-to-grid) considering charging request and battery condition. In *Innovative Smart Grid Technologies Conference Europe (ISGT Europe), 2010 IEEE PES* (pp. 1–6): IEEE.
- Papathanassiou, S., Hatziargyriou, N., Strunz, K., & others (2005). A benchmark low voltage microgrid network. In *Proceedings of the CIGRE Symposium: Power Systems with Dispersed Generation* (pp. 1–8).
- parliament, E. & the council (2009). Directive 2009/28/EC of the European Parliament and of the Council of 23 April 2009 on the promotion of the use of energy from renewable sources and amending and subsequently repealing Directives 2001/77/EC and 2003/30/EC.
- Pecas Lopes, J., Soares, F. J., & Almeida, P. M. (2011). Integration of Electric Vehicles in the Electric Power System. *Proceedings of the IEEE*, 99(1), 168–183.
- Pecas Lopes, J. A., Rocha Almeida, P. M., & Soares, F. J. (2009). Using vehicle-to-grid to maximize the integration of intermittent renewable energy resources in islanded electric grids. In *2009 International Conference on Clean Electrical Power* (pp. 290–295): IEEE.
- Pillai, J. R. & Bak-Jensen, B. (2010a). Vehicle-to-Grid for islanded power system operation in Bornholm. In *Power and Energy Society General Meeting, 2010 IEEE* (pp. 1–8): IEEE.
- Pillai, J. R. & Bak-Jensen, B. (2010b). Vehicle-to-grid systems for frequency regulation in an Islanded Danish distribution network. In *Vehicle Power and Propulsion Conference (VPPC), 2010 IEEE* (pp. 1–6): IEEE.
- Pillai, J. R. & Bak-Jensen, B. (2011). Integration of Vehicle-to-Grid in the Western Danish Power System. *Sustainable Energy, IEEE Transactions on*, 2(1), 12–19.
- Pinson, P., Madsen, H., & others (2014). Benefits and challenges of electrical demand response: A critical review. *Renewable and Sustainable Energy Reviews*, 39, 686–699.
- R Ball, Keers, N., Alexander, M., & Bower, E. (2011). MERGE d2.1 project deliverable 2.1.
- Rakhmatov, D., Vrudhula, S., & Wallach, D. A. (2003). A model for battery lifetime analysis for organizing applications on a pocket computer. *Very Large Scale Integration (VLSI) Systems, IEEE Transactions on*, 11(6), 1019–1030.
- Rebours, Y. G., Kirschen, D. S., Trotignon, M., & Rossignol, S. (2007a). A Survey of Frequency and Voltage Control Ancillary Services-Part I: Technical Features. *IEEE Transactions on Power Systems*, 22(1), 350–357.

- Rebours, Y. G., Kirschen, D. S., Trotignon, M., & Rossignol, S. (2007b). A Survey of Frequency and Voltage Control Ancillary Services-Part II: Economic Features. *IEEE Transactions on Power Systems*, 22(1), 358–366.
- REE (2006). Procedimiento de operación, REE red electrica de espana.
- REE (2013). REE red electrica de espana.
- Rosekeit, M. & De Doncker, R. W. (2011). Smoothing power ripple in single phase chargers at minimized dc-link capacitance. In *Power Electronics and ECCE Asia (ICPE & ECCE), 2011 IEEE 8th International Conference on* (pp. 2699–2703): IEEE.
- Ruiz, N., Claessens, B., Jimeno, J., Lopez, J. A., & Six, D. (2015). Residential load forecasting under a demand response program based on economic incentives. *International Transactions on Electrical Energy Systems*, 25(8), 1436–1451.
- Ruiz, P. A. & Sauer, P. W. (2008). Spinning Contingency Reserve: Economic Value and Demand Functions. *IEEE Transactions on Power Systems*, 23(3), 1071–1078.
- Sarker, M., Dvorkin, Y., & Ortega-Vazquez, M. (2015a). Optimal Participation of an Electric Vehicle Aggregator in Day-Ahead Energy and Reserve Markets. *IEEE Transactions on Power Systems*, PP(99), 1–10.
- Sarker, M., Ortega-Vazquez, M., & Kirschen, D. (2015b). Optimal Coordination and Scheduling of Demand Response via Monetary Incentives. *IEEE Transactions on Smart Grid*, 6(3), 1341–1352.
- Serban, I. & Marinescu, C. (2012). An enhanced three-phase battery energy storage system for frequency control in microgrids. In *Optimization of Electrical and Electronic Equipment (OPTIM), 2012 13th International Conference on* (pp. 912–918): IEEE.
- Serban, I. & Marinescu, C. (2014). Control Strategy of Three-Phase Battery Energy Storage Systems for Frequency Support in Microgrids and with Uninterrupted Supply of Local Loads. *IEEE Transactions on Power Electronics*, 29(9), 5010–5020.
- Shi, L., Meintz, A., & Ferdowsi, M. (2008). Single-phase bidirectional AC-DC converters for plug-in hybrid electric vehicle applications. In *Vehicle Power and Propulsion Conference, 2008. VPPC'08. IEEE* (pp. 1–5): IEEE.
- Sigrist, L., Egido, I., Sanchez-Ubeda, E. F., & Rouco, L. (2010). Representative Operating and Contingency Scenarios for the Design of UFLS Schemes. *IEEE Transactions on Power Systems*, 25(2), 906–913.
- Singh, B., Singh, B. N., Chandra, A., Al-Haddad, K., Pandey, A., & Kothari, D. P. (2003). A review of single-phase improved power quality AC-DC converters. *Industrial Electronics, IEEE Transactions on*, 50(5), 962–981.
- Singh, B., Singh, B. N., Chandra, A., Al-Haddad, K., Pandey, A., & Kothari, D. P. (2004). A review of three-phase improved power quality AC-DC converters. *Industrial Electronics, IEEE Transactions on*, 51(3), 641–660.
- Singh, H. & Papalexopoulos, A. (1999). Competitive procurement of ancillary services by an independent system operator. *Power Systems, IEEE Transactions on*, 14(2), 498–504.

- Slootweg, J. G. & Kling, W. L. (2003). Aggregated modelling of wind parks in power system dynamics simulations. In *Power Tech Conference Proceedings, 2003 IEEE Bologna*, volume 3 (pp. 6–pp).
- Soler, D., Frias, P., Gomez, T., & Platero, C. A. (2010). Calculation of the Elastic Demand Curve for a Day-Ahead Secondary Reserve Market. *IEEE Transactions on Power Systems*, 25(2), 615–623.
- Su, W. & Wang, J. (2012). Energy management systems in microgrid operations. *The Electricity Journal*, 25(8), 45–60.
- Sun, Y., Liu, W., Su, M., Li, X., Wang, H., & Yang, J. (2014). A unified modeling and control of a multi-functional current source-typed converter for V2g application. *Electric Power Systems Research*, 106, 12–20.
- Taleb, M., Akbaba, M., & Abdullah, E. A. (1994). Aggregation of induction machines for power system dynamic studies. *Power Systems, IEEE Transactions on*, 9(4), 2042–2048.
- Teece, D. J. (1980). Economies of scope and the scope of the enterprise. *Journal of economic behavior & organization*, 1(3), 223–247.
- UCTE (2009). *Policy 1. Load-Frequency Control and Performance*. Technical report, Technical Report UCTE OH.
- Ulbig, A., Galus, M. D., Chatzivasileiadis, S., & Andersson, G. (2010). General frequency control with aggregated control reserve capacity from time-varying sources: The case of PHEVs. In *Bulk Power System Dynamics and Control (iREP) - VIII (iREP), 2010 iREP Symposium* (pp. 1–14).: IEEE.
- Ullah, N. R., Thiringer, T., & Karlsson, D. (2008). Temporary primary frequency control support by variable speed wind turbines - potential and applications. *Power Systems, IEEE Transactions on*, 23(2), 601–612.
- Vidyanandan, K. V. & Senroy, N. (2013). Primary frequency regulation by deloaded wind turbines using variable droop. *Power Systems, IEEE Transactions on*, 28(2), 837–846.
- Vrakopoulou, M. & Andersson, G. (2010). An Adaptive Load Shedding Technique for Controlled Islanding.
- Williamson, O. E. (1985). *The economic institutions of capitalism*. Simon and Schuster.
- Yang, Y., Li, H., Aichhorn, A., Zheng, J., & Greenleaf, M. (2014). Sizing strategy of distributed battery storage system with high penetration of photovoltaic for voltage regulation and peak load shaving. *Smart Grid, IEEE Transactions on*, 5(2), 982–991.
- Yilmaz, M. & Krein, P. (2013). Review of the Impact of Vehicle-to-Grid Technologies on Distribution Systems and Utility Interfaces. *IEEE Transactions on Power Electronics*, 28(12), 5673–5689.
- Zhang, L., Gari, N., & Hmurcik, L. V. (2014). Energy management in a microgrid with distributed energy resources. *Energy Conversion and Management*, 78, 297–305.
- Zhang, X.-P., Rehtanz, C., & Pal, B. (2012). Autonomous Systems for Emergency and Stability Control of FACTS. In *Flexible AC Transmission Systems: Modelling and Control* (pp. 301–320). Springer.

Candidate's Curriculum Vitae

Seyedmahdi Izadkhast was born on November 26th 1986 in Tehran, Iran. He received the B.Sc. degree in Electrical Engineering from University of Tehran (Fanni), Tehran, Iran, in 2008, and the M.Sc. degree in Power Electronics and Electrical Machines from Sharif University of Technology, Tehran, Iran, in 2010. Over the past years, he has been pursuing the Erasmus Mundus Joint Doctorate in sustainable energy technologies and strategies (SETS) delivered by Comillas Pontifical University, Spain; Royal Institute of Technology, Sweden; and Delft University of Technology, The Netherlands. Since 2011, he has been pursuing the Ph.D. degree at the Institute for Research in Technology (IIT), Comillas Pontifical University, Madrid, Spain, and since 2014, he has been also collaborating with the DC Systems, Energy Conversion and Storage (DCE&S) group of the Electrical Sustainable Energy (ESE) Department at the Delft University of Technology. Also, he has been involved in various international research projects like Advanced Smart Grid Solutions for Europe (GRID4EU), NICE GRID, and Cellular Smart Grid Platform (CSGriP) in the Netherlands. Currently, he is working as a researcher in DCE&S group at the Delft University of Technology, where his main research focus is on the large-scale integration of dispersed energy storage systems across AC and DC electrical networks. Within DCE&S group, he also assists in the coordination of European projects (e.g., ERA Net Smart Grids Plus DC Distribution Smart Grids (DCSMART)), technical courses (e.g., AC/DC microgrids and “Systems Engineering”), and the daily supervision of M.Sc. students. S. Izadkhast is a reviewer for several prestigious Journals and international conferences including IEEE Transactions on Power Systems, IEEE Transactions on Industrial Informatics, IEEE Transactions on Smart grid, IET Generation, Transmission, Distribution (GTD), Elsevier, Sustainable Energy, Grids, and Networks (SEGAN), and IEEE PES General Meeting.

His research interests include modeling and control strategies for plug-in electric vehicles integration in power systems, battery energy storage system technologies, technical scalability and replicability analysis, power system dynamics, stability, and control.

For KTH Royal Institute of Technology:
DOCTORAL THESIS IN ELECTRICAL ENGINEERING
TRITA-EE
www.kth.se

[EAN-code]

[TRITA xxxx]
ISSN
ISBN